Cellular and molecular mechanisms of human endothelial cell plasma membrane remodeling by Neisseria meningitidis

Arthur Charles-Orszag

Paris Descartes University
Doctoral school BioSPC (ED 562)
Unit of Pathogenesis of Vascular Infections
Department of Cell Biology and Infection, Institut Pasteur

Cellular and molecular mechanisms of human endothelial cell plasma membrane remodeling by *Neisseria meningitidis*

Arthur Charles-Orszag

Doctoral Thesis in **Cell Biology**

Under the supervision of **Dr. Guillaume DUMÉNIL**
Presented and publicly defended on Tuesday, October 17, 2017

Before the examining committee composed of:

Prof. Catherine ALCAÏDE	Paris Diderot University	President
Dr. Emmanuel BOUCROT	University College London	Reviewer
Dr. Martin PILHOFER	ETH Zürich	Reviewer
Dr. Patricia BASSEREAU	Institut Curie, Paris	Examiner
Dr. Jost ENNINGA	Institut Pasteur, Paris	Examiner
Dr. Guillaume DUMÉNIL	Institut Pasteur, Paris	Thesis director

The all laughed at Christopher Columbus
When he said the world was round
They all laughed when Edison recorded sound
They all laughed at Wilbur and his brother
When they said that man could fly
They told Marconi
Wireless was a phony
It's the same old cry
[...]
But ho, ho, ho!
Who's got the last laugh now?

George & Ira Gershwin, "They All Laughed" (1937)

Remerciements

Ce manuscrit est l'occasion pour moi de remercier les personnes qui ont compté, qui ont apporté un soutien précieux, qui ont travaillé avec moi... en somme ceux qui auront autant participé que moi-même à l'aboutissement de cette thèse.

Je tiens d'abord à remercier **Guillaume** pour m'avoir initialement accueilli en tant que stagiaire au laboratoire. Ce stage aura marqué le début d'une longue collaboration scientifique qui a inclus un an de Master 2 et un peu plus de quatre ans de thèse. Merci de m'avoir fait confiance, de m'avoir laissé tout essayer, de m'avoir toujours encouragé, de m'avoir permis de présenter mon travail en congrès, de m'avoir poussé à toujours explorer plus à fond des hypothèses parfois un peu folles. Grâce à tout ça, je me sens un scientifique accompli. Merci aussi infiniment de nous avoir emmenés avec toi à Pasteur, quelle aventure !

Je tiens ensuite à remercier les membres de mon jury de thèse, à commencer par **Emmanuel Boucrot** et **Martin Pilhofer** pour avoir très gentiment accepté de lire et d'évaluer ce manuscrit, puis à **Patricia Bassereau** et **Jost Enninga** pour avoir accepté d'évaluer ce travail lors de la soutenance, et enfin à **Catherine Alcaïde** pour avoir accepté de présider ce jury.

Je tiens en particulier à remercier **Matthieu Piel**, **Jacomine Krijnse-Locker**, **Patricia Bassereau** et **Françoise Brochard-Wyart** pour nos discussions et nos collaborations scientifiques qui ont été essentielles à l'avancement de ce projet.

Merci à l'ensemble des personnes avec qui j'ai collaboré et/ou qui ont fourni de précieux conseils (dans le désordre) : **Jacomine Krijnse-Locker**, **Matthieu Piel**, **Yong Chen**, **Jian Shi**, **Rafaele Attia**, **Patricia Bassereau**, **Tsai Feng Ching**, **Christophe Lamaze**, **Sven van Teeffelen**, **Guy Tran Van Nhieu**, **Emmanuel Lemichez**, **Arnaud Echard**, **Samy Gobaa**, **Julia Chamot-Rooke**, **Christian Malosse**, **Sergio Grinstein**, **Ana-Maria Lennon-Duménil**, **Martin Sachse**, **Adeline Mallet**, **Maryse Moya-Nilges**, **Christine Schmitt**, **Emmanuelle Quemin**, **Audrey Salles**, **Perinne Bomme**, et tous les membres de **Roper Scientific France**.

Merci à toutes les personnes que du PARCC, où cette thèse a débuté, et en particulier à **Alain Tedgui**, **Andreas**, **Babette**, **Ivana**, **Carole**, **Xavier**, **Véronique**, **Karima**, les membres de l'**équipe Camerer** (en particulier **Sylvain**, **Aline** et **Eric**), pour votre aide, votre amitié, les retraites, les soirées Halloween de folliiiiiie. Merci plus particulièrement à **Stéphanie** pour nos petits déjeuners avant même le lever du soleil, en plein hiver, qui me manquent beaucoup, et à la formidable **Julie**.

Merci à tous les anciens du labo, en particulier à **Mag** et **Anne-Flore** qui m'ont tout appris et avec qui on a bien rigolé, mais également à **Flore**, **Keira**, **Silke**, **Ximing** et **Corinne**.

Merci aux membres actuels du labo, little **Vale**, **Hebert**, la grosse **Pierre**, **Jean-Ficelle**, **Youxin**, **Tomas**, **Marie-Paule**, **Isabelle**, **Dorian**, **Daria** et **Paul**. Mention spéciale à la berrichonne, **Sylvie**, avec qui ça aura été une joie de partager le bureau. J'espère que tu te souviendras encore de moi dans vingt ans quand tu rigoleras en écoutant Radio Swiss Classic.

Merci à l'**institut Pasteur** et aux **pasteuriens**, et en particulier aux voisines les plus stylées du monde : **Raqui**, **Babinetta** et **Fabi**.

Merci à l'**équipe pédagogique** du département de biologie cellulaire de Paris 7 et aux préparatrices qui nous facilitent beaucoup la vie. Merci également à **tous mes étudiants de TP** qui ont (presque) toujours été vraiment mignons avec moi. Merci à mes deux super stagiaires, **Athénaïs** et **Maëlys**. Merci à mes collègues moniteurs **Virginie**, **Tamara** et **Hicham**.

Merci à **Marie-Jeanne Barets** et **Odile Riberty** pour le virus de la biologie.

Merci aux encadrants merveilleux avec qui j'ai eu la chance de travailler au cours de mon cursus : **Seb**, **Tobi** et **Mag**. Merci d'ailleurs au **Pr. Laure Bonnaud** (et toute son équipe au Muséum National d'Histoire Naturelle) et au **Pr. Laura Machesky** (et toute son équipe au Beatson Institute de Glasgow).

Merci infiniment aux amis (dans le désordre) : **Mikou**, **Meliss** et **Ripoldingue** (mes BFF), **Camilla** (*Shantay, you stay* djirect), **Mel** (ma coloc pour *UN MOIS*), *monkey* **Nhito**, **Hicham** (le joli casse-noix), **Mémelle**, **Coco** et **Cécilou** (la vieille garde), **No**, **Youss**, **Bruno** (qui m'éclaire de sa toute petite lanterne, qu'il trimballe souvent quand on se promène), **Antho** (ma co-sicilienne), **Louise**, **Charlotte** et **Anne-Lise** (les babloches), the amazing **Max Nobis**, **Doubidou** (qui en plus d'être un amour s'est avéré être un super collègue), et enfin **Matthieu** et **Darinetta** (la génialissime). Heureusement que vous êtes tous là, je vous aime !

Merci à **Alexis**, avec qui j'ai vécu des années vraiment heureuses, pour avoir été là dans les moments les plus durs, et sans qui je n'aurais jamais été aussi loin. Merci pour des milliards de raisons.

Mention spéciale à **Catherine** (encore toi). Il n'y a pas assez de place ici pour dresser la liste de tout ce pour quoi je te suis reconnaissant, mais principalement : pour ton amitié indéfectible, pour ton soutien dans les moments difficiles, pour ton esprit de contradiction (pour rester poli), pour ton humour, et surtout pour ton immense tendresse.

Merci à **Paul** (le chaton fou) pour tout, mais entre autres : pour ton aide, pour ton scepticisme (qui peut s'avérer super utile), pour ta tendresse, et parce que tu es si drôle (*mongolieeeeenne*).

Merci infiniment à toute ma famille. Les **Orszag** d'un côté, à commencer évidemment par ma merveilleuse maman, mes amours de frères et sœurs, mon oncle (miaou), et en particulier à mes grands-parents qui ont fait naître chez moi l'esprit de découverte. Tous les **Charles** aussi de l'autre côté, mais surtout mon papa bien sûr, et les Despert. Merci infiniment à **Hélène** et **Jo**, et à **Alzira**.

Enfin, merci (dans le désordre) à **Anita**, **Camille**, **Billie**, **Ella**, **Amy**, **Francis**, **Chet**, **Vladimir**, **Aretha**, **Véronique**, **Blossom**, **Donny**, **Chico**, **João**, **Barbara**, **Mary J.**, **Caetano**, **Nina**, **Erroll**, **Erykah**, **Janis**, **Lauryn**, **Marvin** & **George** pour la musique, **l'infirmerie de Pasteur** et **Mercurochrome** pour les soins, la **cantine** de Pasteur, et surtout **Fred** pour les bières.

* * *

Cette thèse est dédiée à **Fabienne Orszag-Sperber** (1937-2014), docteur en géologie, maître de conférence à Paris XI, et ma grand-mère. Tu gravites toujours autour de moi, quelque part, mais tu me manques terriblement. J'arrête bientôt de fumer et de me ronger les ongles, c'est promis !

Table of contents

Index of figures and tables

List of abbreviations

AAA	ATPases Associated with diverse cellular Activities
Arp2/3	Actin-related proteins 2/3
BAR	Bin/Amphiphysin/Rvs
BBB	Blood-brain barrier
CEACAM	Carcinoembryonic antigen-related cell adhesion molecule
ECM	Extracellular matric
ERM	Ezrin/Radixin/Moesin
F-actin	Filamentous actin
LOS	Lipooligosaccharide
MOI	Multiplicity of infection
SCID	Severe combined immunodeficiency
T2SS	Type II secretion system
T3SS	Type III secretion system
T4P	Type IV pili

OBJECTIVES & OVERVIEW

The bacterial genus *Neisseria* was named after Alfred Neisser who identified its first member, *Neisseria gonorrhoeae* (or gonococcus), as the causative agent of gonorrhea (Neisser, 1879). Another member of this genus, *Neisseria meningitidis* (or meningococcus), is responsible for meningococcal disease in human.

Meningococcal disease refers to a group of life-threatening bacterial infections caused by meningococcus and that occur in the blood vessels. It includes meningococcal meningitis and septic shock. The pathophysiology of the disease is tightly linked to the ability of the bacterium to interact with human endothelial cells. In particular, after bacterial adhesion to host cells via filamentous organelles called type IV pili, bacteria reshape the host cell plasma membrane in the form of actin-rich finger-like protrusions. This allows bacterial microcolonies to resist shear forces that are met in the bloodstream during vascular colonization. The global objective of this PhD project was to understand the cellular and molecular mechanisms of human endothelial cells plasma membrane remodeling by *N. meningitidis*.

The originality of plasma membrane reorganization by meningococcus is that it does not depend on a reorganization of the actin cytoskeleton, as is the case for other bacterial pathogens. During this PhD, I have been investigating the actin-independent mechanisms of membrane bending that could be at play, involving either host cell or bacterial factors. This project has been structured around two main goals, namely:

1) Refining our understanding of the dynamics of plasma membrane remodeling by meningococcus;
2) Investigating more specifically the role of meningococcal type IV pili in this process.

In this thesis, I describe the pathophysiology of *N. meningitidis* and review the virulence factors that mediate its interaction with host endothelial cells. In particular, a section is dedicated to the biology of type IV pili, which are the major adhesins of meningococcus. Next, I detail the complex crosstalk that takes place between bacteria and endothelial cells that lead to the reorganization of the host cell surface. Finally, I describe the cellular mechanisms of membrane remodeling in animal cells and show more specifically how different bacterial pathogens usually remodel the plasma membrane of their target cells.

Then I present our experimental data and discuss its relevance regarding the biological question of this thesis.

INTRODUCTION

1. *Neisseria meningitidis* & meningococcal disease

The genus *Neisseria* is a diverse group of diderm β-proteobacteria mainly composed of non-pathogenic species that colonize mucosal surfaces in animals. In particular, 11 species are human commensals (Liu et al., 2015). Among these, two can be pathogenic: *N. gonorrhoeae* (or gonococcus), the causative agent of gonorrhea, and *N. meningitidis* (or meningococcus), the causative agent of life-threatening meningococcal disease. This section will describe the carriage of meningococcus and the features of meningococcal disease in human.

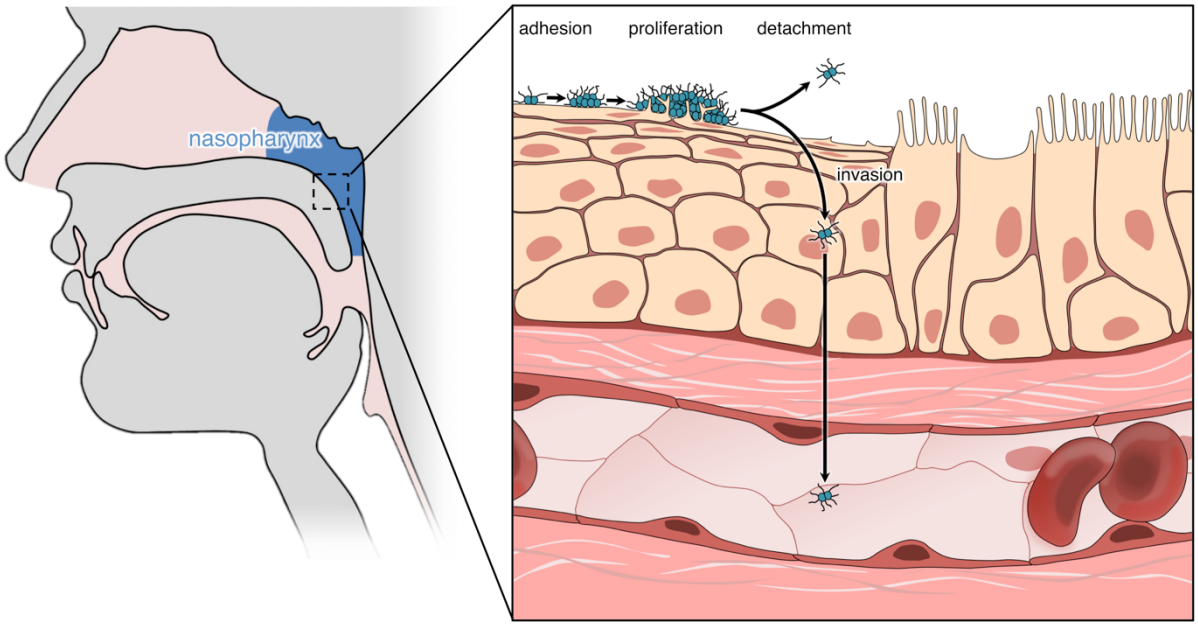

Figure 1 | Life cycle of *N. meningitidis*. The human nasopharynx is the sole natural reservoir of *N. meningitidis*. From there, bacteria colonize the mucosal surface as a commensal and can disseminate to the next host. They are sometimes found to cross the mucosal barrier and reach the underlying blood vessels, where meningococcal disease occurs.

1.1. Meningococcal carriage

Neisseria meningitidis is a capsulated and piliated diplococcus-shaped bacterium. It is exclusively found in the human nasopharynx (Fig. 1) where it mainly adheres to columnar epithelial cells that lack microvilli (de Vries et al., 1996; Pujol et al., 1997; Stephens et al., 1983; Stephens and McGee, 1981). In Europe and in North America, it colonizes 10 to 35% of the population. Carriage rates are mainly influenced by individuals age: they are very low in young children, increase in teenagers and peak between ages 20 and 24. Less than 10% of older people carry meningococcus (Caugant et al., 1994; Claus et al., 2005). In Africa, on the other hand, carriage rates do not seem to depend on age (Trotter and Greenwood, 2007). Other than age, male gender, active or passive smoking, and low socio-economic status also increase the risk of carrying meningococcus, although to a lesser extent (Blackwell et al., 1990). Meningococcal carriage can be either chronic or transient. It is likely that any given individual once carried meningococcus in its nasopharynx (Broome, 1986; Kuzemenska et al., 1978).

Transmission between carriers and non-carriers occurs either via direct contact or through respiratory droplets. Therefore, person-to-person transmission is facilitated in confined environments, such as military camps and childcare facilities, where carriage rates can almost be of 100% (Caugant et al., 1992; Olcen et al., 1981).

There is no obvious link between the carriage of meningococcus and the onset of meningococcal disease, as the vast majority of carriers never develop meningococcal infections. Of note, meningococcus is constantly exposed to the mucosal immune system in the nasopharynx, which has implications for the population dynamics of the bacterium (see section **2.8.**).

1.2. Traversal of the mucosal barrier

For reasons that are yet unknown, bacteria can sometimes cross the nasopharyngeal barrier, which is a prerequisite to the establishment of meningococcal disease (Fig. 1). Although a transcellular passage of bacteria has been proposed, only a small percentage of *N. meningitidis* get internalized into epithelial cells *in vitro* (Pujol et al., 1997). Besides, epidemiological studies have demonstrated that the seasonal peaks of meningococcal disease were tightly correlated in time with the peaks of influenza virus infections. Also, a part of the cases of meningococcal infections can be directly inferred to a previous case of influenza virus infection, suggesting that influenza facilitates meningococcal infections (Jacobs et al., 2014). It was proposed that this might be due to a lowering of the immune defenses in flu patients, but other hypotheses, including physical weakening of the upper respiratory tract mucosa due to flu, are not excluded. In the sub-Saharian region, individuals are thought to be at higher risk of meningococcal disease due to damages to the respiratory mucosa caused by the dust-wind Harmattan that blows during the dry season.

1.3. Meningococcal disease

1.3.1. Epidemiology of meningococcal infections

Meningococcal infections occur worldwide but display two very contrasted epidemiologic profiles in different parts of the world (Caugant and Maiden, 2009; Jafri et al., 2013).

In most countries of Europe, North America, South-East Asia and Western Pacific Region, since the introduction of antibiotics, the disease has become rare. Annual incidence rates vary from less than 2 to 10 cases per 100,000 individuals, and disease occurs mainly sporadically, in clusters or localized outbreaks. Occasionally, localized hyperendemic disease can occur with incidence rates of 5 to 10 cases per 100,000. The last outbreak of meningogoccal disease in France occurred in late 2016. Three cases of meningogoccal meningitis in students at the University of Dijon, including two deaths, prompted an exceptional vaccination campaign on the campus with more than 13,000 persons vaccinated.

In sharp contrast, in Africa, meningococcal disease presents mainly as epidemic or even pandemic outbreaks, with incidence rates of up to 1,000 cases per 100,000 individuals. It is particularly pronounced in countries of the sub-Saharian region, especially in Burkina Faso, Chad, Ethiopia and Niger. This area was named the "meningitis belt". This particular epidemic profile could stem from a lower access to healthcare and to the Harmattan wind that could facilitate the traversal of the mucosal barrier in the respiratory tract. Typically, 20,000 to 200,000 cases of meningococcal disease occur in Africa annually, causing 2,000 to 20,000 deaths (source: World Health Organization, http://www.who.int/csr/disease/OP_meningitis_FINAL.pdf?ua=1).

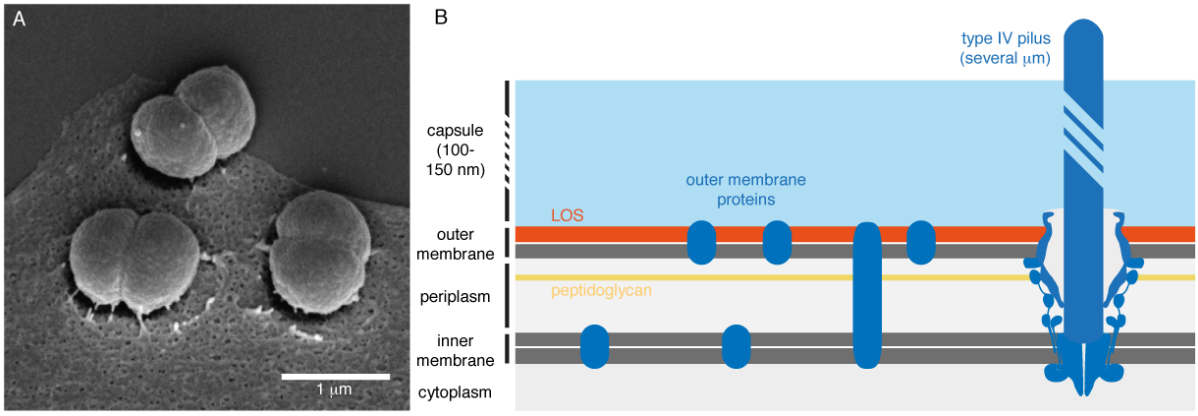

Figure 2 | Morphology and general cellular organization of *N. meningitidis*. (A) Scanning electron micrograph of three meningococci on the surface of a human endothelial cell, showing the classical diplococcus shape of the bacteria. **(B)** *N. meningitidis* is a diderm bacterium. It possesses two membranes separated by a periplasmic space containing peptidoglycan. It typically expresses type IV pili and a polysaccharide capsule (neither are visible on the electron micrograph). LOS, lipooligosaccharide.

1.3.2. Disease-associated serogroups

Contrary to *N. gonorrhoeae*, *N. meningitidis* possesses a polysachharide capsule anchored to its outer membrane (Fig. 2, and see section **2.2.**). Based on antigenic variation of the capsule (i.e. the nature of the polysaccharide), 12 serogroups have been defined. Only 6 of them, serogroups A, B, C, W135, Y and X, are responsible for over 90% of meningococcal infections worldwide, including hyperendemic and epidemic outbreaks (Boisier et al., 2007; Caugant and Maiden, 2009; Jafri et al., 2013). Capsular polysaccharides are the main targets of currently available vaccines, with the exception of serogroup B. The polysaccharide in this serogroup being too similar to a polysaccharide present in human neural tissues (Finne et al., 1987), a combination of conserved surface proteins has been used to generate a vaccine that was only approved in 2013 (Serruto et al., 2012).

In Africa, most epidemics have been associated with serogroup A, and to a lesser extent to serogroups W135 and X. However, since the introduction of a conjugate vaccine against serogroup A in 2010 that lowered the number of serogroup A infections, serogroup C infections have begun to emerge in some countries (Sidikou et al., 2016).

In the rest of the world, especially in industrialized countries, it is mostly serogroups B and C that were shown to cause hyperendemic outbreaks. In North America, serogroup Y has emerged in the last fifteen years as an important cause of disease (Stephens et al., 2007).

1.3.3. Clinical manifestations of meningococcal disease

1.3.3.1. Bacteremia, septic shock and meningitis

Bacteremia is clinically described as the presence of bacteria in the blood. In the case of meningococcus, it can evolve towards meningitis, septic shock, or a combination of the two. Each of these pathologies displays distinct clinical features with different fatality and morbidity rates (Brandtzaeg and van Deuren, 2012; de Greeff et al., 2008; Gedde-Dahl et al., 1983; Halstensen et al., 1987; van Deuren et al., 2000).

Patients with meningococcal bacteremia represent 18 to 33% of the cases of meningococcal disease. They usually present with fever but show no signs of septic shock or meningitis. Meningococci are found in the blood (with a median number of $7{,}7.10^3$ copies of meningococcal DNA per mL of blood (Ovstebo et al., 2004)) but there is no infiltration of leucocytes or bacteria in the cerebrospinal fluid, as evidenced by spinal puncture.

If not treated, meningococcal bacteremia can lead to septic shock (or fulminant septicemia) that accounts for 10 to 18% of the cases of meningococcal disease. Patients show no signs of meningitis and have little leucocyte and meningococci counts in the cerebrospinal fluid. However, they usually have fever. The number of bacteria in the blood can be high (up to 10^8 DNA copies per mL of blood). Small hemorrhagic lesions in the skin that do not blanch on applying pressure, called purpuric rashes, are a hallmark of meningococcal septic shock. They are found in 28 to 78% of the patients. During disease, and even sometimes after antiobiotherapy, meningococci can be consistently recovered from the skin by needle puncture and aspiration. In the blood, exponentially growing meningococci induce an exaggerated and destructive inflammatory response in the vasculature, heart, kidneys, and lungs. Consequently, patients can develop acute respiratory distress or renal failure. Importantly, meningococcus cause severe vascular damage that can translate into large hemorrhagic skin lesions (*purpura fulminans*, see Fig. 3), but also hemorrhages throughout the body organs. Vascular dysfunction is accompanied by a deregulation of coagulation and anti-coagulation systems, which leads to severe disseminated intravascular coagulation.

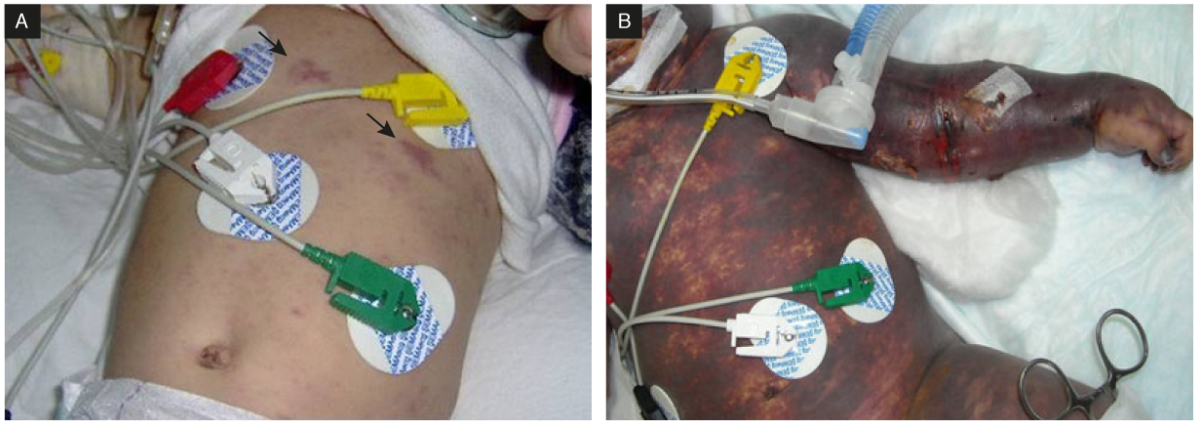

Figure 3 | Purpuric rashes and *purpura fulminans* in a case of meningococcal infection. (A) A 6-month-old girl with fever and vomiting, showing purpuric rashes on the abdomen (arrows), on the day of hospital admission. **(B)** The same child after 58 hours of medical care in the hospital. *Purpura fulminans* and extensive necrosis all over the body of the patient was associated with disseminated intravascular coagulation and multi-organ failure, which eventually led to death. Adapted from (Ozdemir et al., 2012) (see **Credits** section).

The most frequent clinical presentation of meningococcal disease is meningitis, where meningococcus crosses the blood-brain barrier and proliferates in the cerebrospinal fluid. Meningitis occurs in 37 to 49% of the cases of meningococcal disease. Patients typically present with neck and back rigidity, vomiting, photophobia and headache. Few or no bacteria are found in the blood (less than 10^3 DNA copies per mL of blood) but bacterial numbers can be very high in the cerebrospinal fluid (up to $10^9.mL^{-1}$ DNA copies) which also typically contains high numbers of leucocytes (up to $100.10^6.L^{-1}$) and an elevated concentration of proteins. Finally, in 13 to 20% of the cases, patients present with symptoms of both septic shock and meningitis.

Several histological studies on *post mortem* samples from patients with meningococcal infections have found bacterial aggregates inside the lumen of blood vessels in the skin, liver, brain and kidney, pointing to the importance of the vascular pathology in meningococcal disease (Dupin et al., 2012; Guarner et al., 2004; Hill and Kinney, 1947; Mairey et al., 2006) (also see Fig. 4A). These findings also stress the importance of the interaction of meningococcus with endothelial cells, which is the topic of this thesis.

1.3.3.2. Case fatality rates and morbidity

Each clinical manifestation of meningococcal disease features a different case fatality rate. It is lower than 5% in simple meningococcal bacteremia because patients do not develop circulatory dysfunction or massive inflammation. In meningitis, it is around 1% but surviving patients can keep severe sequelae such as deafness, blindness or reduced IQ. In shock combined to meningitis, the case fatality rate can reach 12%.

The most severe form of meningococcal disease is the septic shock. Hypotension and hypoperfusion of different organs due to vascular leakage, or multi-organ failure, can persist even after fluid resuscitation and eventually lead to acidosis and hypoxia. 50% of patients die of arrhythmia within 12h after hospital admission. Overall, the case fatality rate can reach 52%. Meningococcal septic shock also shows the highest level of morbidity. Surviving patients may require extensive care with prolonged ventilation for acute respiratory distress syndrome, dialysis for renal failure, extensive skin grafting or amputation of peripheral parts of the extremities.

1.4. Recapitulation of vascular colonization in an animal model of infection

Several animal models have been developed to study meningococcal infections *in vivo*. Since infection by meningococcus is strictly specific to human, all the animal models were based on partial humanization of mice. Transgenic mice expressing either human transferrin (see section **2.4.**) (Zarantonelli et al., 2007) or the putative pilus receptor CD46 (see section **3.3.1.**) (Johansson et al., 2003) were used, but none of these models recapitulates the vascular aspects of meningococcal disease. In particular, no bacterial aggregates were found in the blood vessels of infected animal as observed in *post mortem* samples of infected patients (Fig. 4A).

In 2013, a mouse model of meningococcal infection has been developed in the lab that allows the study of meningococcus interaction with human vasculature *in vivo* (Melican et al., 2013). In this model, immunodeficient SCID/Beige mice are partially humanized by the grafting of human skin. The 200 μm-thick piece of human skin contains a large number of capillaries. Three weeks after grafting, mice vessels are seen connected to human vessels in the skin. Therefore, human vessels are perfused and alive. Since the human specificity of meningococcus is partly due to the acquisition of iron through human transferrin (see section **2.4.**), this model includes addition of human transferrin to support bacterial growth. Infection of the grafted mice via intravenous injection of *N. meningitidis* demonstrated that meningococcus associated exclusively to human blood vessels in the grafted skin, as compared to non-grafted mice or mice grafted with mouse skin.

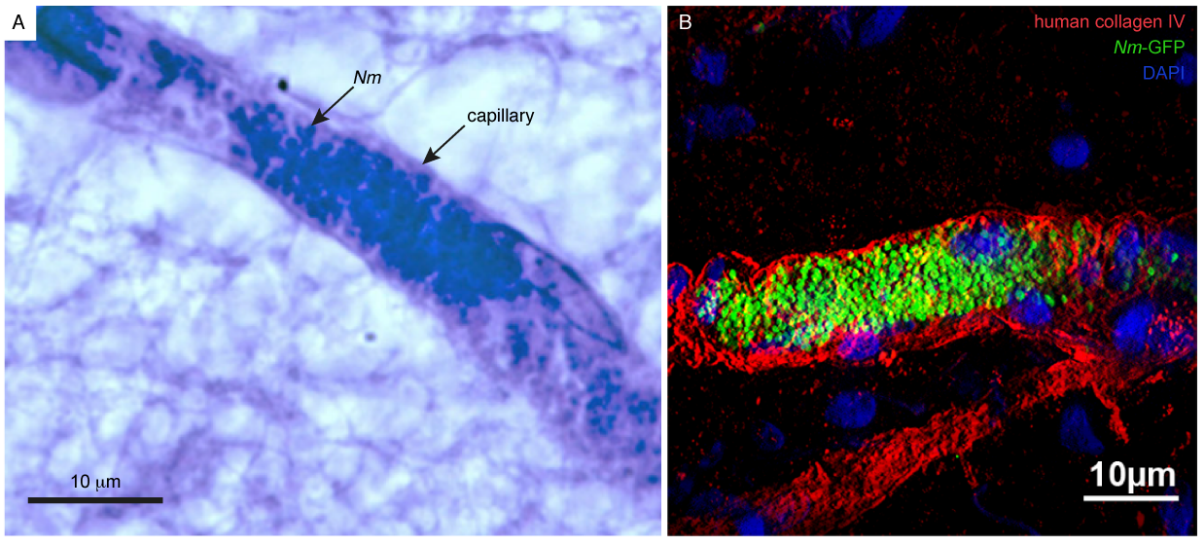

Figure 4 | Vascular colonization by *N. meningitidis*. (A) Aggregates of meningococci (*Nm*) can be found in blood capillaries of meningococcal disease patients *post mortem*, here in the brain. Adapted from (Mairey et al., 2006). **(B)** Infection of mice grafted with human skin also leads to vascular colonization by meningococcus (in green). Colonization is specific to human blood vessels (in red). Here the lumen is completely filled with bacteria. Adapted from (Melican et al., 2013). (Also see **Credits** section.)

At 30 minutes post-infection, individual bacteria were seen to adhere to human vessels walls. At 24 h post-infection, although bacterial counts decreased in the blood, bacterial aggregates were seen in the lumen of human vessels. They occasionally filled entirely the vessel lumen (Fig. 4B). Expression of type IV pili and capsule was maintained in the vessels. Upon infection, expression of the human cytokines IL-6 and -8 by the human endothelium was detected, as well as infiltration of inflammatory cells at the site of bacterial colonization. Vascular damage, as evidenced by vascular congestion, thrombosis and vascular leakage was seen in all infected animals. 30% of infected mice even developed visible rashes on the grafted skin, reminiscent of the *purpura* seen in meningococcal septic shock.

Most importantly, it was shown that adhesion to human vessels, release of cytokines, and vascular damage were strictly dependent on the expression of functional type IV pili by meningococcus. Non-piliated bacteria remained in the circulation and were never seen to associate with human vessels. Furthermore, no inflammation or vascular damage were measured in that case, despite the expression of endotoxin (or lipooligosaccharide, see section **2.3.**) by non-piliated bacteria. Of note, this conclusion was supported by another study in which the authors used the same model (Join-Lambert et al., 2013).

Therefore, recapitulation of vascular colonization by meningococcus in an animal model of infection clearly demonstrates that vascular damage in meningococcal disease is not caused by the endotoxin of circulating bacteria, as is commonly the case in bacterial sepsis (see section **2.3.**). Instead, it requires a localized type IV pili-mediated adhesion to human endothelial cells, pointing to the central role of type IV pili as virulence factors in *N. meningitidis* (see section **3.3.**).

2. Virulence factors of *Neisseria meningitidis*

A number of bacterial species acquire pathogenic abilities by the integration of mobile genetic elements, called pathogenicity islands, via horizontal gene transfer. These sets of genes are often carried on plasmids or bacteriophages and code for key virulence factors in a given species, such as secretion systems, toxins and adhesins (Hacker and Kaper, 2000). Examples include *Vibrio cholerae*, *Staphylococcus aureus*, *Listeria monocytogenes*, *Escherichia coli*, *Helicobacter pylori*, *Shigella* spp., *Salmonella* spp. and *Yersinia* spp.. In *N. meningitidis*, the comparison of disease-associated versus non disease-associated isolates has identified several strains possessing an 8-kb bacteriophage that is associated with meningococcal disease in adults only (Bille et al., 2008; Bille et al., 2005; Meyer et al., 2016). However, it was recently shown to be dispensable for virulence *in vivo* in a serogroup A strain (Bille et al., 2017). As most meningococcal isolates lack pathogenicity islands, meningococcus does not express any of the secretion systems that are usually employed by other bacterial pathogens to deliver toxins to host cells.

A set of specific tools has been employed to determine the genetic bases of virulence in meningococcus. In the late 90s, the development of Multilocus sequence typing (MLST) has allowed the study of meningococcal strains diversity (Maiden et al., 1998). This method, based on nucleotide sequencing, analyzes genetic variations of 7 housekeeping genes in order to sort a given strain within a sequence type (ST). Since 2003, next-generation sequencing (NGS) has been progressively used to get whole genome sequences (WGS) of meningococal isolates. At the time of writing, over 19,000 meningococcal WGS have been obtained (Harrison et al., 2017). Together, MLST and NGS have permitted the classification of 43,053 isolates of both pathogenic and carriage strains from different parts of the world into 12,944 STs. STs that shared more than 4 similar allelic variants among the 7 housekeeping genes were further grouped into so-called clonal complexes. So far, 53 clonal complexes have been identified (see the online database https://pubmlst.org/neisseria/info/complexes.shtml). A small number of clonal complexes are termed hyperinvasive lineages because they comprise a large proportion of disease-associated isolates relative to carriage-associated ones. Thesy are responsible for a large percentage of meningococcal disease worldwide (Caugant, 2008).

From these genomic studies has emerged the notion that the capacity of meningococcus to cause disease is not determined by a set of virulence genes in the strictest sense of the word. Instead, it rather depends on different combinations of allelic variants of genes that are evenly shared by virulent and non-virulent strains. In line with this idea, since the late 60s, multiple species of commensal *Neisseria* other than gonococcus and meningococcus have caused over 80 cases of bacterial infections, including speticaemia and meningitis (Liu et al., 2015).

Nevertheless, a number of bacterial factors that are usually required for the colonization of the host mucosal surfaces also happen to be involved in virulence. These factors are all surface-exposed bacterial components such as the type IV pili, the capsule, the lipooligosaccharide, iron acquisition systems, and non-pilus adhesins, which are described in this section. In addition, a striking feature of *Neisseria* spp. bacteria is the ability to constantly modulate their repertoire of surface components due to a remarkably fluid genome. Therefore, genetic variability in meningococcus also greatly contributes to virulence (as discussed in section **2.8.**).

2.1. Type IV pili

Important to this work, type IV pili are the outermost structures in contact with the environment and the major adhesins of *N. meningitidis*. They are expressed by all disease-causing isolates (DeVoe and Gilchrist, 1975). Their structure, assembly, biological functions and role in host cell interaction are the described in dedicated sections of this Introduction (see sections **3.** and **4.**).

2.2. Polysaccharide capsule

After type IV pili, the capsule is the second structure accessible to the environment. The ability to synthesize a polysaccharide capsule seemingly occurred by horizontal gene transfer from *Pasteurella multocida* or *Haemophilus influenzae* (Lam et al., 2011; Putonti et al., 2013; Schoen et al., 2008). Among invasive meningococcal strains, it is one of the most frequently found virulence determinant. The genetic locus for capsule biosynthesis contains over 20 genes grouped in 6 regions (Harrison et al., 2013). Region A contains the genes responsible for the synthesis of the polysaccharide polymer and is specific to each serogroup. Regions B and C contain the genes required for capsule translocation and transport. Regions D and D' contain genes of unknown functions as well as a gene encoding the GalE protein responsible for the synthesis of uridine diphosphate (UDP)-Galactose, which is necessary for the synthesis of serogroups W135 and Y capsules and of the lipooligosaccharide, and utilized in protein glycosylation. Region E contains a gene of unknown function, *tex*, that has sequence similarities with transcription factors.

The capsule is as an approximately 100 nm-thick hydrated gel (Fig. 5). As such, it was first thought to protect bacteria against desiccation, but this hypothesis was ruled out in a study of environmental survival capacities of meningococcus (Tzeng et al., 2014). It rather seems that the capsule prevents bacterial killing by the complement system. Non-capsulated meningococci are much more sensitive to complement-mediated killing than capsulated meningococci (Uria et al., 2008).

The complement system is the first line of innate immune defense against bacteria in the blood. It mainly relies on the recognition of surface molecules, such as outer membrane proteins or specific saccharides, via the binding of antibodies or lectins. It rapidly leads to the assembly of a the membrane attack complex (MAC) at the surface of the pathogen, which forms pores in the membrane of the bacterium and causes it to lyse (see (Lewis and Ram, 2014) for a review). The partial role of complement-mediated killing initiated by antibodies against *N. meningitidis* has been demonstrated in the late 60s by comparing the bactericidal activity of sera drawn from healthy and infected children and army recruits (Goldschneider et al., 1969a; Goldschneider et al., 1969b). It was found that only 5.6% of sera from previously infected individuals had a bactericidal activity against meningococcus, compared to 82% of sera from non-previously infected individuals. The role of complement-mediated killing in the protection against meningococcal infections is also suggested by the high incidence of meningococcal disease in persons with a deficiency in the proteins of the complement system (Figueroa et al., 1993; Figueroa and Densen, 1991). In these patients, phagocytosis of bacteria mediated by antibodies, or opsonophagocytosis, is still possible but not direct killing by the complement system.

However, the mechanisms of protection against the complement by the capsule are largely undetermined. One possible reason with respect to serogroups B, C, W135 and Y is that their capsules all contain sialic acid, which is known to inhibit complement activation on host cells. However, capsules from serogroups A and X do not. Other studies have shown that the polysaccharides of the capsule could inhibit the insertion of the MAC (Drogari-Apiranthitou et al., 2002), and it is also suggested that the capsule could inhibit the binding of antibodies to surface components. Moreover, the incidence of meningococcal disease in

complement-deficient individuals is decreased following vaccination with polysaccharide-based vaccines, suggesting an additional role of opsonophagocytosis in protection against meningococcal infections (Platonov et al., 2003).

Some rare cases of infections by meningococci with a capsule null locus have been reported (Findlow et al., 2007; Hoang et al., 2005; Vogel et al., 2004) and may challenge the idea of a central role of the capsule in the infection process. However, the genes for capsule biosynthesis are subject to phase variation and thermoregulation (see section **2.8.**), and it was suggested that meningococcus might express a capsule during disease and downregulate it during carriage (Dolan-Livengood et al., 2003). Moreover, approximately 50% of carrier strains do not express a capsule (Caugant et al., 2007) and it is likely that downregulation of the capsule might aid in the interaction with epithelial cells in the nasopharynx via non-pilus adhesins, which are likely masked otherwise (see sections **2.6.** and **2.7.**) (Deghmane et al., 2002; Hammerschmidt et al., 1996; Virji et al., 1992). Therefore, there is convincing evidence supporting the role of the capsule as a virulence factor, although the mechanisms of capsule-mediated virulence are not fully understood. Still, it cannot account for meningococcal virulence on its own.

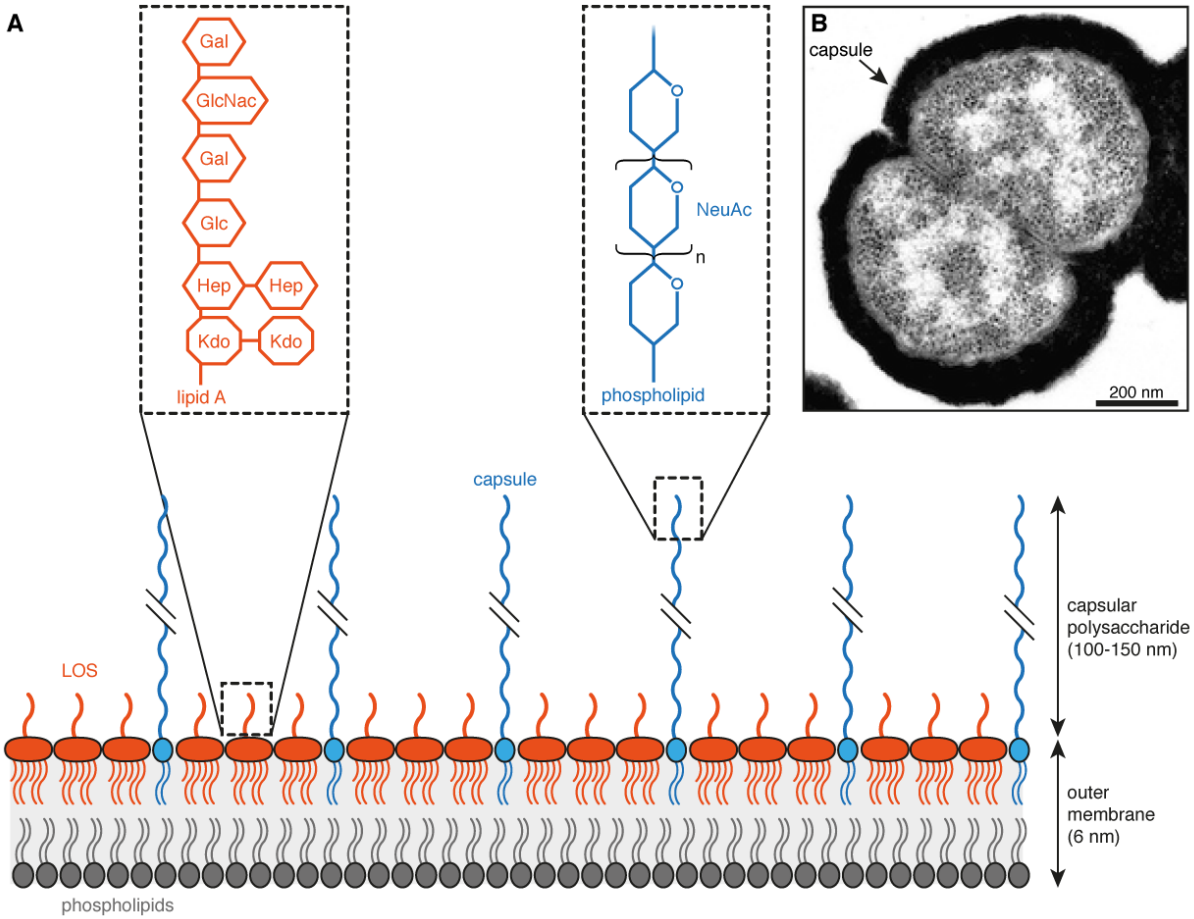

Figure 5 | Chemical structure of the lipooligosaccharide and of the capsular polysaccharide of *N. meningitidis*. (A) The outer leaflet of the outer membrane mainly contains lipooligosaccharide (LOS) that consists of a short oligosaccharide anchored to lipid A (orange). The capsular polysaccharide (serogroup C here, blue) is anchored to phospholipids and can measure up to 150 nm. LOS, lipooligosaccharide; Gal, galactose; GlcNac, N-Acetylglucosamine; Glc, glucose; Hep, heptose; Kdo, ketodeoxyoctonic acid; NeuAc, N-Acetylneuraminic acid. **(B)** Transmission electron micrograph of a serogroup W meningococcus stained with alcian blue, revealing the polysaccharide capsule as a dark layer surrounding the bacterial body. Adapted from (Ganesh et al., 2017) (see **Credits** section).

2.3. Lipooligosaccharide

In diderm bacteria, the major lipid component of the outer leaflet of the outer membrane is the lipopolysaccharide, or LPS (also called endotoxin). It is a large molecule composed of a lipid A moiety, a core oligosaccharide and a long repetitive glycan polymer called the O antigen, or O polysaccharide. LPS is also a major virulence factor that is robustly recognized by the Toll-like receptor 4 (TLR-4) within the host. TLR-4 activation by LPS triggers a massive proinflammatory response with a release of the inflammatory cytokines interleukine (IL)-1 and -6 and tissue necrosis factor (TNF)-α, as well as chemokines such as monocyte chemoattractant protein (MCP)-1, macrophage inflammatory protein (MIP)-1α and IL-8. This inflammatory response eventually leads to endotoxic shock (Janeway and Medzhitov, 2002). In *N. meningitidis* and other bacteria such as *Haemophilus influenzae*, LPS lacks the long O antigen and is therefore referred to as lipo*oligo*saccharide (LOS, Fig. 5). Of note, meningococcus is the only bacterium that is viable in the absence of LOS (Steeghs et al., 1998).

High levels of LOS can be found in individuals infected with meningococcus, and the level of circulating LOS correlates with the mortality and morbidity of meningococcal infections (Brandtzaeg et al., 1989a). LOS may originate from the large number of bacteria in the blood, but also from outer membrane vesicles (OMVs) shed by the bacteria (Namork and Brandtzaeg, 2002). Although it was found that LOS-expressing meningococcal strains trigger a "sepsis-like" inflammatory response in pigs, but not LOS-deficient strains (Hellerud et al., 2008), *in vitro* studies showed that only 9% of 464 meningococcal isolates were able to trigger a modest release of cytokines in macrophages cell lines (Fransen et al., 2009).

Meningococcal LOS was shown to be a poor activator of the complement system (Sprong et al., 2004). However, a direct correlation between LOS levels and complement activation was observed (Brandtzaeg et al., 1989b) and it was postulated that LOS could exacerbate disease progression after initial lysis of the bacteria by the complement system (Lewis and Ram, 2014).

Genes coding for the glycosyltransferases involved in the biosynthesis of LOS are subject to high frequency phase variation and to thermoregulation, which generates structural diversity (see section **2.8**.). In meningococcus, 12 different LOS structures have been identified (L1 to L12) and are used as an immunotyping system (Scholten et al., 1994). It was observed that some clinical isolates expressed the L3, L7 and L9 LOS to a greater extent than nasopharyngeal isolates that expressed more frequently L1, L8 and L10 (Jones et al., 1992). Since the three latter LOS immunotypes cannot be sialylated, it was hypothesized that sialylation of the LOS could have a role in virulence of meningococcus. LOS can act as a site of deposition for some components of the complement, and variations in the LOS structure may thus impact resistance to serum. Yet, the mechanisms by which LOS mediate resistance to serum are still poorly understood (Lewis and Ram, 2014). Moreover, the isolation of disease-causing strains that possessed a non-sialylated LOS (Mackinnon et al., 1993) suggested that, even if LOS can play a role in the virulence of meningococcus, it is anyway not strictly required.

2.4. Iron acquisition systems

Iron is a key element in several biological functions. In bacteria, several enzymes involved in DNA replication, electron transfer and the metabolism of oxygen, peroxide and superoxide depend on the utilization of ferric iron (Griffiths, 1999). In particular, iron acquisition in meningococcus is essential for bacterial growth (Archibald and DeVoe, 1978). However, in the human body, the majority of iron is either stored intracellularly on ferritin and hemoglobin proteins, or transported by high-affinity iron-binding

proteins in body fluids, such as transferrin in serum and lymph and lactoferrin in milk and mucosal secretions (Evans et al., 1999). In the blood for instance, iron-binding proteins have high binding constants for iron but are only partially saturated with iron, which means that there is virtually no free iron available for bacterial metabolism (Griffiths and Williams, 1999). Therefore, *N. meningitidis* has evolved several systems that allow the acquisition of iron from transferrin, lactoferrin, hemoglobin and haptoglobin-hemoglogin.

The most efficient iron acquisition system in meningococcus is the transferrin receptor, formed by the proteins transferrin-binding protein (Tbp) A and B. Found in all meningococcal strains, they are upregulated under iron-restricted conditions. TbpA and B expression is not regulated by phase variation (Mickelsen and Sparling, 1981; Schryvers and Morris, 1988b; Schryvers and Stojiljkovic, 1999). A lactoferrin receptor, formed by the proteins lactoferrin-binding protein (Lbp) A and B, has also been identified but its contribution to iron acquisition is undetermined (Mickelsen et al., 1982; Schryvers and Lee, 1989; Schryvers and Morris, 1988a). There is a strict specificity for human transferrin and lactoferrin by meningococcus transferrin and lactoferrin receptors (Schryvers and Gonzalez, 1990). The periplasmic import of ferric iron acquired through transferrin and lactoferrin receptors requires a specific system based on a protein called ferric-binding protein (Fbp).

Meningococcus also expresses a hemoglobin receptor (HmbR) and a haptoglobin-hemoglobin receptor (HpuAB) (Lewis and Dyer, 1995; Stojiljkovic et al., 1995). Some meningococcal strains express either receptor, while others express both (Stojiljkovic et al., 1996). Although hemoglobin is sequestered in red blood cells, low levels can be released by spontaneous hemolysis in normal human serum. Of the two receptors, HmbR is the best-characterized. It binds hemoglobin with high affinity, takes up its heme and transports it into the periplasm. It is not specific for human hemoglobin (Stojiljkovic et al., 1996). Both HmbR and HpuAB expressions are regulated by phase variation (Lewis et al., 1999). It is not known how ferric iron acquired through these receptors is transported through the periplasm, although it is not dependent of the Fbp-based system.

Transferrin, lactoferrin, hemoglobin and haptoglobin-hemoglobin iron acquisition systems all depend on energy provided by the TonB-ExbBD system (Stojiljkovic and Srinivasan, 1997). The proteins TonB, ExbB and D sit in the inner membrane of the bacterium and transduce the energy generated by the proton motive force into conformational changes in TonB-associated membrane receptors, such as the iron-acquisition systems receptors (Postle and Kadner, 2003).

2.5. Other virulence factors related to survival in the blood

Other meningococcal proteins have been suggested to be virulence factors during the blood phase of infection. The outer membrane porin PorA was shown to bind to the complement inhibitor protein C4bp (Jarva et al., 2005) and, since its expression is phase-variable, it could also contribute to evasion to antibodies. The outer membrane porin PorB2 has been shown to contribute to serum resistance (Lewis et al., 2013), as well as the autotransporter Neisseria hia homolog A (NhhA) (Griffiths et al., 2011; Peak et al., 2000; Pizza et al., 2000; Scarselli et al., 2006). The β-barrel Neisserial surface protein A (NspA) (Martin et al., 1997; Vandeputte-Rutten et al., 2003) and the factor H binding protein (fHbp) were both shown to bind human factor H, thereby impairing the alternative pathway of the complement system and mediating serum resistance (Lewis et al., 2010; Madico et al., 2006; McNeil et al., 2013), and are upregulated in human blood (Echenique-Rivera et al., 2011). fHbp expression was incidentally shown to be regulated by an increase in temperature (Loh et al., 2013). Finally, a secreted immunoglobulin (Ig) A1 protease was shown to cleave antibodies, thereby inhibiting their binding and function (Vidarsson et al., 2005).

2.6. Non-pilus adhesins: the Opacity proteins

Opa and Opc opacity proteins got their name from the opaque appearance they induce in *N. gonorrhoeae* colonies (Swanson, 1978). Although this phenotype is not as clear in *N. meningitidis* (Virji et al., 1992), Opa and Opc are expressed in meningococcus. Opa proteins are eight-stranded transmembrane β-barrel proteins encoded by three to four different genes in meningococcus. *opa* genes are subject to phase and antigenic variation and therefore generate a large number of Opa variants (see section **2.8.**) (Aho et al., 1991; Hobbs et al., 1998). Opc is a ten-stranded β-barrel protein that is encoded by a single *opc* gene which is also subject to phase variation, but not to antigenic variation (Prince et al., 2002; Sarkari et al., 1994).

Opa proteins can specifically bind to human carcinoembryonic antigen (CEA) and CEA-related cell adhesion molecules (CEACAM) 1, 3 and 6 (de Jonge et al., 2003). CEACAM1 is the most abundant of these receptors in human, although expression levels are quite low and interaction with Opa proteins requires high levels of expression (Griffiths et al., 2007; Hammarstrom, 1999), which is presumably achieved through upregulation by inflammatory cytokines (Muenzner et al., 2000). Although the expression of Opa proteins alone is not sufficient to promote adhesion to human host cells, interaction of Opa with CEACAM1 was shown to result in cellular invasion by meningococcus (Muenzner et al., 2000; Virji et al., 1999).

Opc was shown to bind indirectly to $\alpha_V\beta_3$ and $\alpha_5\beta_1$ integrins via interaction with serum vitronectin and fibronectin (Unkmeir et al., 2002; Virji et al., 1994). Vitronectin binding by Opc was shown to contribute to serum resistance (Hubert et al., 2012). Opa and Opc proteins also bind to heparin sulphate proteoglycans and sialic acids, although it was suggested that binding to sialic acid contained in some LOS immunotypes could interfere with adhesion to host cells (de Vries et al., 1998; Moore et al., 2005; Virji et al., 1995). Of note, heterologous expression of meningococcal Opc in *E. coli* does not promote adhesion of *E. coli* to human endothelial cells (Virji et al., 1994).

2.7. Other non-pilus adhesins

N. meningitidis possesses several other adhesins that are less well described and that were mostly shown to enhance binding to epithelial cells. They include the autotransporters Adhesion and penetration protein (App) (Hadi et al., 2001; Serruto et al., 2003) and Meningococcal serine protease (MspA) (Turner et al., 2006), the oligomeric coiled coil neisserial adhesion protein NadA (Capecchi et al., 2005; Comanducci et al., 2004), and the two-partner secretion system proteins TpsA and B (Schmitt et al., 2007; Tala et al., 2008; van Ulsen et al., 2008). The modes of action of these adhesins and their receptors are not clearly determined yet.

In summary, *N. meningitidis* possesses a wide variety of bacterial factors that can contribute to virulence. However, there is no evidence that any of these factors can support every aspect of meningococcal pathogenesis on its own. Furthermore, the plasticity of meningococcal genome yields a plethora of meningococcal variants which probably have very different pathogenic abilities.

2.8. Adaptive capacity

During its commensal life in the nasopharynx and during the blood phase of meningococcal infection, *N. meningitidis* must avoid recognition and killing by the immune system. However, compared to other bacteria, it is not very good at adapting through transcriptional control of gene expression. Yet, meningococcus has evolved a highly dynamic genome that allows rapid adaptation by the continuous generation of a surplus of genetic variants. Therefore, meningococcal populations are not clonal. The adaptive capacity of *N. meningitidis* relies on phase variation, antigenic variation, natural competence for transformation and a reduced repertoire of genes involved in DNA repair.

2.8.1. Transcriptional control of gene expression

Commonly studied bacteria must adapt to changing environments and have therefore developed tools to sense and respond to environmental signals, in particular by differentially regulating the expression of sets of target genes. Examples include σ factors, which are subunits of the RNA polymerase that are activated by specific environmental stresses (Paget, 2015), and two-component regulatory systems, that usually function through a membrane-bound histidine kinase sensor protein and a response regulator protein (Zschiedrich et al., 2016). The model bacterium *Escherichia coli* K-12 for instance, with a genome of 4.6 Mb and 4,288 genes in total, possesses 7 σ factors and approximately 30 two-component regulatory systems (Blattner et al., 1997). In contrast, *N. meningitidis* has a fairly small genome of 2.2 Mb and 2,065 genes in total, and possesses only 3 σ factors and 5 putative two-component regulatory systems, some of which with potentially redundant functions (Parkhill et al., 2000; Tettelin et al., 2000). This probably reflects the relative stability of meningococcus single natural habitat (Davidsen and Tonjum, 2006).

Recently, three RNA thermosensors located in the 5' untranslated region of meningococcal genes were found. As temperature increases, which occurs during infection, these RNA thermosensors upregulate the expression of genes involved in capsule biosynthesis, expression of the factor H binding protein and sialylation of the LOS (Loh et al., 2013).

2.8.2. Phase and antigenic variation

Phase variation is a mechanism that leads to an on/off switching of a gene product. It is present in many bacteria (Moxon et al., 1994). At the molecular level, it relies on the presence of short repeat sequences in the genome. Addition or deletion of repeat units in the coding or promoter regions of a gene, usually due to slipped-strand mispairing during DNA replication or DNA repair, can ultimately change the transcriptional or translational state of that gene in an on/off fashion (Fig. 6A).

Antigenic variation is the process by which functionally conserved genes can produce a range of antigenic variants within a population (Borst, 1991). It is used by numerous pathogens to modulate the antigenic properties of surface components and evade the host immune system (Deitsch et al., 2009). One of the best-characterized examples of antigenic variation are the type IV pili of *N. meningitidis*. Type IV pili consist of a polymeric assembly of thousands of subunits called pilins (see section **3.**). The *pilE* gene, which codes for the major pilin PilE, exists as a single copy in the meningococcal genome. However, recombination events with several silent coding sequences called *pilS* cassettes, that are partially homologous to the 3' coding sequence of *pilE*, result in high variability of the C-terminal part of the PilE protein (Fig. 6B, and see section **3.3.3.**).

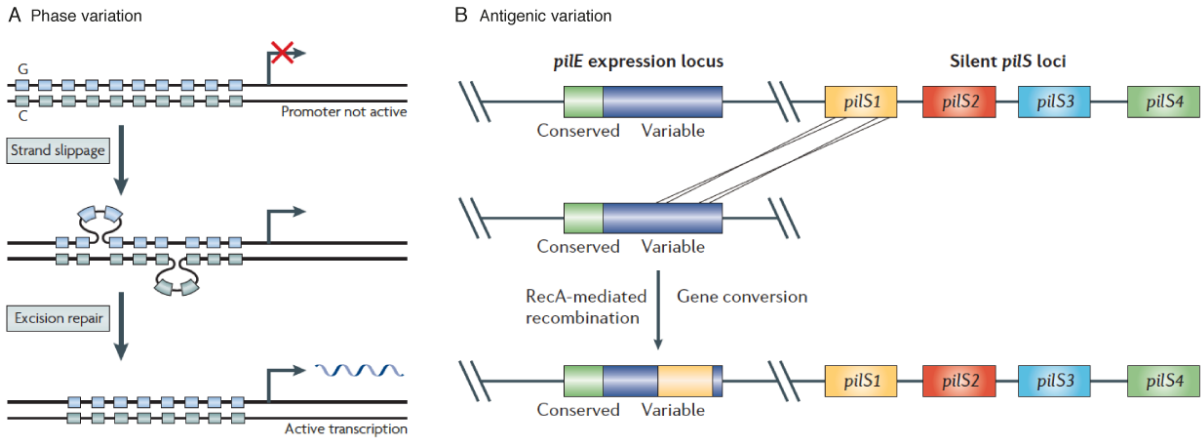

Figure 6 | Mechanisms of phase and antigenic variation used by *N. meningitidis*. (A) Example of transcriptional control of gene expression by phase variation. Here the promoter region contains multiple short repeat elements that can be deleted during DNA replication or repair due to slipped-strand mispairing, switching the gene from an off phase to an on phase. Adapted from (Deitsch et al., 2009). **(B)** Example of the mechanism of antigenic variation of the *pilE* gene coding for the major pilin in *N. meningitidis*. Silent partial pilin genes, or *pilS*, can recombine with the variable region of *pilE* via the RecA recombinase, resulting in partial pilin gene conversion. Reproduced from (Davidsen and Tonjum, 2006). (Also see **Credits** section.)

In *E. coli*, less than 10 genes are subject to phase and antigenic variation. In *N. meningitidis* there are more than a hundred (Davidsen and Tonjum, 2006), which mostly code for surface structures. In particular, several virulence factors other than type IV pili are regulated by phase and antigenic variation, such as the LOS, the capsule, and several outer membrane proteins and adhesins (see sections **2.1.** to **2.7.**) (Hammerschmidt et al., 1996; Jennings et al., 1999; Jonsson et al., 1991; Lewis et al., 1999; Martin et al., 2003; Sarkari et al., 1994; Segal et al., 1986; Stern and Meyer, 1987; van der Ende et al., 1995).

2.8.3. Natural competence for transformation

Transformation is the ability of a bacterium to uptake exogenous DNA and subsequently recombine it into its own chromosome (Chen and Dubnau, 2004). Natural competence for transformation exists in several monoderm and diderm bacteria. While it is subject to regulation in *Bacillus subtilis*, *Streptococcus pneumoniae* or *Haemophilus influenzae* (Havarstein et al., 1995; MacFadyen et al., 2001; Singh and Pitale, 1968), it is constitutively active in *N. gonorrhoeae* and *N. meningitidis* (Davidsen and Tonjum, 2006; Jyssum and Lie, 1965; Sparling, 1966).

Transformation in *N. gonorrhoeae* and *N. meningitidis* depends on the expression of type IV pili (see section **3.2.**), on the presence of the minor pilin ComP, on homologous recombination by the RecA recombinase and on the presence of 10-bp sequences in the exogenous DNA called DNA uptake sequences (DUS) (Biswas et al., 1977; Elkins et al., 1991; Graves et al., 1982; Koomey and Falkow, 1987). Approximately 1,900 DUS exist in gonococcal and meningococcal genomes (Davidsen and Tonjum, 2006; Parkhill et al., 2000; Tettelin et al., 2000), which explains why gonococcus and meningococcus preferentially uptake DNA from their own genus. Transfer of DNA by transformation between gonococcal and meningococcal strains is very efficient and can occur at frequencies of 10^{-3} to 10^{-1} per cell (Kroll et al., 1998).

Natural competence for transformation is associated with the acquisition of antibiotic resistance genes (Spratt et al., 1992), but is also believed to participate to genome maintenance by restoring damaged genes (Davidsen and Tonjum, 2006). Over the last few years, a new type of *N. meningitidis* has emerged as a new cause of genital infections. Interestingly, it has presumably acquired its ability to colonize the human genital tract by exchange of DNA with *N. gonorrhoeae*. In that case, uptake of DNA has resulted in a loss of the

polysccharide capsule and acquisition of a set of genes allowing anaerobic growth (Tzeng et al., 2017). This is a very striking example of the fluidity of the meningococcal genome and of how genome instability can impact meningococcal virulence.

2.8.4. DNA-repair systems

Like other organisms, bacterial cells must cope with DNA damage that results from both normal intracellular metabolic activity, that generates reactive oxygen species harmful to DNA, and from environmental stresses. Inability to repair lesions to the DNA can be lethal, but can also generate mutations that are beneficial to the cell. In *E. coli*, a rich repertoire of genes ensures diverse and redundant DNA-repair mechanisms, which allows efficient genome maintenance and minimal genome variation. Although homologues of these genes are found in *N. meningitidis*, this repertoire is overall reduced (Davidsen and Tonjum, 2006), and lack of robustness in the DNA-repair pathways is likely to contribute to the high variability of meningococcal genome.

2.9. Reference strain 8013

In this study, we used the reference strain 8013 (or 2C4.3). It is a serogroup C capsulated clinical isolate that expresses type IV pili, but not Opa or Opc adhesins. Due to genome plasticity, bacterial cultures consist of genetically diverse populations. This is an important experimental aspect because it can make mutagenesis more challenging, and because it brings overall variability to the experiments.

3. Type IV pili: multi-function organelles of *Neisseria meningitidis*

Type IV pili are widespread prokaryotic filamentous organelles. In the particular case of bacterial pathogens, they are key virulence factors. In this chapter, I will describe the general properties of type IV pili and related organelles in prokaryotes and discuss how type IV pili contribute to virulence in meningococcus.

3.1. Type IV pili and related organelles in bacteria and archaea

Type IV pili and type IV pili-like fibers, collectively called type IV filaments (Berry and Pelicic, 2015), are filamentous organelles, mostly surface-exposed, that are found both in monoderm and diderm bacteria, including human pathogens, as well as in archaea. Type IV filaments include proper type IV pili (T4P, Fig. 7), the type II secretion system (T2SS) and the archaellum (Fig. 7).

T4P

Homologs of genes coding for components of the type IV piliation system are found in all phyla of bacteria, and in all but one phylum of archaea, representing overall more than 2,000 prokaryotic species (Berry and Pelicic, 2015) (see sections **3.1.2.** and **3.1.3.**). T4P are subdivided into type IVa and type IVb pili according to the sequence of the type of major pilin that is expressed (detailed in section **3.1.2.**). T4P support a wide range of functions in prokaryotes, including motility, uptake of exogenous DNA, cell-cell interactions or adhesion to biotic and abiotic surfaces (detailed in sections **3.2.** and **3.3.**).

T2SS

Many pathogenic and non-pathogenic bacteria use a T2SS to secret folded (or partially folded) proteins in the extracellular milieu. T2SS-secreted proteins include enzymes that support bacterial growth and survival, as in *Pseudomonas aeruginosa* or *Klebsiella pneumoniae*, but also the cholera toxin of *Vibrio cholerae* (see (Nivaskumar and Francetic, 2014) for a review).

Archaellum

The archaellum is a highly-conserved motility structure found in archaea (Fig. 7). Due to its resemblance to bacterial flagella in electron microscopy and its role as a swimming device, it was first designated as the archaeal flagellum. However, subsequent studies demonstrated that it has structural and sequence similarities with T4P, and not with bacterial flagella (see (Albers and Jarrell, 2015) for a review). Interestingly though, unlike T4P, the archaellum was shown to rotate (Shahapure et al., 2014). Therefore, it does functionally resemble a bacterial flagellum.

Although T4P, the T2SS and the archaellum are highly diverse in structure and function, they share important core properties of type IV filaments.

3.1.1. Morphologies of type IV filaments

T4P are characterized by their hair-like morphology (Fig. 7A), as observed by electron microscopy (Ottow, 1975). Individual fibers are typically 5 to 9 nm wide. Type IVa pili (T4aP), for example in *Neisseria*, have an average diameter of 6 nm (Fig. 7B and C) (Kolappan et al., 2016). Type IVb pili (T4bP), for instance the toxin co-regulated pilus of *Vibrio cholerae*, has a diameter of 9 nm (Li et al., 2012). Although very thin, their length can reach several micrometers, the most extreme example being the plasmid-encoded longus

pilus of enterotoxigenic *E. coli* that can measure up to 20 µm (Giron et al., 1997). T4P fibers can be highly flexible and associate laterally to form bundles (Berry and Pelicic, 2015; Biais et al., 2010; Biais et al., 2008; Craig et al., 2004). The archaellum, a type IV filament expressed in archaea, also has a hair-like morphology but is wider (approximately 10 nm, Fig. 7D and E) (Albers and Jarrell, 2015; Poweleit et al., 2016).

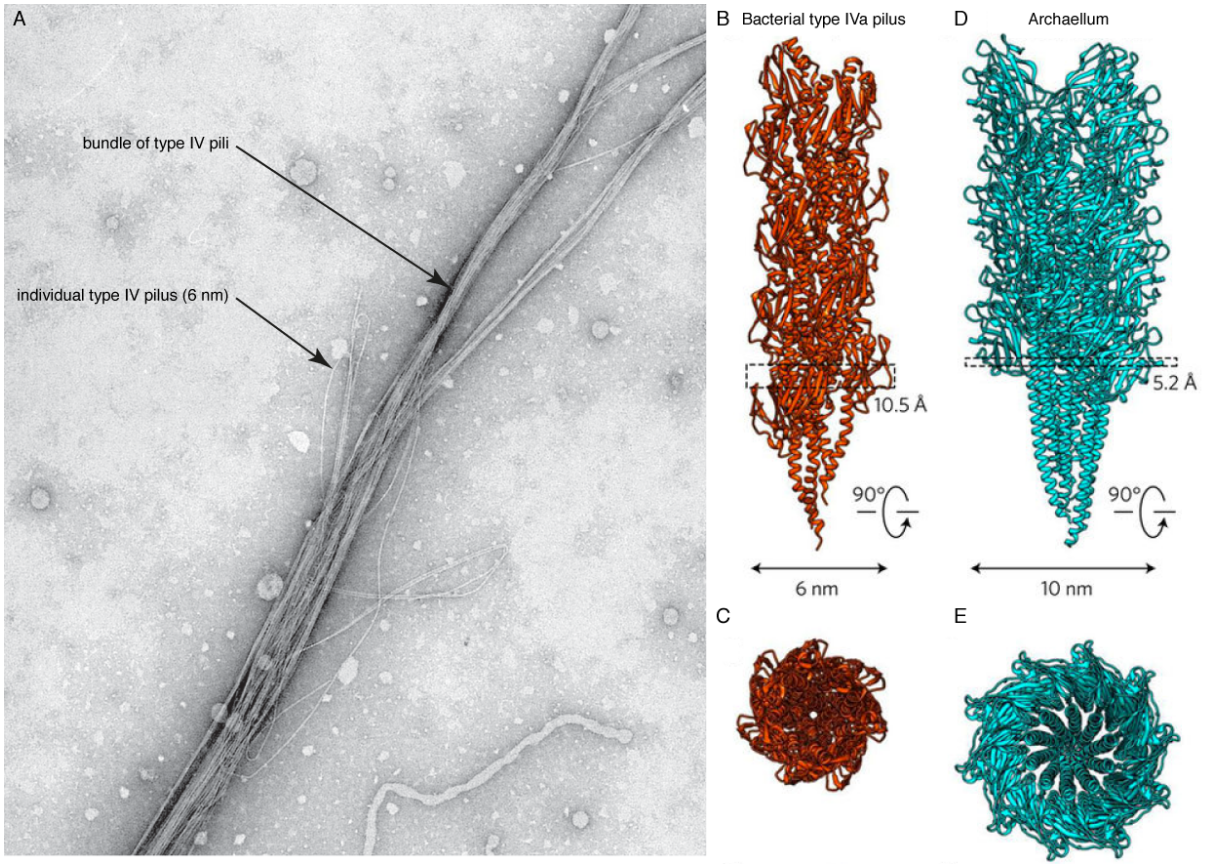

Figure 7 | Morphology of type IV filaments in bacteria and archaea. (A) Transmission electron micrograph of negatively stained type IV pili from *N. meningitidis* showing individual pili, which are 6 nm wide, as well as pili bundles. Adapted from (Berry and Pelicic, 2015). **(B,C)** Side and top views of the crystal structure of the type IVa pilus from *N. gonorrhoeae*. **(D,E)** Side and top views of the crystal structure of the archaellum from *Methanospirillum hungatei*. Adapted from (Poweleit et al., 2016) Both type IV filaments are helical assemblies of a type IV pilin protein. (Also see **Credits** section.)

In contrast, the T2SS in diderm bacteria (Nivaskumar and Francetic, 2014) and most of the competence pili in monoderm bacteria (Chen and Dubnau, 2004; Chen et al., 2006) assemble filaments, called pseudopili, that only span the periplasmic space and are thus too short to be seen by electron microscopy. One exception to this rule is the competence pseudopilus of the monoderm bacterium *Streptococcus pneumoniae*, that has been found to assemble long extracellular fibers (Balaban et al., 2014; Laurenceau et al., 2013). In the case of the T2SS, the extension of the pseudopilus is thought to act as a piston or as an Archimedes' screw that pushes the secreted protein through the periplasm prior to translocation across the outer membrane via the secretin (see (Nivaskumar and Francetic, 2014) for a review). Interestingly, bacteria that artificially overexpress the major pseudopilin subunit of the T2SS assemble long extracellular filaments, or hyper-pseudopili, that closely resemble T4P fibers with a diameter of 6,5 nm (Kohler et al., 2004; Sauvonnet et al., 2000; Vignon et al., 2003).

3.1.2. Type IV pilin proteins and the prepilin peptidase

At the molecular level, the key common feature of type IV filaments is that they are homopolymeric assemblies of proteins called type IV pilins. Type IV pilins are expressed as prepilins that need to undergo maturation steps prior to assembly into fibers. Type IV prepilins are characterized by a highly conserved and unique N-terminal signal sequence called class III signal sequence (Szabo et al., 2007) followed by a conserved stretch of hydrophobic amino acids that form a transmembrane hydrophobic α-helix (Giltner et al., 2012) (Fig. 8A). In diderm bacteria, class I and II signal sequences are required for maturation of commonly secreted proteins and lipoproteins, respectively. After translocation of the protein across the inner membrane by the Sec translocon, signal sequences are recognized by several peptidases that catalyze the cleavage of the leader peptide in the periplasm. The class III signal sequence of type IV prepilins is recognized and cleaved by a single peptidase, called the prepilin peptidase (PilD in the case of *Neisseria* spp.). Following cleavage of the leader peptide after a conserved glycine residue on the cytoplasmic side of the inner membrane, the prepilin peptidase can additionally methylate the next residue of type IVa prepilins. Type IVa prepilins have typically shorter class III signal sequences (less than 10 residues) than type IVb prepilins (15 to 30 residues) (Fig. 8).

Mature type IV pilins have molecular weights between 15 and 20 kDa. Apart from their signature N-terminus, they have quite divergent sequences. However, they share a common structural fold with a N-terminal α-helix and a C-terminal globular head (Fig. 8B and C), except in *Geobacter* spp. were the C-terminal domain is almost absent (Reardon and Mueller, 2013). The N-terminal α-helix is divided in two domains: α1-N is highly hydrophobic and is embedded in the cytoplasmic membrane prior to assembly, later constituting the inner core of the assembled fiber, while α1-C is amphipathic and packs against the head domain (Giltner et al., 2012). The C-terminal globular domain, composed of 4 to 7 stranded β-sheets, is the most divergent part of type IV pilins. Except in T2SS pseudopilins, loops connecting the N-terminal α-helix to the C-terminal domain, loops between consecutive β-sheets and the C-terminal loop are hypervariable. The latter, called the D region, is the most important one. In most type IV pilins, the D-region is a loop formed by a disulfide bond between two highly conserved C-terminal cysteines residues (Fig. 8B). The type IV pilin from the ovine pathogen *Dichelobacter nodosus* is the only one that lacks these two cysteines, however the D-region is structurally conserved through a network of hydrogen bonds (Hartung et al., 2011). The D-region can greatly vary in length and in secondary structures, even among strains of the same species (see section **3.3.3.**). It has an important structural role though, as perturbation of the formation of the disulfide bond between the two C-terminal cysteines inhibits assembly of the pilus fiber. In *N. meningitidis*, the structure of the D-region of the minor pilin PilX was proposed to function as a hook that promotes pilus-pilus lateral interactions involved in bacterial aggregation (Helaine et al., 2005).

Another level of diversity in type IV pilins originates from differences in post-translational modifications, especially in the D-region. The most frequent post-translational modification of type IV pilins is O-glycosylation. In bacteria, it is not required for pilus assembly but can be essential to some pilus functions or for evasion to the immune system (Allison et al., 2015; Gault et al., 2015). Oppositely, in archaea, pilin glycosylation is essential to pilus assembly (Chaban et al., 2006; VanDyke et al., 2008; Yurist-Doutsch et al., 2008). Other modifications include the addition of phosphoethanolamine, phosphorylcholine or phosphoglycerol groups to serine residues (Chamot-Rooke et al., 2011; Forest et al., 1999; Gault et al., 2013; Hegge et al., 2004).

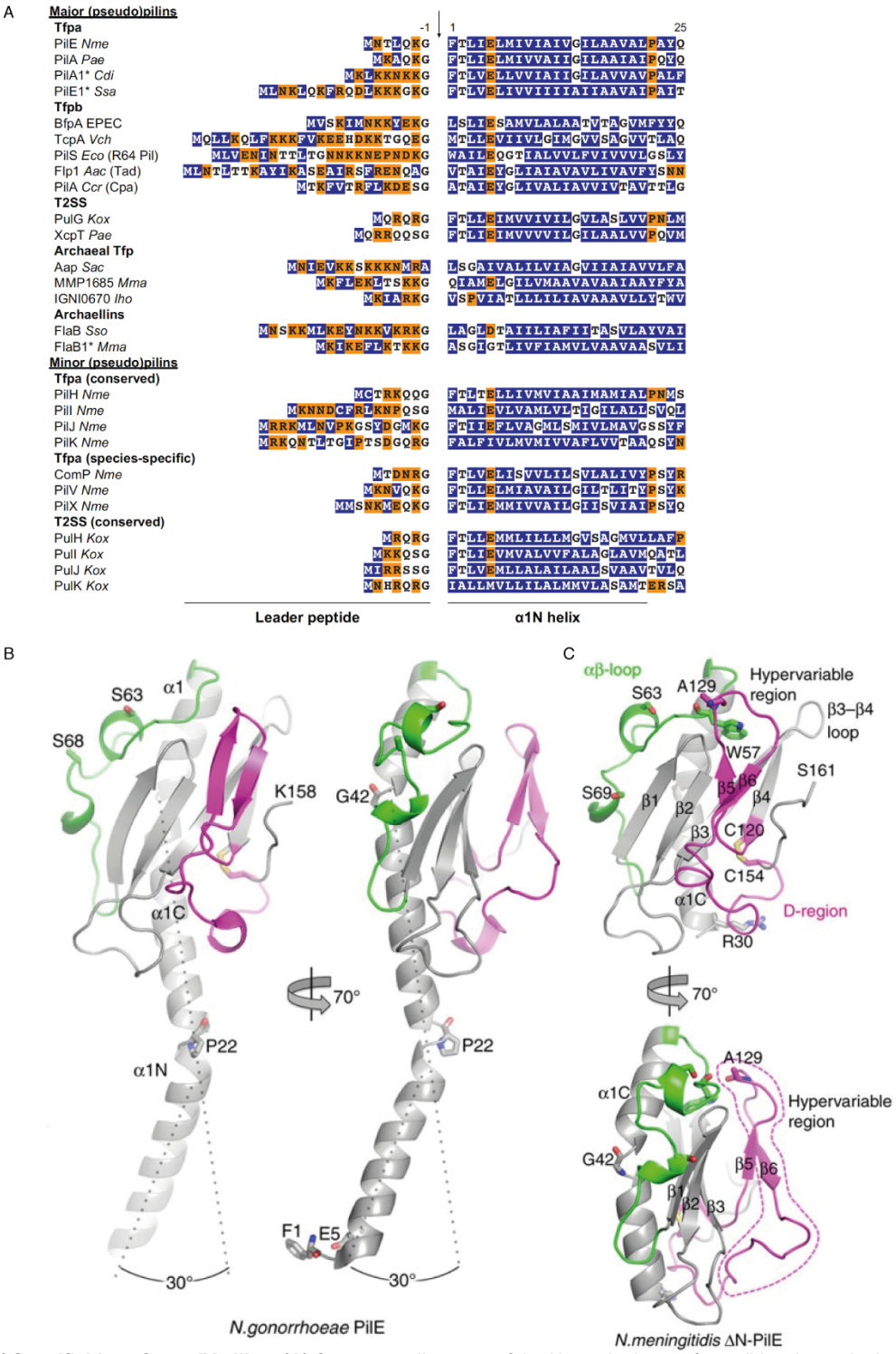

Figure 8 | Specificities of type IV pilins. (A) Sequence alignment of the N-terminal part of type IV major and minor prepilins (or pseudoprepilins) showing the class III signal sequence with the conserved glycine residue (-1) recognized by the prepilin peptidase and the hydrophobic α1-N helix. Tfpa, type IVa pilus; Tfpb, type IVb pilus; T2SS, type II secretion system; *Nme*, *Neisseria meningitidis*; *Pae*, *Pseudomonas aeruginosa*; *Cdi*, *Clostridium difficile*; *Ssa*, *Streptococcus sanguinis*; *Vch*, *Vibrio cholerae*; *Eco*, *Escherichia coli*; *Aac*, *Actinobacillus actinomycetemcomitans*; *Ccr*, *Caulobacter crescentus*; *Kox*, *Klebsiella oxytoca* (bacteria); *Sac*, *Sulfolobus acidocaldarius*; *Mma*, *Methanococcus maripaludis*; *Iho*, *Ignicoccus hospitalis*; *Sso*, *Sulfolobus solfataricus* (archaea). Adapted from (Berry and Pelicic, 2015) **(B)** Crystal structure of the mature major pilin PilE from *N. gonorrhoeae* showing the typical "lollipop" architecture with the N-terminally methylated α helix and the globular head domain connected by the αβ loop (green). The D-region is shown in magenta. **(C)** Crystal structure of the C-terminal domain of the mature major pilin PilE from *N. meningitidis* showing the same typical arrangement of stranded β sheets and the D-region. Adapted from (Kolappan et al., 2016). (Also see **Credits** section.)

3.1.3. Major pilin and minor pilins

Type IV filaments are mainly composed of copies of one type IV pilin which is thus called the major pilin (or the major pseudopilin in the case of the T2SS). It is called PilE in meningococcus and gonococcus.

Other type IV pilin proteins, called minor pilins (or minor pseudopilins), are expressed in fewer quantities. Four of them, PilH, I, J and K in meningococcus (which are also called pseudopilins in that case), are highly conserved and are essential for piliation (Carbonnelle et al., 2006). Although their role in T4P assembly remains undetermined, their homologs in the T2SS were shown to prime the assembly of the pseudopilus (Cisneros et al., 2012) and are therefore believed to sit at the tip of T4P fibers (Fig. 9).

In meningococcus, three minor pilins, PilV, PilX and ComP, are associated to T4P functions. Minor pilins share some degree of structural homology with PilE. Mutant bacteria that do not express PilV or PilX still express T4P but lose specific T4P-associated functions. Therefore, it has been commonly admitted that minor pilins are assembled in the pilus fiber, although in lower copy numbers than the major pilin, and that they carry specific T4P functions. PilV is thought to mediate signaling within the host cell (Bernard et al., 2014; Coureuil et al., 2010; Maissa et al., 2017; Mikaty et al., 2009; Soyer et al., 2014) (see section **4**.), while PilX is thought to promote bacterial aggregation (Helaine et al., 2005). However, a recent study demonstrated that PilV and PilX can exert their functions from the periplasm. There, they regulate the amount of T4P expressed, thereby indirectly controlling T4P-associated functions (Imhaus and Dumenil, 2014). ComP is required for the uptake of DNA during transformation (Wolfgang et al., 1999). Meningococcal ComP directly binds DNA (Cehovin et al., 2013) but its localization and mode of action are undetermined, so it could arguably function in the periplasm similarly to PilV and PilX.

3.1.4. Assembly machinery of type IV filaments

Homopolymeric assembly of mature type IV pilins into helical fibers requires a set of 10 to 18 proteins, according to species. The complete architectures of type IVa and type IVb pili machineries has recently been solved by electron cryotomography in the diderm bacteria *Myxococcus xanthus* (Chang et al., 2016) and *Vibrio cholerae* (Chang et al., 2017) (Fig. 9A). The exact mechanism by which pilin monomers are assembled into a helix is not fully understood. However, extraction of the pilin from the inner membrane requires energy provided by the cytoplasmic protein PilF. PilF is a highly-conserved AAA-ATPase that forms hexamers and interacts with the T4P machinery intermittently. ATP hydrolysis by PilF induces conformational changes in an inner membrane protein, PilG, that acts as the platform for pilus assembly (Goosens et al., 2017). Conformational changes in PilG are thought to result in the addition of pilin monomers to the nascent pilus fiber in a rotational step-wise fashion (McCallum et al., 2017; Nivaskumar et al., 2014). PilF and PilG are likely recruited to a pre-assembled multimeric PilMNOP complex (Chang et al., 2017; Chang et al., 2016; Goosens et al., 2017). A recent study proposed a new model where the core complex PilNO would recruit pilin monomers to the PilG platform, then PilM, that would interact with PilF in the cytoplasm, and then PilP that would stabilize the PilNO complex (Goosens et al., 2017). PilE, PilD, PilF, PilG, and PilMNOP are all essential to pilus biogenesis, as exemplified in *Neisseria* spp. where deletion of any of these proteins prevents pilus assembly (Carbonnelle et al., 2006).

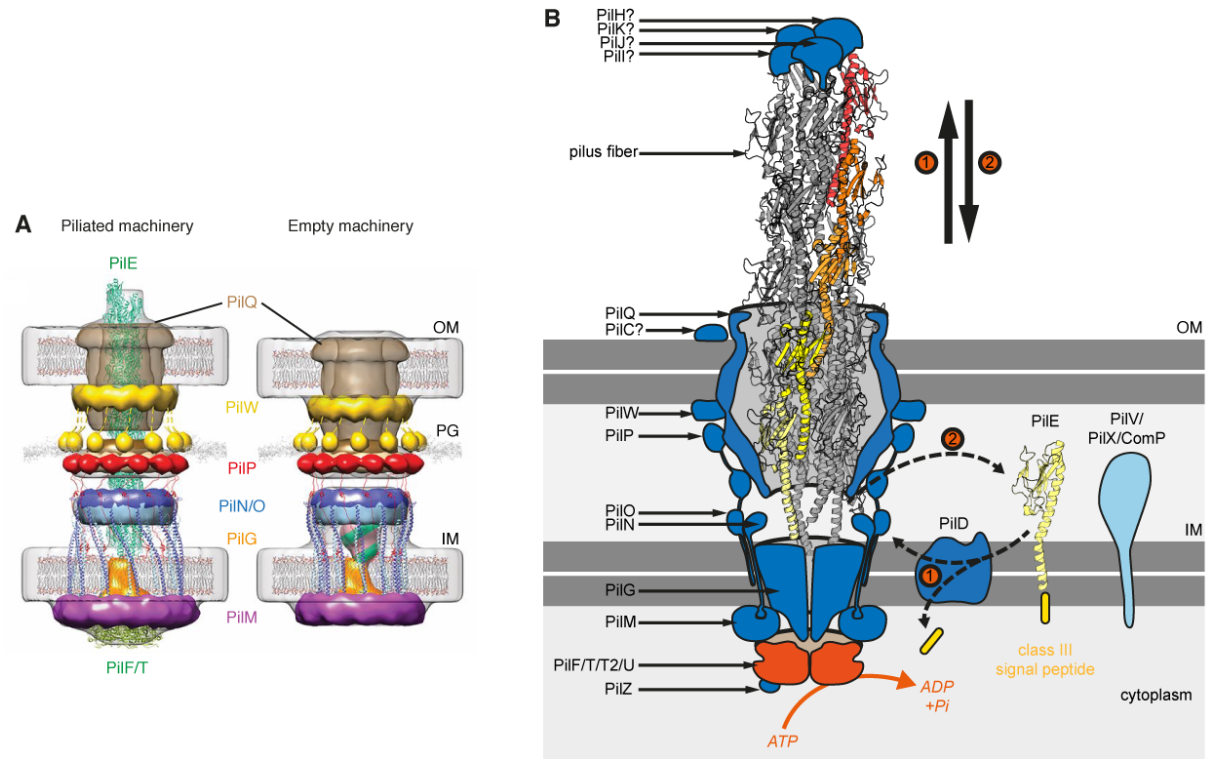

Figure 9 | The assembly machinery of type IV pili. (A) Model of the T4P machinery in *M. xanthus* based on subtomogram averaging of electron cryotomograms and crystal structures of individual components. The model shows that the whole machinery undergoes massive conformational changes upon assembly of T4P fibers under the action of the PilF ATPase (the labels correspond to the names of the homolog proteins in *Neisseria* spp.). Adapted from (Chang et al., 2016) (see **Credits** section). **(B)** The type IV pilus fiber in meningococcus is a helical assembly of copies of the mature major pilin, PilE. The prepilin is cleaved by the prepilin peptidase, PilD, prior to assembly that requires energy from the PilF ATPase (1). ATP hydrolysis by PilF induces conformational changes in the assembly platform protein PilG where new PilE monomers are added. The PilMNOP complex is essential to pilus assembly. The pilus fiber exits the outer membrane via the PilQ secretin channel that is stabilized by PilW. The pseudopilins PilHIJK are thought to initiate pilus assembly and to localize at the tip of the pilus. ATP hydrolysis by the PilT ATPase powers pilus retraction (2). The PilT2 ATPase regulates pilus retraction speed. The function of the PilU ATPase is undetermined. The pilus associated non-pilin protein PilC is described as an adhesin, although its localization is controversial. The function of PilZ is unknown. Other type IV pilins called minor pilins, PilV, PilX and ComP, are processed as PilE but function in the periplasm by regulating the number of type IV pili that are assembled. The major pilin PilE is colored in shades of yellow to red to highlight the helical structure of the pilus fiber.

Recently, Berry and Pelicic found that homologs of PilD, PilF and PilG exist in all phyla of bacteria, and in all but one phylum of archaea (over 2,000 prokaryotic species in total). However, only 1,800 species possess homologs of the canonical type IV prepilins, suggesting the existence of type IV filaments that assemble non-canonical type IV pilins (Berry and Pelicic, 2015).

In addition to PilF, some species express other cytoplasmic ATPases that are not essential to pilus biogenesis but modulate T4P functions (Brown et al., 2010). For example, the PilT ATPase is responsible for depolymerization, or retraction, of the pilus fiber (Brown et al., 2010; Maier et al., 2002) (Fig. 9). A single PilT motor can generate forces of up to 100 pN, powering the retraction of T4P fibers at a speed of up to 1 μm per second (Maier et al., 2002; Merz et al., 2000). T4P retraction allows a specific kind of surface motility known as "twitching" motility (Merz et al., 2000). In *Neisseria* spp., the speed of pilus retraction is further modulated by the PilT2 ATPase (Brown et al., 2010; Kurre et al., 2012). It is still unknown what is the function of the fourth ATPase, PilU.

In diderm bacteria, type IV filaments must cross the outer membrane through secretin proteins, which are widely conserved between T2SS and T4P and also share similarities with secretins of the type III secretion system (T3SS) (Tosi et al., 2014). In *Neisseria*, the secretin is called PilQ. 12 to 14 PilQ monomers form a

channel in the outer membrane (Fig. 9) (Berry et al., 2012; Collins et al., 2001; Collins et al., 2004; Jain et al., 2011). PilQ interacts with PilP, thereby forming a trans-periplasmic channel for T4P (Balasingham et al., 2007; Berry et al., 2012), and is stabilized at the outer membrane by the protein PilW (Carbonnelle et al., 2005; Jain et al., 2011). PilQ is not essential for pilus biogenesis, as overproduction of pili by deletion of the retraction ATPase PilT in a Δ*pilQ* background results in the production of T4P fibers that remain trapped in the periplasm (Carbonnelle et al., 2006; Goosens et al., 2017). In monoderm bacteria, only homologs of inner membrane proteins are found and T4P fibers are surface-exposed as soon as they are assembled. Therefore, the inner membrane components of the T4P assembly machinery in diderm bacteria can be considered the minimal unit for pilus assembly (Goosens et al., 2017).

In some bacteria, including *Neisseria* spp., PilZ and PilY1/PilC are other accessory proteins involved in pilus biogenesis (Alm et al., 1996; Brown et al., 2010). PilZ interacts with PilF (Georgiadou et al., 2012), but its function remains unknown. The specific case of PilY1/PilC, which is described as an adhesin, will be discussed in section **3.3.1**.

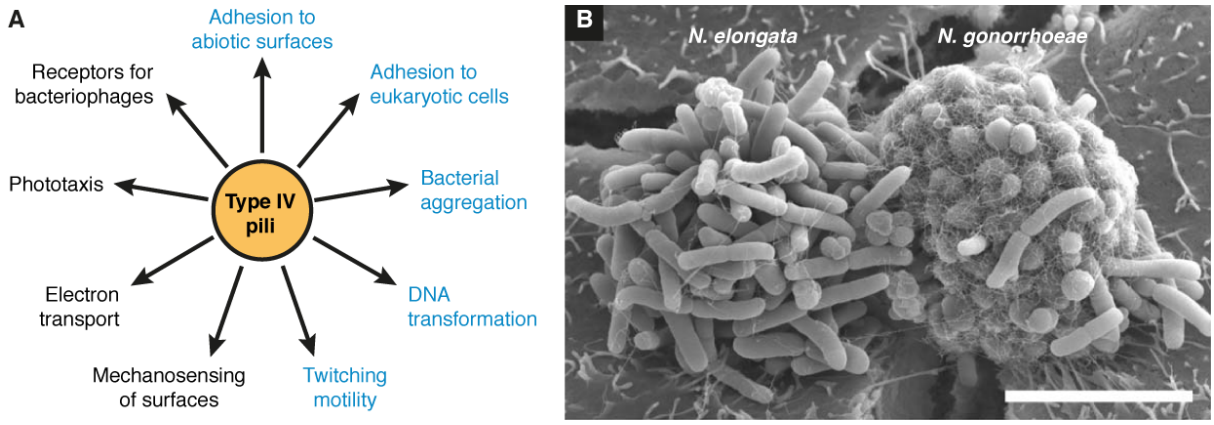

Figure 10 | Biological functions of type IV pili in prokaryotes. (A) T4P mediate a wide range of functions in prokaryotes. T4P-mediated functions found in *N. meningitidis* are indicated with blue letters. **(B)** Scanning electron micrograph of bacterial aggregates formed by the commensal *N. elongata* (rods, left) and the pathogen *N. gonorrhoeae* (diplococci, right) after 3h of co-culture on human epithelial cells. In this study, type IV pili from *N. elongata* were shown to promote genetic exchange between the two species. Scale bar, 5 μm. Adapted from (Higashi et al., 2011) (see **Credits** section).

3.2. Diverse functions of type IV pili in prokaryotes

Like other pili, the most important feature of T4P is that they are the outermost structure in contact with the environment. As such, they have evolved the ability to bind a wide variety of substrates and are typically used by bacteria to attach to surfaces. Attachment to abiotic surfaces like metal, glass or plastics can be a major challenge to the maintenance of sterility in medical facilities. Colonization of biotic surfaces, such as host cells or extracellular matrices, make T4P key colonization factors in commensal species and major virulence factors in pathogenic ones (Berry and Pelicic, 2015).

T4P also commonly mediate bacteria-bacteria interactions and promote the formation of microcolonies or bacterial aggregates, on surfaces or in suspension (Chamot-Rooke et al., 2011; Imhaus and Dumenil, 2014; Kirn et al., 2000) (Fig. 10). The ability to form microcolonies can be important for survival, for instance by promoting biofilm formation (Alcantar-Curiel et al., 2013; Dunger et al., 2014; Pohlschroder and Esquivel, 2015; Wang et al., 2013), or for the efficient transfer of DNA between cells (Chimileski et al., 2014; Yoshida et al., 1999). In *N. meningitidis*, it is still debated whether it is the major pilin PilE (Imhaus and Dumenil,

2014) or the minor pilin PilX (Helaine et al., 2005; Helaine et al., 2007) that mediates bacterial aggregation. Yet, posttranslational modification of PilE with a phosphoglycerol upon contact with host cells was shown to disfavor T4P-T4P interactions, thereby promoting bacterial dissemination (Chamot-Rooke et al., 2011). Regulation of bacterial aggregation in meningococcus could therefore contribute to transmission between people and traversal of the nasopharyngeal barrier (see section **1.2.**).

In species possessing the PilT ATPase, T4P allow the exploration of surfaces via twitching motility. The characteristic of twitching motility is that the motile cells exhibit apparently non-directional, jerky movements (Henrichsen et al., 1972). This irregular movement is due to the differential retraction of a subset of T4P fibers while other fibers still adhere to the surface, in a tug-of-war fashion (Marathe et al., 2014; Merz et al., 2000).

As mentioned earlier, T4P also mediate the uptake of exogenous DNA during natural transformation. Binding to DNA occurs either directly through the major pilin (van Schaik et al., 2005) or through a minor pilin (Cehovin et al., 2013). Uptake of exogenous DNA can be species- or genus-specific, like in *Neisseria*, or not, like in *Vibrio cholerae* (Matthey and Blokesch, 2016). Extracellular DNA can serve as a source of genetic information, as food or as template for DNA-repair (Chen and Dubnau, 2004).

Other genus- or species-specific T4P-associated functions include binding to bacterial viruses in *P. aeruginosa* and *C. crescentus* (Bradley, 1972; Skerker and Shapiro, 2000), reduction of metal and sulphur by transport of electrons along the pili fibers towards extracellular electron acceptors in members of the genus *Geobacter* (Boesen and Nielsen, 2013; Tan et al., 2017; Vargas et al., 2013), negative phototaxis (the movement of a cell away from a light source) in the cyanobacteria *Synechocystis* spp. (Nakane and Nishizaka, 2017), and mechanoperception of surface properties by the pilus associated protein PilY1 in *P. aeruginosa* (Siryaporn et al., 2014).

3.3. Role of type IV pili as virulence factors in *Neisseria meningitidis*

3.3.1. Major adhesins

The mechanism by which T4P bind the host cell surface is controversial. Nevertheless, on-piliated bacteria are unable to adhere to host cells *in vitro* (Lecuyer et al., 2012; Miller et al., 2014; Nassif et al., 1993) as well as *in vivo* (Join-Lambert et al., 2013; Melican et al., 2013), demonstrating the role of T4P as the major adhesins of meningococcus. In other species, adhesive properties of T4P can be mediated directly by the major pilin, like BfpA in the bundle-forming pilus of enteropathogenic *E. coli* which binds N-acetyllactosamine on host cells via a lectin domain (Hyland et al., 2008). Alternatively, pilus-associated non-pilin proteins, such as the PilY1 protein in *P. aeruginosa*, can mediate adhesion to host cells (Heiniger et al., 2010). In this case, PilY1 contains an Arg-Gly-Asp (RGD) motif that binds human integrins in a calcium-dependent manner (Johnson et al., 2011). However, it is not clear whether PilY1 associates with T4P or with the bacterial surface (Nguyen et al., 2015; Siryaporn et al., 2014).

In *N. meningitidis*, several pilus-associated proteins were shown to be involved in adhesion to host cells. The minor pilin PilV, which might be assembled in the pilus fiber, was shown to bind to human CD46 (Kallstrom et al., 1997), β2-adrenergic receptor (Coureuil et al., 2010; Maissa et al., 2017) and CD147 (Bernard et al., 2014; Maissa et al., 2017). However, the finding that PilV functions in the periplasm challenges the very notion that the protein is surface-exposed and that it can bind to any of these receptors (Imhaus and Dumenil, 2014). PilC1, the ortholog of *P. aeruginosa* pilus-associated adhesin PilY1 in *Neisseria* spp., was also identified as an adhesin because a Δ*pilC1* mutant fails to adhere to human cells while still expressing T4P.

It is believed to be located at the tip of the pilus fiber (Asmat et al., 2014; Morand et al., 2001; Nassif et al., 1994; Rudel et al., 1995) and to allow adhesion via a release of calcium within the host cell (Asmat et al., 2014). Yet, the mode of action of PilC1 remains unclear. On the one hand, the protein could be associated with the bacterial surface rather than with the pilus tip, as suggested for *P. aeruginosa*. PilC proteins were also shown to regulate pilus retraction (Morand et al., 2004). In addition, deletion of both *pilC1* and its allelic variant *pilC2*, which is not an adhesin and does not exist in *P. aeruginosa*, prevents T4P assembly, suggesting that PilC1 is not an adhesin per se but indirectly modulates adhesion.

The meningococcal major pilin subunit, PilE, was also found to bind directly to human CD46 (Johansson et al., 2003; Kallstrom et al., 1997), although it is still controversial (Kirchner et al., 2005), as well as to the β2-adrenergic receptor and CD147 (Bernard et al., 2014; Coureuil et al., 2010). Recently, it was further shown that optimal adhesion of T4P to CD147 requires its hetero-oligomerization with the β2-adrenergic receptor at the plasma membrane via scaffolding by the protein α-actinin-4 (Maissa et al., 2017). Indeed, atomic force microscopy measurements of detachment forces of beads coated with purified pilins showed that it is easier to unbind PilE from the host cell plasma membrane when the formation of CD147/β2-adrenergic receptor clusters is impaired. The major pilin itself is thus a proper adhesin in *N. meningitidis*. Interestingly, T4P in *Neisseria* spp. are able to stretch under tension, thereby exposing hidden epitopes in PilE (Biais et al., 2010). In this case, the pilus diameter can be narrowed by 40%. This was recently supported by a 3D structure of the meningococcal pilus fiber resolved by cryo-electron microscopy, where a stretch of unstructured amino acids was found within the N-terminal α-helix of PilE, providing the whole pilus fiber with high flexibility (Kolappan et al., 2016). Conformational change of the pilus fiber was also found to be mediated by the minor pilin PilX and to regulate signaling within host cells (Brissac et al., 2012). In conclusion, it is still not very clear what explains the adhesive properties of T4P towards human cells.

3.3.2. Natural competence for transformation by DNA

In contrast to *P. aeruginosa* T4P (van Schaik et al., 2005), meningococcal pili do not seem to bind directly to DNA. Instead, it is the minor pilin ComP that acts as a receptor for DNA (Cehovin et al., 2013). DNA uptake is also strictly dependent on pilus retraction, as a Δ*pilT* deficient mutant is no longer competent for transformation (Wolfgang et al., 1998). The PilQ secretin, which is thought to be partially surface-exposed (Lieberman et al., 2015), was also shown to bind DNA (Assalkhou et al., 2007). In addition, a recent study in *N. gonorrhoeae* showed that pili fibers that are not surface-exposed still support uptake of exogenous DNA (Obergfell and Seifert, 2016), suggesting that the role of T4P in natural transformation could be indirect. For example, T4P fibers could allow opening of PilQ channels in the outer membrane and subsequent uptake of the DNA in the periplasm by the minor pilin ComP.

Again, even if the mechanism for DNA uptake is not clear, transformation in *Neisseria* is strictly dependent on the presence of T4P. Therefore, as a source of genetic variability in meningococcus, T4P-mediated natural competence for transformation is likely to contribute to virulence.

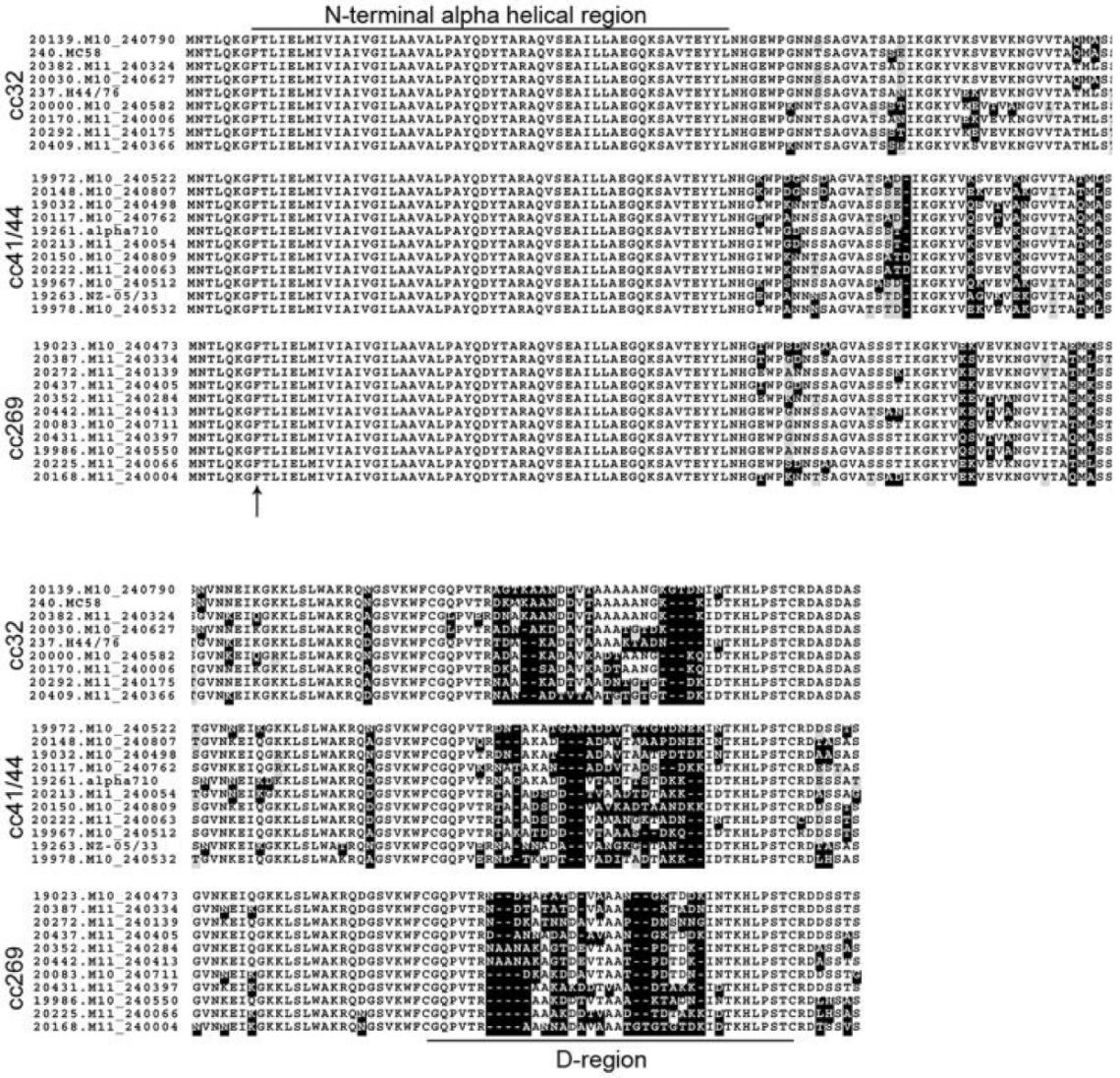

Figure 11 | Antigenic diversity in meningococcal major pilin. Amino acids sequence alignments of the major pilin in different clonal complexes (cc) of meningococcus, showing the high conservation of the N-terminal part of the protein, including the conserved site of clevage by PilD (denoted by an arrow) and the high variability in the C-terminal part due to antigenic variation (black boxed-residues). Importantly, the sequence of the major pilin can highly diverge even among different isolates from a same clonal complex. Adapted from (Wormann et al., 2014) (see **Credits** section).

3.3.3. Immune evasion

T4P in *N. meningitidis* have immunogenic properties, since antibodies directed against meningococcal pili can be found in human sera (Poolman et al., 1983). However, glycosylation of the major pilin PilE can shield the pilus fiber from immune recognition (Gault et al., 2015), and the *pilE* gene can undergo antigenic variation, which generates a wide diversity of T4P (Helm and Seifert, 2010) (Fig. 11 and see section **2.8.2.**). Pilin antigenic variation was shown to alter interactions with host cells (Miller et al., 2014; Nassif et al., 1993), and it is likely that it also helps avoiding recognition by the immune system.

3.3.4. Signaling within host cells and cell surface reorganization

An important aspect of the virulence mediated by meningococcal T4P is their ability to trigger or manipulate specific signaling pathways within host cells as well as cell surface reorganization, which are required for bacterial colonization. This is a central aspect of this thesis which will be discussed in the section **4** of this Introduction.

4. Crosstalk between *Neisseria meningitidis* and the human endothelial cell

As described earlier in this Introduction, a key aspect of meningococcal disease is the ability of *N. meningitidis* to interact with human endothelial cells. Upon adhesion, meningococci engage in a complex crosstalk with the host endothelial cell that involves the local remodeling of the host cell plasma membrane and the manipulation of intracellular signaling cascades that promote actin polymerization at the site of adhesion. In this chapter, I will describe these interactions and discuss their relevance in terms of meningococcal pathogenesis.

4.1. Plasma membrane remodeling and actin polymerization

In the late 90s, a seminal study on the interaction of pathogenic *Neisseria* with cultured epithelial cells demonstrated that gonococci and meningococci devoid of Opa and Opc adhesins but expressing T4P, elicit a reorganization of the F-actin cytoskeleton at the site of adhesion, showing that there is a response from the host cell to the colonization by gonococcus and meningococcus (Merz and So, 1997). The authors also noticed the accumulation of tyrosine-phosphorylated proteins underneath bacterial microcolonies, further suggesting that the host cell response involved the activation of intracellular signaling pathways.

Soon after, it was found that upon proliferation of *N. meningitidis* on the surface of cultured endothelial cells, there was a formation of microvilli-like protrusions at the site of bacterial adhesion (Eugene et al., 2002). These protrusions of plasma membrane were suggested to allow the internalization of bacteria, although it is not clear how the authors measured it and what experimental values are presented. Nevertheless, microvilli-like structures accumulated the membrane protein CD44, as well as F-actin and the ERM (ezrin/radixin/moesin) protein ezrin (Fig. 12). The whole structure was named the "cortical plaque" (Merz et al., 1999). Consistent with the role of ezrin as a regulator of microvilli biogenesis (Yonemura et al., 1999), the authors found that recruitment of ezrin via its interaction with CD44 was necessary to F-actin reorganization by meningococcus. Furthermore, they showed that actin polymerization at the site of bacterial adhesion was dependent on the activity of the small GTPases Rho and Cdc42, which are known regulators of actin polymerization (Ridley, 2006; Sit and Manser, 2011), but not on the activity of Rac1 which belongs to the same family of GTPases and is also involved in actin polymerization. The signaling pathway(s) involved in the activation of Rho and Cdc42, as well as Rho terminal effectors involved in actin polymerization, have not been identified so far.

Numerous studies went on identifying the remaining signaling cascade that supports actin polymerization after meningococcal adhesion to endothelial cells (Fig. 13). In particular, it is the phosphorylation of cortactin (or cortical actin-binding protein) by the protein kinase Src that is thought to be the main regulator of actin polymerization in plasma membrane protrusions (Hoffmann et al., 2001; Lambotin et al., 2005). Cortactin is a cytoplasmic protein that regulates cortical actin dynamics, directly or indirectly, via the actin-related protein (Arp)2/3 complex (Uruno et al., 2001; Weaver et al., 2002; Weaver et al., 2001). However, there has been no experimental evidence for the implication of Arp2/3 (or, as a matter of fact, of any other actin nucleator) in the actin polymerization induced by meningococcus so far.

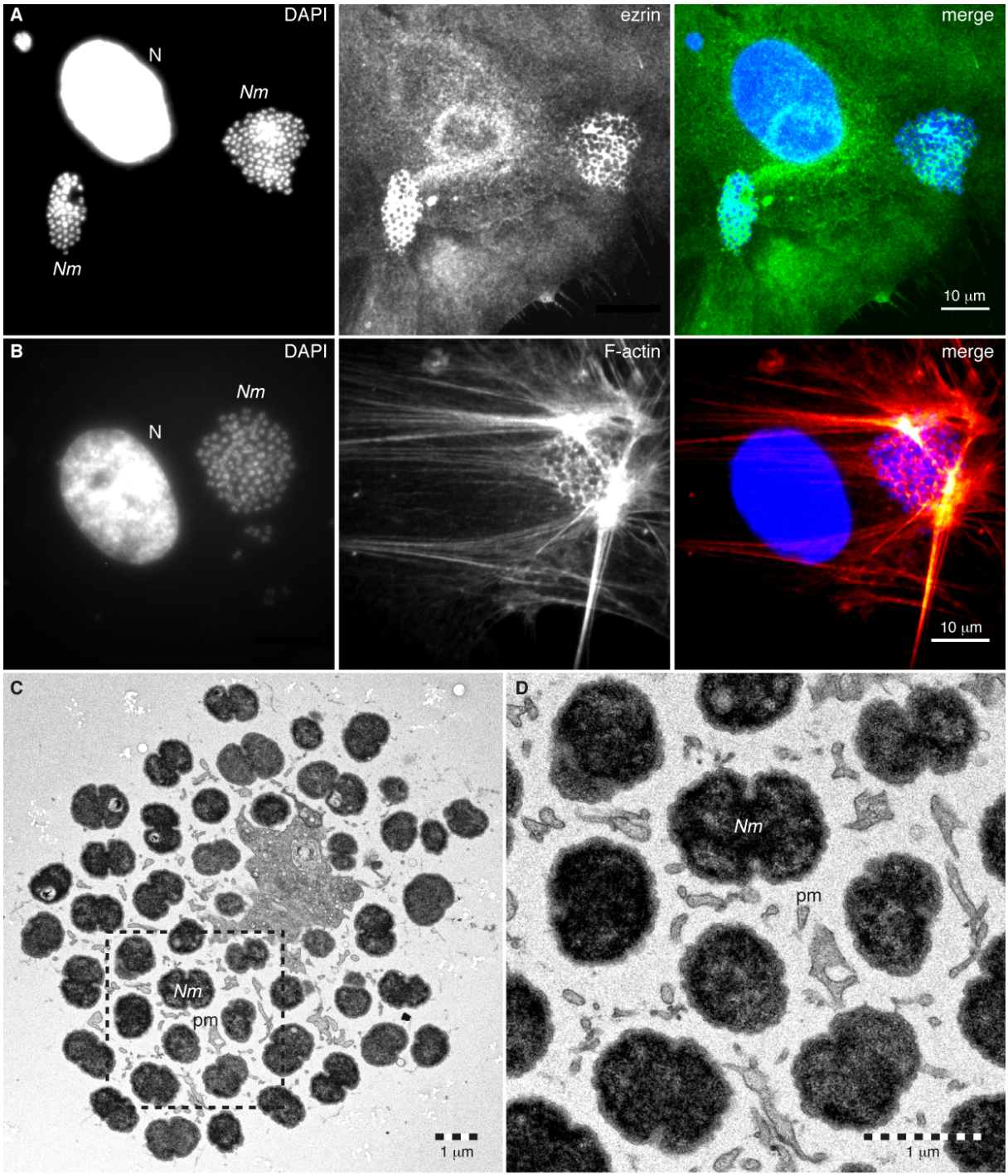

Figure 12 | *N. meningitidis* adhesion induces cortical plaque formation in human endothelial cells *in vitro*. Following type IV pili-mediated adhesion, meningococci proliferate at the surface of the host endothelial cell as microcolonies. After 2h of infection, the host cell plasma membrane is found accumulated within the microcolonies in an "honeycomb lattice" fashion as evidence by the immunostaining of the plasma membrane marker ezrin **(A)**. Plasma membrane remodeling is accompanied by a reorganization of the F-actin cytoskeleton, as revealed by staining with fluorescent phalloidin **(B)**. N, nucleus; *Nm*, *N. meningitidis* microcolonies. **(C, D)** Transmission electron micrograph of an ultrathin sagittal section taken through a meningococcal microcolony (therefore representing the top view as in **(A)** and **(B)**). Bacteria have recruited the host cell plasma membrane that appears as microvilli-like protrusions (pm) intercalated between aggregated bacteria (*Nm*). **(D)** is an enlargement of the dashed box in **(C)**.

It was later found that cortactin recruitment by meningococcus is also promoted by the activation of the phosphoinositide 3-kinase (PI3K) pathway, leading to the production of phosphatidylinositol-3,4,5-triphosphate (PtdIns(3,4,5)P_3) and the recruitment of Rac1 at the plasma membrane. Rac1, in turn, was shown to promote actin polymerization and bacterial internalization (Lambotin et al., 2005) (Fig. 13). This is in clear contradiction with the study by Eugene *et al.* that excluded Rac1 as an actin polymerization factor within the cortical plaque (Eugene et al., 2002), however Lambotin *et al.* argued that Rac1 promoted the specific polymerization of actin stress fibers rather than actin-rich plasma membrane protrusions. They also showed that the activation of the PI3K pathway depended on the meningococcal LOS rather than on T4P, although they failed to activate this pathway with purified LOS. It is not clear anyway how the formation of actin stress fibers would promote bacterial internalization. Moreover, the authors call "bacterial internalization" the intracellular localization of as little as 0,0005 to 0,012% of total adherent meningococci after 3h of interaction with endothelial cells (or in other words, 5 to 120 over 10,000 bacteria). Thus, the implication of Rac1 in meningococcal induction of actin polymerization within the endothelial host cell is overall quite enigmatic.

Nevertheless, it was shown that upon binding of meningococcal T4P proteins PilE and PilV to the G protein coupled receptor (GPCR) β2-adrenoreceptor, the protein β-arrestin-2 is specifically recruited and promotes the phosphorylation of Src, which in turn phosphorylates cortactin and leads to actin polymerization (Coureuil et al., 2010). Sequestration of Src in the cortical plaque by the epidermal growth factor receptor (EGFR) related protein ErbB2 was also shown to promote cortactin phosphorylation (Hoffmann et al., 2001) (Fig. 13). Interestingly, binding of T4P to the β2-adrenoreceptor does not trigger the canonical activation of the adenylyl cyclase/cAMP pathway via the heterotrimeric Gαs protein. Therefore, meningococcal activation of this GPCR was referred to as "biased". In addition, overexpression of the β2-adrenoreceptor and of β-arrestin-2 in HEK293 cells, which are typically not competent for colonization by meningococcus, is sufficient to trigger actin polymerization by meningococci in these cells (Coureuil et al., 2010).

Recruitment of F-actin at the plasma membrane is promoted by the linker protein ezrin, which was shown to bind phosphatidylinositol-4,5-biphosphate (PtdIns(4,5)P_2), CD44 and the intercellular adhesion molecule (ICAM)-1 at the plasma membrane through its C-terminal domain as well as F-actin through its N-terminal domain (Eugene et al., 2002; Merz et al., 1999; Merz and So, 1997).

In the closely related species *N. gonorrhoeae*, it was proposed that the resembling reorganization of the epithelial cell surface was dependent on the forces generated by pilus retraction via the PilT ATPase (Higashi et al., 2009; Lee et al., 2005). Pilus retraction in that context promotes expression of survival genes in the host cell (Howie et al., 2005). Moreover, mimicking of pilus retraction by optical tweezers pulling of gonococcal pili-coated beads adhered to epithelial cells leads to a recruitment of actin at the site of membrane deformation (Opitz and Maier, 2011), suggesting that pilus retraction could act on plasma membrane morphology. In *N. meningitidis*, it was shown that PilT-mediated pilus retraction allows intimate attachment of meningococci to epithelial cells, probably by promoting the interaction of outer membrane adhesins with the host cell plasma membrane (Pujol et al., 1999). This point is addressed in the Results chapter. Moreover, recruitment of the plasma membrane seems to be promoted by a conformational change of the pilus fiber (Brissac et al., 2012), which could occur upon pilus retraction. However, how forces generated by pilus retraction influence plasma membrane remodeling is unknown.

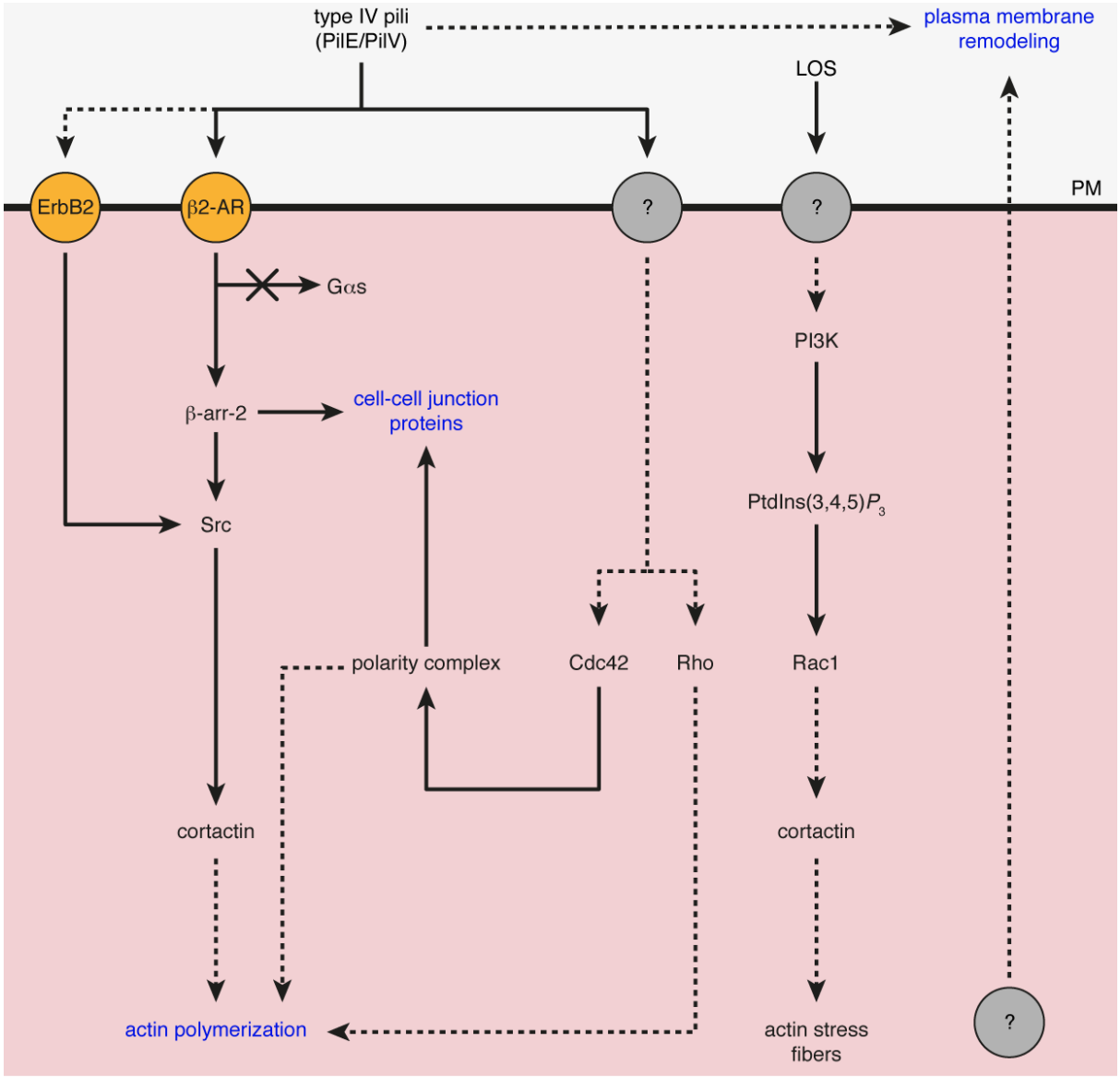

Figure 13 | Major signaling events associated with *N. meningitidis* adhesion to human endothelial cells. Upon adhesion to endothelial cells, meningococcus elicits intracellular signaling events that mainly lead to a reorganization of the F-actin cytoskeleton and a relocalization of cell-cell junction proteins at the site of bacterial adhesion. The reader is invited to refer to the main text for a detailed description of these signaling cascades. Solid arrows indicate direct interactions, whereas dashed arrows denote indirect or unknown interactions. β2-AR, β2-adrenoreceptor; β-arr-2, β-arrestin-2; LOS, lipooligosaccharide; PI3K, phosphoinositide 3-kinase; ?, unidentified host cell components; PM, plasma membrane. The mechanism for plasma membrane remodeling is unknown.

Despite the early observation of Eugene *et al.* that the deformation of the endothelial cell surface does not depend on the rearrangement of the F-actin cytoskeleton, it has been paradoxically well admitted in the field that actin polymerization promotes plasma membrane protrusions. In a study by Mikaty *et al.*, it was demonstrated again that neither disruption of the actin or the microtubule cytoskeleton impacts plasma membrane reshaping by meningococcus (Mikaty et al., 2009). However, the authors noticed that cholesterol was accumulated in plasma membrane protrusions, and that plasma membrane remodeling by meningococcus does not occur in the absence of plasma membrane cholesterol. In terms of bacterial factors, it was found that mutant bacteria lacking the minor pilin PilV failed to remodel the host cell plasma membrane. In line with the role of T4P or T4P associated proteins in host cell surface reorganization, other studies showed that adhesion of meningococcus via alternative non-pilus adhesins does not lead to plasma membrane remodeling (Brissac et al., 2012).

In conclusion, plasma membrane remodeling and F-actin reorganization by meningococcus appear to be two distinct events. In addition, although plasma membrane cholesterol and T4P (or T4P associated proteins) were proved necessary for plasma membrane remodeling, the precise underlying mechanisms are not understood.

Nevertheless, reorganization of the host cell surface by *N. meningitidis* has important implications for the pathophysiology of meningococcal disease. First, it can lead to a weakening of cell-cell junctions, which is thought to facilitate the traversal of the blood-brain barrier during meningitis. Second, it allows bacterial microcolonies to resist shear forces that are found in the bloodstream.

4.2. Opening of the endothelial cell-cell junctions

One of the main scientific challenges with respect to the pathogenesis of meningococcal meningitis has been to understand how meningococcus can get access to the central nervous system. The passage of cells and molecules into and out of the brain is indeed tightly regulated by a structure known as the blood-brain barrier (BBB). It normally protects the neural tissue by acting as a highly selective filter against microorganisms, immune cells, toxins, or inflammatory molecules (Fig. 14).

Non-BBB endothelial cell-cell contacts mainly consist of adherens junctions, characterized by the presence of the transmembrane protein vascular endothelial (VE)-cadherin, that establishes homotypic interactions between two adjacent cells through its extracellular domains, and the cytoplasmic proteins p120-catenin, α-, β- and γ-catenins that anchor VE-cadherin to the actin cytoskeleton. The BBB endothelium is well differentiated and cell-cell contacts have additional tight junctions. Tight junctions prevent the transcellular passage of water-soluble molecules that circulate in the blood. They comprise the membrane proteins claudins and occludins that form the actual junction, and the peripheral membrane zona occludens (ZO) proteins that anchor them to the actin cytoskeleton (for a review, see (Coureuil et al., 2017; Hartsock and Nelson, 2008)) (Fig. 14A).

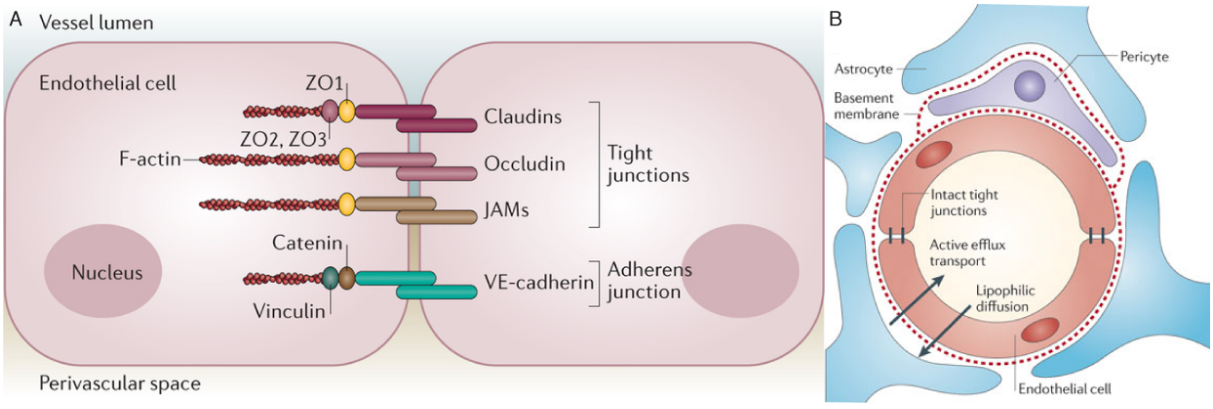

Figure 14 | Molecular organization of cell-cell junctions in human endothelial cells from the blood-brain barrier (BBB) and structure of the BBB. (**A**) Endothelial cell-cell contacts in the BBB consist of adherens and tight junctions. ZO, zona occludens; JAMs, junctional adhesion molecules; VE-cadherin, vascular endothelial-cadherin. Adapted from (Coureuil et al., 2017). (**B**) The neural tissue of the brain is separated from the blood compartment by the blood-brain barrier which consists of microvascular endothelium, astrocytes and pericytes. Endothelial cells in the BBB are highly differentiated and possess cell-cell junctions that are impermeable to immune cells, microorganisms and water-soluble molecules such as toxins and inflammatory molecules. Adapted from (Steeg et al., 2011). (Also see **Credits** section.)

In addition, endothelial cells in the BBB show very low levels of pinocytosis, i.e. the uptake of large volumes of fluids from the extracellular milieu, and of transcytosis, i.e. the vesicular transport of molecules from the luminal to the abluminal membranes across the cytoplasm. Compared to other endothelia, the BBB endothelium lacks structures such as fenestrae that allow the passage of cells and fluids across the vascular bed. Instead, BBB endothelial cells express specific transporters to shuttle molecules and macromolecules from the blood to the brain and back. The differentiated status of endothelial cells in the BBB is maintained by the action of pericytes and astrocytes (for a review, see (Banks, 2016; Steeg et al., 2011)) (Fig. 14B). Yet, meningococci are found in large numbers in the cerebrospinal fluid of meningitis patients (Brandtzaeg and van Deuren, 2012; Ovstebo et al., 2004) (see section **1.3.3.**), clearly indicating that *N. meningitidis* must somehow bypass the BBB function.

In 2009, it was found that proteins of the polarity complex are recruited to the meningococcal cortical plaque in endothelial cells. The polarity complex consists of the proteins Par3, Par6 and the protein kinase Cζ (PKCζ). It is normally found at the basolateral membrane of epithelial and endothelial cells where it allows formation and maintenance of intercellular junctions via the recruitment of adherens and tight junctions proteins and Cdc42-mediated actin polymerization (Joberty et al., 2000; Koh et al., 2008; Vasioukhin et al., 2000; Yamanaka et al., 2001). Upon T4Pmediated cortical plaque formation in endothelial cells, activated Cdc42 was shown to recruit the polarity complex, leading to the trafficking of the adherens junction molecules VE-cadherin, p120-catenin and β-catenin and the tight junction molecules ZO-1, ZO-2 and claudin-5 to the site of bacterial adhesion (Coureuil et al., 2009) (Fig. 13). Cell junction proteins were relocalized from the existing cell-cell contacts via clathrin-mediated endocytosis and resulted in the depletion of these components from the cell-cell junctions. This in turn led to the formation of gaps between endothelial cells, promoting the transcellular passage of meningococci across the cell monolayer. Interestingly, it was found that the recruitment of VE-cadherin and p120-catenin is also mediated by β-arrestin-2 after the biased activation of the β2-adrenoreceptor by meningococcus (Coureuil et al., 2010) (Fig. 13). Recruitment of the polarity complex and of cell-cell junction molecules by *N. meningitidis* was shown to be specific to endothelial cells, as compared to epithelial cells (Lecuyer et al., 2012). Adhesion of meningococcus to endothelial cells was also associated with the cleavage of occludin by the matrix metalloproteinase (MMP)-8 *in vitro*, which could contribute to the opening of endothelial cell junctions (Schubert-Unkmeir et al., 2010).

It is not known whether the interaction of *N. meningitidis* with the endothelial cells of the BBB leads to such a weakening of cell-cell junctions *in vivo*.

4.3. Resistance to shear stress

Another key aspect of the blood phase of meningococcal pathogenesis is that bacteria adhering to endothelial cells are expected to experience an important shear stress in the bloodstream. Shear stress refers to the drag forces, parallel to the blood vessel walls, generated by the circulation of blood. It is expressed in dynes.cm^{-2}. Blood flow-generated shear stress depends on blood velocity and viscosity and varies according to the blood vessel type and diameter. *In vivo*, it ranges from 1 to 60 dynes.cm^{-2} (Loscalzo and Schafer, 2002), with arteries and capillaries showing the highest and lowest values, respectively (Pries et al., 1994). Since meningococci are found to adhere to capillaries in various tissues, they are expected to be able to cope with this shear stress.

Surprisingly, the study of meningococcal adhesion under shear stress *in vitro* showed that shear forces as low as 0,22 dynes.cm^{-2} efficiently inhibit T4P-mediated adhesion to endothelial cells (Mairey et al., 2006).

However, in capillaries of living rats, intravital imaging through cranial windows showed that shear stress could reach 3 dynes.cm^{-2} but occasionally fall in a range of values compatible with T4P-mediated adhesion of meningococci for periods of time of up to 30 seconds. *In vitro*, meningococci that initially adhered via their T4P can subsequently withstand shear stress levels of up to 30 dynes.cm^{-2} (Mairey et al., 2006). More specifically, resistance to shear stress is strictly dependent on the remodeling of the plasma membrane at the site of bacterial adhesion (Mikaty et al., 2009) (Fig. 15).

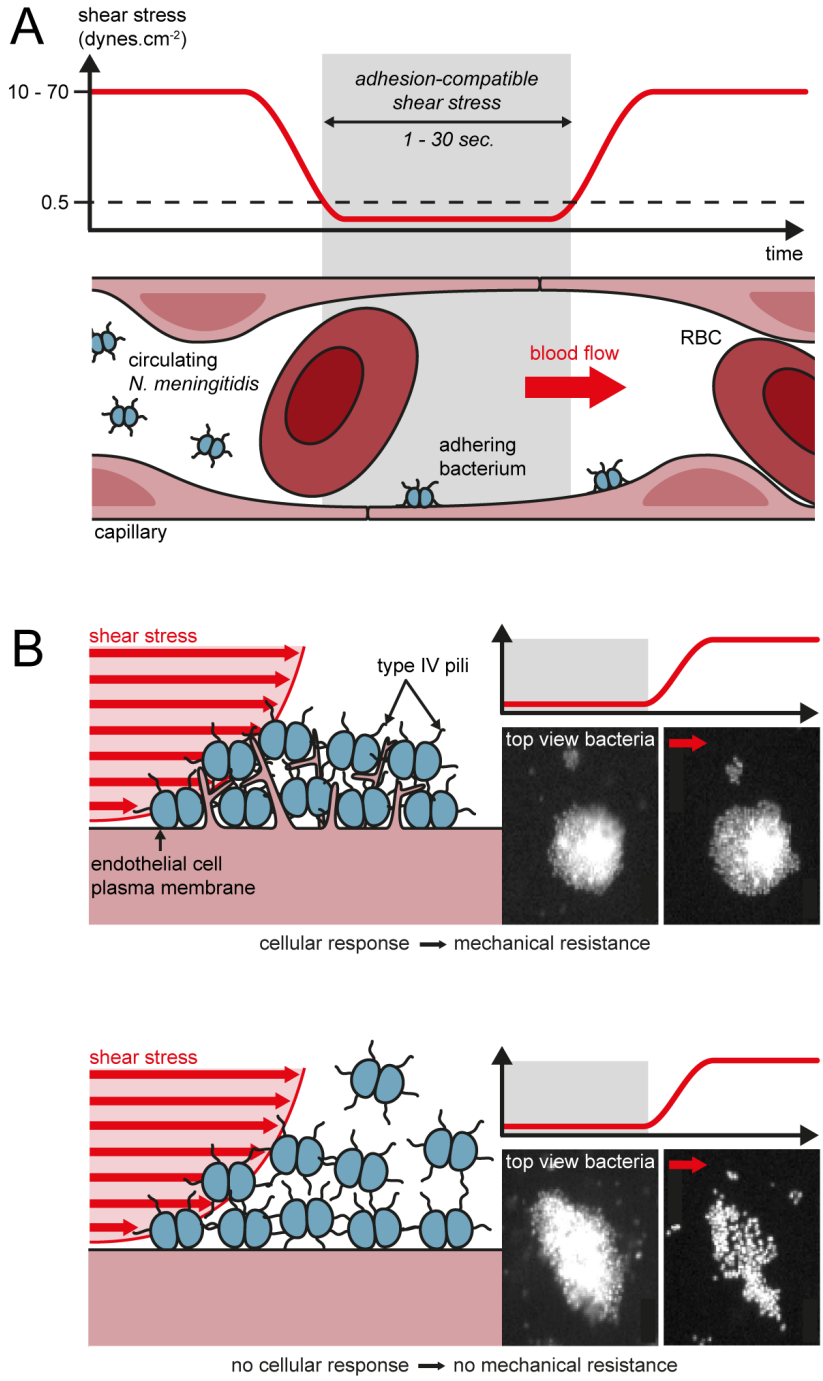

Figure 15 | Impacts of blood shear stress on *N. meningitidis* pathophysiology. (**A**) *N. meningitidis* that has entered the human circulation cannot bind vessels walls until the blood flow-generated shear stress levels reach values compatibles with bacterial adhesion. Irreversible adhesion of meningococcus to the endothelial cells through type IV pili allows bacterial proliferation and subsequent damage to the vessels. (**B**) Reshaping of the endothelial cell plasma membrane by adherent meningococci provides bacterial microcolonies mechanical resistance to high shear stress levels (top panel). Mutants that are unable to trigger this cellular response lack mechanical resistance and remain sensitive to shear stress (bottom panel). For each case, snapshots from live cell imaging experiments show bacterial microcolonies adhering to human endothelial cells before (left) and after (right) the addition of flow. Reproduced from (Charles-Orszag et al., 2016) (see **Credits** section).

Therefore, remodeling of the endothelial cell plasma membrane upon T4P-mediated adhesion of meningococcus provides bacterial microcolonies with the ability to resist shear stress levels compatible with those encountered in human blood. Although the role of resistance to shear stress in meningococcal pathogenesis was not tested *in vivo*, it is expected to play an important role, as non-adhering bacteria do not cause symptoms of meningococcal disease in animal models of vascular colonization (Join-Lambert et al., 2013; Melican et al., 2013) (see section **I.4.**).

In summary, remodeling of the host cell plasma membrane by *N. meningitidis* following pilus-mediated adhesion and associated signaling events have important effects on the physiology of endothelial cells and of bacteria that are relevant to meningococcal pathogenesis. While several studies suggest that plasma membrane remodeling and cytoskeletal rearrangements are two separate steps during cell surface reorganization, the precise mechanisms of plasma membrane reshaping are not understood, which is the focus of this PhD project.

5. General mechanisms of membrane curvature & functions of plasma membrane remodeling in animal cells

The ability of *N. meningitidis* to remodel the endothelial cell plasma membrane allows bacterial microcolonies to resist shear forces that are found in the bloodstream. Therefore, it is likely to play an important role in the blood phase of meningococcal infections. However, the mechanisms by which meningococcus reshapes the host cell plasma membrane are not known. In this chapter, I will describe how biological membranes can generally be remodeled in animal cells. Next, I will focus more specifically on the functions of plasma membrane remodeling. Finally, I will describe common strategies used by bacterial pathogens to hijack these mechanisms at the surface of host cells for their own benefits.

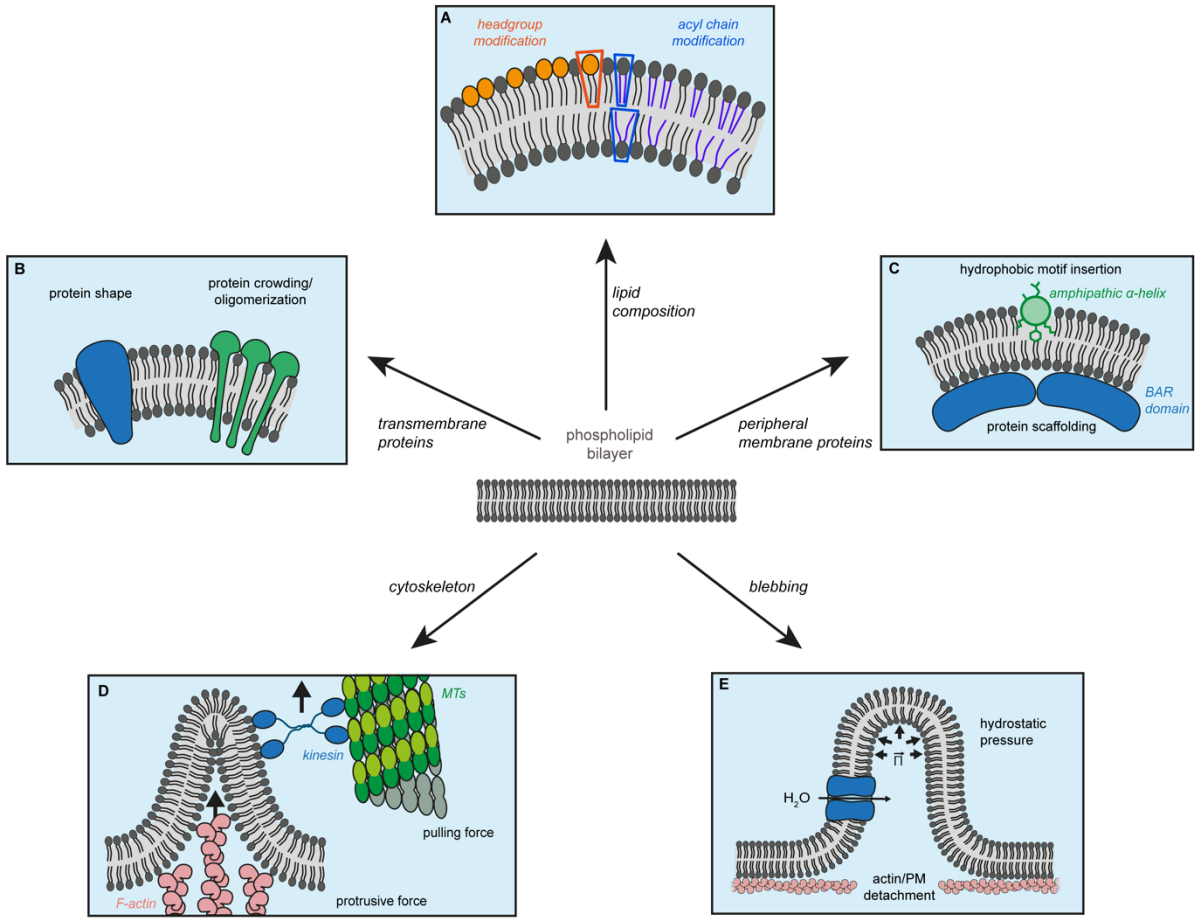

Figure 16 | Molecular mechanisms of membrane curvature. In animal cells, bending of membranes can be achieved by (**A**) asymmetrical distribution of lipids species with different shapes, resulting from different headgroups or acyl chains, (**B**) intrinsic shapes and/or crowding or oligomerization of transmembrane proteins, (**C**) insertion of hydrophobic protein motifs (wedge mechanism) or scaffolding by peripheral membrane proteins with curved shapes, (**D**) protrusive or pulling forces exerted by the cytoskeleton, directly or through molecular motors such as kinesins or (**E**) pushing forces by exerted by the hydrostatic pressure from the cytoplasm after detachment of the plasma membrane from the actin cortex. BAR, Bin/Amphiphysin/Rvs; MTs, microtubules; PM, plasma membrane.

5.1. General mechanisms of membrane curvature

Biological membranes consist of a bilayer of phospholipids, of varying amounts of cholesterol, and of transmembrane proteins. In eukaryotic cells, they are subject to a constant remodeling which supports proper compartmentalization and timing of biochemical reactions within the cell as well as intracellular trafficking. However, at steady state, lipid bilayers are flat (Helfrich, 1973). Modification of their shape thus requires energy (Helfrich and Jakobsson, 1990) and greatly depends on the bilayer tension (Simunovic et al., 2015). Over the past twenty years has emerged the notion that membrane curvature is highly regulated in cells and that it can be achieved by a set of conserved mechanisms. It is now well described that membrane bending can result from the intrinsic properties of the bilayer, i.e. of its lipid and protein constituents, or can be induced by extrinsic factors such as peripheral membrane proteins or cytoskeletal components (Fig. 16).

5.1.1. Shapes of the bilayer components

Different phospholipid species constitute the plasma membrane bilayer. They differ owing to the size of their hydrophilic headgroups and to the occupancy of their hydrophobic acyl chains that results from differences in the number of saturations. The size ratio between the two parts gives a specific shape to the phospholipid, which ranges from cylindrical to conical or inverted conical. Since phospholipids of the same kind tend to cluster together, asymmetry in phospholipid composition between two opposing lipid leaflets can locally change the topography of the bilayer (Cooke and Deserno, 2006). For example, cylindrical phospholipids (such as phosphatidylcholine) will tend to make flat bilayers, whereas phospholipids with large headgroups (such as phosphatidylinositol phosphates) will have a conical shape that will tend to locally bend the bilayer outwards (Fig. 16A). Transmembrane proteins, which are embedded in the lipid bilayer, also have intrinsic shapes (Aimon et al., 2014; Caltagarone et al., 2015; Fribourg et al., 2014; Unwin, 2005) that can promote positive or negative membrane curvature, according to the side of the bilayer where protein domains occupy more space (McMahon and Boucrot, 2015) (Fig. 16B).

5.1.2. Membrane bending by peripheral membrane proteins

Some non-transmembrane proteins may interact with membranes and bend them through shallow insertion of amino acids or through insertion of hydrophobic loops into one lipid leaflet. Proteins such as epsin and amphiphysin (Ford et al., 2002; Isas et al., 2015; Peter et al., 2004) contain amphipathic helices with hydrophobic amino acids that mostly localize on one side of the helix and insert beneath the phospholipid headgroups. Other proteins, such as synaptotagmin-1 and Doc2b (Groffen et al., 2010; Hui et al., 2009), contain a calcium-regulated C2 domain that inserts even more deeply in the bilayer. Proteins like caveolin-1 and flotillins interact with membranes by inserting hydrophobic loops that span one lipid leaflet (Morrow and Parton, 2005; Parton and del Pozo, 2013; Schlegel and Lisanti, 2000). In all three cases, asymmetric insertion of hydrophobic protein domains into one lipid leaflet acts like a wedge that generates membrane curvature (Fig. 16C). This effect is largely enhanced by protein oligomerization that stabilizes membrane curvature by a scaffolding effect (Isas et al., 2015; Parton et al., 2006; Simunovic et al., 2015). Of note, it has been shown that aspecific protein crowding at the surface of the membrane was sufficient to drive membrane curvature, without insertion of any hydrophobic protein domains (Stachowiak et al., 2010; Stachowiak et al., 2012), although it was argued that this mechanism requires very high local concentrations of proteins that are probably not met in real life (Kirchhausen, 2012).

Membrane curvature can further be generated or stabilized by peripheral membrane proteins that contain Bin/Amphiphysin/Rvs (BAR) domains. BAR domains are typically crescent-shaped and can bind to membranes, thereby impressing their shape (Fig. 16C). N-BAR and F-BAR domains promote positive

curvature. They are respectively found in proteins such as amphiphysin and FCH domain only proteins (FCHo)1 and 2 that are involved in clathrin-mediated endocytosis (Henne et al., 2007; Isas et al., 2015) and differ by their degree of curvature, with F-BAR domains being more shallowly curved. I-BAR domains promote negative curvature. They are found in proteins such as the insulin receptor substrate protein of 53 kD (IRSp53) or missing-in-metastasis (MIM) that are involved in the biogenesis of filopodia (Ahmed et al., 2010; Mattila et al., 2007; Prevost et al., 2015). BAR domain-containing proteins can further oligomerize in a head-to-tail or side-by-side fashion, which increases their density on the membrane and provides an additional scaffolding effect (Mim and Unger, 2012; Rao and Haucke, 2011; Simunovic et al., 2015).

Scaffolding can also be exerted by proteins that do not interact with membranes but with membrane-bending proteins, as is the case for clathrin that interacts with epsin and amphiphysin. The clathrin coat assembles as the membrane bends and further stabilizes its curvature in the clathrin-coated pit (McMahon and Boucrot, 2011).

5.1.3. Membrane bending by cytoskeletal components

While the aforementioned mechanisms of membrane bending generate curvatures at the nanoscale (a few to 100 nm in radius), components of the cytoskeleton can generate macroscopic membrane curvature. Scaffolding by actin, intermediate filaments and microtubules, or membrane pushing and pulling through motor proteins like kinesins, dyneins and myosins, shape intracellular organelles such as the endoplasmic reticulum, the Golgi or endosomes (for a review, see (Jarsch et al., 2016)) (Fig. 16D). At the plasma membrane, it is mainly the actin cytoskeleton that shapes the bilayer at macroscopic scales, essentially by pushing on the membrane, generating negative membrane curvature.

5. 2. Cellular functions of plasma membrane remodeling

The plasma membrane is the cellular compartment that separates the cytoplasm from the surrounding environment. As such, it must protect the cell mechanically and chemically while supporting communication with the environment, uptake of nutrients, secretion into the extracellular milieu and locomotion. These cellular functions all depend on the ability of the cell to control the shape of the plasma membrane, which relies on combinations of mechanisms of membrane remodeling that can act in concert. Plasma membrane can undergo either positive curvature toward the cytoplasm (invagination), or negative curvature toward the extracellular milieu (protrusion).

5.2.1. Plasma membrane invaginations

Positive curvature of the plasma membrane is required for endocytosis (the uptake of extracellular material by the cell). Clathrin-mediated endocytosis is the best-studied endocytic pathway. It is also a good example of how a combination of different mechanisms of membrane curvature cooperates during the same process. The formation of clathrin-coated pits is initiated by the F-BAR containing proteins FCHo1/2 (Henne et al., 2010) that promote a shallow positive membrane curvature. Plasma membrane is further bent by i) membrane insertion and membrane scaffolding and ii) asymmetrical clustering of inverted conical lipids (e.g. phosphatidylserine and PtdIns(4,5)P_2) by epsin and amphiphysin, as well as by scaffolding by the clathrin coat (McMahon and Boucrot, 2011). Constriction of the neck of the clathrin-coated vesicle prior to fission is generated by oligomerization of the GTPase protein dynamin (Chappie et al., 2011; McMahon and Boucrot, 2011; Morlot et al., 2012) and helped by polymerization of actin from the plasma membrane that is thought to push on the vesicle (Collins et al., 2011). The clathrin-independent carriers/glycosylphosphatidylinositol-enriched early endosomal compartment (CLIC/GEEC) pathway is

another endocytic pathway that is used for fluid uptake and plasma membrane turnover (Doherty and McMahon, 2009). It involves the plasma membrane curvature sensing activity of the BAR domain containing protein GTPase Regulator Associated with Focal Adhesion Kinase (GRAF)-1 that localizes to PtdIns(4,5)P_2-enriched membrane domains (Lundmark et al., 2008). Fast endophilin-mediated endocytosis is another pathway that mediates the internalization of a number of surface receptors. It is initiated both by the BAR domain and the amphipathic helix of endophilin (Boucrot et al., 2015; Watanabe and Boucrot, 2017). Finally, uptake of the Shiga toxin is triggered by its binding to the glycosphingolipid receptor globotriaosyl ceramide (Gb3). Clustering of Gb3 then induces the invagination of the plasma membrane (Romer et al., 2007).

Positive curvature of the plasma membrane is also required for the biogenesis of caveolae, which serve as plasma membrane reservoirs that physically buffer membrane tension (Cheng et al., 2015; Parton and del Pozo, 2013; Sinha et al., 2011). In that case, membrane curvature is achieved by insertion of caveolin-1 hydrophobic loops into the membrane, oligomerization of caveolin-1, of the cytoplasmic cavin proteins, of the ATPase EH domain-containing protein EHD2 (Moren et al., 2012; Stoeber et al., 2012), and of the BAR domain-containing protein kinase C and casein kinase substrate in neuron 2 (PACSIN2) (Hansen et al., 2011; Senju et al., 2011).

5.2.2. Plasma membrane protrusions

Plasma membrane negative curvature, or protrusion towards the outside of the cell, is particularly relevant to this study since this is the topology that is induced by meningococcus upon T4P-mediated adhesion (see section **4**).

Plasma membrane protrusions can support the uptake of extracellular material, for example in macropinocytosis and phagocytosis where large volumes of fluid or large particles are internalized via the closure of membrane ruffles or membrane cups (see (Doherty and McMahon, 2009) and (Levin et al., 2016) for reviews). More recently, it was shown that small protrusions of the plasma membrane allow the clathrin-independent internalization of the IL2 receptor (IL2R) (Basquin et al., 2015). In these three cases, plasma membrane protrusions are generated by actin polymerization pushing on the membrane after transmsmembrane signaling.

Animal cells also use plasma membrane protrusions to explore and move into their environment (Insall and Machesky, 2009; Ridley, 2011). For example, filopodia are 100-500 nm actin-based protrusions that can be used to adhere to the cell substrate, sense chemotactic cues and migrate (Albuschies and Vogel, 2013; Jacquemet et al., 2015; Mattila and Lappalainen, 2008). Filopodia formation involves an initial step of membrane bending by I-BAR domain-containing proteins such as IRSp53 (Ahmed et al., 2010; Prevost et al., 2015), or non-BAR domain-containing proteins such as the exocyst complex subunit Exo70 (Zhao et al., 2013b). In turn, these proteins recruit actin polymerization proteins, thereby generating long plasma membrane protrusions by pushing on the membrane (Ahmed et al., 2010; Prevost et al., 2015; Suetsugu and Gautreau, 2012; Svitkina et al., 2003). Invadopodia are specific filopodia-related protrusions that are used to degrade the extracellular matrix locally and promote cell migration through tissues. Their formation follows the same principles than that of filopodia (Garcia et al., 2012; Machesky et al., 2008). Depending on the actin polymerization machinery involved, plasma membrane protrusions can also become flat and large migratory structures called lamellipodia (Hansen and Mullins, 2015; Kuhn et al., 2015; Ridley, 2011; Suetsugu and Gautreau, 2012; Svitkina et al., 2003). In contrast, blebs are migratory structures where plasma membrane bending is not dependent on actin polymerization. In that case, it is the hydrostatic pressure exerted by the cytoplasm on the plasma membrane that pushes it outwards when the cortical actin detaches from the membrane (Fig. 16E). Actin polymerization is subsequently used to resorb the bleb (for a review,

see (Fackler and Grosse, 2008)). Finally, the plasma membrane can protrude upon water influx through aquaporin 9 (Karlsson et al., 2013) or under the action of the endosomal sorting complex required for transport (ESCRT)-III complex upon plasma membrane damage (Jimenez et al., 2014; Nabhan et al., 2012).

Other plasma membrane protrusions include cilia and flagella, which are microtubule-based, and microvilli in epithelial cells, which are actin-based. It is possible that the microtubule and actin cytoskeletons push the membrane forwards in these two cases. However, to my knowledge, there are no studies that have addressed the role or the regulation of membrane curvature in these protrusions so far. Yet, the septin cytoskeleton was recently proposed to sense membrane curvature at the base of cilia and flagella (Palander et al., 2017).

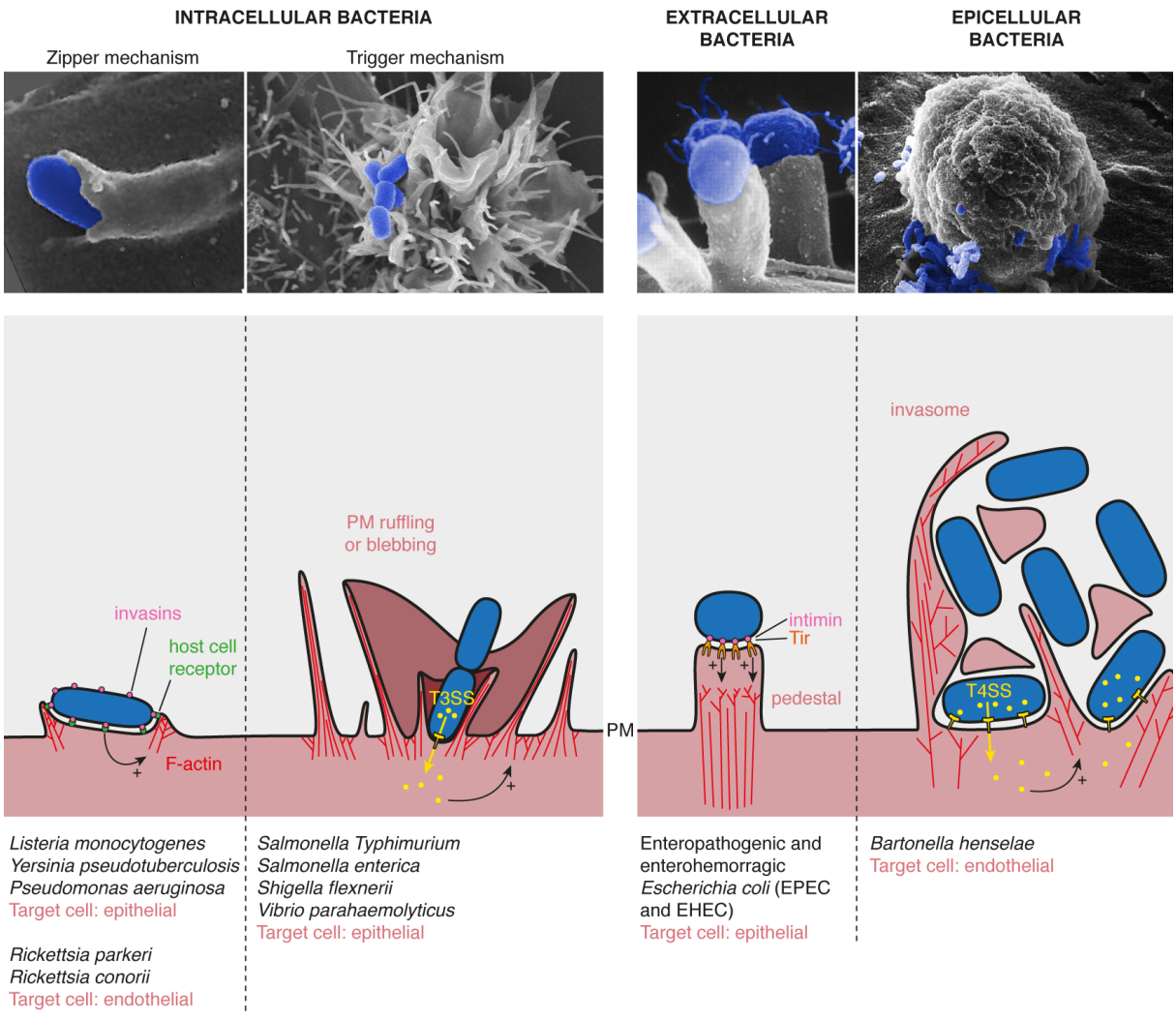

Figure 17 | Mechanisms of plasma membrane remodeling used by bacterial pathogens. Numerous bacterial pathogens exploit actin-based plasma membrane remodeling to invade host cells or to support their extracellular lifestyle. Obligate intracellular pathogens either use a zipper or a trigger mechanism to induce their internalization, while non-intracellular bacteria trigger plasma membrane protrusions that do not lead to bacterial engulfment. Scanning electron micrographs illustrating each mechanism were colorized for clarity, with bacteria in blue. They were adapted from (Parida et al., 1998), (Charles-Orszag et al., 2016), (Knutton et al., 1998) and (Dehio et al., 1997) (from left to right, also see **Credits** section). The reader is invited to refer to the main text for a detailed description of the signaling cascades involved. Arrows marked with a "+" denote activation of actin polymerization. T3SS, type III secretion system; T4SS, type IV secretion system; PM, plasma membrane.

5.3. Plasma membrane remodeling triggered by bacterial pathogens

5.3.1. Internalization of intracellular bacteria in non-phagocytic cells

The extracellular environment can be a source of numerous stresses and dangers to bacterial pathogens, such as shear stress in the blood and urinary tract, low pH, complement deposition, opsonization by antibodies and phagocytosis, etc. Therefore, in contrast with *N. meningitidis* that remains extracellular, successful infection by some pathogens requires bacterial internalization into the host cell. Obligate intracellular bacterial pathogens have evolved diverse strategies to induce their uptake by non-phagocytic cells. These strategies broadly rely on a "zipper" or on a "trigger" mechanism.

The zipper mechanism

The zipper mechanism of cell invasion involves bacterial surface proteins called invasion proteins. Upon binding to their host cell receptor, invasion proteins trigger intracellular signaling cascades that lead to actin polymerization and engulfment of the bacterium (Fig. 17).

In *Yersinia pseudotuberculosis* and *Yersinia enterolitica*, the invasion protein was called invasin (Isberg et al., 1987). It binds to the β_1 chain integrin family of proteins on epithelial cells with high affinity, thereby competing with fibronectin (Isberg and Leong, 1990). In turn, the cytoplasmic domain of the β_1 chain recruits the focal adhesion kinase (FAK) and the Src kinase (Alrutz and Isberg, 1998; Bruce-Staskal et al., 2002) and promotes actin polymerization at the site of bacterial adhesion via the small GTPases Rac1 and Arf6 and the phosphatidylinositol-phosphate-5-kinase Iα that induces the local production of PtdIns(4,5)P_2 (Wong and Isberg, 2003), resulting in bacterial invasion.

In *Listeria monocytogenes*, two different invasion proteins called internalin (Inl) A and B mediate two different pathways of bacterial internalization via a zipper mechanism. InlA binds to the epithelial cell adhesion molecule E-cadherin in a cholesterol-dependent fashion (Lecuit et al., 1999; Lecuit et al., 2004; Lecuit et al., 2001; Seveau et al., 2004). Engagement with InlA leads to the recruitment of α- and β-catenin to the cytoplasmic C-terminus of E-cadherin (Lecuit et al., 2000) and, eventually, to actin polymerization and bacterial uptake via the small GTPase Rac1, the actin regulator cortactin and the Arp2/3 complex (Pizarro-Cerda and Cossart, 2006). The InlB-dependent pathway involves the interaction of InlB with the hepatocyte growth factor (HGF) receptor tyrosine kinase Met (Shen et al., 2000). Activation of Met leads to the recruitment of adaptor proteins that promote PI3K association with the plasma membrane. PI3K then activates Rac, which leads to Wiskott-Aldrich syndrome protein-family verprolin-homologous protein (WAVE)2- and Arp2/3-mediated actin polymerization. Interestingly in this case, bacterial internalization is also helped by the internalization of Met itself through clathrin-mediated endocytosis (Li et al., 2005; Veiga and Cossart, 2005).

In epithelial and endothelial cells, *Rickettsia* spp. induce their internalization via a zipper mechanism through the engagement of the invasion proteins rOmpA and B with host cell receptors (Li and Walker, 1998; Uchiyama, 2003). While rOmpB binds the protein Ku70 in a cholesterol-dependent manner, the target of rOmpA is not known yet (Martinez et al., 2005; Pizarro-Cerda and Cossart, 2006). Bacterial internalization is mediated by FAK and Src kinases, the small GTPase Cdc42, PI3K, cortactin and the Arp2/3 complex (Martinez and Cossart, 2004).

Finally, the pathogenic diffuse-adhering *E. coli* (DAEC) has been shown to trigger the formation of long microvilli via a CEACAM/Cdc42/ERM proteins pathway (Berger et al., 2004) and to induce its

internalization in epithelial cells via binding to $\alpha_5\beta_1$ integrins (Plancon et al., 2003), although the functional link between these two events has not been described.

Overall, despite a wide variety of bacterial invasion proteins and of host intracellular pathways involved, the zipper mechanism of bacterial invasion always relies on the activation of actin polymerization within the host cell from the extracellular milieu through activation of surface receptors.

The trigger mechanism

The trigger mechanism differs from the zipper mechanism because intracellular signaling that leads to actin polymerization is a result of direct injection of bacterial effectors into the host cell cytoplasm by dedicated secretion systems. Actin polymerization in this case results in massive plasma membrane ruffling that is used for bacterial internalization (Fig. 17).

In *Salmonella enterica*, several pathogenicity islands encode different T3SS involved in the secretion of bacterial effectors that trigger actin polymerization in the host cell cytoplasm. Two of these effectors, SopE and SopE2, act as guanine exchange factors (GEFs) that activate the small GTPases Cdc42 and Rac1, leading to actin polymerization and massive ruffling of the host cell plasma membrane (Hardt et al., 1998). Two other T3SS effectors contribute to actin polymerization. SipA inhibits the F-actin depolymerization activity of coffilin and gelsolin (McGhie et al., 2004), while SipC directly induces F-actin bundling (Hayward and Koronakis, 1999).

In *Shigella flexnerii*, the T3SS effector IpaC (homologous to *S. enterica* SipC) promotes actin polymerization at the site of bacterial adhesion (Kueltzo et al., 2003). Another effector, IpaB, binds to the host cell protein CD44 and induces its clustering within lipid rafts, thereby triggering actin polymerization at the site of bacterial entry via Src, cortactin, Cdc42, Rac1 and the Arp2/3 complex (Bougneres et al., 2004; Burton et al., 2003). The effector protein VirA is also indirectly involved in actin polymerization via Rac1 and WAVE2 (Yoshida et al., 2002). Interestingly, *Salmonella enterica* and *Shigella flexnerii* have also evolved strategies to subsequently inhibit actin polymerization at the site of bacterial entry. Therefore, the intense membrane ruffling required for bacterial engulfment is transient, and the plasma membrane quickly recovers its initial shape after bacterial internalization (Bourdet-Sicard et al., 1999; Fu and Galan, 1999; Niebuhr et al., 2002).

In summary, internalization of bacterial pathogens always relies on the manipulation of the host cell actin cytoskeleton, which powers plasma membrane protrusions and subsequent engulfment of the bacteria.

5.3.2. Plasma membrane remodeling triggered by extracellular bacterial pathogens

In contrast to the previously described pathogens, some bacteria do not invade their host cell. Instead, they either remain extracellular (as is essentially the case for meningococcus) or are wrapped in a membrane structure so large that it seems to sit on the cell surface rather than being properly internalized, and can then be referred to as "epicellular" (Dumenil, 2011).

Enteropathogenic and enterohemorragic *E. coli* (EPEC and EHEC) are the prototypical examples of extracellular bacterial pathogens. After T4P-mediated adhesion to epithelial cells, they trigger typical lesions that result from the local effacement of microvilli (attaching and effacing lesions). Then, they trigger actin polymerization very locally, which leads to the formation of typical actin pedestals (Fig. 17). The originality of EPEC and EHEC is that they use a T3SS to inject their own adhesion receptor into host cells. This receptor, Tir (translocated intimin receptor), inserts in the host cell plasma membrane after injection and acts as a receptor for the bacterial surface protein intimin (Kenny et al., 1997). In EPEC, phosphorylation

of Tir by host kinases recruits the host adaptor proteins Nck, which activates the actin polymerization regulator neuronal-Wiskott-Aldrich syndrome protein (N-WASP) and the Arp2/3 complex, leading to the formation of actin pedestals (Phillips et al., 2004; Swimm et al., 2004). Another pathway, independent of Tir phosphorylation, has been described to result in N-WASP and Arp2/3 activation (Campellone and Leong, 2005). EPEC Tir has also evolved the ability to mediate actin depolymerization (Kenny et al., 2002). In EHEC, the T3SS effector $EspF_U$ directly binds to N-WASP and mediates actin pedestal formation by Tir, independently of Tir phosphorylation (Campellone et al., 2004; Garmendia et al., 2004).

Bartonella henselae is a bacterial pathogen whose lifestyle can be considered "epicellular". After adhesion to endothelial cells, it secretes *Bartonella* effector proteins (Beps) into the host cell cytoplasm through a type IV secretion system. BepC and F induce a massive rearrangement of the actin cytoskeleton that results in the formation of a plasma membrane structure around aggregated bacteria called the invasome (Dehio et al., 1997; Eicher and Dehio, 2012; Rhomberg et al., 2009; Truttmann et al., 2011) (Fig. 17). Although described as an internalization structure, the invasome is usually larger than the thickness of the endothelial cell itself and is therefore unlikely to entirely end up in the cytoplasm. The molecular mechanism of actin polymerization by Beps has not been determined yet.

In summary, intracellular as well as extracellular bacterial pathogens use sophisticated mechanisms to promote plasma membrane remodeling, which is required for efficient infection, via the hijacking of the host cell actin polymerization machineries. The case of *N. meningitidis* is unique because bacteria induce a remodeling of the host cell plasma membrane that does not depend on actin polymerization. Moreover, plasma membrane protrusions induced by meningococcus are morphologically distinct from the ruffles induced by intracellular pathogens, EPEC-induced pedestals or *Bartonella*–induced invasome. Therefore, *N. meningitidis*-induced plasma membrane remodeling needs to be studied, especially because it is likely to play a central role in the pathophysiology of meningococcal disease.

RESULTS

1. Paper I: Early sequence of events triggered by the interaction of *Neisseria meningitidis* with endothelial cells

Background

Until the late 2000s, no fluorescence live cell imaging was used to study of the interaction of *N. meningitidis* with host endothelial cells. Therefore, the host cell response was mainly observed at late time points of infection, and no information was available regarding the dynamics of plasma membrane remodeling or F-actin accumulation. These shortcomings were mainly linked to the difficulty to transfect endothelial cells. However, the development of electroporation eventually made live cell imaging of endothelial cells much easier. Subsequently, the engineering of plasmids for the expression of fluorescent proteins in meningococcus allowed the visualization of the bacteria-host cell crosstalk in a dynamic fashion.

In the following study, we used spinning disc confocal live cell imaging to visualize the early steps of the host cell response to meningococcus bacterial aggregates. This led to the description of the sequence of events that takes place within the first minutes of contact between *N. meningitidis* and the host cell plasma membrane.

Main conclusions

The main findings of this first study are i) that plasma membrane remodeling, but not F-actin accumulation, is the first event that occurs upon T4P-mediated adhesion of meningococcus to endothelial cells, ii) that actin polymerization follows plasma membrane remodeling, iii) that plasma membrane remodeling is a rapid process, iv) that plasma membrane remodeling is dependent on host cell plasma membrane cholesterol and of meningococcus minor pilin PilV, v) that plasma membrane remodeling is not dependent on ERM proteins, F-actin polymerization or host cell ATP and vi) that pilus retraction promotes intimate contact between bacteria and the host cell surface rather than plasma membrane remodeling per se.

Of note, soon after this study, it was shown in the lab that the minor pilin PilV does not mediate directly plasma membrane remodeling but rather maintains an optimal amount of T4P at the surface of the bacteria, thus allowing T4P-mediated functions. In a Δ*pilV* insertion mutant, the number of T4P decreases by 30-40% compared to the wildtype strain. This modest decrease is sufficient to render the Δ*pilV* bacteria incompetent for host cell surface reorganization (Imhaus and Dumenil, 2014).

Therefore, our first study demonstrates that initial plasma membrane remodeling induced by meningococcus can exist in the absence of any other response from the host cell and is a T4P-driven process.

Cellular Microbiology (2014) doi:10.1111/cmi.12248

Early sequence of events triggered by the interaction of *Neisseria meningitidis* with endothelial cells

Magali Soyer,[1,2†] Arthur Charles-Orszag,[1,2] Thibault Lagache,[3] Silke Machata,[1,2] Anne-Flore Imhaus,[1,2] Audrey Dumont,[1,2] Corinne Millien,[1,2] Jean-Christophe Olivo-Marin[3] and Guillaume Dum nil[1,2*]

[1]*Universit Paris Descartes, Facult de M decine Paris Descartes, Paris F-75006, France.*

[2]*INSERM, U970, Paris Cardiovascular Research Center, Paris F-75015, France.*

[3]*Institut Pasteur, Unit d'Analyse d'Images Quantitative, Centre National de la Recherche Scientifique, Unit de Recherche Associ e 2582, Paris, France.*

Summary

***Neisseria meningitidis* is a bacterium responsible for severe sepsis and meningitis. Following type IV pilus-mediated adhesion to endothelial cells, bacteria proliferating on the cellular surface trigger a potent cellular response that enhances the ability of adhering bacteria to resist the mechanical forces generated by the blood flow. This response is characterized by the formation of numerous 100 nm wide membrane protrusions morphologically related to filopodia. Here, a high-resolution quantitative live-cell fluorescence microscopy procedure was designed and used to study this process. A farnesylated plasma membrane marker was first detected only a few seconds after bacterial contact, rapidly followed by actin cytoskeleton reorganization and bulk cytoplasm accumulation. The bacterial type IV pili-associated minor pilin PilV is necessary for the initiation of this cascade. Plasma membrane composition is a key factor as cholesterol depletion with methyl-β-cyclodextrin completely blocks the initiation of the cellular response. In contrast membrane deformation does not require the actin cytoskeleton. Strikingly, plasma membrane remodelling under microcolonies is also independent of common intracellular signalling pathways as cellular ATP depletion is not inhibitory. This study shows that bacteria-induced plasma membrane reorganization is a rapid event driven by a direct cross-talk between type IV pili and the plasma membrane rather than by the activation of an intracellular signalling pathway that would lead to actin remodelling.**

Received 19 June, 2013; revised 12 November, 2013; accepted 3 December, 2013. *For correspondence. E-mail guillaume.dumenil@inserm.fr; Tel. (+33) 01 53 98 80 49; Fax (+33) 01 53 98 79 53.
†Present address: Randall Division of Cell and Molecular Biophysics, Room 2.34, King's College London, New Hunt's House, Guy's Campus, London SE1 1UL, UK.

Introduction

Neisseria meningitidis (or meningococcus) is a Gram-negative bacterium responsible for two severe forms of infection, sepsis and meningitidis, that can occur either separately or together (van Deuren *et al.*, 2000). The reservoir of meningococcus is the human upper airways, and particularly the nasopharynx mucosa. Meningococcus can be isolated from the throat of a large percentage of the human population in the absence of symptoms. In the case of invasive infection bacteria can be isolated from the bloodstream and/or the cerebrospinal fluid (Pron *et al.*, 1997; Nassif *et al.*, 2002).

The ability of meningococci to adhere to host cells has emerged as a key step in the pathogenesis process (Melican and Dumenil, 2012). In the nasopharynx the bacterium adheres to epithelial cells and forms microcolonies on the cellular surface likely allowing its survival and proliferation at this site prior to accessing the blood (Stephens *et al.*, 1983). Histological analysis of human cases of invasive infection reveals bacteria in tight association with blood vessels in different organs including the brain. Bacteria appear as tight clusters that can completely fill capillaries (Mairey *et al.*, 2006). Infected capillaries in the brain are likely sites of cerebrospinal fluid colonization in meningitis cases. Recently, the importance of bacterial interaction with endothelial cells in triggering vascular damage during sepsis has been demonstrated in an animal model of infection (Melican *et al.*, 2013).

Neisseria meningitidis expresses several adhesins. Type IV pili (tfp) have emerged as central players because they are expressed by all clinical strains and because adhesion is drastically reduced in the absence of these bacterial structures. Tfp are long filamentous organelles that can measure up to several microns. Tfp are helical polymers of a protein known as the major pilin, PilE in the

case of *Neisseria* species (Giltner *et al*., 2012). Functional pilus expression on the bacterial surface requires a complex machinery composed of over 20 proteins (Carbonnelle *et al*., 2006).

Following adhesion, bacteria and host cells engage in an elaborate cross-talk process, which also involves type IV pili (Merz *et al*., 1999; Mikaty *et al*., 2009). Adhering meningococci trigger a local remodelling of host cell plasma membrane. The area of plasma membrane located under bacterial microcolonies forms numerous flexible filopodia-like structures intertwined between aggregated bacteria (Eugene *et al*., 2002). This cellular response has been observed *in vitro* on cells in culture and has been seen in human cases of meningococcemia (Nassif *et al*., 2002). Bacteria-induced protrusions allow most bacteria to be in direct contact with host cells and this has been shown to enhance the cohesion of bacterial microcolonies. In the absence of cellular protrusions the mechanical forces generated by blood flow dissociate bacterial aggregates thus preventing efficient endothelium colonization (Mikaty *et al*., 2009). Type IV pili are multicomponent machineries that are known to be involved in the cross-talk with host cells but the exact mechanism by which tfp induce plasma membrane reorganization is not known. We previously described the importance of the minor pilin PilV in this process (Mikaty *et al*., 2009). PilV is a protein with structural features common to the major pilin and is thought to insert in the pilus structure and modify its properties. Other studies pointed to the importance of pilus retraction, a process powered by the PilT ATPase (Merz *et al*., 1999; Higashi *et al*., 2009).

At the molecular level, membrane remodelling is accompanied by the accumulation of several proteins under the microcolony that organize in a shape reminiscent of a honeycomb. This structure is sometimes referred to as a 'cortical plaque'. Such structures are formed by the accumulation of adhesion molecules, membrane receptors (Merz *et al*., 1999; Doulet *et al*., 2006), molecular linkers, such as ezrin and moesin (Eugene *et al*., 2002), components of the actin cytoskeleton and junctional proteins (Coureuil *et al*., 2009). Another important consequence of the recruitment of junctional proteins is the weakening of existing junctions between endothelial cells, potentially providing a way for bacteria to exit the vessel lumen (Coureuil *et al*., 2009). A key aspect of this cross-talk is the activation of a number of signalling pathways, including the activation of Src kinase (Hoffmann *et al*., 2001), of Rho, Cdc42 (Eugene *et al*., 2002), Rac1 (Lambotin *et al*., 2005) GTPases, PI3-kinase, mitogen-activated protein kinases (Sokolova *et al*., 2004) and most recently of the β2 adrenergic receptor/β arrestin pathway (Coureuil *et al*., 2010). The exact relationship between these different pathways, their impact on protein accumulation and plasma membrane remodelling remain unclear.

The aim of this study is to better understand the mechanisms of the cross-talk between the bacterium and the host cell, a key feature of the pathogenesis process that stabilizes bacterial aggregates on the host cell surface and favours the opening of cellular junctions. Although numerous components involved in bacterial cross-talk with host cells have been described both on the cellular and bacterial side, the functional connections and sequence of events remain unclear. Most studies were performed on fixed cell preparations taken from a few infection time points, thus only providing a static view of the tfp-mediated cellular response. The value of dynamic studies is increasingly recognized to understand cellular biology processes in general (Taylor *et al*., 2011) and host pathogen interactions in particular (Ray *et al*., 2010). The present study was designed to decrypt how the multiple components involved in meningococcus-induced cellular response are organized temporally with high resolution both in time and in space. To gain high temporal and spatial resolution we took advantage of spinning disc confocal microscopy. This approach allowed multidimensional imaging with rapid acquisition of Z-stacks at several wavelengths every 5 s over selected periods of time. We found that meningococci-triggered plasma membrane remodelling occurs prior to actin reorganization and independently of ATP-dependent intracellular pathways.

Results

High spatio-temporal resolution imaging of cellular components under meningococcus aggregates

Ezrin, a cytoplasmic protein linking the actin cytoskeleton with the cytoplasmic tail of transmembrane receptors, was chosen as a reporter protein using a GFP fusion protein. Ezrin has been frequently used as a read-out of cortical plaque formation on fixed samples (Eugene *et al*., 2002; Mikaty *et al*., 2009). Bacteria-induced cellular response occurs only after a number of bacterial divisions and is visible only under aggregates containing over 10 bacteria (Movie S1). To avoid issues linked to bacterial proliferation and to synchronize the infection process, bacterial aggregates that spontaneously form in culture were used for the infection. Human umbilical vein endothelial cells (HUVECs) were transfected with a construct expressing carboxy-terminally tagged ezrin (Lamb *et al*., 1997) and infected with bacterial aggregates expressing the mCherry fluorescent protein.

Contact of bacterial aggregates with transfected cells led to the rapid formation of a typical 'honeycomb

lattice' type of organization of ezrin under microcolonies (Fig. 1A, Movie S2). Ezrin accumulation was detectable as early as 5 s after initial contact in certain cases. The effect was robust as over 90% of bacterial aggregates triggered a visible response upon contact with the cells.

To obtain quantitative evaluation of cellular protein accumulation under microcolonies we designed a plug-in in the ICY image analysis software called *Intensity profiler* (de Chaumont *et al*., 2012). Analysis is performed within a volume defined by a region of interest (Fig. 1A, ROI-1). Another ROI is selected on the same cell in a similar area relative to the nucleus and cell border to determine the background signal (Fig. 1A, ROI-2). *Intensity profiler* first determines the time of contact between the bacterial aggregates and the cells using the mCherry channel (t_{ini}). To ensure a three-dimensional quantification of the GFP fusion protein, an averaged projection over the Z-axis was used. The raw fluorescence intensity in both ROI was quantified and plotted over time (Fig. 1B). The raw fluorescence intensity was then corrected for background and bleaching, to obtain the net fluorescence intensity (Fig. 1C). Next, the ratio between the corrected signal at a given time relative to the time of contact was calculated to minimize potential effects of local differences in intensity (Fig. 1D). The same procedure was repeated to accumulate 28 adhesion events and 10 representative curves are presented (Fig. 1E). The same approach based on averaging of curves was used for the remainder of the study. Ezrin recruitment typically showed a strikingly rapid increase. Fluorescence continued to increase until a plateau value of about 1.8-fold over the initial value after 5 min.

Spinning disc confocal microscopy combined with the *Intensity profiler* plug-in for the ICY software thus provides an efficient way to quantitatively assess the recruitment of cellular proteins under bacterial aggregates with high resolution in time and space. This approach reveals a potent and rapid response following bacterial contact.

Bacterial factors involved in membrane remodelling

To determine at which stage PilV is involved in the cross-talk with host cells, aggregates formed by a mutant defective for PilV expression (Δ*pilV*) were used for infection of ezrin-GFP transfected cells. Cells challenged with the mutant strain failed to initiate the accumulation of ezrin (Fig. 2A). Similar results were obtained for actin and membrane accumulation (Fig. S1). Complementation of the *pilV* mutation with a wild-type copy restored the cellular response (Fig. S2). The Δ*pilT* mutant displayed a strong heterogeneity, some aggregates triggered a potent response and others no visible response (Fig. 2B). On average, ezrin recruitment under Δ*pilT* aggregates was largely impaired but with a progressive increase in time at a low rate (Fig. 2C). Similar results were obtained for the recruitment of actin and membrane (Fig. S1). Complementation of the *pilT* mutation with a wild-type copy restored the ezrin recruitment (Fig. S2). These results suggested that the Δ*pilT* mutant might be altered in the time at which the cellular components start to accumulate. To demonstrate this possibility the time at which the response was initiated was determined with longer times of infection in intervals of 5 min. While wild-type bacteria triggered the cellular response within seconds after contact, the Δ*pilT* mutant was slow in triggering ezrin reorganization (Movie S3). The time of response initiation was highly variable with an average of 40 min (Fig. 2D). Interestingly, in certain instances Δ*pilT* aggregates initiated a response, which then disappeared, a phenomenon that was never observed in wild-type bacteria. Pilus retraction is thus necessary to determine the time of initiation and maintenance of the response.

Our observations indicate that the minor pilin PilV acts as a trigger on the host cell to induce membrane remodelling and subsequent cellular components accumulation underneath aggregates. The PilT-dependent retraction is not in itself necessary to trigger the response as many aggregates eventually trigger this response but it provides the appropriate conditions for the initiation and maintenance of the process.

Kinetics of accumulation of cellular components under N. meningitidis *microcolonies*

A large number of proteins have been described to accumulate in the cortical plaque under *N. meningitidis* microcolonies and as a first approach we chose to focus the study on four representative cellular components: the actin cytoskeleton, the plasma membrane, the cytoplasm and ezrin as described above. The LifeAct peptide fused to mCherry was used as a probe for F-actin accumulation. A GFP targeted to the inner leaflet of the plasma membrane with a farnesylation signal (CAAX box) was used to visualize membrane remodelling and accumulation (Aronheim *et al*., 1994). Cytoplasm was visualized by expression of unmodified GFP. HUVECs cells were transfected with these plasmids, infected with pre-formed aggregates and data were analysed using *Intensity profiler* as described before.

At first glance, accumulation of plasma membrane, F-actin and cytoplasm was similar to that of ezrin both morphologically and kinetically (Fig. 3A). A typical 'honeycomb' type of morphology could be observed for all reporter proteins. In the case of F-actin, stress fibres were frequently observed radiating from the site of

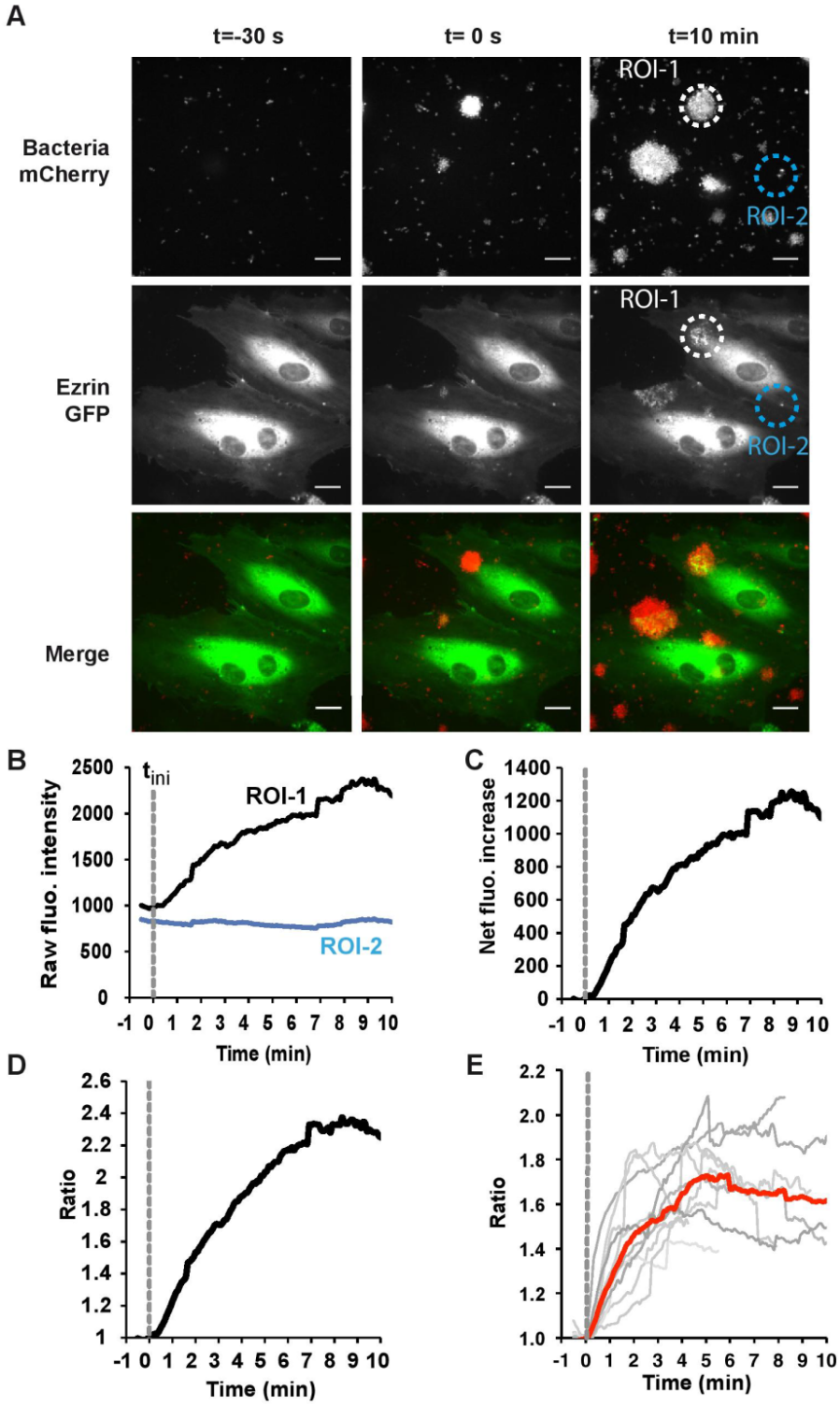

Fig. 1. Quantitative assessment of host cell protein accumulation under adhering *N. meningitidis* aggregates.
A. Endothelial cells expressing ezrin-GFP (middle panels) were infected with mCherry-expressing meningococcus aggregates (top panels). Bottom panels show the merged images. Scale bars represent 20 μm. Region of interest 1 (ROI-1) was selected for being a site of contact of an aggregate and ROI-2 arbitrarily chosen as a 'background' area in a similar area of the same cell.
B. The raw fluorescence intensity in the volume defined by the two ROIs was plotted as a function of time. The time of contact of the bacterial aggregate with the endothelial cell, t_{ini}, is determined automatically by the *Intensity profiler* plug-in.
C. The net fluorescence intensity inside ROI-1 was calculated by correcting the raw intensity from bleaching, thermal fluctuations and background as determined from ROI-2.
D. The ratio of the fluorescence intensity at the different times points relative to the intensity at t_{ini} (fold induction) was plotted as a function of time.
E. The ratio of fluorescence of 10 representative adhesion events were plotted and the average of 28 events represented (red line).

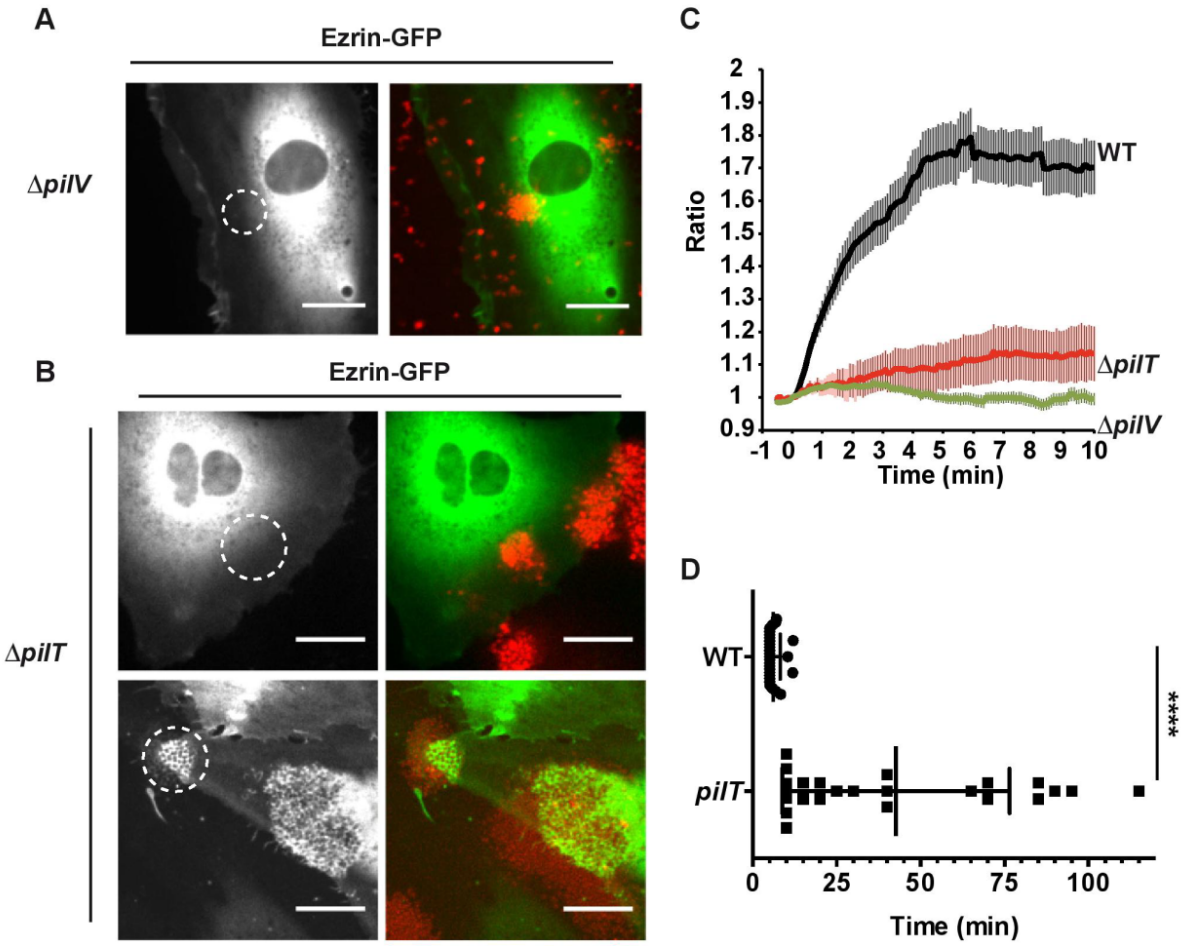

Fig. 2. Bacterial factors involved in bacteria-induced plasma membrane remodelling. Endothelial cells transfected with ezrin-GFP were infected with aggregates formed by the *pilV*- and *pilT*-deficient strains (Δ*pilV*, Δ*pilT*).
A. Snapshot from a *pilV*-infected cell.
B. Snapshots from two adhesion events with the *pilT* strain representing the two types of behaviours.
C. Kinetics of ezrin accumulation in the Δ*pilV* (green curve) and Δ*pilT* (red curve) strains.
D. The time at which ezrin accumulation is detectable was plotted as a function of time within intervals of 5 min. Each dot corresponds to a single adhesion event. Stars indicate significance using a Student *t*-test.
Error bars are ± SEM. Scale bars represent 20 μm.

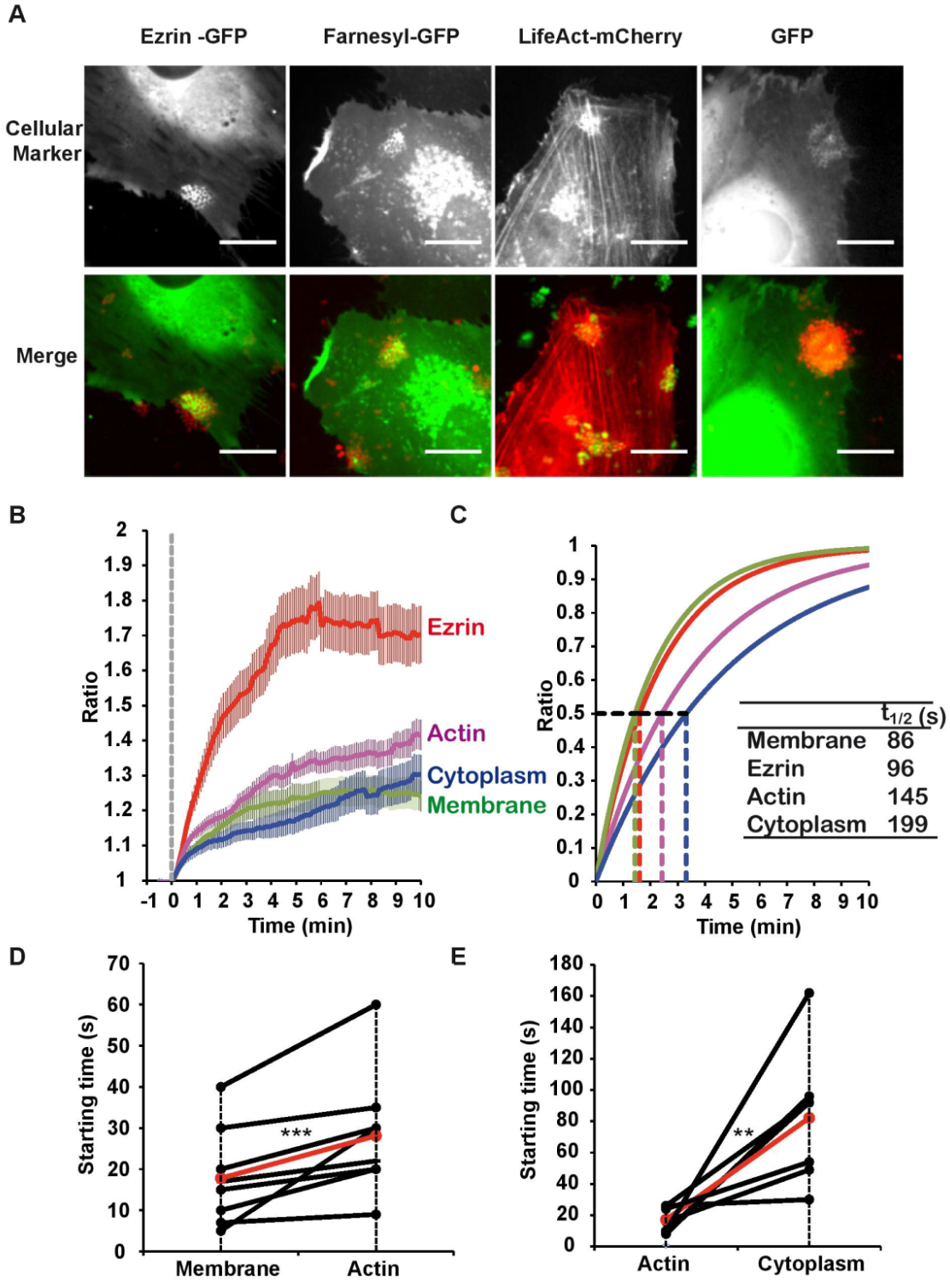

Fig. 3. Kinetics of accumulation of cellular components under bacterial aggregates.
A. Endothelial cells were transfected with fluorescent markers for ezrin (ezrin-GFP), plasma membrane (Farnesyl-GFP), actin cytoskeleton (LifeAct-mCherry) or cytoplasm (GFP) and infected for 10 min with preformed aggregates. Scale bars represent 20 μm.
B. The ratio of fluorescence intensity was determined and averaged for 25–30 events of aggregates contacting endothelial cells transfected with the four fusion proteins. The dotted line represents time of contact (t_{ini}). Errors bars indicate SEM.
C. Each average curve was normalized between 0 (t_{ini}) and 1 (t_{max}) and fitted to an exponential curve. Times corresponding to a 50% increase are indicated in the table ($t_{1/2}$) in seconds.
D. Endothelial cells were co-transfected with constructs allowing expression of Farnesyl-GFP and LifeAct-mCherry and infected with bacteria expressing a blue fluorescent protein. Time at which accumulation of the two fusion proteins is first detected (starting time) was plotted for individual adhesion events ($n = 8$). The line corresponding to the average appears in red.
E. Endothelial cells were co-transfected with constructs allowing expression of LifeAct-mCherry and unmodified GFP, infected and analysed as in (D).
Stars indicate significance according to a paired Student *t*-test.

adhesion. All markers accumulated rapidly after bacterial contact and reached a maximum intensity after 2–4 min. To reduce the variation between individual adhesion events and to enhance resolution, curves of protein accumulation following 20–30 adhesion events were averaged (Fig. 3B). Ezrin recruitment was markedly more intense than other markers. Whereas ezrin accumulation showed a 1.8-fold increase, actin only exhibited a 1.4-fold rise. To compare the kinetics of recruitment of the different proteins, values were normalized and an exponential regression was performed (Fig. 3C). A time at which recruitment reaches 50% of maximum can be inferred from these curves ($t_{1/2}$). Membrane, ezrin, actin and bulk cytoplasm showed a $t_{1/2}$ of ~86, ~96, ~145 and ~199 s respectively. This analysis suggests a sequence of events with ezrin and membrane being recruited first, followed by actin and finally bulk cytoplasm. To confirm these results, double transfections were performed to follow the recruitment of two cellular components at the same time in a single adhesion event. In these experiments bacteria expressing the blue fluorescence protein mTagBFP2 were used (Subach *et al.*, 2011). For each adhesion event the time at which recruitment of the membrane marker and actin could be detected were analysed (Fig. 3D). For every event analysed the membrane marker was detected before actin. The lag between membrane and actin was diverse varying from 2 to 25 s with an average time difference of 10 s. The same strategy was used to compare actin and bulk cytoplasm accumulation also confirming previous observations with actin reaching the microcolony 60 s before bulk cytoplasm (Fig. 3E).

Our results show that the accumulation of plasma membrane under the bacterial microcolony is extremely rapid, starting nearly immediately after contact of the microcolony with the host cell and rapidly reaching a maximum intensity. They further point to an unexpected sequence of events with membrane and ezrin accumulating first under the bacterial aggregates followed by F-actin and finally bulk cytoplasm.

Actin polymerization is not the triggering event for bacteria induced plasma membrane reorganization

The above results indicated that membrane accumulation precedes F-actin accumulation and raised the question of a functional role of actin in this process. To address this, actin cytoskeleton was disrupted by cytochalasin D (CD) treatment prior to infection. Treatment of endothelial cells with 1 μM CD for 20 min led to a complete disruption of actin filaments (Movie S4). On CD-treated cells both membrane and ezrin started to accumulate soon after contact between the aggregate and the cell surface (Fig. 4A). Strikingly, maximal intensities for ezrin and membrane were higher than in untreated conditions with 2.2- and 1.7-fold increases respectively (Fig. 4B and C). The accumulation only reached saturation 10 min after contact. Similar results were obtained when bulk cytoplasm was measured in the presence of the actin-disrupting drug.

Given the role of ezrin as a linker between the actin cytoskeleton and transmembrane receptors these results questioned the implication of ezrin in bacteria induced plasma membrane reorganization. To evaluate the role of ERM proteins in this process their level of expression was decreased using an siRNA knock-down strategy. ERM levels were reduced to an average of 26.12% ± 2.647 (Fig. 4D and E; Fig. S3). Bacterial aggregates accumulated the same amount of plasma membrane marker in the knock-down cells when compared with the cells treated with the control siRNA (Fig. 4F). ERM proteins thus do not participate in the early phases of the process when plasma membrane is recruited. Nevertheless, knock-down of ERM proteins reduced the accumulation of actin under microcolonies. After 2 h of infection only 32.1 ± 5.2% of microcolonies showed efficient actin accumulation in cells treated with the knock-down siRNA whereas in cells treated with the control siRNA, 77.0 ± 7.5% of microcolonies showed intense actin staining.

These observations show that actin polymerization is not the leading event of the cellular response, as polym-

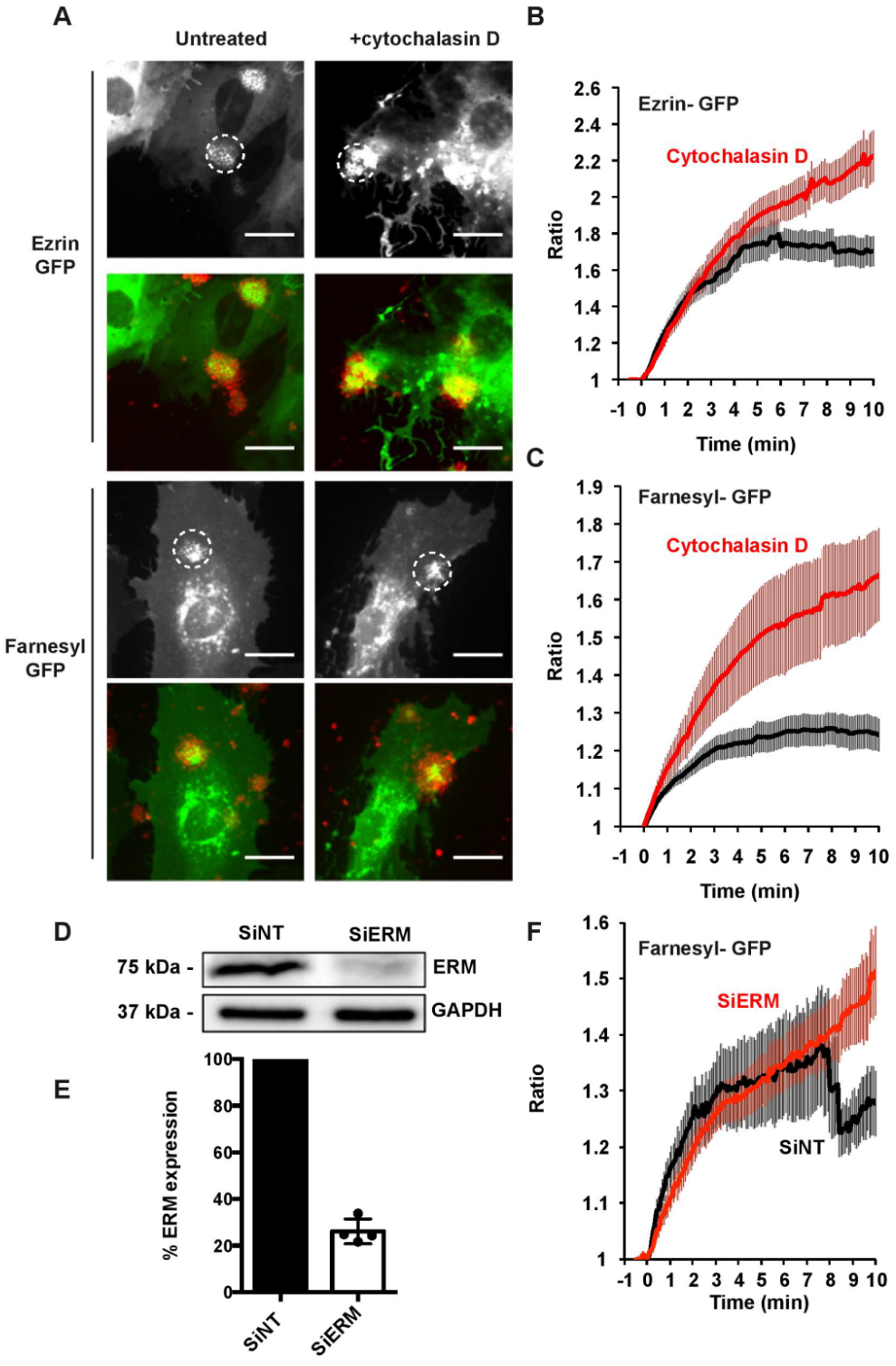

Fig. 4. Membrane remodelling and ezrin accumulation do not require an active actin cytoskeleton.
A. Endothelial cells transfected with ezrin-GFP (top panels) or Farnesyl-GFP (bottom panels) were treated with the actin-disrupting agent cytochalasin D (1 μM) and infected for a period of 10 min. Scale bars represent 20 μm.
B. Ratio of fluorescence intensity for ezrin-GFP. The red line corresponds to samples treated with cytochalasin D ($n = 20$) while the black line the untreated controls ($n = 28$).
C. Ratio of fluorescence intensity for Farnesyl-GFP. The red line corresponds to samples treated with cytochalasin D ($n = 20$) while the black line the untreated controls ($n = 28$). Errors bars are ± SEM.
D. Level of ERM family of proteins following siRNA knock-down assessed by Western blot. GAPDH was used as a control.
E. Quantitative analysis of ERM depletion in four experiments.
F. Ratio of fluorescence intensity for Farnesyl-GFP. The red line corresponds to samples treated with ERM siRNA ($n = 20$) while the black line to samples treated with the control siRNA ($n = 10$). Errors bars are ± SEM.

erization inhibition does not affect membrane remodelling. On the contrary actin cytoskeleton disruption favoured plasma membrane accumulation possibly by releasing cellular membrane tension. ERM proteins also do not play a role in the early events but are important for actin accumulation.

Cholesterol depletion blocks the initiation of bacteria-induced plasma membrane reorganization and actin cytoskeleton accumulation

As the plasma membrane reorganization was the earliest event detectable following bacterial contact we focused on the properties of the plasma membrane itself. Cholesterol depletion from cell membranes with methyl-β-cyclodextrin (MβCD) was previously shown to affect bacteria induced cellular response after 2 h of infection (Mikaty *et al*., 2009) and we then evaluated the impact of this drug on the kinetics of the process. When MβCD-treated cells were infected by meningococci, membrane remodelling, F-actin or ezrin accumulations were not found underneath aggregates (Fig. 5A–D).

Cholesterol is known to be an important structuring component of the lipid bilayer, allowing clustering of lipids and proteins in specific domains. The results presented above demonstrate that plasma membrane properties are critical in the cross-talk between the bacteria and host cells but the exact mechanism of this effect still needs to be established. These results are also in favour of a sequence of events where membrane deformation is the initial event leading to actin cytoskeleton reorganization and accumulation of associated proteins.

Membrane remodelling does not require intracellular ATP

As the actin cytoskeleton does not appear to play a significant role in bacteria-induced plasma membrane reorganization, intracellular pathways activated upon bacterial adhesion were investigated. Recently, the β2-adrenoceptor (β2AR) was reported to participate in a pathway leading to the recruitment of cellular components under adhering *N. meningitidis* (Coureuil *et al*., 2010; Lecuyer *et al*., 2012). On fixed samples, induction of the β2AR endocytosis by the specific agonist isoproterenol (ISO) was shown to reduce the recruitment of ezrin under microcolonies after 2 h of infection (Coureuil *et al*., 2010) but the impact on membrane reorganization or the kinetics of this effect is not known.

Cells were treated for 2 h prior to infection with 10 μM ISO and accumulation of cellular components was monitored. The accumulation of ezrin started as rapidly as on control cells (Fig. 6A), almost immediately after contact between the aggregates and the cell surface. However, in isoproterenol-treated cells ezrin reached a plateau earlier and at a lower ratio (1.5 compared with 1.8). Similar results were obtained for F-actin accumulation with normal initiation and lower plateau values (Fig. 6B). Thus perturbation of β2AR signalling does not affect the initiation of ezrin and F-actin accumulation but rather the extent of the process. Accumulation of the plasma membrane marker showed a strikingly different pattern with a higher rate of accumulation at initial time points and a delayed time prior to reaching plateau at a higher value (Fig. 6C). These observations indicate that the β2AR is not involved in the induction of plasma membrane remodelling but affects the extent of intracellular components accumulation.

Rather than testing individual signalling pathways, a strategy blocking intracellular signalling in a global way was sought. Since many signalling cascades engage secondary messengers whose production or activation require energy in the form of ATP, we assessed the effect of energy depletion on the accumulation of cellular components underneath meningococcus aggregates. Treatment of HUVECs with an energy-depleting medium (see *Experimental procedures*) blocking glycolysis and respiration led to inhibition of ATP production (9 ± 5% of normal ATP levels). When energy-depleted cells were challenged with bacterial aggregates, ezrin and actin accumulated slower compared with control cells (Fig. 6D and E). Membrane, however, still accumulated underneath aggregates on energy-depleted cells with a similar profile as on control cells (Fig. 6F) and even reaching higher values. To evaluate the functional impact of the ATP depletion, this treatment was tested on the ability of the pathogenic bacterium *Shigella flexneri* to induce the formation of entry foci upon invasion. In the same conditions, ATP

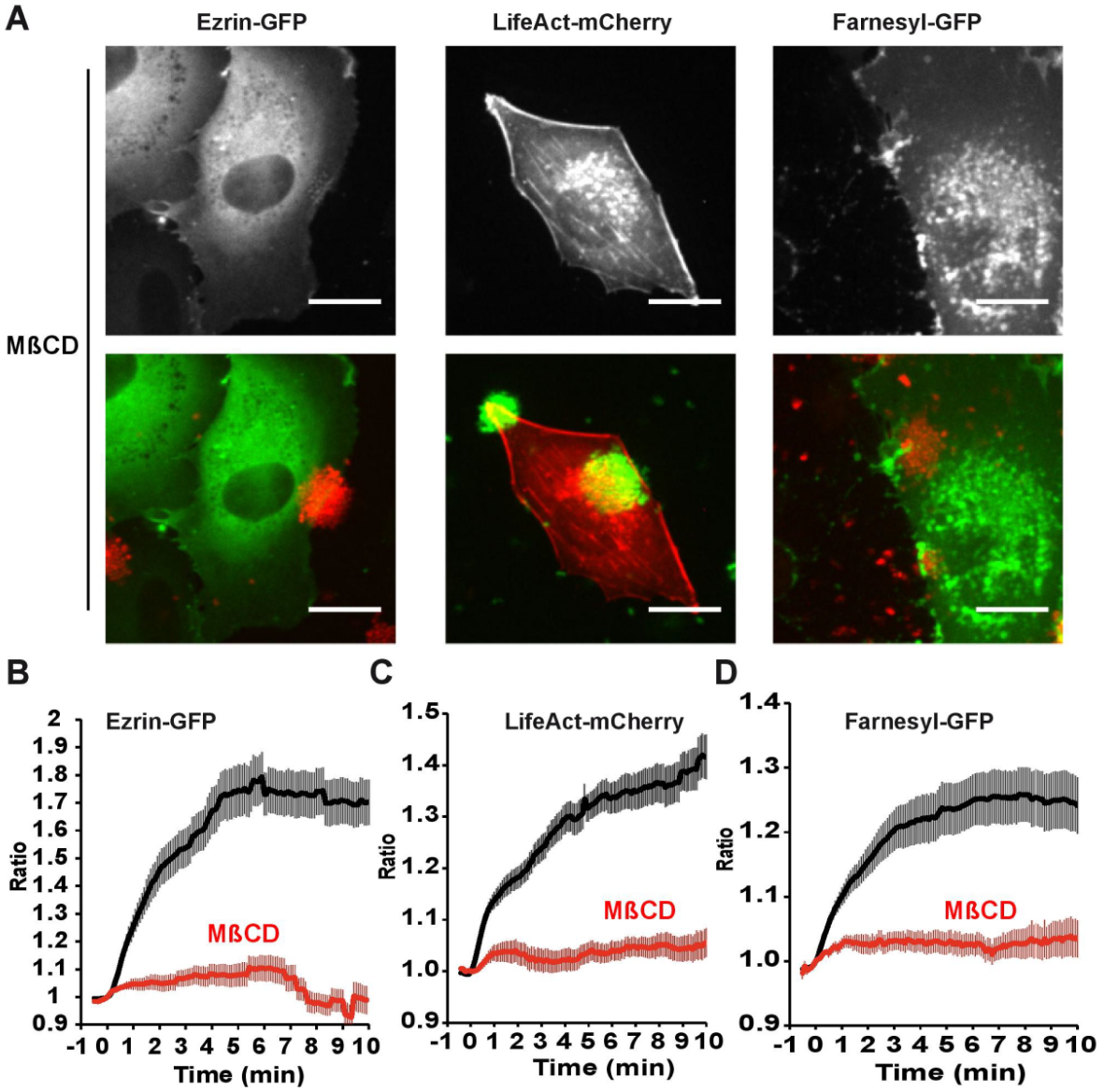

Fig. 5. Cholesterol depletion from the plasma membrane blocks the initiation of meningococcus-induced cellular response. Endothelial cells transfected with ezrin-GFP, LifeAct-mCherry and Farnesyl-GFP were treated with the cholesterol-depleting drug Methyl-β-cyclodextrin (MβCD) and infected with pre-formed aggregates.
A. Snapshots after 10 min of infection show ezrin (left), LifeAct (middle) and farnesyl (right) fusion proteins. Scale bars represent 20 μm.
B–D. Kinetics of accumulation of the fusion proteins was determined. Red curves represent the MβCD-treated samples. (B) Ezrin-GFP; (C) LifeAct-mCherry; (D) Farnesyl-GFP.

depletion decreased the ability of *S. flexneri* to form entry foci by over 10-fold, confirming the efficiency of the depletion. Strikingly, energy in the form of ATP in host cells is thus not required for meningococcus to induce plasma membrane remodelling indicating that common intracellular pathways are not required for this process.

Discussion

In the past, our knowledge of the interaction of *N. meningitidis* with host cells largely relied on static immunofluorescence or electron microscopy images. The present study, based on live cell imaging, provides a more

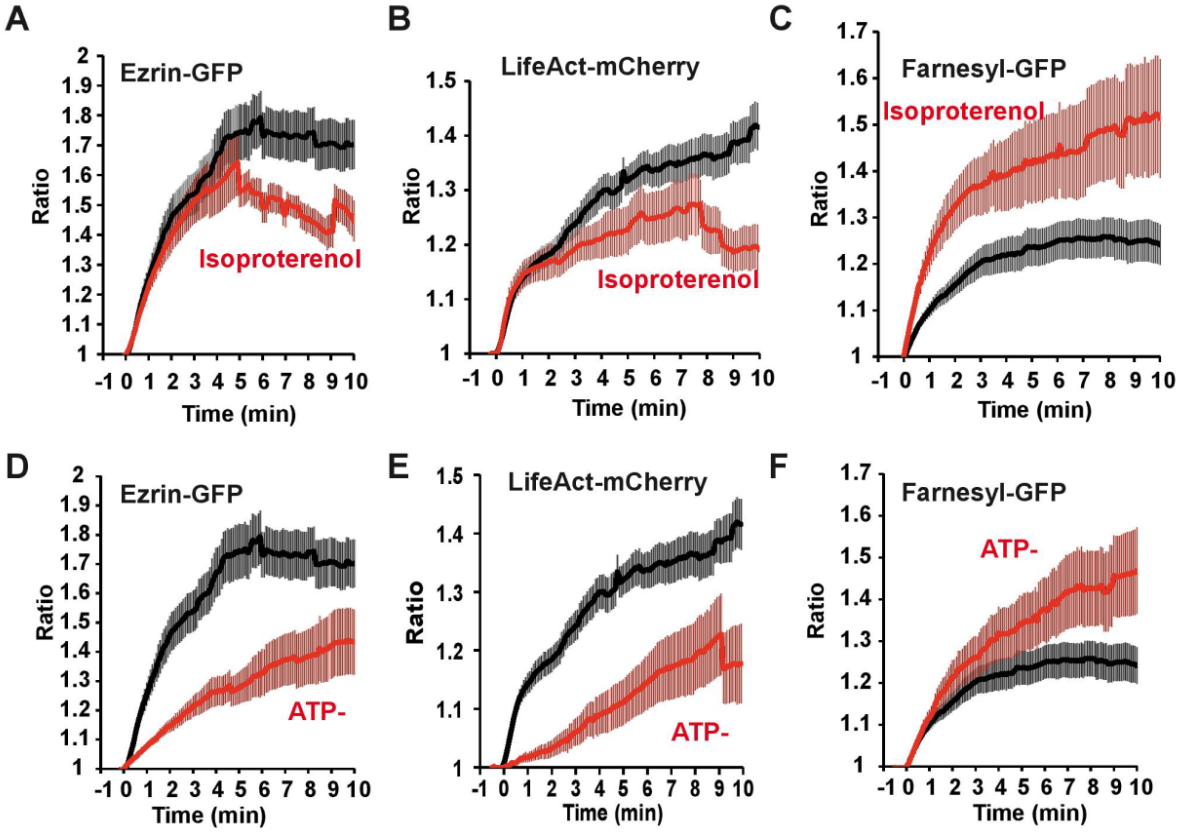

Fig. 6. Relationship between membrane remodelling and intracellular signalling cascades. Endothelial cells were transfected with ezrin-GFP (A and D), LifeAct-mCherry (B and E), Farnesyl-GFP (C and F), and infected with pre-formed aggregates. Curves corresponding to the ratio of fluorescence in cells pre-treated with the β2AR agonist isoproterenol (A, B and C) or ATP-depletion medium (D, E and F) appear in red.

complete view by taking into account the complex spatio-temporal dimension of the process. This approach reveals a rapid sequence of events depicted in Fig. 7A that starts a few seconds only after bacterial contact with cells.

Each individual bacterium expresses a large number of pili on its surface that interact with pili from neighbouring bacteria thus forming a meshwork that allows the formation of spherical bacterial aggregates. Type IV pili are heterogeneous in length and can measure up to several microns. The first contact between bacterial aggregates and host cells is most probably mediated by the pili themselves, rapidly followed by the bacterial bodies. The first cellular event that could be detected was the plasma membrane reorganization and accumulation under the bacterial aggregates. Ezrin accumulation followed the kinetics of the plasma membrane and about 15 s later reorganization of actin cytoskeleton could be detected. Finally, bulk cytoplasm started to accumulate with an average value of 80 s. The most striking result of this kinetic analysis is the accumulation of membrane prior to actin as the opposite would be expected in classical filopodia formation.

The use of pharmacological inhibitors and knock-down experiments allowed the dissection of cellular pathways involved and validated a two-steps model with plasma membrane being recruited first followed by reorganization of the actin cytoskeleton (Fig. 7B). Consistently with the kinetics study, we showed that plasma membrane reorganization occurs separately from the actin cytoskeleton as perturbation of actin polymerization with cytochalasin D does not slow down the process. On the contrary, actin cytoskeleton disorganization in fact enhanced the amount of plasma membrane accumulation under bacterial aggregates. This observation could be related to the implication of the actin cytoskeleton in maintaining surface tension (Hochmuth *et al.*, 1996). In the absence of actin cytoskeleton the surface tension is lower and bacteria may be better able to induce the local accumulation of plasma membrane. In agreement with an actin-independent process ERM knock-down experiments did

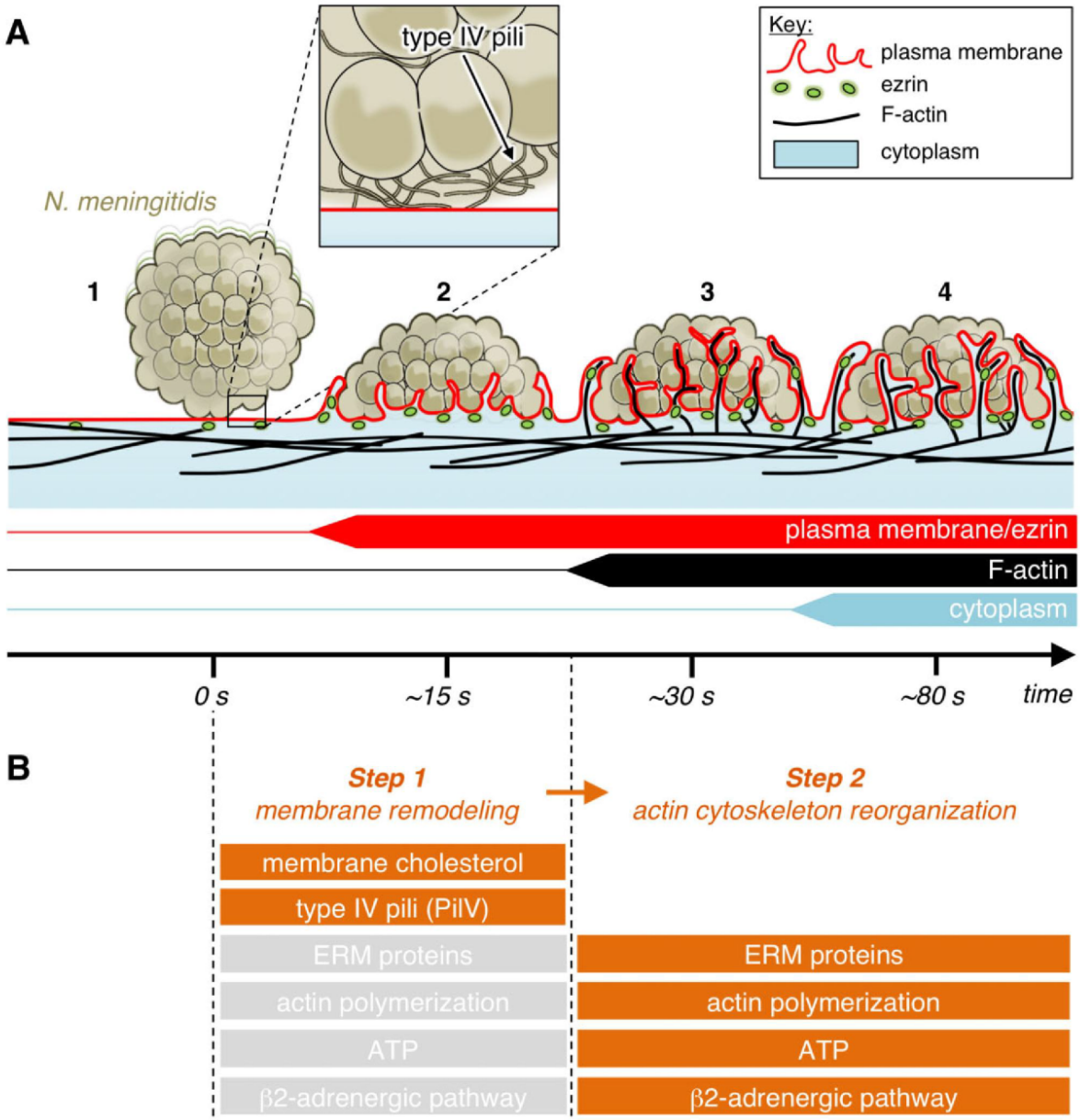

Fig. 7. Chronological sequence and functional relationship between the different early events that follow bacterial adhesion.
A. Schematic representation of the sequence of events triggered by the contact of meningococcus with endothelial cells. (1) Bacterial contact is initiated by type IV pili; (2) Plasma membrane accumulates under the microcolony (red) along with membrane-bound ezrin (green); (3) Cortical actin reorganizes under the remodelled plasma membrane; (4) Bulk cytoplasm accumulates.
B. Early events triggered by bacterial contact can be best described in the form of two sequential steps. Step 1 is dominated by the reorganization of the plasma membrane under the microcolony to form 100 nm cellular protrusions. Step 1 is dependent on the presence of type IV pili (more specifically the activity of the PilV protein) and on the presence of cholesterol in the plasma membrane. Step 1 does not depend on ERM protein, actin polymerization, cellular ATP pools or the β2 adrenergic pathway. Step 2 is dominated by reorganization of cortical actin. This step is dependent on ERM protein, intracellular ATP levels and the β2 adrenergic pathway.

not decrease plasma membrane reorganization indicating that the actin binding ERM family proteins are not involved in these early events. In agreement with their role as a linker between plasma membrane receptors and the actin cytoskeleton, the accumulation of ezrin under the microcolony follows a complex pattern, related both to plasma membrane and to actin reorganization. Ezrin accumulation is detected as early as the plasma membrane and follows a similar pattern in untreated samples. When the actin cytoskeleton is disrupted, large amounts of ezrin are still recruited indicating that a pool of ezrin is associated with the membrane independently of the actin cytoskeleton.

Surprisingly, common signalling pathways are not necessary for the plasma membrane remodelling by the bacterium. The β2-adrenergic-dependent signalling pathway described recently (Coureuil *et al.*, 2010) does not seem to participate in the reorganization of the plasma membrane but rather on subsequent events involving the actin cytoskeleton. In addition, plasma membrane reorganization does not require any ATP-dependent signalling pathway. This likely excludes a role for a large number of intracellular signal transduction pathways in particular those involving protein or lipid kinases. The absence of implication of common intracellular pathways and of the actin cytoskeleton could be explained by a direct impact of bacteria on the plasma membrane rather than an indirect effect via intracellular intermediates although this point will require further work. In line with this hypothesis proper plasma membrane composition and organization with appropriate cholesterol content is necessary for the initiation of the process.

Although the actin cytoskeleton does not appear to play a role in the initial events involving the plasma membrane F-actin is nevertheless recruited under the bacterial aggregates in large amounts. The fact that alteration of plasma membrane composition blocks F-actin accumulation suggests that actin reorganization is a consequence of the initial membrane deformation. Several studies have shown that mechanical membrane deformation leads to intracellular signal transduction and actin cytoskeleton reorganization (Galbraith *et al.*, 2002). If bacteria trigger membrane deformation from the outside, the actin cytoskeleton would thus be predicted to reorganize under the microcolony. As previously described, perturbation of the β2AR-dependent signalling pathway led to a decrease in the amount of actin recruited under the microcolony. It is not clear at this point how this signalling pathway comes into play. Isoproterenol treatment affects the plateau value of actin accumulation rather than the initial accumulation. This suggests that the β2 adrenergic signalling pathway is necessary to attain the full extent of actin reorganization rather than being involved in the initiation of actin reorganization.

After the initiation of F-actin reorganization under the microcolony, bulk cytoplasm accumulates. This accumulation likely reflects the content of the cellular projections in cytoplasm. The fact that cytoplasm accumulation is delayed compared with plasma membrane accumulation suggests that once projections are formed they undergo a change in morphology enabling access of more cytoplasm. The precise nature of this potential morphological change is unknown at this point. An alternative would be that the access of cytoplasmic content is initially restricted and only after release of this restriction can the cytoplasm access the protrusion. Actin cytoskeleton disruption did not perturb bulk cytoplasm accumulation indicating that the actin cytoskeleton is not involved in this late event.

A key point of the experimental strategy used in this study was the use of preformed aggregates rather than individual bacteria. Using aggregates permitted definition of a clear starting point in the sequence of events. Another advantage was the dissociation of plasma membrane reorganization, which occurs at the scale of seconds from bacterial division, which takes about 1 h. Nevertheless, it is difficult to assert whether our observations based on preformed aggregates apply to individual bacteria growing on the cellular surface. A prediction is that as the microcolony grows on the cellular surface the plasma membrane will immediately reorganize around the newly divided bacteria. This can be observed in Movie S1 for instance. One implication is that growing bacteria are constantly wrapped in plasma membrane projections. Furthermore, the precise events taking place *in vivo* are not clear at this point, whether the initial adhesion event only involves a single bacterium or whether small aggregates first interact with endothelial cells.

Two pili-associated bacterial factors have been described as playing a role in triggering the cellular response following bacterial adhesion, the minor pilin PilV and the PilT ATPase. A strain deficient for PilV expression is unable to trigger plasma membrane reorganization or the accumulation of any of the proteins tested in this study. These results show that PilV is involved in the initial events that trigger the cellular response although the mechanisms of action of this protein still remain unidentified. The PilT ATPase powers the pilus retraction motor (Merz *et al.*, 2000). As this retraction generates intense force it was suggested that retraction could be responsible for plasma membrane accumulation and actin cytoskeleton reorganization (Higashi *et al.*, 2009). In contrast with the results presented here, we had shown in a previous publication that the Δ*pilT* mutant triggered plasma membrane reorganization nearly as efficiently as the wild-type strain on fixed samples after 2 h of infection (Mikaty *et al.*, 2009). The present dynamic study perhaps reconciles these studies by showing that the Δ*pilT* mutant is slower in initializing the response but once initiated the

intensity of the response is unaltered. Certain aggregates can stay in apparent contact with host cells for over an hour without triggering plasma membrane reorganization. Interestingly, in certain cases we observed intermittent accumulation of cellular components. Based on these results and the observation of numerous interaction events we propose that pilus retraction, mediated by PilT, is necessary to maintain intimate contact between the cells and the bacterial bodies rather than triggering the response itself. In the absence of PilT, pili grow continuously and it can be envisioned that this elongation pushes the bacterial bodies away from the cells rather than bringing them closer.

Studying the dynamics of the interaction of *N. meningitidis* with endothelial cells reveals some unique features, in particular the speed at which this occurs as the process is initiated in less than 1 min. The other striking feature is the fact that the bacteria induce the formation of membrane structures that are morphologically related to filopodia but form independently of actin and of common intracellular signalling pathways. Rather, plasma membrane deformation appears to trigger a cascade of events leading to intracellular signalling and actin reorganization. We have shown in a previous study that it is the plasma membrane reorganization rather than the actin remodelling that enhances the cohesion of bacterial aggregates on the endothelial surface and that allows resistance of the microcolonies to drag forces generated by blood flow (Mikaty *et al.*, 2009). Thus, identifying the mechanisms that allow *N. meningitidis* to trigger the plasma membrane remodelling represents a central challenge for future studies.

Experimental procedures

Antibodies and reagents

Custom small-interfering RNAs (siRNA) against human ezrin (siEZR), radixin (siRDX) and moesin (siMSN) were purchased from ThermoScientific. Sequences are the following: siEZR 5′-UCCACUAUGUGGAUAAUAA-3′; siRDX 5′-CUCGUCUGA GAAUCAAUAA-3′; siMSN 5′-AGAUCGAGGAACAGACUAA-3′. A non-targeting siRNA, also from ThermoScientific, was used as a negative control (ON-TARGETplus Non-targeting siRNA #1). For Western blots, rabbit polyclonal anti-total ERM (#3142, Cell Signaling Technology) was diluted 1:5000 and mouse monoclonal anti-GAPDH antibody (clone 6C5, Millipore) was diluted 1:10 000. Goat polyclonal anti-mouse or -rabbit IgG secondary antibodies coupled to HRP were diluted 1:10 000. For immunofluorescence, polyclonal anti-ezrin antibody (gift from P. Mangeat) was diluted 1:1000, mouse monoclonal anti-CD44 (clone J.173, Beckman Coulter) was diluted 1:300, phalloidin-AlexaFluor568 was diluted 1:200 and DAPI (4′,6-diamidino-2-phenylindole) was diluted 1:10 000. Goat polyclonal anti-mouse or -rabbit IgG antibodies coupled to AlexaFluor488 and 568 were diluted 1:10 000. All secondary antibodies as well as phalloidin and DAPI were from Sigma-Aldrich.

Cell culture

Human umbilical vein endothelial cells (HUVECs, Promocell) were maintained in Endo-SFM L-glutamine 2 mM (Gibco) supplemented with 10% (v/v) fetal bovine serum (FBS, PAA Laboratories), and 10 μg ml^{-1} endothelial cells growth supplement (ECGS, Harbor Bioproducts). For transfection experiments, cells were used between passage 3 and 9 and 5×10^5 cells were transfected with 4 μg plasmid DNA using the Amaxa Nucleofector Kit for HUVECs (Amaxa Biosystem, Lonza) according to the manufacturer protocol (http://www.lonzabio.com). Plasmids encoding for ezrin-GFP (Lamb *et al.*, 1997), Farnesyl-GFP which contains a CAAX box (Clonetech, pEGFP-F) and cytoplasmic-expressed GFP (pMax-GFP, Lonza) were described previously. The plasmid encoding LifeAct-mCherry was a kind gift from Guillaume Montagnac (Institut Curie, Paris). Transfected cells were then cultivated at 37°C + 5% CO_2 in moist atmosphere either in disposable μ-slides (μ-Slide VI^{0,4} Ibitreat, IBIDI, Biovalley) for microcolony proliferation experiments, or in disposable μ-dishes (μ-Dish$^{35mm,\ low}$, IBIDI) or in 96-well plates (μ-clear®, Greiner BioOne) coated with 0.1% rat tail collagen I (Sigma-Aldrich).

Treatments with inhibitors were performed in Endo-SFM + 10% FBS for cytochalasin D (CD, 1 μM), isoproterenol [ISO, 10 μM, (Coureuil *et al.*, 2010)] and methyl-β-cyclodextrin (MβCD, 4 mM). For ATP depletion, treatment was performed in DMEM without glucose (Invitrogen) + 10% FBS containing 10 mM sodium azide (Sigma-Aldrich) and 10 mM 2-deoxy-D-glucose (2-DG, Sigma-Aldrich). Control cells were incubated in DMEM without glucose supplemented with 5 mM glucose [Sigma-Aldrich (Romer *et al.*, 2007)]. Treatments were performed 2 h prior to infection for ISO and MβCD, 30 or 20 min prior to infection for ATP depletion and CD respectively and maintained through the course of the experiment. ATP depletion efficiency was assessed using the commercially available kit Adenosine 5′-triphosphate Bioluminescent Assay (Sigma-Aldrich).

Bacterial strains and culture

Neisseria meningitidis strains were derived from the 8013 clone 12, a serogroup C clinical isolate expressing capsule and class I SB piline, Opa$^-$ and Opc$^-$ (Nassif *et al.*, 1993; Rusniok *et al.*, 2009). *N. meningitidis* is grown on solid GCB Agar (Difco) containing Kellogg's supplements (Kellogg *et al.*, 1968) and antibiotics when required: kanamycin (100 μl ml^{-1}), chloramphenicol (5 μl ml^{-1}) or erythromycin (4 μl ml^{-1}), at 37°C + 5% CO_2 under moist atmosphere. For infection experiments, overnight cultures on solid plates were suspended in Endo-SFM + 10% FBS at an OD_{600} = 0.05 and cultivated for 2 h with shaking at 37°C + 5% CO_2. Formation of bacterial aggregates after this period was assessed microscopically. Δ*pilV* and Δ*pilT* mutant strains are described elsewhere (Pujol *et al.*, 1999; Mikaty *et al.*, 2009).

A series of plasmids were constructed to allow chromosomal expression of fluorescent proteins under the control of the *pilE* promoter. Inducible genes were inserted between the *recC* (NMV_0648) and *mrtF* (NMV_0649) genes. Two fragments on either side of the insertion site were PCR amplified from *N. meningitidis* chromosomal DNA with the RecCF/R and MrtFF/R primer pairs (see Table 1 for primer sequences), cloned in the Topo 2.1 and checked for sequence. Both fragments were restricted with the enzymes indicated in bold and cloned in the

Table 1. Primers use to generate plasmid constructs.

Name	Sequence[a]	Enzyme
GFPF	**TTAATTAA**TTTAAGAAGGAGATATACATATGAGTAAAG	PacI
GFPR	**GTCGAC**TTATTTGTATAGTTCATCCATGCCATGTG	SalI
PrPilEF	**AGTACT**CCATGCCAATAGAGATACCCCACG	ScaI
PrPilER	**TTAATTAA**AATTGGAAAGGAAATGCCTCAAGC	PacI
RecCF	**GAG CTC** GGA CGA ATT TAT CCG CTT CTG G	SacI
RecCR	**CCG CGG** CCC ACA TTC TAT CCC GCA CC	SacII
mrtFF	**CTC GAG** GCA TGC GTT TAA ACG CAG CGG AAA AAA AGG AAG AGG	XhoI
mrtFR	**GGT ACC** CAT TCG ACA TTC CAA TGA AAT CAC G	KpnI
mCherryF	**TTAATTAA**AGGAGTAATTTTATGGTGAGCAAGGGCGAGGAGGATAACATG	PacI
mCherryR	**GTCGAC**CCTCTACAAATGTGGTATGGCTG	XhoI
BFPF	**TTAATTAA**AGGAGTAATTTTATGAGCGAGCTGATTAAGGAG	PacI
BFPR	**CTCGAGTC**AATTAAGCTTGTGCCCCAG	XhoI
PilT1	**TTA-ATT-AA**A-GGA-GTA-ATT-TTA-TGC-AGA-TTA-CCG-ACT-TA	PacI
PilT2	**GTT-TAA-AC**T-CAG-AAA-CTC-ATA-CTT-TC	PmeI

a. Sequences highlighted in bold represent restriction sites.

pBluescript vector (Stratagene) generating plasmid pMGC1. A chloramphenicol cassette bordered by two BamHI sites from the pT1Cm1 vector (Klee *et al.*, 2000) was then inserted in the BamHI site in between the two chromosomal regions in pMGC1 generating pMGC3. A 305-nucleotide-long promoter region of *pilE* was amplified from genomic DNA with primers PrPilEF/R, cloned in Topo2.1, sequenced, restricted by indicated enzymes and subcloned in the pMGC3. The mCherry open reading frame was amplified from the pmCherry-N1 vector (Clonetech) with primers mCherryF/R, restricted and subcloned in obtained vector thus generating pMGC5. The GFP open reading frame was amplified from the pAM239 plasmid (Solomon *et al.*, 2003) with primers GFPF/R, restricted with indicated enzymes and subcloned in pMGC5 thus generating pMGC7. The mTagBFP2 protein was amplified from the pBadmTagBFP2 plasmid [Addgene (Subach *et al.*, 2011)] using the primer BFPF/R, restricted and cloned in pMGC5 generating pMGC8. The $pilV_{ind}$ strain has been described previously (Mikaty *et al.*, 2009). To complement the *pilT* mutant, the WT *pilT* allele was amplified using primers PilT1 and PilT2, which contained overhangs with underlined restriction sites for PacI and PmeI and cloned in the PCR2.1Topo plasmid. This fragment was restricted with PacI and PmeI and cloned into PacI/PmeI-cut pGCC4 vector, adjacent to lacIOP regulatory sequences (Mehr *et al.*, 2000). This placed *pilT* under the transcriptional control of an IPTG-inducible promoter within a DNA fragment corresponding to an intragenic region of the gonococcal chromosome conserved in *N. meningitidis*. The $pilT_{ind}$ allele was then introduced into the chromosome of a *pilT* mutant by homologous recombination.

Fluorescence microscopy

All experiments were performed on an inverted microscope (Eclipse T*i*, Nikon) through a 1.30 NA oil-immersion objective (CFI Plan Fluor 40× oil, Nikon). To perform spatial high-resolution acquisition, a fast Z-piezo stage (Piezo Nano Z100) was adapted onto the XY platform of the microscope and the set-up coupled to a laser-based spinning disk confocal microscopy system (CSU-X1, Yokogawa), equipped with lasers at 405 nm, 491 nm and 561 nm. All experiments were performed at 37°C in an incubation chamber adapted for the microscope (LIS Microscope Temperature Control System). Focus was maintained with Perfect Focus System (PFS, Nikon). A high-resolution digital camera (Evolve, Photometrics) was used for Image acquisition. The set-up was controlled by the MetaMorph software (Universal Imaging, Molecular Devices).

For infection, overnight culture medium was replaced by 100 μl of fresh or treatment medium for the indicated times prior to infection. The plate was placed on the microscope stage and 50 μl of medium removed and 50 μl of the bacterial culture (OD_{600} ~0.3) was added. Acquisition was started when bacteria appeared in the observation field. Images were acquired over 5 μm along the Z-axis with 1 μm steps for all experiments. Time-lapse parameters were set-up for image acquisition every 5 s over a period of 10–20 min.

ERM proteins knock-down

Ezrin, radixin and moesin (ERM) proteins were knocked-down by electroporating 2×10^6 HUVEC cells on day 1 and 3 with 200 nM control siRNA (siNT) or 200 nM of each of the three siRNA targeting human ezrin, radixin or moesin (siERM). On day 3, cells were co-transfected with 4 μg plasmid DNA encoding farnesyl-GFP and seeded in 96-well plates for imaging on day 4. To evaluate knock-down efficiency, cells grown in six-well plates were washed with PBS 1× and lysed in Laemmli buffer. Samples were immediately boiled for 5 min and stored at −20°C. Proteins were subjected to SDS-PAGE in 10% polyacrylamide gels and transferred onto PVDF membranes (Amersham Hybond-P, GE Healthcare). Membranes were blocked at room temperature with TBST-5% BSA for 30 min, incubated for 1 h with primary antibodies and 1 h with secondary antibodies. ERM proteins and GAPDH were detected using Pierce ECL2 and Bio Rad ECL Clarity kits respectively and quantified using ImageJ (http://rsb.info.nih.gov/ij/). For immunofluorescence assays, treated cells were seeded onto 25 mm glass coverslips coated with type I collagen and infected the next day with 10^7 bacteria (moi = 100) in culture medium for 2 h at 37°C + 5% CO_2. Cells were then washed three times with culture medium, fixed with 4% PFA, permeabilized with 0.1% Triton 100× and blocked with PBS-2% gelatin. Primary antibodies were incubated at room temperature for 1 h, as well as phalloidin, DAPI and secondary antibodies coupled to AlexaFluor488 or 568. Actin recruitment index is given as the percentage of bacterial microcolonies positive for F-actin

from a total of at least 300 microcolonies in three independent experiments performed in duplicate.

Image analysis

A plug-in called *intensity profiler* described below was developed specifically to analyse the images in the context of the ICY community platform for bioimage informatics (de Chaumont *et al.*, 2012; http://icy.bioimageanalysis.org).

ROI selection. Multidimensional files (5D hyperstacks) acquired with MetaMorph were processed with ImageJ software (Schneider *et al.*, 2012; http://rsbweb.nih.gov/ij/) to generate stacks corresponding to timelapse images acquired in the blue, green and red channel, with an averaged projection along the Z-axis. The ICY software was used to select two regions of interest, ROI-1, around a bacterial aggregate establishing a contact with a cell, and ROI-2, in an uninfected part of the same cell to determine the background intensity. Each ROI is assigned a 'bacteria' and a 'protein' channel.

Time of initial contact of the aggregate, t_{ini}. Time of initial of contact (t_{ini}) between the bacterial aggregate and the cell was determined by identifying the first sharp increase (+ 20%) between two time points of the average fluorescence intensity within ROI-1 on the 'bacteria' channel.

Net fluorescence intensity, $S(t)$. The raw intensity $I(t)$ is equal to the sum of a nearly constant background intensity B_1 and the fluorescence variation $S(t)$ triggered by the contact between the bacteria aggregate and the cell membrane. In addition, thermal fluctuations can induce jumps $h(t)$ in fluorescence intensity and the bleaching was modelled with a decreasing exponential function (Molski, 2001) leading to the formula

$$I(t) = (B_1 + S(t))h(t)\exp(-t/\tau),$$

where τ is the time constant of the bleaching process. Similarly, variations of the averaged intensity $B(t)$ in the background ROI-2 are mainly due to thermal fluctuations and bleaching, leading to the relation

$$B(t) = B_2 h(t)\exp(-t/\tau),$$

where B_2 is the constant background intensity in ROI-2. Because we assumed that $S(t_{ini}) = 0$ and $h(t_{ini}) = 0$, the background constants are equal to $B_1 = I(t_{ini})$ and $B_2 = B(t_{ini})$, leading to

$$I(t) = (I(t_{ini}) + S(t))h(t)\exp(-t/\tau), \quad \text{and}$$
$$B(t) = B(t_{ini})h(t)\exp(-t/\tau).$$

Finally, combining equations above, we were able to extract the marginal fluorescence variation $S(t)$ induced by the bacteria aggregate from the measurements of the raw intensities $I(t)$ and $B(t)$:

$$S(t) = I(t)B(t_{ini})/B(t) - I(t_{ini}).$$

Ratio of fluorescence. To access quantitative variations of fluorescence intensity, the relative net increase in signal intensity $R(t)$ between signal intensity at t_{ini}, $I(t_{ini})$, and corrected intensity at time t, $I(t_{ini}) + S(t)$, was computed and plotted over time.

$$R(t) = (I(t_{ini}) + S(t))/I(t_{ini}).$$

Acknowledgements

Authors would like to thank: Fabrice de Chaumont at the Pasteur Institute for initial help with ICY Software; Keira Melican, Ana Maria Lennon-Dumenil and Jost Enninga for critical reading of the manuscript; Guy Tran Van Nhieu for providing the M90T *Shigella flexneri* strain as well as for fruitful discussions; and Patricia Bassereau for fruitful discussions. This work was supported by Fondation pour la Recherche M dicale FRM and the French ministry for research and higher education (MS); the Avenir INSERM Starting Grant; a CODDIM equipment grant (R gion Ile de France) and by a European Research Council starting grant.

References

Aronheim, A., Engelberg, D., Li, N., al-Alawi, N., Schlessinger, J., and Karin, M. (1994) Membrane targeting of the nucleotide exchange factor Sos is sufficient for activating the Ras signaling pathway. *Cell* **78:** 949–961.

Carbonnelle, E., Helaine, S., Nassif, X., and Pelicic, V. (2006) A systematic genetic analysis in *Neisseria meningitidis* defines the Pil proteins required for assembly, functionality, stabilization and export of type IV pili. *Mol Microbiol* **61:** 1510–1522.

de Chaumont, F., Dallongeville, S., Chenouard, N., Herve, N., Pop, S., Provoost, T., *et al.* (2012) Icy: an open bioimage informatics platform for extended reproducible research. *Nat Methods* **9:** 690–696.

Coureuil, M., Mikaty, G., Miller, F., Lecuyer, H., Bernard, C., Bourdoulous, S., *et al.* (2009) Meningococcal type IV pili recruit the polarity complex to cross the brain endothelium. *Science* **325:** 83–87.

Coureuil, M., Lecuyer, H., Scott, M.G., Boularan, C., Enslen, H., Soyer, M., *et al.* (2010) Meningococcus Hijacks a beta2-adrenoceptor/beta-Arrestin pathway to cross brain microvasculature endothelium. *Cell* **143:** 1149–1160.

van Deuren, M., Brandtzaeg, P., and van der Meer, J.W. (2000) Update on meningococcal disease with emphasis on pathogenesis and clinical management. *Clin Microbiol Rev* **13:** 144–166, table of contents.

Doulet, N., Donnadieu, E., Laran-Chich, M.P., Niedergang, F., Nassif, X., Couraud, P.O., and Bourdoulous, S. (2006) *Neisseria meningitidis* infection of human endothelial cells interferes with leukocyte transmigration by preventing the formation of endothelial docking structures. *J Cell Biol* **173:** 627–637.

Eugene, E., Hoffmann, I., Pujol, C., Couraud, P.O., Bourdoulous, S., and Nassif, X. (2002) Microvilli-like structures are associated with the internalization of virulent capsulated *Neisseria meningitidis* into vascular endothelial cells. *J Cell Sci* **115:** 1231–1241.

Galbraith, C.G., Yamada, K.M., and Sheetz, M.P. (2002) The relationship between force and focal complex development. *J Cell Biol* **159:** 695–705.

Giltner, C.L., Nguyen, Y., and Burrows, L.L. (2012) Type IV pilin proteins: versatile molecular modules. *Microbiol Mol Biol Rev* **76:** 740–772.

Higashi, D.L., Zhang, G.H., Biais, N., Myers, L.R., Weyand, N.J., Elliott, D.A., and So, M. (2009) Influence of type IV pilus retraction on the architecture of the *Neisseria*

gonorrhoeae-infected cell cortex. *Microbiology* **155:** 4084–4092.
Hochmuth, F.M., Shao, J.Y., Dai, J., and Sheetz, M.P. (1996) Deformation and flow of membrane into tethers extracted from neuronal growth cones. *Biophys J* **70:** 358–369.
Hoffmann, I., Eugene, E., Nassif, X., Couraud, P.O., and Bourdoulous, S. (2001) Activation of ErbB2 receptor tyrosine kinase supports invasion of endothelial cells by *Neisseria meningitidis*. *J Cell Biol* **155:** 133–143.
Kellogg, D.S., Jr, Cohen, I.R., Norins, L.C., Schroeter, A.L., and Reising, G. (1968) *Neisseria gonorrhoeae*. II. Colonial variation and pathogenicity during 35 months in vitro. *J Bacteriol* **96:** 596–605.
Klee, S.R., Nassif, X., Kusecek, B., Merker, P., Beretti, J.L., Achtman, M., and Tinsley, C.R. (2000) Molecular and biological analysis of eight genetic islands that distinguish *Neisseria meningitidis* from the closely related pathogen *Neisseria gonorrhoeae*. *Infect Immun* **68:** 2082–2095.
Lamb, R.F., Ozanne, B.W., Roy, C., McGarry, L., Stipp, C., Mangeat, P., and Jay, D.G. (1997) Essential functions of ezrin in maintenance of cell shape and lamellipodial extension in normal and transformed fibroblasts. *Curr Biol* **7:** 682–688.
Lambotin, M., Hoffmann, I., Laran-Chich, M.P., Nassif, X., Couraud, P.O., and Bourdoulous, S. (2005) Invasion of endothelial cells by *Neisseria meningitidis* requires cortactin recruitment by a phosphoinositide-3-kinase/Rac1 signalling pathway triggered by the lipo-oligosaccharide. *J Cell Sci* **118:** 3805–3816.
Lecuyer, H., Nassif, X., and Coureuil, M. (2012) Two strikingly different signaling pathways are induced by meningococcal type IV pili on endothelial and epithelial cells. *Infect Immun* **80:** 175–186.
Mairey, E., Genovesio, A., Donnadieu, E., Bernard, C., Jaubert, F., Pinard, E., *et al.* (2006) Cerebral microcirculation shear stress levels determine *Neisseria meningitidis* attachment sites along the blood-brain barrier. *J Exp Med* **203:** 1939–1950.
Mehr, I.J., Long, C.D., Serkin, C.D., and Seifert, H.S. (2000) A homologue of the recombination-dependent growth gene, *rdgC*, is involved in gonococcal pilin antigenic variation. *Genetics* **154:** 523–532.
Melican, K., and Dumenil, G. (2012) Vascular colonization by *Neisseria meningitidis*. *Curr Opin Microbiol* **15:** 50–56.
Melican, K., Michea Veloso, P., Martin, T., Bruneval, P., and Dumenil, G. (2013) Adhesion of *Neisseria meningitidis* to dermal vessels leads to local vascular damage and purpura in a humanized mouse model. *PLoS Pathog* **9:** e1003139.
Merz, A.J., Enns, C.A., and So, M. (1999) Type IV pili of pathogenic Neisseriae elicit cortical plaque formation in epithelial cells. *Mol Microbiol* **32:** 1316–1332.
Merz, A.J., So, M., and Sheetz, M.P. (2000) Pilus retraction powers bacterial twitching motility. *Nature* **407:** 98–102.
Mikaty, G., Soyer, M., Mairey, E., Henry, N., Dyer, D., Forest, K.T., *et al.* (2009) Extracellular bacterial pathogen induces host cell surface reorganization to resist shear stress. *PLoS Pathog* **5:** e1000314.
Molski, A. (2001) Statistics of the bleaching number and the bleaching time in single-molecule fluorescence spectroscopy. *J Chem Phys* **114:** 1142–1147.
Nassif, X., Lowy, J., Stenberg, P., O'Gaora, P., Ganji, A., and So, M. (1993) Antigenic variation of pilin regulates adhesion of *Neisseria meningitidis* to human epithelial cells. *Mol Microbiol* **8:** 719–725.
Nassif, X., Bourdoulous, S., Eugene, E., and Couraud, P.O. (2002) How do extracellular pathogens cross the blood-brain barrier? *Trends Microbiol* **10:** 227–232.
Pron, B., Taha, M.K., Rambaud, C., Fournet, J.C., Pattey, N., Monnet, J.P., *et al.* (1997) Interaction of *Neisseria meningitidis* with the components of the blood-brain barrier correlates with an increased expression of PilC. *J Infect Dis* **176:** 1285–1292.
Pujol, C., Eugene, E., Marceau, M., and Nassif, X. (1999) The meningococcal PilT protein is required for induction of intimate attachment to epithelial cells following pilus-mediated adhesion. *Proc Natl Acad Sci USA* **96:** 4017–4022.
Ray, K., Bobard, A., Danckaert, A., Paz-Haftel, I., Clair, C., Ehsani, S., *et al.* (2010) Tracking the dynamic interplay between bacterial and host factors during pathogen-induced vacuole rupture in real time. *Cell Microbiol* **12:** 545–556.
Romer, W., Berland, L., Chambon, V., Gaus, K., Windschiegl, B., Tenza, D., *et al.* (2007) Shiga toxin induces tubular membrane invaginations for its uptake into cells. *Nature* **450:** 670–675.
Rusniok, C., Vallenet, D., Floquet, S., Ewles, H., Mouze-Soulama, C., Brown, D., *et al.* (2009) NeMeSys: a biological resource for narrowing the gap between sequence and function in the human pathogen *Neisseria meningitidis*. *Genome Biol* **10:** R110.
Schneider, C.A., Rasband, W.S., and Eliceiri, K.W. (2012) NIH Image to ImageJ: 25 years of image analysis. *Nat Methods* **9:** 671–675.
Sokolova, O., Heppel, N., Jagerhuber, R., Kim, K.S., Frosch, M., Eigenthaler, M., and Schubert-Unkmeir, A. (2004) Interaction of *Neisseria meningitidis* with human brain microvascular endothelial cells: role of MAP- and tyrosine kinases in invasion and inflammatory cytokine release. *Cell Microbiol* **6:** 1153–1166.
Solomon, J.M., Leung, G.S., and Isberg, R.R. (2003) Intracellular replication of *Mycobacterium marinum* within *Dictyostelium discoideum*: efficient replication in the absence of host coronin. *Infect Immun* **71:** 3578–3586.
Stephens, D.S., Hoffman, L.H., and McGee, Z.A. (1983) Interaction of *Neisseria meningitidis* with human nasopharyngeal mucosa: attachment and entry into columnar epithelial cells. *J Infect Dis* **148:** 369–376.
Subach, O.M., Cranfill, P.J., Davidson, M.W., and Verkhusha, V.V. (2011) An enhanced monomeric blue fluorescent protein with the high chemical stability of the chromophore. *PLoS ONE* **6:** e28674.
Taylor, M.J., Perrais, D., and Merrifield, C.J. (2011) A high precision survey of the molecular dynamics of mammalian clathrin-mediated endocytosis. *PLoS Biol* **9:** e1000604.

Supporting information

Additional Supporting Information may be found in the online version of this article at the publisher's web-site:

Fig. S1. Actin and membrane accumulation in Δ*pilV* and Δ*pilT* strains. Endothelial cells transfected with actin-mCherry or Farnesyl-GFP were infected with aggregates formed by the *pilV*- and *pilT*-deficient strains (Δ*pilV*, Δ*pilT*).
A. Kinetics of actin accumulation in the Δ*pilV* (green curve) and Δ*pilT* (red curve) strains.
B. Kinetics of membrane marker accumulation in the Δ*pilV* (green curve) and Δ*pilT* (red curve) strains.
Fig. S2. Complementation of the Δ*pilV* and Δ*pilT* mutations. Strains expressing wild-type copies of *pilV* and *pilT* under the control of the *lac* promoter in the presence of 1 mM and 0.05 mM of IPTG respectively were used to infect endothelial cells transfected with ezrin-GFP.
A. Kinetics of ezrin accumulation in the $pilV_{ind}$ (red curve).
B. Kinetics of ezrin accumulation in the $pilT_{ind}$ (red curve).
Fig. S3. Evaluation of the effect of ERM knock-down by immunofluorescence. Expression of ezrin and of CD44 as a control were visualized by immunofluorescence in cells treated with ERM siRNA (SiERM) and cells treated with control siRNA. The scale bar corresponds to 20 μm.
Movie S1. Meningococcus growth as a microcolony is accompanied by ezrin accumulation. Ezrin-GFP transfected cells were infected by individual mCherry-expressing meningococci. Following initial adhesion (white arrows), behaviour of ezrin underneath the nascent microcolony was monitored over a 4 h period. As the microcolony reached a size of about 10 diplococci (30 min), ezrin started to accumulate and the cortical plaque size increased with the size of the microcolony. The scale bar corresponds to 20 μm.
Movie S2. Ezrin accumulation underneath pre-formed meningococcus aggregates. Ezrin-GFP transfected cells (middle panel) were infected with pre-formed mCherry-expressing meningococcus aggregates (left panel). Ezrin accumulation was monitored over 10 min and started immediately after contact of the aggregate with the cell. Right panel shows the merged images. Scale bar corresponds to 20 μm.
Movie S3. Delayed plasma membrane remodelling by the Δ*pilT* strain. Endothelial cells were transfected with ezrin-GFP and infected with the Δ*pilT* strain for a period of 4 h. The arrow points to a bacterial aggregate that triggers a detectable response only after 1 h and 15 min. Bacteria (left), ezrin-GFP (middle) and merge (right) are shown on the movie. Scale bar corresponds to 20 μm.
Movie S4. Treatment of endothelial cells with cytochalasin D leads to disruption of actin cytoskeleton. Endothelial cells were co-transfected with LifeAct-mCherry, allowing direct visualization of the actin cytoskeleton, and with ezrin-GFP. Actin cytoskeleton behaviour following cytochalasin D treatment was monitored over 20 min. Soon after drug addition, actin fibres started to depolymerize and led to a punctuate labelling of actin throughout the cell. Scale bar corresponds to 20 μm.

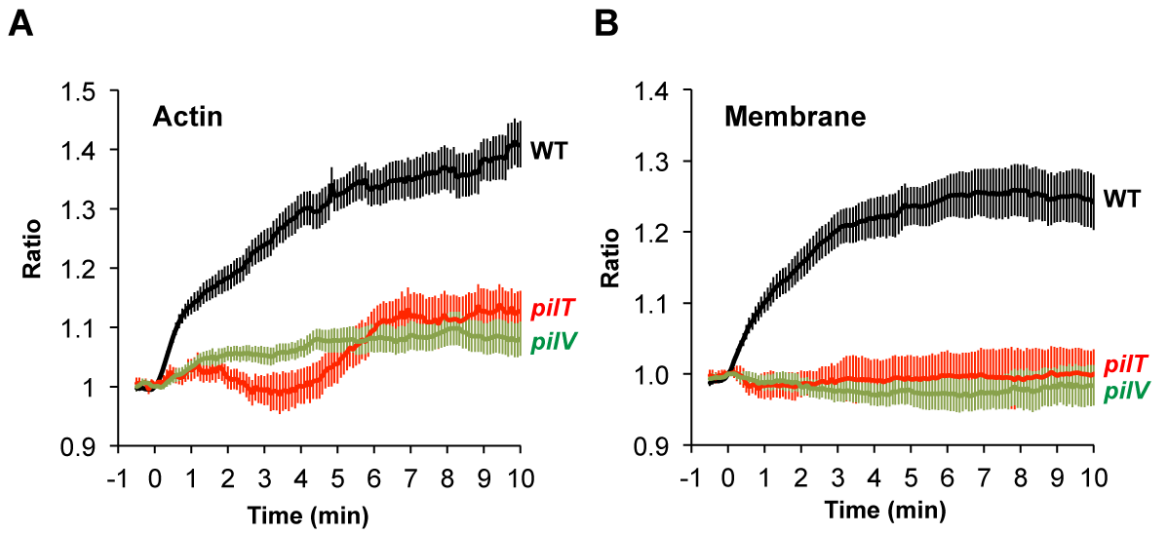

Supplementary figure 1

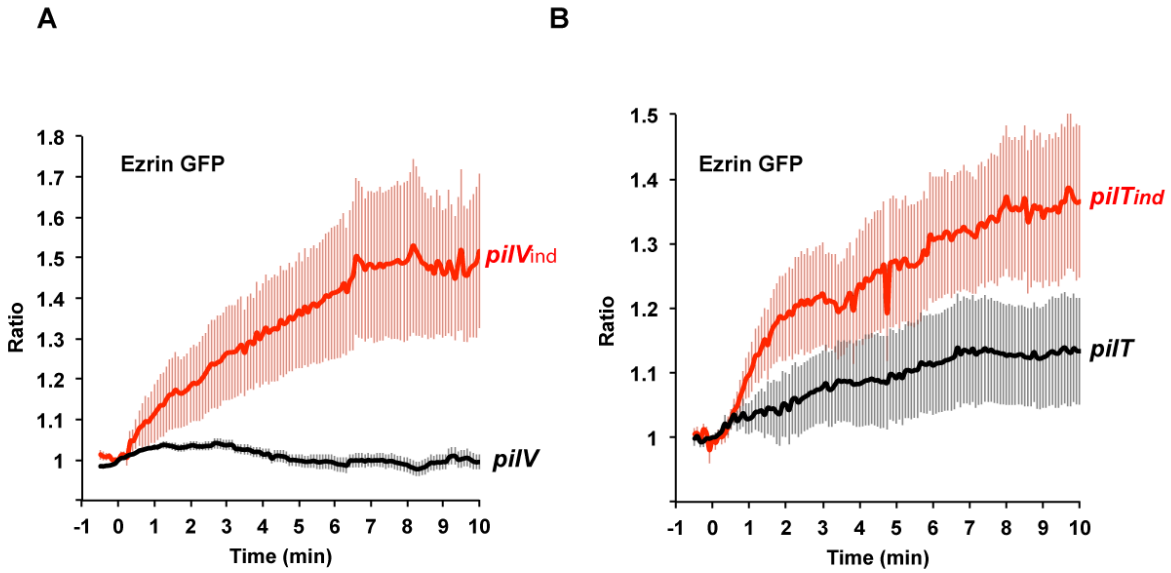

Supplementary figure 2

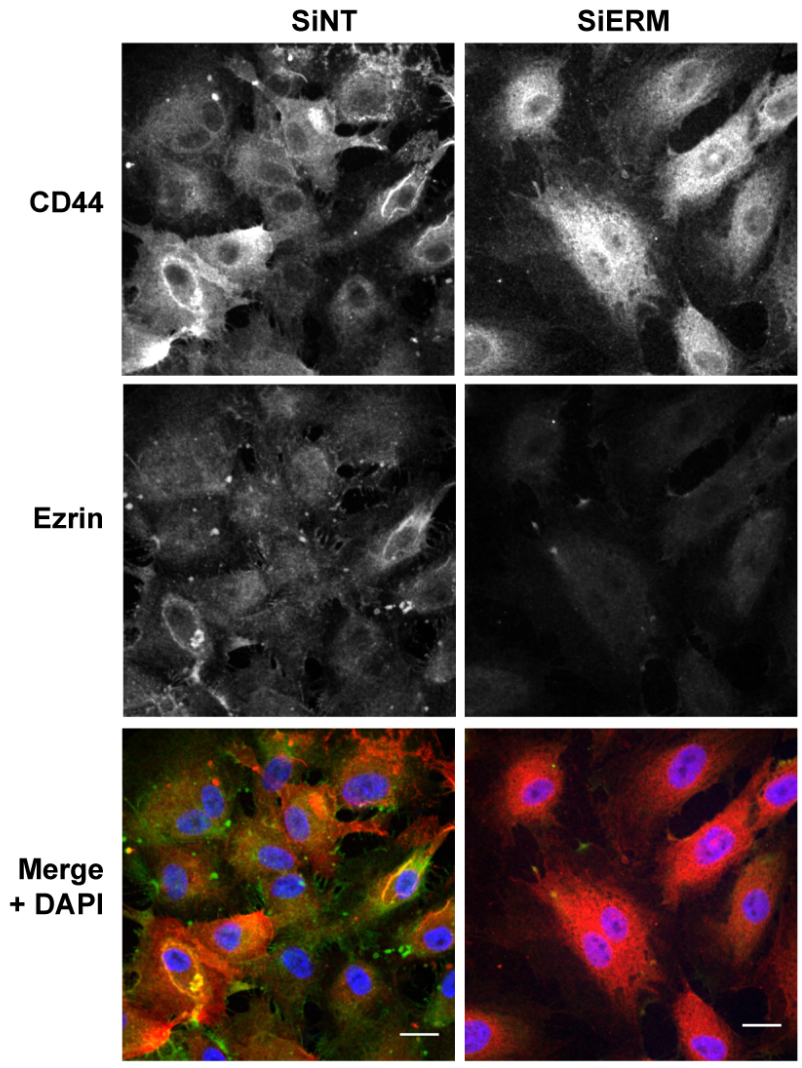

Supplementary figure 3

2. Paper II: Plasma membrane remodeling is triggered by adhesion on *Neisseria meningitidis* type IV pili fibers

Background

Following the previous study, I dedicated the rest of this PhD to understanding how T4P drive plasma membrane remodeling in an F-actin-independent fashion.

Since bacteria expressing only 60% of the wildtype levels of T4P can no longer remodel the host cell plasma membrane, we more specifically wondered whether the density or spatial organization of T4P fibers played a role in this process. To answer this question, we used a combination of light and electron microscopy approaches.

Previous electron microscopy studies of meningococci, alone or adhered to human cells, taught us that i) pili are 6 nm wide, ii) plasma membrane protrusions diameter fall in the 100 nm range and iii) only a very few number of T4P are seen on meningococcus cells compared to gonococcus. Therefore, this project had two main technical challenges. On the one hand, both our biological objects of interest are smaller than the smallest objects that can be observed through diffraction-limited optical systems (i.e. about 200 nm). On the other hand, meningococcal T4P are seemingly more difficult to preserve for electron microscopy than other pili. As a result, this study required the use and optimization of super resolution light microscopy approaches, and the optimization of electron microscopy sample preparation methods for meningococcus. In addition, we found that oblique illumination, combined with live cell fluorescence imaging, allowed visualization of plasma membrane remodeling dynamics at the level of the single bacterium.

Main conclusions

In this study, we show that plasma membrane remodeling occurs during vascular colonization of human blood vessels *in vivo*.

In vitro, we found that the plasma membrane of endothelial cells is remodeled because it adheres along T4P fibers at the level of the single bacterium. Plasma membrane protrusions that adhere to T4P are dynamic and reflect T4P retraction. Oppositely, actin polymerization stabilizes plasma membrane protrusions. Finally, we show that deformation along nanoscale adhesive structures is an intrinsic property of the plasma membrane.

(At the time of writing, the following manuscript has not yet been submitted.)

Plasma membrane remodeling is triggered by adhesion on *Neisseria meningitidis* type IV pili fibers

Arthur Charles-Orszag[1,2], Daria Bonazzi[1], Valeria Manriquez[1,2], Martin Sachse[3], Adeline Mallet[3], Audrey Salles[4], Keira Melican[1,‡], Corinne Millien[6], Sylvie Goussard[1], Pierre Lafaye[7], Spencer Shorte[4], Matthieu Piel[8,9], Jacomine Krijnse-Locker[3] & Guillaume Duménil[1,*]

[1]Pathogenesis of Vascular Infections Unit, INSERM, Institut Pasteur, 75015 Paris, France
[2]Université Paris Descartes, Sorbonne Paris Cité, 75006 Paris, France
[3]Ultrapole, Institut Pasteur, 75015 Paris, France
[4]Imagopole, Institut Pasteur, 75015 Paris, France
[6]Paris Cardiovascular Research Center, 75015 Paris, France
[7]Antibody Engineering, Institut Pasteur, 75015 Paris, France
[8]Systems Biology of Cell Polarity and Cell Division, Institut Pierre-Gilles De Gennes, 75005 Paris, France
[9]Institut Curie, 75005 Paris, France
[‡]Current address: Swedish Medical Nanoscience Center, Department of Neuroscience, Karolinska Institutet, 171 77 Solna, Sweden
*Correspondence: guillaume.dumenil@pasteur.fr

Abstract

Neisseria meningitidis is a bacterial pathogen that colonizes human blood vessels and causes septic shock and meningitis. Adhesion of meningococci to host endothelial cells via type IV pili is accompanied by a potent remodeling of the host cell plasma membrane, forming filopodia-like protrusions that intercalate between aggregated bacteria. While the mechanism behind plasma membrane remodeling remains unknown, the plasma membrane protrusions have been shown to increase microcolony resistance to shear stress. Here we show that plasma membrane remodeling does occur during bacterial colonization of human blood vessels *in vivo* and demonstrate that remodeling occurs as discrete short-lived protrusions at the level of the single adhering bacterium *in vitro*. Cortical actin polymerization is not necessary for protrusion formation but does stabilize them. Disappearance of the protrusions correlates with type IV pili retraction. Electron microscopy shows that membrane protrusions grow alongside type IV pili fibers, suggestive of a scaffolding mechanism. By perturbing the architecture of the type IV pili meshwork, we show that spatial organization of the type IV pili fibers is necessary to impose a specific geometry to plasma membrane remodeling. Finally, by using an artificial adhesive nanostructured substrate, we show that local deformations of

the plasma membrane in response to adhesive nanotopographical cues is an intrinsic property of human cells.

Introduction

The control of the shape of biological membranes is a fundamental process for the maintenance of multiple functions in the eukaryotic cell (1). Acting as the interface of the cell with its surrounding environment, the plasma membrane is a particularly important compartment that is subject to a precise control of its shape and dynamics. Plasma membrane remodeling occurs at very small scales, for example in the biogenesis of caveolae (2) or during the formation of clathrin coated pits (3). At larger scales, remodeling of the plasma membrane plays an important role in a wide variety of biological processes, such as the uptake of large particles by phagocytosis (4) or in the formation of membrane structures that support cell migration and probing of the extracellular milieu, such as filopodia or lamellipodia (5). In the context of pathological conditions, especially in bacterial, viral and fungal infections, pathogens manipulate the shape of the plasma membrane in particular to achieve their entry into the host cell (6-8). The bacterium *Neisseria meningitidis* (or meningococcus) is a human pathogen that, while remaining extracellular (9), massively remodels the host cell plasma membrane upon adhesion to the host cell surface. This remodeling provides bacterial microcolonies with an important mechanical cohesion, in particular when facing shear stress (10). Understanding this process is both important in the study of infectious processes and a useful model to probe the mechanisms of plasma membrane dynamics.

N. meningitidis is a human obligate diderm bacterium that is carried asymptomatically in the nasopharynx of 10 to 35% of the worldwide population (11). Occasionally, it can cross the mucosal barrier and reach the underlying blood vessels where it can cause septic shock and/or meningitis, particularly in children and young adults. Colonization of the blood vessels by *N. meningitidis* leads to a loss of vascular function that translates into hemorrhagic lesions in organs throughout the body, including in the skin where it presents as characteristic purpuric rashes (12-14). Despite the use of efficient antibiotics, the case fatality rates for *N. meningitidis* infection can still reach 11% for sporadic cases and 20% for epidemic outbreaks. Surviving patients frequently experience severe physical or mental sequelae (15). Therefore, it is important to improve our understanding of the pathophysiology of meningococcal diseases, in particular of the blood phase of infection where bacterial interaction with the vascular endothelium is crucial.

Adhesion of *N. meningitidis* is specific to human cells and is mediated by filamentous adhesins referred to as type IV pili (T4P). Bacteria lacking these organelles are unable to adhere to human endothelial cells *in vitro* (16) as well as *in vivo* (12). T4P are fibers with a diameter of 6 nm and a length of up to several micrometers that can associate laterally to form

bundles. T4P are made by helical assembly of the major pilin protein PilE (17). It is still under debate if other proteins, including PilV, PilX, ComP or PilC1 co-assemble with PilE and decorate the pilus fiber (18-20). PilV and PilX for instance have been shown to function in the periplasm and regulate T4P assembly (21). T4P polymerization depends on a complex machinery of around twenty different proteins. Fibers can go through rapid cycles of elongation and retraction through the action of two ATPases, PilF and PilT, respectively. Two host cell surface proteins, CD46 and more recently CD147, have been described as receptors for PilE and PilV (22, 23). The strength of T4P adhesion to the plasma membrane relies on the specific hetero-oligomerization of CD147 with the β2-adrenergic receptor, which is mediated by the scaffolding protein α-actinin-4 (24).

Following adhesion, *N. meningitidis* remodels the host cell plasma membrane in the form of filopodia-like protrusions that are found interdigitated between aggregated bacteria in the microcolony (25). It was shown *in vitro* that plasma membrane remodeling allows *N. meningitidis* to proliferate outside of the host cell while mechanically resisting high shear stress levels (10). This suggests a central role for plasma membrane remodeling in the blood phase of *N. meningitidis* pathogenesis, where bacteria would be subject to high shear.

The molecular mechanisms by which *N. meningitidis* remodels the host cell plasma membrane are still elusive. As the membrane protrusions are enriched in F-actin (25), the mechanisms of actin polymerization in the remodeling process have been extensively studied. Reorganization of the F-actin cytoskeleton underneath microcolonies of *N. meningitidis in vitro* have been shown to rely on the phosphorylation of cortactin by the Src kinase through the biased activation of a β2-adrenergic receptor/β-arrestin pathway (19), and depends on the small GTPases Rho, Cdc42 and Rac (25, 26). Activation of the ErbB2 receptor (27) and of the PI3-kinase pathway (26) were also proposed to contribute to this process. Our previous work has however shown that plasma membrane remodeling actually precedes accumulation of F-actin (28). Consequently, inhibition of actin polymerization (10, 25, 28) or depletion of host cell ATP (28) have no effect on the remodeling of the host cell plasma membrane, which takes only seconds to accumulate underneath bacterial aggregates (28). F-actin reorganization therefore appears to be a consequence of plasma membrane remodeling, rather than its cause.

Parallel to their role in adhesion to the host cell, T4P have been shown to be required for plasma membrane remodeling, as adhesion of non-piliated bacteria mediated by alternative adhesins does not lead to the formation of plasma membrane protrusions in host cells (18). Furthermore, plasma membrane remodeling is tightly linked to the amount of T4P expressed by the bacteria, as a 30% decrease in T4P is sufficient to strongly decrease cell surface remodeling (21). Since the retraction of T4P mediated by the PilT ATPase can generate forces

in the order of 100 pN (29), it has been proposed that T4P retraction could trigger plasma membrane protrusions in the closely related species *N. gonorrhoeae* (30, 31). However, this is unlikely to be the mechanism used by *N. meningitidis* in view of recent results demonstrating that meningococcal aggregates deficient for pilus retraction were still able to remodel the host cell plasma membrane (28).

Here, we address the relevance of *N. meningitidis* plasma membrane remodeling *in vivo* using a recently developed humanized mouse model of infection (12, 13). We show that the surface of human blood vessels is indeed remodeled by *N. meningitidis in vivo*. Using a combination of several light and electron microscopy approaches, we then explore the mechanism of plasma membrane remodeling *in vitro* and provide evidence of a wetting-like mechanism for plasma membrane remodeling driven by adhesion along T4P fibers.

Results

Plasma membrane remodeling by *N. meningitidis* occurs during vascular colonization *in vivo*

A crucial question that needed to be addressed in this field was whether plasma membrane remodeling by *N. meningitidis* occurs *in vivo*. To answer this we took advantage of our humanized mouse model of infection that involves the xenotransplantation of human dermal vessels (12).

After 2 to 3h of infection, we analyzed infected human blood vessels by immunostaining of histological sections. Fluorescent aggregated bacteria filled the human vessel lumen completely. Specific labeling of human endothelial plasma membrane with a human specific lectin revealed a heterogeneous staining with regularly spaced circular shapes at the site of bacterial adhesion (Fig. 1A). Closer examination revealed that every bacterium matched the plasma membrane cup-like structures (Fig. 1A, crop, arrowheads). T4P were present and localized all along the bacterial aggregate (Fig. 1A), filling the space between aggregated bacteria (Fig. 1A, crop).

Since F-actin is recruited to plasma membrane protrusions *in vitro*, we wondered if this was also the case *in vivo*. Labeling of F-actin in infected vessels revealed a similar staining (Fig. 1B). Observation of single planes revealed extensive remodeling of the surface of endothelial cells, with F-actin rich cellular protrusions found extending between aggregated bacteria (Fig. 1B, crop). T4P filled the space between neighboring bacteria and were in close proximity to F-actin (Fig. 1B). These observations show similarities to the description of the local plasma membrane remodeling induced by *N. meningitidis in vitro*, but also demonstrate that these rearrangements occur all along the endothelial layer in a 3D tube-like organization.

To gain ultrastructural information on the shape of the plasma membrane in infected human vessels, we performed transmission electron microscopy. The surface of the vascular endothelial cells was reshaped around the bacterial bodies and extended in between aggregated meningococci (Fig. 1C). Small plasma membrane protrusions were also seen in close association with the bacterial cells surface (Fig. 1C, arrowheads).

These data demonstrate that plasma membrane remodeling by *N. meningitidis* does occur during vascular colonization *in vivo*. Further studies are therefore warranted to understand the underlying cellular mechanisms governing this remodeling.

Single bacteria trigger short lived plasma membrane protrusions

We previously showed that upon entering the circulation, *N. meningitidis* initially binds to blood vessel walls as individual bacteria before proliferating as aggregates that fill the vessel lumen (12). Therefore, we sought to study plasma membrane remodeling first at the level of the single bacterium, then in proliferating bacteria, and finally within the bacterial microcolony on endothelial cells in culture.

Using the high contrast yielding technique of oblique dark field illumination (also known as Highly Inclined and Laminated Optical sheet illumination, or HILO) (32) we imaged human umbilical vein endothelial cells (HUVEC) expressing a GFP targeted to the plasma membrane by lipidation (either GFP-Farnesyl, GFP or Palmitoyl-Myristoyl-EGFP, PM-EGFP). Individual *N. meningitidis* induced the formation of several contrasted fluorescent dots within seconds of adhesion to the host cell (Fig. 2A and Movie S1). These dots dynamically appeared and disappeared, remaining in close proximity to the bacterial bodies. F-actin was not detectable in these protrusions, demonstrated by the absence of the LifeAct-mCherry signal in the fluorescent dots (see Movie S2). Scanning electron microscopy (SEM) of endothelial cells 10 min post-infection showed individual bacteria surrounded by plasma membrane protrusions of diverse morphologies, from finger-like to small ruffle-like structures (Fig. 2B). These results strongly suggest that the fluorescent signal observed in endothelial cells within seconds of bacterial interaction are actually protrusions of the host cell plasma membrane. This indicates that single bacteria are sufficient to induce plasma membrane protrusions and that they occur almost instantaneously.

To fully characterize the dynamics of these plasma membrane protrusions, we performed high-speed oblique illumination live cell imaging (Fig. 2C). Over observation periods of 10 seconds, single bacteria triggered the formation of 1 to 9 small protrusions, with a distribution centered around 4 to 5 protrusions per bacterium (Fig. 2d). These protrusions had diverse lifetimes. Some were static over the entire observation window (Fig. 2C, red), some disappeared (Fig. 2, orange) or appeared (Fig. 2, green) and others had short lifetimes (Fig. 2, blue). Small subsets of protrusions could be identified with extremely short lifetimes, in the

order of a few seconds, and below (minimum was 166 milliseconds) (Fig. 2E). We then measured on- and off-rates (k_{on} and k_{off}) that corresponded to the mean rate of appearance and disappearance of protrusions per second. Consistent with the stable number of protrusions per bacterium over time, k_{on} and k_{off} values were similar, suggesting that plasma membrane protrusions are a dynamic system at equilibrium over the observation period (Fig. 2F and G), consistent with the stable number of protrusions per bacterium over time. By taking the inverse value of k_{off}, we found that the plasma membrane protrusions had an estimated average lifetime of 44 ± 7 seconds (Fig. 2H).

We next wondered what would be the fate of *N. meningitidis*-induced small protrusions over a longer time scale, as bacteria multiply on the surface of the host cell. Live cell imaging of the plasma membrane protrusions caused by individual meningococci showed that protrusions remained present around the bodies of dividing bacteria over the course of 1 h (Fig. 2I). Although bacteria moved laterally on the cell surface, plasma membrane protrusions remained present during the first cycles of bacterial division (Fig. 2I, arrowheads, and Movie S3). In addition, observation of membrane remodeling within large bacterial aggregates also revealed an accumulation of discrete membrane protrusions (Fig. 2J). Interestingly though, protrusions within the center of the bacterial aggregate were now stable over the 10-second observation time, suggesting an increase in the lifetime of the protrusions inside aggregates (Fig. 2K, black arrowhead and Movie S4).

Therefore, *N. meningitidis*-induced plasma membrane remodeling occurs at the level of the single bacterium as dynamic discrete plasma membrane protrusions. These protrusions remain associated with the bacterial bodies and accumulate between aggregated bacteria while the pathogen multiplies on the cell surface.

Factors regulating plasma membrane protrusions dynamics

With *N. meningitidis*-induced plasma membrane protrusions proving unexpectedly dynamic, we went on to investigate which cellular and bacterial factors were involved in their regulation.

While F-actin is not required to induce plasma membrane remodeling by *N. meningitidis*, actin polymerization may be involved in regulating membrane protrusion dynamics. Therefore, we measured the dynamic parameters of plasma membrane protrusions in cells treated with the F-actin polymerization inhibitor cytochalasin D. Consistent with previous studies (10, 25, 28), treatment of the cells did not prevent the formation of the protrusions (Fig. 3A and Movies S5 and S6). Interestingly, bacteria were even able to induce significantly more protrusions with an average of 7 protrusions in cytochalasin D-treated cells compared to 4 protrusions in non-treated ones (Fig. 3B). We measured significantly higher values of k_{on} (Fig. 3C) and k_{off} (Fig. 3D) and found a significantly reduced protrusion lifetime

(Fig. 3E) in treated cells with an average of 15 ± 2 seconds compared to 36 ± 7 seconds in control cells. Actin polymerization is thus not required for the formation of *N. meningitidis*-induced plasma membrane protrusions but rather slows down their formation and stabilizes them once they are formed.

T4P produced by *N. meningitidis* can extend and retract at speeds of up to 1 $\mu m.s^{-1}$ (29). We therefore sought to determine whether T4P dynamics could regulate the lifetime of plasma membrane protrusions. We analyzed protrusions dynamics in endothelial cells infected with a mutant strain of *N. meningitidis* that lacks the PilT ATPase and is therefore unable to achieve T4P retraction (*pilT* mutant). We found that the *pilT* mutant bacteria were still capable of triggering plasma membrane remodeling (Fig. 3F), in line with previous data (28). The total number of protrusions triggered by the mutant bacteria was moderately smaller than those induced by the wild-type strain (Fig. 3G). While most protrusions induced by the *pilT* mutant appeared as discrete dots, in 22% of bacteria they presented as thick rings that conceivably correspond to multiple protrusions unable to be individually resolved at this resolution (Fig. 3F and H). This suggests that the total number of protrusions caused by the hyper-piliated *pilT* mutant may be underestimated (Fig 3G and H). The most striking difference between the wild-type and the *pilT* strains was that in the absence of T4P retraction, protrusions were extremely stable (Fig. 3I and Movie S7). Membrane protrusions induced by the *pilT* mutant strain were rarely seen to disappear or to appear de novo over the observation period (Fig. 3i and Movie S7).

These data show that T4P retraction does not induce plasma membrane protrusions. Protrusions dynamics do however depend on T4P dynamics. Our data suggests that the disappearance of plasma membrane protrusions is related to T4P retraction, leading to a hypothesis that T4P play a direct role in plasma membrane remodeling.

Plasma membrane protrusions grow alongside type IV pili fibers and become embedded in a dense type IV pili meshwork

To follow up on this hypothesis, we sought to determine the spatial organization of T4P-plasma membrane interaction. As plasma membrane protrusions are in the range of a few tens of nanometers and T4P fibers are only 6 nm wide, high resolution approaches were required to achieve this.

Observation of individual or pairs of bacteria on endothelial cells by 3D Structured Illumination Microscopy (3D SIM) revealed that T4P adopted a complex architecture. Whereas a few T4P extended away from the bacteria over several microns, as has previously been reported, the majority of T4P however appeared as a dense meshwork of fibers wrapping the bacterial bodies in all directions (Fig. 4A). Within small aggregates of bacteria, T4P appeared to equally wrap every bacterium (Fig. 4C). Some gaps within the meshwork of T4P fibers were

found to be empty (Fig. 4B and D, empty arrowheads), but importantly, others were seen to enclose host cell plasma membrane protrusions (filled arrowheads).

To reach ultrastructural resolution of the T4P, we performed SEM on endothelial cells after 10 min of infection with wildtype *N. meningitidis*. Consistent with the previous observations, individual bacteria harbored a rich meshwork of fibers (Fig. 4E and F). Some T4P fibers extended away from the bacterial bodies and could measure up to 20 microns, whereas other fibers built a complex meshwork that closely surrounded the bacterium in a cage-like fashion (Fig. S1). Plasma membrane protrusions were seen and appeared to be closely attached to T4P fibers and to adjust to their shapes (Fig. 4E and F, crops). Importantly, plasma membrane remained flat along T4P fibers away from the bacterial bodies (Fig. 4E and F, and Fig. S1). Immunogold labelling unambiguously confirmed that the fibers scaffolding the plasma membrane protrusions were indeed T4P fibers (Fig. 4F). Therefore, the host cell plasma membrane is only remodeled in the vicinity of the bacteria, where T4P fibers draw away from the host cell surface.

To analyze T4P-plasma membrane interaction at the level of the bacterial microcolony, we used high pressure freezing and freeze substitution (HPF-FS) to ensure the best possible ultrastructural preservation. TEM of ultrathin sections of endothelial cells infected by *N. meningitidis* for 2 h revealed a remarkably dense and complex meshwork embedding both bacteria and plasma membrane protrusions (Fig. 4G and Fig. S2). The meshwork embedded every plasma membrane protrusion seen (Fig 4G). Immunogold labeling of T4P prior to HPF-FS confirmed that this meshwork stained positive for T4P (Fig 4H). T4P structures were again seen to run in parallel to plasma membrane protrusions (Fig. 4H). Protrusions were sometimes found tightly wrapped around bacterial bodies in a thin layer of T4P that embedded both the bacterium and the protrusion even in the absence of a neighboring bacterium (Fig. S2).

Our results show that the morphology of the plasma membrane protrusions is tightly linked to the morphology of T4P fibers at the level of the single adhering meningococcus. As bacteria divide and aggregate, plasma membrane protrusions are progressively embedded in an extracellular matrix-like meshwork of T4P. Together, these data suggest that plasma membrane protrusions align along the T4P fibers, which may act as a scaffold type guide.

T4P fibers act as a scaffold that imposes a specific geometry to the plasma membrane

To test whether the fibrous architecture of T4P could act as a scaffold and impose a specific shape to plasma membrane remodeling, we addressed the following questions: 1) what is the native state of T4P prior to contact with the host cell? 2) what is the shape of the plasma membrane when the spatial organization of the adhesive structure is modified? and 3) can the plasma membrane be remodeled in the absence of bacteria, in response to any adhesive nanostructured substrate?

We first analyzed the ultrastructure of T4P in individual bacteria. TEM after immunogold labeling of T4P and negative stain revealed extensive fibrous structures around bacteria that were entirely decorated with gold particles (Fig. 5A). SEM also revealed an extensive meshwork of fibers emanating from individual bacteria (Fig. 5B) similar to the architecture of T4P on bacteria adhered to host cells (Fig. 4E and F).

To directly test whether the spatial organization of T4P fibers has an impact on the shape of host cell plasma membrane remodeling, we used a T4P-deficient (T4P-) and capsule-deficient (caps-) mutant of a natural derivative of *N. meningitidis* that uniformly expresses the OpaB alternative adhesin (Opa+) on its outer membrane (18). When adhered to endothelial cells overexpressing the Opa adhesins receptor carcinoembryonic antigen-related cell adhesion molecule 1 (CEACAM1), the remodeling of the host cell plasma membrane was seen in oblique illumination as partial or complete plasma membrane rings surrounding the bacterial bodies (Fig. 5C, arrowheads). In contrast, restoration of T4P production (T4P+) in the same *N. meningitidis* strain was sufficient to reestablish a dot-like appearance of plasma membrane remodeling (Fig. 5D, arrowheads).

We then sought to infect endothelial cells while perturbing the meshwork-like organization of T4P fibers. To do so, we infected endothelial cells for 2h in the presence of an anti-T4P monoclonal antibody in order to cross-link the T4P meshwork. We then assessed the ability of bacterial microcolonies to recruit the plasma membrane by the staining of endogenous ezrin, as commonly done (10, 19). Control microcolonies showed a typical regular arrangement of T4P and most of them accumulated host cell plasma membrane visible as a honeycomb-like lattice at this resolution (Fig. 5E and F). In sharp contrast, increasing concentrations of antibodies progressively altered the spatial organization of T4P that appeared loosely packed and eventually no longer fibrous. Plasma membrane remodeling was strongly impaired underneath these microcolonies (Fig. 5E and F). This strongly suggests that it is the architecture of T4P that dictates the specific geometry of the plasma membrane protrusions they trigger.

To further test whether the endothelial cell plasma membrane has the intrinsic ability to deform in response to any adhesive nanostructured substrate or whether this response is specific to T4P, endothelial cells were cultured on anodized aluminum oxide (AAO) membranes featuring 100 nm pores with pore walls of less than 15 nm, closely mimicking the diameter of T4P individual fibers (6 nm) or small T4P bundles (10 nm) (Fig. 5G and J). To promote adhesion of the plasma membrane to the substrate without altering the nanotopography, we sequentially coated the membranes with an azide functionalized PLL-PEG (azido-(Poly-L-lysine-graft-Poly[ethylene glycol] or APP) and a reactive RGD peptide (BCN-RGD) (33). Observation of these cells using high resolution SEM showed that the plasma membrane at the cell contour was periodically pinching along the pore walls (Fig. 5H).

Filopodia were also frequently seen to follow the complex geometry of the pore walls along their whole length (Fig. 5I). Interestingly, the plasma membrane in filopodia also seemed to deform periodically when meeting with a pore wall (Fig. 5I). Upon depolymerization of the F-actin cytoskeleton with cytochalasin D, local deformation of the plasma membrane onto the pore walls was still observed on the cell contour (Fig. 5K) and filopodia were still seen to follow the edges of the pore walls along their length. The filopodia appeared flattened, and periodic deformation of the plasma membrane on pore walls was more pronounced (Fig. 5L).

Taken together, these data strongly suggest that the plasma membrane has the intrinsic ability to deform locally onto an adhesive nanostructure in an F-actin independent fashion

Discussion

In this study, we investigated how the plasma membrane of host human cells is remodeled by an extracellular bacterial pathogen. Our data show that the host cell plasma membrane is remodeled by adhesion onto T4P fibers expressed by the bacteria. We propose a model in which bacterial T4P adhere over their whole length to the cellular surface, and trigger a remodeling of the plasma membrane in the vicinity of the bacterial body (Fig. 6).

A key element of our study is our improved ability to actually visualize T4P fibers at high resolution, including at the single bacterium level. While previous studies on *N. meningitidis*-infected cells only showed rare T4P fibers (10, 25, 34), the use of more preservative preparation methods has allowed us to show that T4P fibers are very abundantly expressed by piliated bacteria. Moreover, we show that T4P have a particular spatial organization in which they form a meshwork that encloses the bacterium in a cage-like structure and extends as fibers over long distances. Numerous other bacteria have been shown to produce pili in large amounts, particularly at the surface of host cells. This is the case for the T4P of the closely related species *Neisseria gonorrhoeae* (35), but also of other human pathogens such as *Vibrio cholerae* (36, 37), *Francisella tularensis* (38) and *Burkholderia cepacia* (39). Other types of pili, like the curli pili of *Mycobacterium tuberculosis* (40) and *Escherichia coli* (41), the type I pili of *Salmonella enteritidis* (42) and the mixed pili types of *Klebsiella pneumoniae* (43) and *Enterococcus faecalis* (44), were seen to be produced in large amounts. Even filamentous organelles produced by archaea (45), like the hami fibers in the SM1 Euryarcheon (46), were seen to harbor dense and complex architectures in vitro and in the context of natural multispecies biofilms. To our knowledge however, the three-dimensional architecture of these different fibers at the single cell level is not known. It would be of great interest to see whether the architecture of such pili and other surface appendages in these organisms have complex 3D architectures as seen in *N. meningitidis* at the single bacterium

level. It would also be of interest to see whether specific architectures of prokaryotic appendages contribute to the interactions between microorganisms and their environment or host cells.

Here we identified a link between T4P retraction and the disappearance of plasma membrane protrusions, meaning that plasma membrane and T4P dynamics mirror one another. We estimated a lifetime for the protrusions of around 44 seconds. Considering typical T4P fibers between 5 and 20 μm long and that can extend and retract at speeds in the order of 1 $\mu m.s^{-1}$ (29), it would take a few tens of seconds for one fiber to completely extend and retract. Therefore, the lifetime of T4P fibers is in good accordance with the lifetime of the protrusions. In addition, our observation that plasma membrane protrusions appear very stable within a bacterial aggregate implies that T4P dynamics change as bacteria proliferate on top of the host cell. It may be that the T4P stop retracting within the microcolony. Alternatively, T4P could also accumulate in a way that retraction of one pilus would not lead to the disappearance of a particular plasma membrane protrusion since it would be compensated by the remaining T4P. Both hypotheses would be consistent with the dense meshwork of T4P observed by electron microscopy within microcolonies (Fig. 4). Stabilization of, or increase in the number of T4P would greatly increase the interaction surface between bacteria and the plasma membrane, which could account for the greater mechanical coherence of the bacterial microcolonies and their resistance to shear stress (10).

Our results show that plasma membrane remodeling at the single bacterium level is F-actin-independent, consistent with previous findings performed on bacterial aggregates (10, 25, 28). We further identify actin polymerization as a negative regulator of plasma membrane remodeling. Low doses of cytochalasin D in endothelial cells were shown to alter the morphology of the actin cortex (47, 48), and as protrusions are likely areas of plasma membrane that detached from the cortex, one could imagine that decreasing the density of cortical F-actin would facilitate the formation of plasma membrane protrusions. Another role of cortical F-actin is to physically stabilize plasma membrane protrusions. Polymerization of actin inside newly formed plasma membrane protrusions could be a direct response to plasma membrane deformation, as has been shown for filopodia initiation (49, 50).

In this study, the T4P meshwork appears to shape the host cell plasma membrane. Other biological processes, such as the initial remodeling of the plasma membrane during phagocytosis (51, 52) or the adaptation of the plasma membrane to mechanical stress (53, 54) involve a step of plasma membrane deformation that is independent of actin polymerization. The geometry of proteins has been shown to be sufficient to change the shape of a lipid bilayer, even in liposomes where no F-actin is present. Intracellular membranes can be reshaped by crescent-shaped BAR-domain containing proteins (55). From outside of the cell, invaginations of the plasma membrane can be initiated through a nanoscaffolding mechanism by the SV40

virus (56) or the protein galectin-3 alone (57). The human opportunistic pathogen Pseudomonas aeruginosa was also shown to trigger its internalization by a lipid zipper mechanism that could be reconstituted in a synthetic lipid bilayer system (58). The interaction of *N. meningitidis* with endothelial cells is a unique case in this family of mechanisms, as the remodeling of the plasma membrane occurs outwards and is driven by adhesion to fibers. Our present description of what we term "scaffolded adhesion" challenges the notion that cell surface reorganization occurs sequentially after initial adhesion of the bacteria to the host cell. Instead, it suggests that adhesion and plasma membrane remodeling are indistinguishable. The discrete fluorescent dots observed in oblique illumination (Fig. 2) reflect individual adhesion points between the bacterium and the host cell surface, in addition to individual points of T4P assembly and retraction.

Our study demonstrates that the plasma membrane of human cells can deform by aligning onto adhesive nanostructures even in the absence of F-actin. From a physical standpoint, this process could be compared to the wetting of a liquid on a wettable solid with a particular geometry. Indeed, earlier studies have shown that lipid vesicles can wet onto adhesive fibers (59) and that wetting of supported lipid bilayers could be directed by the nanotopography of an adhesive substrate (60), even at the submicrometer scale (61, 62). A simple gradient of calcium ions near a negatively charged multilamellar vesicles induces protrusions of the bilayer by a simple wetting through electrostatic interactions with the surface (63). In our particular case, the plasma membrane may simply wet onto adhesive T4P fibers (23, 24, 64) (Fig. 6). Since it seems more favorable for the plasma membrane to bend out onto T4P fibers rather than to staying in a 2D plane, it implies that the interaction of the plasma membrane with T4P is very strong, as measured in vitro (24). Furthermore, the fact that plasma membrane remodeling by *N. meningitidis* is completely abolished in the absence of plasma membrane cholesterol (10, 28) is consistent with the fact that the ability of a liquid to wet on a solid also depends on the surface tension of that liquid. Indeed, cholesterol-depleted endothelial cells have a stiffer plasma membrane due to an enhancement of membrane-cytoskeleton interaction (65-67).

It clearly appears here that the endothelial cells plasma membrane in human blood vessels is remodeled at the bacterial adhesion site in vivo, pointing to a key role for plasma membrane remodeling in the context of vascular colonization by *N. meningitidis*. At low resolution, plasma membrane appears cup-shaped. Yet, electron micrographs show that several small plasma membrane protrusions are found associated with each bacterium, correlating to the discrete protrusions that we describe in vitro. Fluorescence imaging further reveals that plasma membrane protrusions are enriched with F-actin, as previously described in vitro, and more importantly that T4P are present at the site of plasma membrane remodeling. These data suggest that the mechanism of plasma membrane remodeling that we describe

here likely occurs in the pathological context of vascular colonization and that it is indeed a strategy employed by *N. meningitidis* to resist blood flow-generated shear stress.

Overall, our study emphasizes the notion that the topography of the environment, even at the nanoscale, can be sensed by cells and can direct their behavior (68). It is likely that the development of high resolution light and electron imaging techniques will help uncovering the cell response to nanotopographical cues. In a recent study by Elkhatib et al., stunning pictures of correlative light and electron microscopy showed how cells plasma membrane closely fits to the morphology of sub-micrometer collagen fibers in a 3D environment (69). In our case, nanotopographical cues are induced by bacterial fibers that elicit a remodeling of the plasma membrane in human endothelial cells in the context of an infectious process. It would be of interest to assess whether such an F-actin-independent wetting-like phenomenon plays a role in the interaction of human cells with their substrate, in particular when exploring complex fibrous environments like extracellular matrices.

Acknowledgments

We gratefully acknowledge the Imagopole – Citech of Institut Pasteur (Paris, France) as well as the France–BioImaging infrastructure network supported by the French National Research Agency (ANR-10–INSB–04; Investments for the Future), and the Région Ile-de-France (program Domaine d'Intérêt Majeur-Malinf) for the use of the Zeiss LSM 780 Elyra PS1 microscope. We thank Dorian Obino for critical reading of the manuscript.

Author contributions

A.C.O. conducted and analyzed most of the experiments, and prepared the figures. D.B. performed and analyzed the micropatterns experiments. V.M. and A.C.O. performed and analyzed the fluorescence experiments in mice. M.S. and A.C.O. performed and analyzed the HPF-FS, negative stain and TEM experiments. A.M. and A.C.O. conducted and analyzed the SEM experiments. A.S. and A.C.O. performed and analyzed the 3D-SIM experiments. K.M. performed the TEM experiment in the mouse. C.M. constructed the pMGC13 plasmid. S.G. and P.L. produced the nanobody against T4P used in the mice experiments. M.P., J.K.L., S.S., G.D. and A.C.O. designed and analyzed the experiments. A.C.O. and G.D. wrote the manuscript. D.B., M.S., A.M., A.S. and K.M. edited the manuscript.

References

1. H. T. McMahon, J. L. Gallop, Membrane curvature and mechanisms of dynamic cell membrane remodelling. Nature 438, 590-596 (2005).

2. R. G. Parton, M. A. del Pozo, Caveolae as plasma membrane sensors, protectors and organizers. Nat Rev Mol Cell Biol 14, 98-112 (2013).

3. H. T. McMahon, E. Boucrot, Molecular mechanism and physiological functions of clathrin-mediated endocytosis. Nat Rev Mol Cell Biol 12, 517-533 (2011).
4. R. Levin, S. Grinstein, J. Canton, The life cycle of phagosomes: formation, maturation, and resolution. Immunol Rev 273, 156-179 (2016).
5. A. J. Ridley, Life at the leading edge. Cell 145, 1012-1022 (2011).
6. H. Ham, A. Sreelatha, K. Orth, Manipulation of host membranes by bacterial effectors. Nat Rev Microbiol 9, 635-646 (2011).
7. J. S. Rossman, R. A. Lamb, Viral membrane scission. Annu Rev Cell Dev Biol 29, 551-569 (2013).
8. D. C. Sheppard, S. G. Filler, Host cell invasion by medically important fungi. Cold Spring Harb Perspect Med 5, a019687 (2014).
9. G. Dumenil, Revisiting the extracellular lifestyle. Cell Microbiol 13, 1114-1121 (2011).
10. G. Mikaty et al., Extracellular bacterial pathogen induces host cell surface reorganization to resist shear stress. PLoS Pathog 5, e1000314 (2009).
11. D. A. Caugant, M. C. Maiden, Meningococcal carriage and disease--population biology and evolution. Vaccine 27 Suppl 2, B64-70 (2009).
12. K. Melican, P. Michea Veloso, T. Martin, P. Bruneval, G. Dumenil, Adhesion of Neisseria meningitidis to dermal vessels leads to local vascular damage and purpura in a humanized mouse model. PLoS Pathog 9, e1003139 (2013).
13. O. Join-Lambert et al., Meningococcal interaction to microvasculature triggers the tissular lesions of purpura fulminans. J Infect Dis 208, 1590-1597 (2013).
14. K. Melican, G. Dumenil, Vascular colonization by Neisseria meningitidis. Curr Opin Microbiol 15, 50-56 (2012).
15. P. Brandtzaeg, M. van Deuren, Classification and pathogenesis of meningococcal infections. Methods Mol Biol 799, 21-35 (2012).
16. X. Nassif et al., Antigenic variation of pilin regulates adhesion of Neisseria meningitidis to human epithelial cells. Mol Microbiol 8, 719-725 (1993).
17. J. L. Berry, V. Pelicic, Exceptionally widespread nanomachines composed of type IV pilins: the prokaryotic Swiss Army knives. FEMS Microbiol Rev 39, 134-154 (2015).
18. T. Brissac, G. Mikaty, G. Dumenil, M. Coureuil, X. Nassif, The meningococcal minor pilin PilX is responsible for type IV pilus conformational changes associated with signaling to endothelial cells. Infect Immun 80, 3297-3306 (2012).
19. M. Coureuil et al., Meningococcus Hijacks a beta2-adrenoceptor/beta-Arrestin pathway to cross brain microvasculature endothelium. Cell 143, 1149-1160 (2010).
20. X. Nassif et al., Roles of pilin and PilC in adhesion of Neisseria meningitidis to human epithelial and endothelial cells. Proc Natl Acad Sci U S A 91, 3769-3773 (1994).

21. A. F. Imhaus, G. Dumenil, The number of Neisseria meningitidis type IV pili determines host cell interaction. Embo J, (2014).
22. H. Kallstrom, M. K. Liszewski, J. P. Atkinson, A. B. Jonsson, Membrane cofactor protein (MCP or CD46) is a cellular pilus receptor for pathogenic Neisseria. Mol Microbiol 25, 639-647 (1997).
23. S. C. Bernard et al., Pathogenic Neisseria meningitidis utilizes CD147 for vascular colonization. Nat Med 20, 725-731 (2014).
24. N. Maissa et al., Strength of Neisseria meningitidis binding to endothelial cells requires highly-ordered CD147/beta2-adrenoceptor clusters assembled by alpha-actinin-4. Nat Commun 8, 15764 (2017).
25. E. Eugene et al., Microvilli-like structures are associated with the internalization of virulent capsulated Neisseria meningitidis into vascular endothelial cells. J Cell Sci 115, 1231-1241 (2002).
26. M. Lambotin et al., Invasion of endothelial cells by Neisseria meningitidis requires cortactin recruitment by a phosphoinositide-3-kinase/Rac1 signalling pathway triggered by the lipo-oligosaccharide. J Cell Sci 118, 3805-3816 (2005).
27. I. Hoffmann, E. Eugene, X. Nassif, P. O. Couraud, S. Bourdoulous, Activation of ErbB2 receptor tyrosine kinase supports invasion of endothelial cells by Neisseria meningitidis. J Cell Biol 155, 133-143 (2001).
28. M. Soyer et al., Early sequence of events triggered by the interaction of Neisseria meningitidis with endothelial cells. Cell Microbiol 16, 878-895 (2014).
29. N. Biais, B. Ladoux, D. Higashi, M. So, M. Sheetz, Cooperative retraction of bundled type IV pili enables nanonewton force generation. PLoS Biol 6, e87 (2008).
30. D. L. Higashi et al., Influence of type IV pilus retraction on the architecture of the Neisseria gonorrhoeae-infected cell cortex. Microbiology 155, 4084-4092 (2009).
31. A. J. Merz, C. A. Enns, M. So, Type IV pili of pathogenic Neisseriae elicit cortical plaque formation in epithelial cells. Mol Microbiol 32, 1316-1332 (1999).
32. M. Tokunaga, N. Imamoto, K. Sakata-Sogawa, Highly inclined thin illumination enables clear single-molecule imaging in cells. Nat Methods 5, 159-161 (2008).
33. S. F. M. van Dongen, P. Maiuri, E. Marie, C. Tribet, M. Piel, Triggering Cell Adhesion, Migration or Shape Change with a Dynamic Surface Coating. Adv Mater 25, 1687-1691 (2013).
34. C. Pujol, E. Eugene, L. de Saint Martin, X. Nassif, Interaction of Neisseria meningitidis with a polarized monolayer of epithelial cells. Infect Immun 65, 4836-4842 (1997).
35. W. J. Todd, G. P. Wray, P. J. Hitchcock, Arrangement of pili in colonies of Neisseria gonorrhoeae. J Bacteriol 159, 312-320 (1984).
36. B. A. Jude, R. K. Taylor, The physical basis of type 4 pilus-mediated microcolony formation by Vibrio cholerae O1. J Struct Biol 175, 1-9 (2011).

37. S. J. Krebs, R. K. Taylor, Protection and attachment of Vibrio cholerae mediated by the toxin-coregulated pilus in the infant mouse model. J Bacteriol 193, 5260-5270 (2011).
38. H. Gil, J. L. Benach, D. G. Thanassi, Presence of pili on the surface of Francisella tularensis. Infect Immun 72, 3042-3047 (2004).
39. U. S. Sajjan, L. Sun, R. Goldstein, J. F. Forstner, Cable (cbl) type II pili of cystic fibrosis-associated Burkholderia (Pseudomonas) cepacia: nucleotide sequence of the cblA major subunit pilin gene and novel morphology of the assembled appendage fibers. J Bacteriol 177, 1030-1038 (1995).
40. C. J. Alteri et al., Mycobacterium tuberculosis produces pili during human infection. Proc Natl Acad Sci U S A 104, 5145-5150 (2007).
41. A. Olsen, A. Jonsson, S. Normark, Fibronectin binding mediated by a novel class of surface organelles on Escherichia coli. Nature 338, 652-655 (1989).
42. S. K. Collinson, L. Emody, K. H. Muller, T. J. Trust, W. W. Kay, Purification and characterization of thin, aggregative fimbriae from Salmonella enteritidis. J Bacteriol 173, 4773-4781 (1991).
43. M. D. Alcantar-Curiel et al., Multi-functional analysis of Klebsiella pneumoniae fimbrial types in adherence and biofilm formation. Virulence 4, 129-138 (2013).
44. C. J. Kristich et al., Development and use of an efficient system for random mariner transposon mutagenesis to identify novel genetic determinants of biofilm formation in the core Enterococcus faecalis genome. Appl Environ Microbiol 74, 3377-3386 (2008).
45. K. F. Jarrell, Y. Ding, D. B. Nair, S. Siu, Surface appendages of archaea: structure, function, genetics and assembly. Life (Basel) 3, 86-117 (2013).
46. A. K. Perras et al., Grappling archaea: ultrastructural analyses of an uncultivated, cold-loving archaeon, and its biofilm. Front Microbiol 5, 397 (2014).
47. C. Kronlage, M. Schafer-Herte, D. Boning, H. Oberleithner, J. Fels, Feeling for Filaments: Quantification of the Cortical Actin Web in Live Vascular Endothelium. Biophys J 109, 687-698 (2015).
48. T. Wakatsuki, B. Schwab, N. C. Thompson, E. L. Elson, Effects of cytochalasin D and latrunculin B on mechanical properties of cells. J Cell Sci 114, 1025-1036 (2001).
49. S. Ahmed, W. I. Goh, W. Bu, I-BAR domains, IRSp53 and filopodium formation. Semin Cell Dev Biol 21, 350-356 (2010).
50. C. Prevost et al., IRSp53 senses negative membrane curvature and phase separates along membrane tubules. Nat Commun 6, 8529 (2015).
51. M. B. Lowry, A. M. Duchemin, J. M. Robinson, C. L. Anderson, Functional separation of pseudopod extension and particle internalization during Fc gamma receptor-mediated phagocytosis. J Exp Med 187, 161-176 (1998).

52. S. Tollis, A. E. Dart, G. Tzircotis, R. G. Endres, The zipper mechanism in phagocytosis: energetic requirements and variability in phagocytic cup shape. BMC Syst Biol 4, 149 (2010).
53. B. Sinha et al., Cells respond to mechanical stress by rapid disassembly of caveolae. Cell 144, 402-413 (2011).
54. A. J. Kosmalska et al., Physical principles of membrane remodelling during cell mechanoadaptation. Nat Commun 6, 7292 (2015).
55. M. Simunovic, G. A. Voth, A. Callan-Jones, P. Bassereau, When Physics Takes Over: BAR Proteins and Membrane Curvature. Trends Cell Biol 25, 780-792 (2015).
56. H. Ewers et al., GM1 structure determines SV40-induced membrane invagination and infection. Nat Cell Biol 12, 11-18; sup pp 11-12 (2010).
57. R. Lakshminarayan et al., Galectin-3 drives glycosphingolipid-dependent biogenesis of clathrin-independent carriers. Nat Cell Biol 16, 595-606 (2014).
58. T. Eierhoff et al., A lipid zipper triggers bacterial invasion. Proc Natl Acad Sci U S A, (2014).
59. N. Borghi, K. Alias, P. G. de Gennes, F. Brochard-Wyart, Wetting fibers with liposomes. J Colloid Interf Sci 285, 61-66 (2005).
60. A. L. Bernard et al., Permeation through lipid bilayers by adhesion of giant vesicles on decorated surfaces. Langmuir 16, 6801-6808 (2000).
61. K. Furukawa, K. Sumitomo, H. Nakashima, Y. Kashimura, K. Torimitsu, Supported lipid bilayer self-spreading on a nanostructured silicon surface. Langmuir 23, 367-371 (2007).
62. J. H. Werner et al., Formation and Dynamics of Supported Phospholipid Membranes on a Periodic Nanotextured Substrate. Langmuir 25, 2986-2993 (2009).
63. T. Lobovkina et al., Protrusive growth and periodic contractile motion in surface-adhered vesicles induced by Ca2+-gradients. Soft Matter 6, 268-272 (2010).
64. S. Lu et al., Nanoscale Pulling of Type IV Pili Reveals Their Flexibility and Adhesion to Surfaces over Extended Lengths of the Pili. Biophys J 108, 2865-2875 (2015).
65. L. Wu et al., AFM of the ultrastructural and mechanical properties of lipid-raft-disrupted and/or cold-treated endothelial cells. J Membr Biol 247, 189-200 (2014).
66. F. J. Byfield, H. Aranda-Espinoza, V. G. Romanenko, G. H. Rothblat, I. Levitan, Cholesterol depletion increases membrane stiffness of aortic endothelial cells. Biophys J 87, 3336-3343 (2004).
67. M. Sun et al., The effect of cellular cholesterol on membrane-cytoskeleton adhesion. J Cell Sci 120, 2223-2231 (2007).
68. V. Ruprecht et al., How cells respond to environmental cues - insights from bio-functionalized substrates. Journal of Cell Science 130, 51-61 (2017).
69. N. Elkhatib et al., Tubular clathrin/AP-2 lattices pinch collagen fibers to support 3D cell migration. Science 356, (2017).

Figure 1

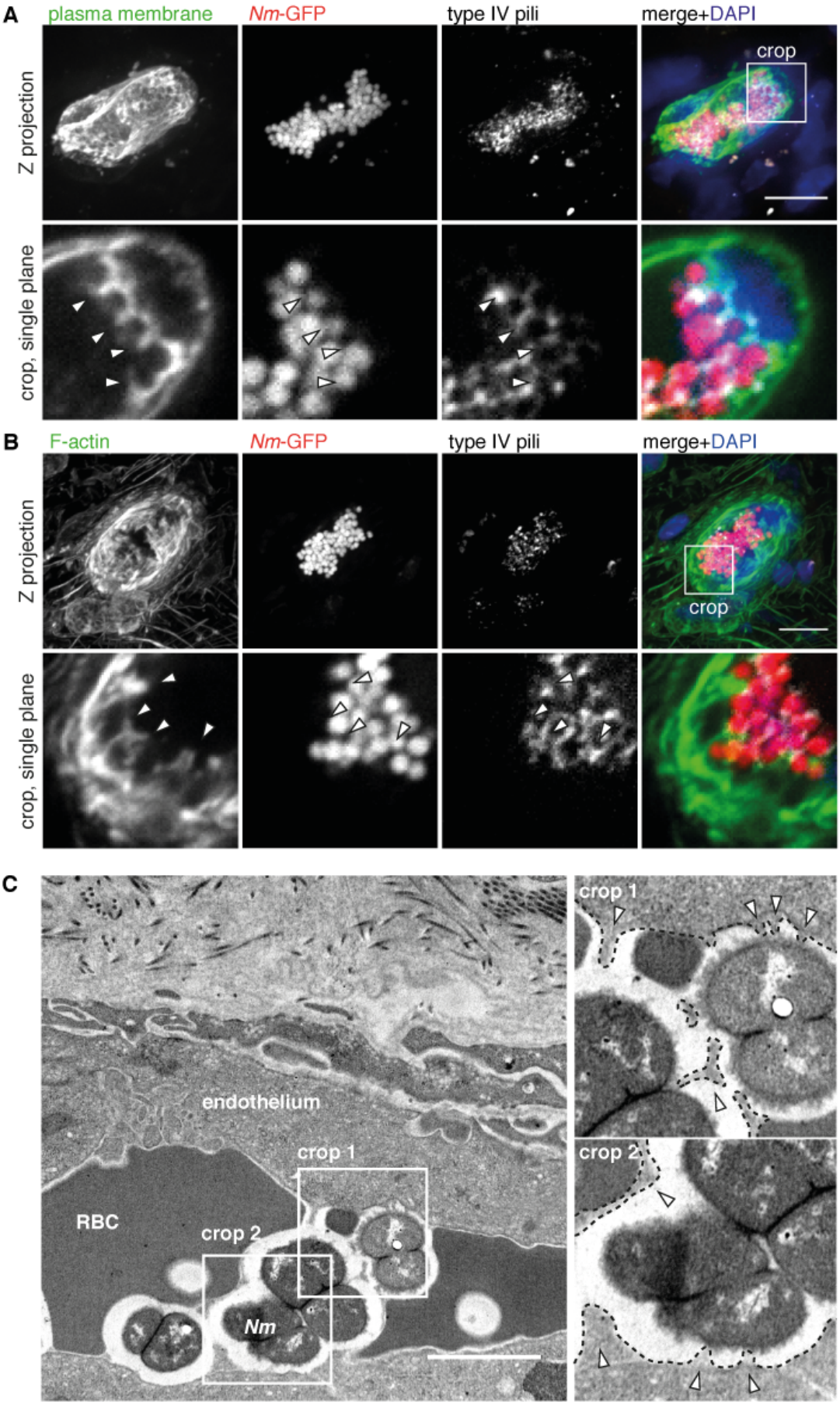
A
plasma membrane
Nm-GFP
type IV pili
merge+DAPI
Z projection
crop
crop, single plane
B
F-actin
Nm-GFP
type IV pili
merge+DAPI
Z projection
crop
crop, single plane
C
endothelium
crop 1
RBC
crop 2
Nm
crop 1
crop 2

Figure 2

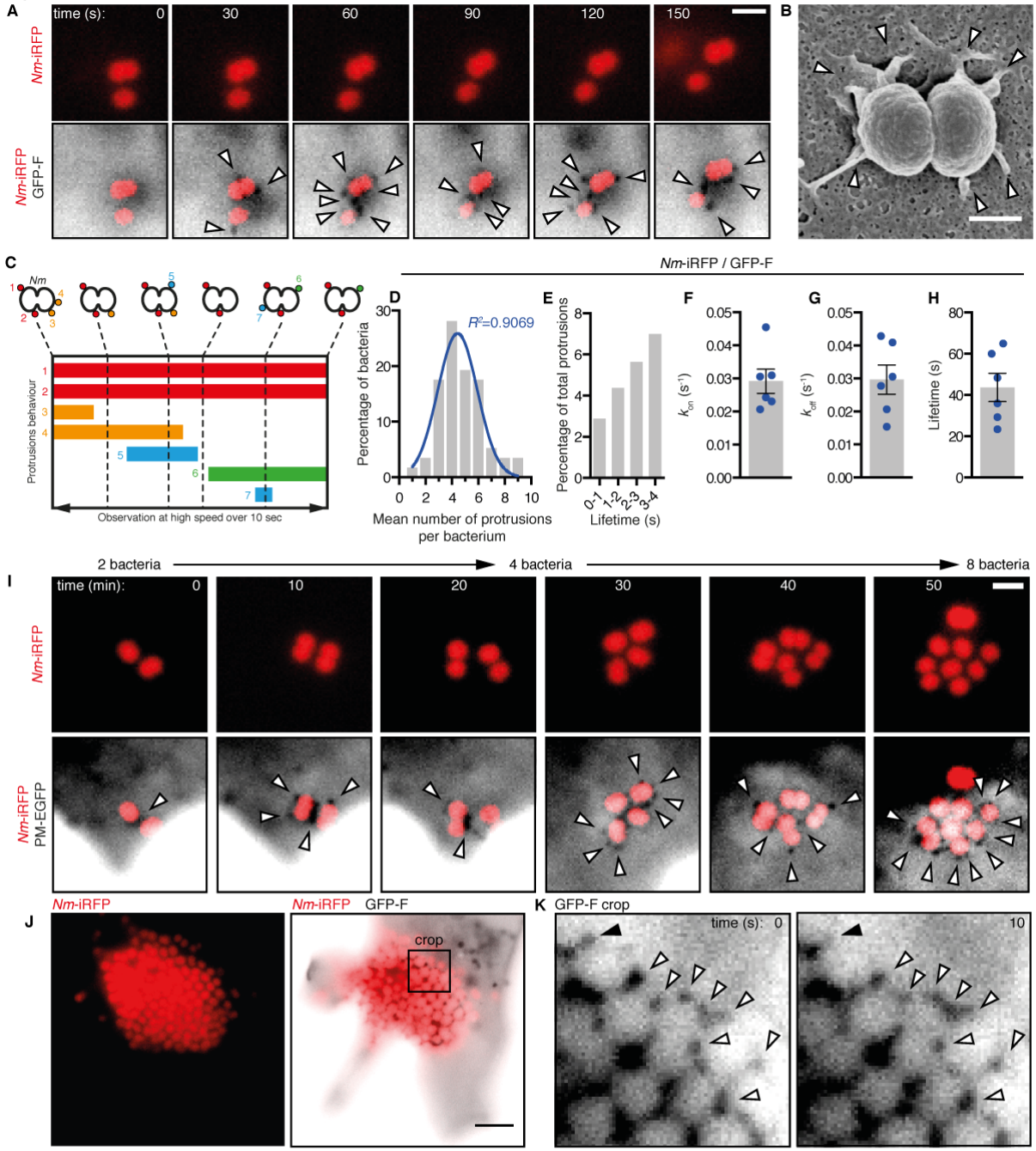
A
time (s): 0 30 60 90 120 150
Nm-iRFP
Nm-iRFP GFP-F
B
C
Nm
Protrusions behaviour
Observation at high speed over 10 sec
Nm-iRFP / GFP-F
D
R²=0.9069
Percentage of bacteria
Mean number of protrusions per bacterium
E
Percentage of total protrusions
Lifetime (s)
F
k_on (s⁻¹)
G
k_off (s⁻¹)
H
Lifetime (s)
2 bacteria
4 bacteria
8 bacteria
I
time (min): 0 10 20 30 40 50
Nm-iRFP
Nm-iRFP PM-EGFP
J
Nm-iRFP
Nm-iRFP GFP-F
crop
K
GFP-F crop
time (s): 0
10

Figure 3

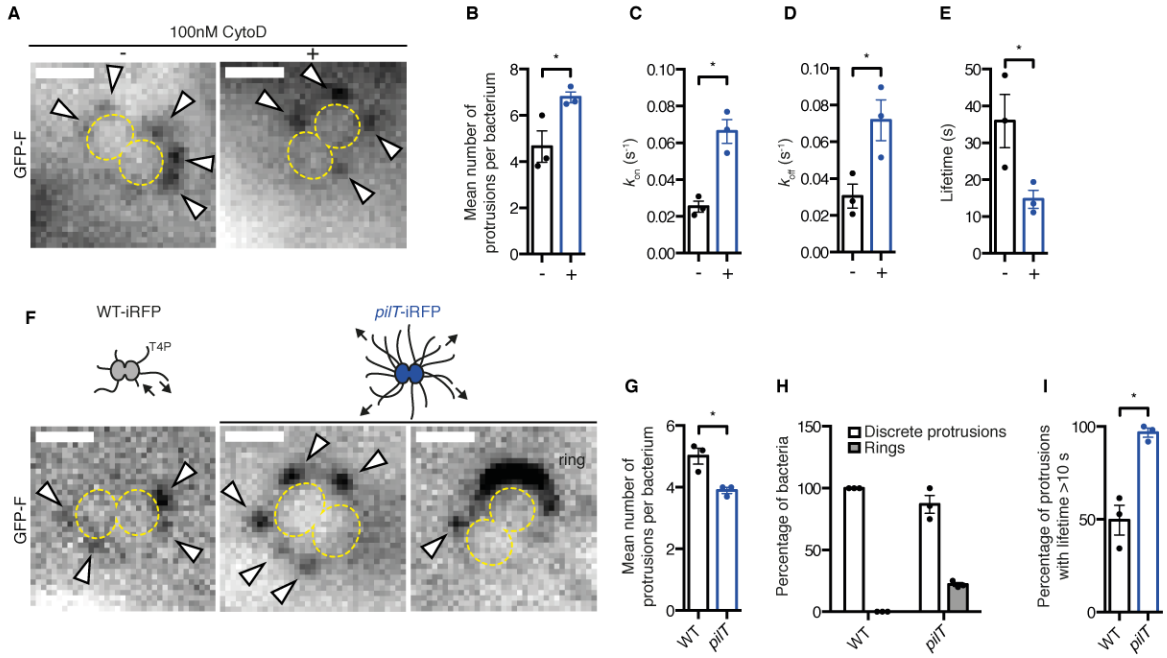
A
100nM CytoD
-
+
GFP-F
B
Mean number of protrusions per bacterium
C
k_{on} (s^{-1})
D
k_{off} (s^{-1})
E
Lifetime (s)
F
WT-iRFP
T4P
pilT-iRFP
GFP-F
ring
G
Mean number of protrusions per bacterium
H
Discrete protrusions
Rings
Percentage of bacteria
WT
pilT
I
Percentage of protrusions with lifetime >10 s

Figure 4

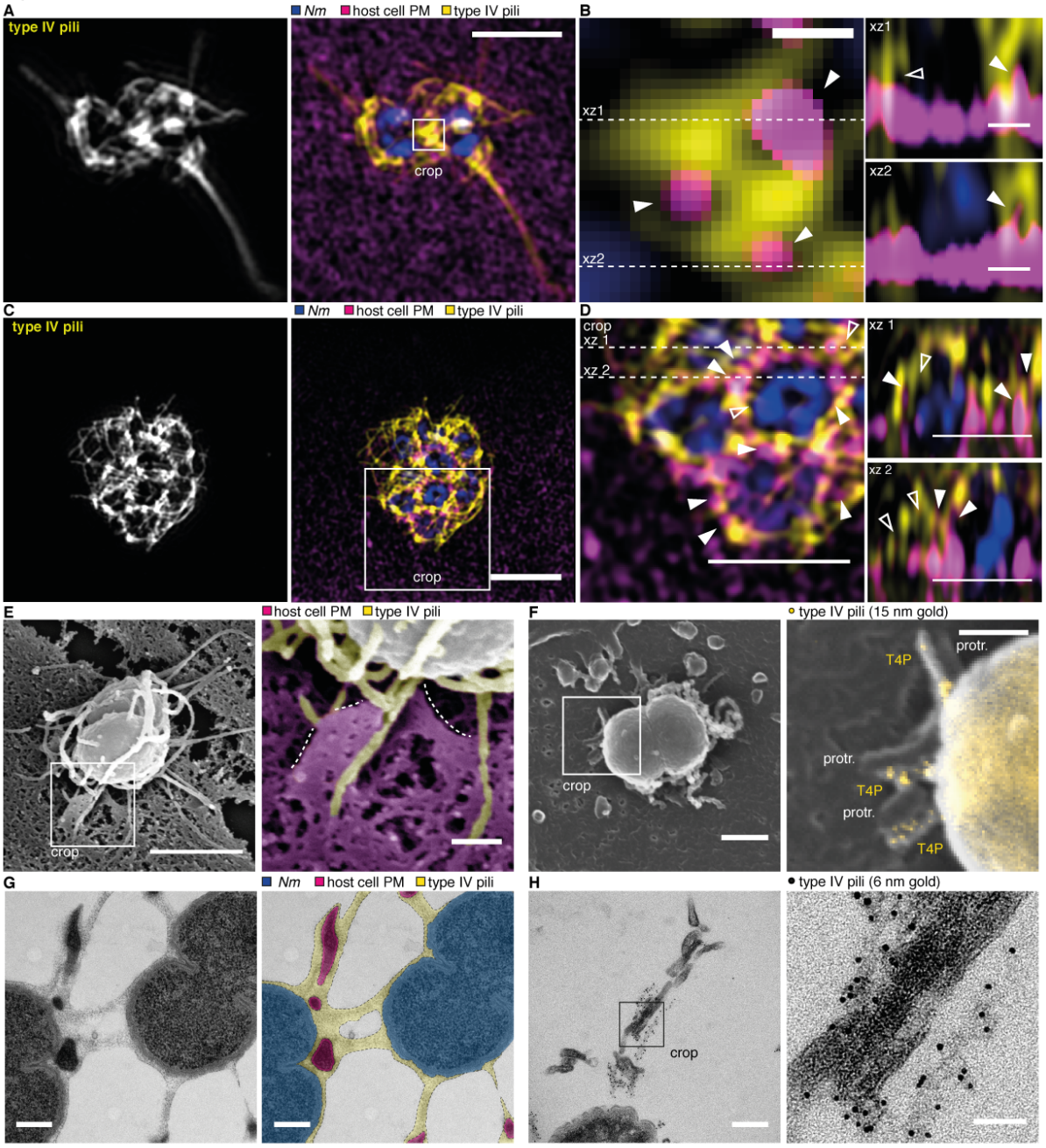
A
type IV pili
Nm
host cell PM
type IV pili
crop
B
xz1
xz2
C
type IV pili
Nm
host cell PM
type IV pili
crop
D
crop
xz 1
xz 2
E
host cell PM
type IV pili
crop
F
type IV pili (15 nm gold)
T4P
protr.
G
Nm
host cell PM
type IV pili
H
type IV pili (6 nm gold)
crop

Figure 5

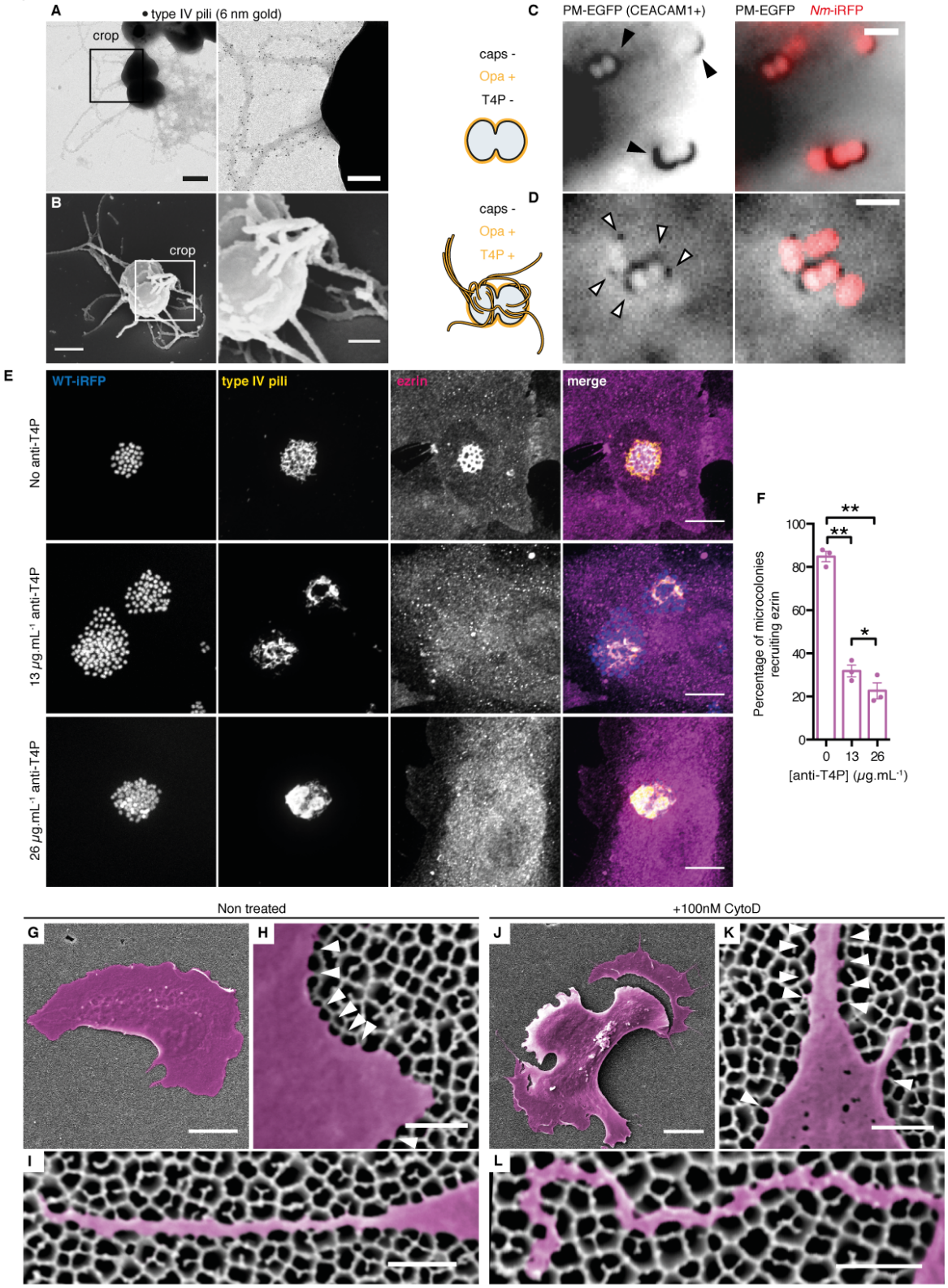
A
type IV pili (6 nm gold)
crop
B
crop
C
PM-EGFP (CEACAM1+)
PM-EGFP Nm-iRFP
caps -
Opa +
T4P -
D
caps -
Opa +
T4P +
E
WT-iRFP
type IV pili
ezrin
merge
No anti-T4P
13 μg.mL-1 anti-T4P
26 μg.mL-1 anti-T4P
F
Percentage of microcolonies recruiting ezrin
[anti-T4P] (μg.mL-1)
Non treated
+100nM CytoD
G
H
I
J
K
L

Figure 6

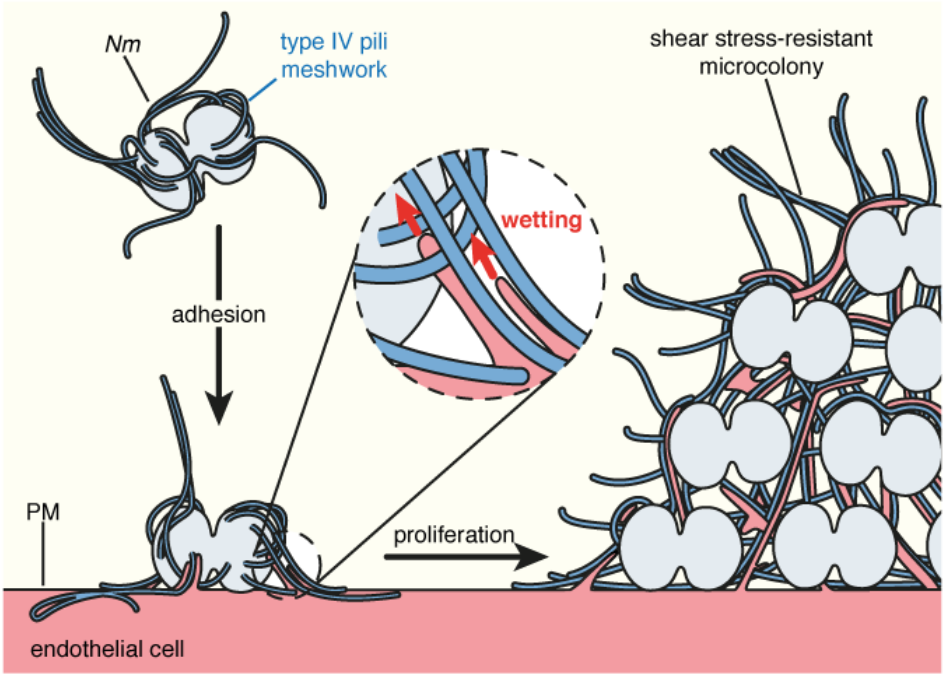
Nm
type IV pili
meshwork
shear stress-resistant
microcolony
wetting
adhesion
PM
proliferation
endothelial cell

Figure S1

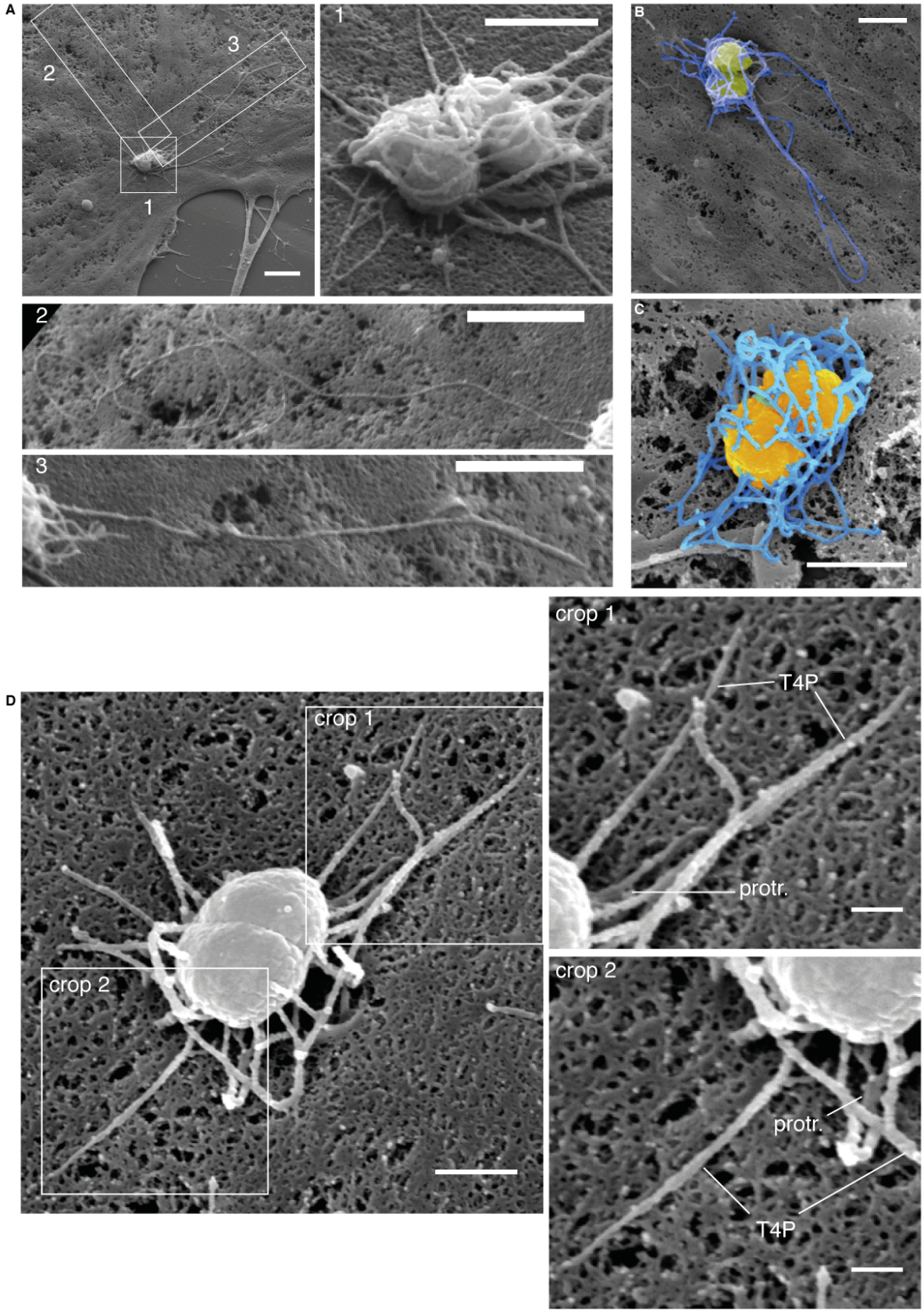

Figure S2

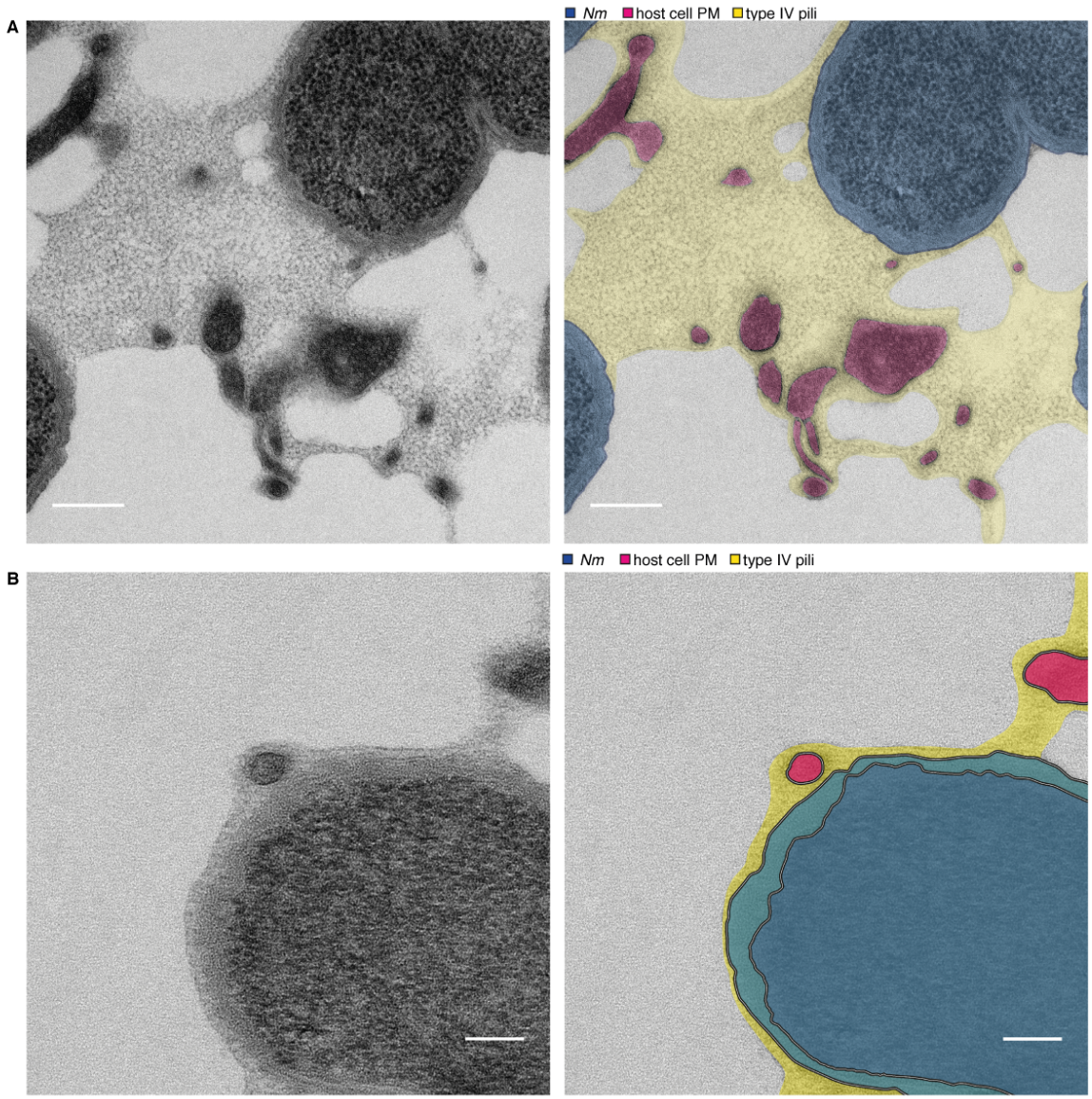

Figures legends

Figure 1. Plasma membrane remodeling occurs during vascular colonization by *Nm in vivo*. (**A**, **B**) Max intensity projections and crops of single focal planes of histoimmunolabeling assays on human blood vessels in mice 3h post infection with *N. meningitidis*(*Nm*)-GFP. Type IV pili were immunostained with a nanobody coupled to AlexaFluor-647. Plasma membrane was detected with the human-specific UEA lectin coupled to rhodamin (**A**) and F-actin was detected with phalloidin coupled to AlexaFluor-568 (**B**). Plasma membrane remodeling between bacteria is shown with arrowheads. Micrographs were taken from samples harvested from the same mouse and are representative of n=2 mice. Dashed lines delimits blood vessels. Scale bars, 10 μm. (**C**) Transmission electron micrograph of human blood vessels in a mouse 2h post infection with *Nm*-GFP. Endothelial cells plasma membrane is delimited with black dotted lines in the two crops. RBC, red blood cells. Plasma membrane protrusions are denoted by arrowheads. n=1 mouse. Scale bar 2 μm.

Figure 2. Plasma membrane remodeling occurs at the level of the single bacterium. (**A**) Representative oblique illumination live cell imaging of HUVEC expressing the membrane marker GFP-F (GFP-Farnesyl, inverted contrast) infected by *Nm*-iRFP. Black dots represent accumulation of plasma membrane fluorescence and are denoted by arrowheads. Scale bar, 2 μm. The movie is representative of n>10 independent experiments. (**B**) Representative scanning electron micrograph of a HUVEC infected by *Nm* for 10 min. Arrowheads show plasma membrane protrusions. n=2 independent experiments. Scale bar, 500 nm. (**C**) Schematic of the classification of the plasma membrane protrusions observed in high speed oblique illumination imaging (6 frames per second). (**D**) Frequency distribution (gray bars) and Gaussian fit (blue line) of the number of protrusions observed per bacterium over 10 seconds. n=57 bacteria in six independent experiments. (**E**) One-second binned frequency distribution of the number of plasma membrane protrusions with short observed lifetimes. (**F-H**) Plasma membrane protrusions on-rate (k_{on}) (**F**) off-rate (k_{off}) (**G**) and estimated mean lifetime (**H**). Gray bars and error bars represent the mean ±SEM over six independent experiments. Dots represent the mean values of 4-14 bacteria in each experiment. (**I**) Oblique illumination live cell imaging of a micropatterned HUVEC expressing the membrane marker PM-EGFP (Palmitoyl-Myristoyl-EGFP, inverted contrast) and infected by *Nm*-iRFP. Arrowheads denote plasma membrane protrusions that can be followed over two bacterial divisions. Scale bar, 2 μm. (**J-K**) Oblique illumination live cell imaging of a HUVEC expressing GFP-F infected with a pre-formed bacterial aggregate (**J**) and enlargement of a region taken from the aggregate periphery showing stability of most of the plasma membrane protrusions (white arrowheads)

and disappearance of one protrusion (black arrowhead) over 10 seconds (**K**) Scale bar, 5 μm. The movie is representative of n>10 independent experiments.

Figure 3. The dynamics of plasma membrane protrusions are differentially regulated by F-actin and T4P retraction. (**A**) Representative oblique illumination live cell imaging of HUVEC expressing the membrane marker GFP-F (inverted contrast), treated (+) or not (-) with 100 nM cytochalasin D (CytoD) and infected by *Nm*-iRFP (yellow dotted lines). Plasma membrane protrusions are denoted by arrowheads. Scale bars, 1 μm. (**B**-**E**) Analysis of plasma membrane protrusions dynamics (as in Fig. 2) of cells shown in **A**: mean number of protrusions per bacterium (**B**), protrusions k_{on} (**C**), k_{off} (**D**), and mean lifetime. Bars and error bars represent the mean ±SEM in three independent experiments. Dots represent the mean of each individual experiment. The total number of bacteria analyzed was 26 and 15 in non-treated and treated cells, respectively. *, P<0.05 (**f**) Representative oblique illumination live cell imaging of HUVEC expressing the membrane marker GFP-F (inverted contrast) infected by *Nm* WT-iRFP or the T4P retraction deficient mutant *pilT*-iRFP (yellow dotted lines). Plasma membrane protrusions are denoted by arrowheads. *pilT*-iRFP bacteria also elicited protrusions in the shape of plasma membrane rings as labeled. Scale bars, 1 μm. (**G**) Mean number of protrusions per bacterium. (**H**) Percentage of bacteria with discrete plasma membrane protrusions and with plasma membrane rings. (**I**) Percentage of plasma membrane protrusions with a lifetime over the observation period of 10 seconds. Bars and error bars in (**G**-**I**) represent the mean ±SEM of three independent experiments. Dots represent the mean of each individual experiment. The total number of bacteria analyzed was 31 WT-iRFP and 28 *pilT*-iRFP. *, P<0.05

Figure 4. Observation of the T4P-plasma membrane interface at high resolution. (**A**-**D**) Representative 3D Structure Illumination Microscopy (SIM) micrographs of a pair (**A**, **B**) and a small aggregate of 8 (**C**, **D**) meningococci (DAPI, blue) after 30 min infection on HUVEC expressing the membrane marker PM-EGFP and immunostained for T4P (yellow) and GFP (magenta). (**A**) and (**C**) show T4P detection and merged images in Z projections. Scale bars, 2 m and 3 m. (**B**) and (**D**) are cropped merged images and Z-sections showing details of T4P organization with empty spaces between fibers (empty arrowheads) and spaces occupied by plasma membrane protrusions (filled arrowheads). Scale bars in (**B**), 200 nm for the first inset then 500 nm. Scale bars in (**D**), 2 μm. n=3 independent experiments. (**E**) Representative scanning electron micrograph of *Nm* after 10 min infection of HUVEC and stabilization of the T4P with a monoclonal anti-T4P antibody. Colorized crop shows plasma membrane protrusions (magenta, dotted lined) attached alongside T4P fibers (yellow). Scale bars, 1 μm (left) and 200 nm (rigth). n=2 independent experiments. (**F**) Representative scanning electron

micrograph of *Nm* after 10 min infection of HUVEC and immunogold labeling of T4P. Crop shows the merge of the secondary electrons detector image (surface features, grayscale) and the backscattered electron detector image (gold particles, yellow). Protr., plasma membrane protrusions. Scale bars, 500 nm (left) and 200 nm (right). One experiment. (**G**) Representative transmission electron micrograph and colorized micrograph of a microcolony of *Nm* on HUVEC after 2h of infection, high pressure freezing and freeze substitution, showing plasma membrane protrusions embedded in a meshwork of T4P. Scale bar, 200 nm. One experiment. (**H**) Same than in (**E**) except that T4P were immunogold labeled prior to high pressure freezing. Crop shows the meshwork of T4P, decorated with gold particles, attached alongside a plasma membrane protrusion. Scale bars, 200 nm (left) and 50 nm (right). One experiment.

Figure 5. T4P fibers act as a scaffold that imposes a specific geometry to the plasma membrane. (**A**) Representative transmission electron micrograph after immunogold labeling of T4P and negative stain of *Nm* adhered on a grid. Crop shows long fibers decorated with gold particles. Scale bars, 500 nm (left) and 200 nm (right). One experiment. (**B**) Representative scanning electron micrograph of *Nm* adhered on glass. T4P were stabilized with a monoclonal anti-T4P antibody. Crop shows details of T4P meshwork-like organization in two bacteria. Scale bars, 500 nm (left) and 200 nm (right). n=2 independent experiments. (**C**) Oblique illumination imaging of HUVEC expressing the plasma membrane marker PM-EGFP and the receptor for Opa adhesins, CEACAM1. Cells were infected for 10 min with a natural variant of *Nm* homogeneously expressing the Opa adhesin on its outer membrane (Opa+) that was further modified to abolish expression of the capsule (caps-) and of T4P (T4P-). Plasma membrane recruitment appears as partial or complete membrane rings (black arrowheads). Scale bar, 2 μm. (**D**) Same experiment than in (**C**) except that the bacterial strain expressed T4P (T4P+). Plasma membrane recruitment appears as discrete protrusions (white arrowheads). Scale bar, 2 μm. (**E**) 2h infection assays of HUVEC with wild-type iRFP expressing *Nm* in the absence or presence of indicated concentrations of an anti-T4P moclonal antibody. Plasma membrane recruitment was detected by immunostaining of ezrin (magenta) and T4P pili immunostaining is shown in yellow. Scale bars, 10 μm. (**F**) Quantification of the percentage of microcolonies recruiting ezrin from cells shown in (**E**). Bars and error bars represent the mean ±SEM of three independent experiments. Dots represent the mean of individual experiments. 216 to 240 microcolonies were counted for each condition. *, $P<0.05$; **, $P<0.01$. (**G**-**I**) Representative scanning electron micrographs of a HUVEC cultured on an anodized aluminum oxide porous membrane functionalized with a RGD peptide. Scale bars, 10 μm (**G**) and 500 nm (**H**, **I**). High magnification images of the plasma membrane at the edge of the cell, showing pinching out along the adhesives walls of the pores (**H**, arrowheads), and

of a filopodium, highlighting plasma membrane alignment alongside the pore walls over its entire length (**I**). n=2 independent experiments. Scale bars, 500 nm. (**J**-**L**) Representative scanning electron micrographs of a HUVEC cultured as in (**G**-**I**) but after treatment with 100 nM of the F-actin depolymerization agent cytochalasin D (CytoD). Scale bars, 10 μm (**J**) and 500 nm (**K**, **L**). High magnification image of the plasma membrane at the edge of the cell, showing pinching out along the adhesives walls of the pores (**K**, arrowheads) and of a filopodium, showing a flattened morphology but still aligning onto the pore walls. n=2 independent experiments.

Figure 6. Working model for the mechanism of scaffold-induced plasma membrane protrusions by *Nm* T4P fibers. *Nm* produces T4P as a meshwork of fibers. Upon adhesion to the host endothelial cell, high adhesiveness of T4P triggers the remodeling of the plasma membrane that grows locally alongside the fibers in a process reminiscent of wetting. As the bacteria proliferate and aggregate extracellularly, the protrusions of plasma membrane remain attached to the T4P fibers and end up embedded in a dense T4P extracellular matrix-like meshwork. This complex T4P-plasma membrane structure provides the microcolony with enough mechanical coherence to resist blood flow-generated shear stress.

Supplementary figures legends

Figure S1. Additional examples of *Nm* T4P architecture and T4P-plasma membrane interface by SEM after stabilization of the T4P with a monoclonal anti-T4P. (**A**) Example of a pair of bacteria (crop 1) with particularly long pili (crop 2 and 3). Scale bars, 10 μm (large view) and 2 μm (crops). (**B**) Example of a single bacterium (yellow) featuring both long pili and a core of dense meshwork of pili (blue) around the bacterial body. Scale bar, 1 μm. (**C**) Example of a single bacterium (yellow) harboring a very dense cage of pili (blue) around the bacterial body. Scale bar, 1 μm. (**D**) Example of a single bacterium where host cell plasma membrane forms protrusions near the bacterial body but not along T4P fiber away from the bacterium, as better seen in the crops. Scale bars, 500 nm (whole picture) and 200 nm (crops).

Figure S2. Additional examples of T4P-plasma membrane interface by TEM. Representative transmission electron micrographs and colorized micrographs of microcolonies of *Nm* on HUVEC after 2h of infection, high pressure freezing and freeze substitution. (**a**) Example of a dense meshwork of T4P embedding plasma membrane protrusions. Scale bar, 200 nm. (**b**)

Example of a protrusion of plasma membrane embedded in a thin layer of T4P at the periphery of a bacterium with no neighboring bacteria. Scale bar, 100 nm.

Movie S1. Oblique illumination live cell imaging of a HUVEC expressing the membrane marker GFP-F (inverted contrast) infected by *Nm*-iRFP. A single focal plan is shown. Plasma membrane protrusions from the host cell are visible as discrete bright dots surrounding the bacterial bodies. Scale bar, 10 μm. Representative of several events in n>10 independent experiments.

Movie S2. Oblique illumination live cell imaging of a HUVEC expressing the membrane marker GFP-F and LifeAct-mCherry infected by *Nm*-iRFP. A single focal plan is shown. Plasma membrane protrusions from the host cell are visible as discrete bright dots surrounding the bacterial bodies. No accumulation of LifeAct-mCherry is observed. Scale bar, 2 μm. Representative of several events in n=2 independent experiments.

Movie S3. Oblique illumination live cell imaging of a micropatterned HUVEC expressing the membrane marker PM-EGFP (inverted contrast) and infected by *Nm*-iRFP. A single focal plan is shown. Plasma membrane protrusions can be followed over two bacterial divisions. Scale bar, 10 μm. Representative of n=2 independent experiments.

Movie S4. Oblique illumination live cell high speed imaging of a HUVEC expressing GFP-F (inverted contrast) infected with a pre-formed bacterial aggregate of *Nm*-iRFP (not visible on the movie, please refer to Fig. 2). A single focal plan is shown. The plasma membrane protrusions barely move over 10 seconds, except at the aggregate periphery. Scale bar, 5 μm. Representative of several events in n>10 independent experiments.

Movie S5. Oblique illumination live cell high speed imaging of a HUVEC expressing GFP-F (inverted contrast) infected with wild-type *Nm*-iRFP bacteria. In this experimental setting, only one channel can be recorded at high speed. The position of 3 bacteria, denoted by a yellow ellipse, was assessed before recording of the GFP-F channel. Plasma membrane protrusions from the host cell are visible as discrete bright dots. Scale bar, 2 μm. Representative of several events in n=10 independent experiments.

Movie S6. Oblique illumination live cell high speed imaging of a HUVEC expressing GFP-F and treated for 20 min with 100nM cytochalasin D (inverted contrast) infected with *Nm*-iRFP bacteria. In this experimental setting, only one channel can be recorded at high speed. The

position of 2 bacteria, denoted by a yellow ellipse, was assessed before recording of the GFP-F channel. Plasma membrane protrusions from the host cell are visible as discrete bright dots. Scale bar, 2 μm. Representative of several events in n=3 independent experiments.

Movie S7. Oblique illumination live cell high speed imaging of a HUVEC expressing GFP-F (inverted contrast) infected with *pilT*-iRFP bacteria which are deficient for T4P retraction. In this experimental setting, only one channel can be recorded at high speed. The position of 2 bacteria, denoted by a yellow ellipse, was assessed before recording of the GFP-F channel. Plasma membrane protrusions from the host cell are visible as discrete bright dots. Scale bar, 2 μm. Representative of several events in n=3 independent experiments.

Experimental procedures

Ethics statement

All experimental procedures involving animals were conducted in accordance with guidelines established by the French and European regulations for the care and use of laboratory animals (Décrets 87–848, 2001–464, 2001–486 and 2001–131 and European Directive 2010/63/UE) and approved by the local ethical committee Comité d'Ethique en matière d'Expérimentation Animale, Universite Paris Descartes, Paris, France. No: CEEA34.GD.002.11. All surgery was performed under anesthesia, and all efforts were made to minimize suffering. For human skin, written informed consent was obtained and all procedures were performed according to French national guidelines and approved by the local ethical committee, Comité d'Evaluation Ethique de l'INSERM IRB 00003888 FWA 00005881, Paris, France Opinion: 11–048.

Animals, grafting and infection

Humanized SCID/Beige (SOPF/CB17 SCID BEIGE. CB17.Cg-Prkdc-Lyst/Crl) mice (Charles River, France) 5–8 weeks of age were used as described in earlier studies (Melican et al., 2013). Briefly, anesthetized mice were grafted with healthy human skin, including epidermis, dermis and dermal microvasculature. 3-4 weeks post graft, the tissue retained human morphology without inflammation. 10^7 CFU of GFP expressing bacteria were injected IV and the animals were sacrificed 2h to 3h post infection.

Preparation of tissue samples for immunohistochemistry

Tissues were fixed with 4% paraformaldehyde (PFA), frozen in OCT (Tissuetek) and sliced at 10 μm. Human vessels were stained for plasma membrane with the human specific Ulex europaeus agglutinin (UEA) lectin coupled to rhodamine (Vector Laboratories) and for F-actin with phalloidin coupled to AlexaFluor-568 (Invitrogen). Type IV pili were detected with an in-house generated anti-PilE nanobody coupled to AlexaFluor-647 (AlexaFluor-647-NHS-ester, Invitrogen).

Preparation of tissue samples for transmission electron microscopy

Tissues were fixed with 4% PFA and 0.5% glutaraldehyde in 0.1M phosphate buffer, for 4h at room temperature. They were then transferred to 1% PFA in 0.1M phosphate buffer and incubated overnight at 4°C. Samples were next processed as for conventional TEM.

Cell culture

Human umbilical vein endothelial cells (HUVEC, Promocell) were maintained in Endo-SFM (human endothelial-SFM, Gibco) supplemented with 10% (v/v) heat-inactivated fetal bovine

serum (FBS, PAA Laboratories) containing 10 µg.mL^{-1} endothelial cells growth supplement (ECGS, Alfa Aesar) and were used between passages 3 and 9.

Bacterial strains and culture

Neisseria meningitidis (*Nm*) serogroup C strain 8013 is a capsulated, piliated, Opa-, Opc- clinical isolate (Nassif et al., 1993). It was grown on GCB-Agar (Difco) plates containing Kellogg's supplements (Kellogg et al., 1968) and antibiotics when required (kanamycin, 100 µg.mL^{-1}; chloramphenicol, 5 µg.mL^{-1}; spectinomycin, 50 µg.mL^{-1}; erythromycin, 2 µg.mL^{-1}) at 37°C and 5% CO_2 under moist atmosphere. For infection experiments, GCB-Agar grown bacteria were resuspended in Endo-SFM supplemented with 10% FBS at an OD_{600} of 0.05 and cultured for 2 h with shaking at 37°C and 5% CO_2. The GFP expressing strain was described elsewhere (Melican et al. 2013). A plasmid allowing stable expression of the iRFP near-infrared fluorescent protein (Filonov et al., 2011) in *Nm*, pMGC13, was constructed as follows: the sequence encoding the iRFP protein was PCR-amplified from the plasmid pBAD/His-B-iRFP (a kind gift from Vladislav Verkhusha, Addgene plasmid #31855) with PacI and SalI restriction sites in 5' and 3' respectively and the ribosome binding site from *Nm pilE* gene just upstream of the start codon. The sequences for the primers are iRFP_F2: TTAATTAAAGGAGTAATTTTATGGGGGGTTCTCATCATCATCA and iRFP_R3: GTCGACTCACTCTTCCATCACGCCGATCTGC (with restriction sites underlined and RBS from *pilE* in italic). The PCR fragment was then cloned in a pCRII-TOPO vector (Invitrogen), checked for sequence and subcloned in the pMGC5 plasmid that allows homologous recombination at an intergenic locus of the *Nm* chromosome and expression under the control of the constitutive *pilE* promoter (Soyer et al., 2014). The *pilT*-iRFP mutant strain deficient for type IV pili retraction was generated by homologous recombination of the chromosomal DNA of the *pilT* insertion mutant strain into the wild-type iRFP strain by natural transformation. The non-capsulated Opa+-*siaD*-iRFP and its non-piliated derivative Opa+-*siaD*-*pilD*-iRFP was generated by homologous recombination of the chromosomal DNA from *siaD* and/or *pilD* insertion mutants strains into a naturally occurring variant of 2C43, which carries a *opaB* gene in the ON phase, by natural transformation.

Cell transfection and plasmids

5.10^5 HUVEC were electroporated with 4 µg plasmid DNA encoding either the enhanced green fluorescent protein fused to palmitoylation and myristoylation signals from the Lyn protein (PM-EGFP, kindly provided by Barbara Baird and David Holowka, Cornell University, Ithaca), a farnesylated GFP (GFP-F, Clonetech), and/or LifeAct-mCherry (kindly provided by Guillaume Montagnac, Institut Curie, Paris) or the Carcinoembryonic antigen-related cell adhesion

molecule 1 (CEACAM1, kindly provided by Alain Servin) with the Amaxa Nucleofector device (Amaxa Biosystem, Lonza).

Oblique illumination (dark field) live cell imaging and stream mode analysis

$2{,}1.10^4$ transfected cells were seeded in 96-well glass bottom plates (Sensoplate, Greiner BioOne) coated with 3 $\mu g.mL^{-1}$ rat tail type I collagen and 50 $\mu g.mL^{-1}$ human fibronectin (Sigma-Aldrich) and cultivated without ECGS. The next day, cells were infected with vortexed Endo-SFM-FBS grown bacteria at a MOI of 200 and gently rinsed after 10 min with Endo-SFM-FBS and screened for presence of adhering bacteria prior imaging. For inhibition of F-actin polymerization, cells were treated with 100 nM cytochalasin D in Endo-SFM-FBS for 20 min at 37°C and 5% CO_2 prior to infection. Live imaging was performed on an Eclipse T*i* inverted microscope (Nikon) equipped with a laser-based iLas2 Total Internal Reflection Fluorescence microscopy (TIRF) module (Roper Scentific) with lasers at 491 nm, 561 nm and 647 nm and an ORCA03 digital CCD camera (Hamamatsu). Dark field images were obtained by using the TIRF module to get the illumination lasers with an incident angle of 31.2° in the widefield mode through an oil immersion 100x Apo TIRF objective with a 1.49 numerical aperture and alternatively an additional 1.5x lens. A 2x2 binning was used. To perform spatial high-resolution acquisition, a fast Z-piezo stage (Piezo Nano Z100) was adapted onto the stage of the microscope. For imaging in the stream mode, images were recorded at the camera frame rate (5 to 6 images per second) for 10 seconds. Focus was maintained with the Perfect Focus System (PFS, Nikon). All experiments were performed at 37°C in an incubation chamber adapted for the microscope (Microscope Temperature Control System, LIS). The set-up was controlled by the MetaMorph software (Molecular Devices). Times of appearance and disappearance of the plasma membrane protrusions around each bacterium were analyzed manually. k_{on} and k_{off} were calculated by dividing the total number of appearing or disappearing protrusions in all the bacteria of a given experiment by the total number of protrusions observed and by 10 seconds, and were consequently expressed in s^{-1}. The mean lifetime for plasma membrane protrusions was calculated as the inverse of k_{off} and was therefore expressed in seconds.

Oblique illumination live cell imaging of HUVEC on micropatterns

Micropatterning on glass coverslips was performed as previously described (Azioune et al., 2009). Briefly, after plasma activation (Plasma Cleaner, Harrick), we passivated the glass with PLL-g-PEG (Surface Solutions GmbH, 0,1 mg.mL-1 in 10 mM HEPES pH 7.4) for 30 min. After washing with water, we illuminated the surface with deep UV light (UVO Cleaner) through a chromium synthetic quartz photomask (Toppan). For imaging, we used channel-shaped sticky slides (Ibidi) that we bound on top of micropatterned coverslips. The home built chambers were

sterilized by 10 minutes UV exposure under the hood. Finally, we incubated 1h with human fibronectin (50 μg.ml^{-1} in water) and seeded PM-EGFP expressing HUVEC cells at a density of 50,000 cells per channel. 1h post seeding, cells were rinsed 3 times with fresh Endo-SFM to get rid of non-adhering cells, and cultured overnight. For infection, iRFP and mCherry wild-type bacteria from liquid cultures were vortexed and loaded into the channels in a 1:10 ratio to a final MOI of 400. Samples were incubated for 10 minutes at 37°C and 5% CO_2 and then rinsed thoroughly 3 times with fresh Endo-SFM to remove non-adhering bacteria. To follow membrane remodeling during bacterial proliferation, oblique imaging with 491, 561 and 642 nm lasers was performed with a 100X ApoTIRF objective (Z-stacks: 1 μm steps over 10 μm; time-lapse: 10 minutes time frame over 10h).

3D Structured Illumination Microscopy (3D-SIM)

1,5.10^5 PM-EGFP expressing cells were seeded onto 12 mm glass coverslips coated with 3 μg.mL^{-1} rat tail type I collagen and 50 μg.mL^{-1} human fibronectin and cultivated without ECGS. The next day, cells were infected for 30 min at a MOI of 200 with Endo-SFM-FBS grown bacteria and fixed by addition of one volume of pre-warmed 8% PFA in PBS and incubation at room temperature for 30 min. Cells were rinsed three times in PBS, permeabilized for 10 min with PBS-0.1% Triton-X100 and blocked for 30 min in PBS-0.2% gelatin (PBSG). Cells were then incubated for 1h with 2 μg.mL^{-1} rabbit polyclonal anti-GFP antibody to amplify the membrane GFP signal (A11122, Invitrogen) and 1,2 μg.mL^{-1} mouse monoclonal anti-PilE antibody 20D9 (Pujol et al., 1997) to detect type IV pili. Cells were incubated with 10 μg.mL^{-1} secondary goat anti-rabbit and goat anti-mouse polyclonal antibodies coupled to AlexaFluor-488 and -568 (Invitrogen) for 1h. DNA was detected with 0,5 μg.mL^{-1} DAPI. All antibodies and DAPI were diluted in PBSG. Coverslips were mounted in Vectashield mounting medium (Vector Laboratories) and sealed with clear nail polish. SIM was performed on the ELYRA system controlled by the Zen software (Carl Zeiss) equipped with diode lasers at 405 nm, 488 nm and 561 nm. Images were acquired with an oil immersion 100x Plan-Apochromat M27 objective with a 1.46 numerical aperture and an additional 1.6x lens. Nominal pixel size was 0.049 and 0.084 µm in the XY and XZ planes, respectively, using a 1x1 binning. Structured illumination grid pattern was shifted by five different phases and three different angles along the whole Z-stack. Super resolved images were computationally reconstructed and channels were aligned with 100 nm TetraSpeck beads (Invitrogen) mounted in Vectashield. To further avoid reconstruction artefacts, raw images were checked for bleaching using the SIMcheck plugin (Ball et al., 2015) in Fiji (Schindelin et al., 2012). Only data sets with total intensity variations below 20% over the whole Z-stack were used. We could detect however the

presence of putative "hammerstroke" artifacts difficult to avoid in SIM (Demmerle et al., 2017). Contrast was linearly enhanced in Fiji for clarity.

Scanning Electron Microscopy (SEM)

$1{,}5.10^5$ HUVEC infected with Nm for 10 min at a MOI of 400 or bacteria alone cultured on 12 mm glass slides were chemically pre-fixed by addition of one volume of pre-warmed 8% PFA in 0,1M HEPES pH 7.4 and incubated at room temperature for 45 min. After three washing steps in HEPES, type IV pili were immunostained or not after 20 min blacking in HEPES-0.2% gelatin (HEPES-G) with 1,2 $\mu g.mL^{-1}$ 20D9 antibody and a fluorescent secondary antibody or 2,4 $\mu g.mL^{-1}$ 20D9 antibody and a secondary antibody coupled to 15 nm colloidal gold particles (EM.GMHL15, BBI Solutions) diluted 1:30. HEPES was used instead of PBS in all steps. Infected cells were then post-fixed with 2.5% glutaraldehyde in HEPES, overnight at 4°C, washed in HEPES, post-fixed with 1% OsO_4 in HEPES for 1h, washed in distilled water, dehydrated in graded series of ethanol (25, 50, 75, 90 and 100%), critical point dried with Leica EM CPD300, mounted on aluminum stubs and sputter-coated with 20 nm gold/palladium with a Gatan PEC 682 gun ionic evaporator. SEM was performed in an Auriga scanning microscope (Carl Zeiss) operated at 7 kV with an in-lens secondary electrons detector. For immunogold labelled samples, images were simultaneously acquired through the secondary electrons detector and the backscattered electrons detector at 20 kV. Colorized images were generated with Adobe Photoshop.

High pressure freezing, freeze substitution and transmission electron microscopy (HPF-FS-TEM)

3x0.05 mm sapphire disks (M. Wohlwend GmbH) were cleaned in 100% ethanol, carbon coated in a Baltec MED 010 evaporator, baked at 130°C for 8h, glow discharged for 5 sec in a Harrick PDC-32G-2 air plasma cleaner at low radiofrequency and coated immediately with 2,5 $\mu g.mL^{-1}$ rat tail type I collagen and 50 $\mu g.mL^{-1}$ human fibronectin. Disks were seeded with $1{,}5.10^5$ cells in 24-well plates. The next day, cells were infected with *Nm* for 2h at a MOI of 400 and chemically pre-fixed by addition of one volume of a mix of pre-warmed 8% PFA and 1% EM-grade glutaraldehyde in 0,1 M HEPES pH 7.4 and incubated at room temperature for 45 min. Cells were rinsed three times in 0,1 M HEPES. Disks were then spaced by a golden O-ring, sandwiched between a 0.4 mm and a 0.5 mm copper spacer, high pressure frozen in a Baltec HPM 010 and stored in liquid nitrogen. Samples were freeze substituted in a RMC Boeckler FS-8500 with a mix of 1% OsO_4, 0.1% uranyl acetate and 5% water in glass distilled acetone. Freeze substitution cycle was as follows: -90°C for 1h, 2.5°C increase per hour for 16h, -50°C for 30 min, 15°C increase per hour for 2h, -20°C for 30 min, 10°C increase per hour

for 2h and 0°C for 1h. After four washes in acetone, sample were embedded in Epon (Epon 812, AGAR1031 kit, hard formula, Agar 100). Alternatively, type IV pili were immunogold labelled before embedding. In this case, cells were chemically pre-fixed with 4% PFA and 0.1% glutaraldehyde (final concentrations), rinsed three times in HEPES, quenched with 50 mM NH4Cl in HEPES for 5 min, blocked with HEPES-G for 20 min, incubated with 12 $\mu g.mL^{-1}$ 20D9 antibody in HEPES-G for 1h, washed twice in HEPES-G, incubated with goat anti-mouse antibody coupled to 6 nm colloidal gold particles (EM.GMHL6, BBI Solutions) diluted 1:30 in HEPES-G for 30 min, washed five times in HEPES-G and post-fixed with 1% glutaraldehyde in HEPES for 15 min. Samples were then high pressure frozen and freeze substituted as described above. Ultrathin sections of 60 nm nominal thickness were cut with a Leica EM UC7 ultramicrotome and collected on carbon coated, formvar-supported hexagonal copper grids, contrasted with 4% uranyl acetate and 3% Reynold's lead citrate and imaged in a FEI Tecnai T12 transmission electron microscope operated at an accelerating voltage of 120 kV.

Negative stain of bacteria immunogold labelled for type IV pili

Formvar-supported, carbon-coated hexagonal copper grids were glow discharged for 20 seconds in a Harrick PDC-32G-2 air plasma cleaner at high radiofrequency and covered with 10 μL of a suspension of GCB-Agar grown *Nm* at a OD_{600nm} of 1 in HEPES. Grids were incubated at 37°C and 5% CO_2 for 15 min and transferred onto a drop of 4% PFA and 0.1% glutaraldehyde in HEPES for 15 min. Grids were then rinsed three times in HEPES and immunogold labelled as described above. After staining, grids were post-fixed with 1% glutaraldehyde in HEPES for 15 min. After two washes in distilled water, grids were contrasted with 4% uranyl acetate for 30 sec and imaged in TEM at 120 kV.

Immunofluorescence on 2h infected cells

$1,5.10^5$ HUVEC were cultured in 96-well glass bottom plates coated with 2,5 $\mu g.mL^{-1}$ rat tail type I collagen and 50 $\mu g.mL^{-1}$ human fibronectin and infected the next day with *Nm* at an MOI of 100. After 30 min adhesion in the presence of 0, 13 or 26 $\mu g.mL^{-1}$ 20D9 antibody, unbound bacteria were washed three times with fresh cell culture medium and allowed to proliferate for 2h in the presence or not of the same concentrations of 20D9. Infected cells were then fixed with 4% PFA and processed for immunofluorescence as for 3D SIM except that the 20D9 staining was omitted in wells were the antibody was already present. Ezrin was detected with a rabbit polyclonal anti-ezrin antibody (kind gift of Paul Mangeat). Images were taken with the Nikon T*i* Eclipse spinning disk through a 100X oil immersion objective and ezrin recruitment was detected manually.

Cell culture on anodized aluminum oxide (AAO) membranes (or Anodiscs)

13 mm Whatman Anodiscs with 100 nm pores (GE Healthcare) were coated for 30 min with 0,1 $\mu g.mL^{-1}$ APP3 in 10 mM HEPES pH 7.4, rinsed three times in 0,1M HEPES and once with distilled water, and then coated for 30 min with 100 μM BCN-RGD in PBS and rinsed three times in PBS (van Dongen et al., 2013). $1,5.10^5$ HUVEC were seeded per disc and cultivated overnight. The next day, cell culture medium was renewed with or without 100 nM cytochalasin D for 20 min at 37°C and cells were fixed in 2.5% glutaraldehyde (final concentration). Cells were then processed as for SEM.

Statistics

Data were analyzed in the Prism software (GraphPad). For comparison of exact values measured in multiple individual bacteria over several independent experiments, the data sets were first tested for normality with a D'Agostino & Pearson test and then tested for statistical difference accordingly, either by an unpaired Mann-Whitney test (no normality) or an unpaired t test (normality). For comparison of mean values pooled over several independent experiments, statistical difference was tested with a paired t test. *, $P<0.05$; **, $P<0.01$.

Supplementary references

Azioune, A., Storch, M., Bornens, M., Thery, M., and Piel, M. (2009). Simple and rapid process for single cell micro-patterning. Lab Chip 9, 1640-1642.

Ball, G., Demmerle, J., Kaufmann, R., Davis, I., Dobbie, I.M., and Schermelleh, L. (2015). SIMcheck: a Toolbox for Successful Super-resolution Structured Illumination Microscopy. Sci Rep-Uk 5.

Demmerle, J., Innocent, C., North, A.J., Ball, G., Muller, M., Miron, E., Matsuda, A., Dobbie, I.M., Markaki, Y., and Schermelleh, L. (2017). Strategic and practical guidelines for successful structured illumination microscopy. Nat Protoc 12, 988-1010.

Schindelin, J., Arganda-Carreras, I., Frise, E., Kaynig, V., Longair, M., Pietzsch, T., Preibisch, S., Rueden, C., Saalfeld, S., Schmid, B., et al. (2012). Fiji: an open-source platform for biological-image analysis. Nat Methods 9, 676-682.

van Dongen, S.F.M., Maiuri, P., Marie, E., Tribet, C., and Piel, M. (2013). Triggering Cell Adhesion, Migration or Shape Change with a Dynamic Surface Coating. Adv Mater 25, 1687-1691.

3. Additional results

Along with the two previous projects, we explored alternative or complementary mechanisms for plasma membrane remodeling by meningococcus (see **Discussion. I.**).

3.1. Role of caveolae in plasma membrane remodeling induced by *N. meningitidis*

Rationale

In mammals, the surface of vascular endothelial cells is constituted by up to 60% by cholesterol-and glycosphingolipid-based plasma membrane domains called caveolae. These 50-100 nm plasma membrane invaginations are characterized by proteins that are specifically associated to them, caveolins and cavins. Caveolins possess acylation sites, cholesterol binding sites and hydrophobic hairpins that can insert in the inner leaflet of the plasma membrane. Caveolin-1 and -2 are ubiquitously expressed, whereas caveolin-3 expression is restricted to muscle. Caveolin-1 in particular in essential to the biogenesis of caveolae. On the one hand, insertion of its hydrophobic hairpin is thought to promote plasma membrane positive curvature (Parton et al., 2006; Schlegel and Lisanti, 2000). On the other hand, it co-traffics with cholesterol, which is essential to caveolae biogenesis, from the Golgi to the plasma membrane (Parton and del Pozo, 2013). Cavins 1, 2, 3 and 4 are cytoplasmic proteins that associate with caveolins (Hansen et al., 2009; Hayer et al., 2010; Kovtun et al., 2014). Their expression and relative importance in caveolae biogenesis are tissue-specific (Hansen et al., 2013). In addition, the BAR domain-containing protein PACSIN2 is thought to help maintaining the structure of caveolae, while the EHD2 ATPase is localized to the neck and stabilizes caveolae at the plasma membrane (Hansen et al., 2011; Moren et al., 2012; Stoeber et al., 2012) (Fig. 18).

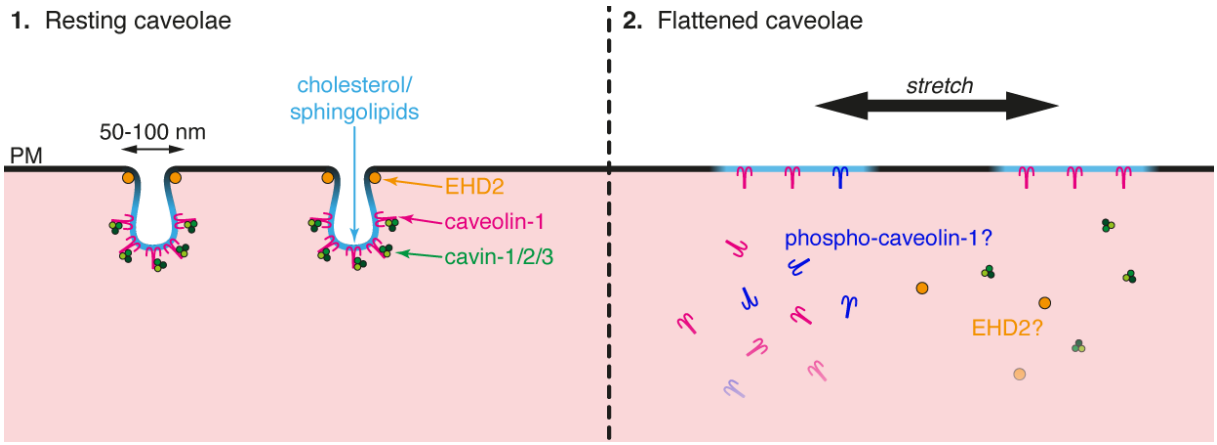

Figure 18 | Molecular composition of caveolae and role as plasma membrane reservoirs. Caveolae are cholesterol- and glycosphingolipid-based invaginations of the plasma membrane **(1)**. Caveolins and cavins proteins specifically associate to caveolae and promote their formation. The ATPase EHD2 stabilizes caveolae by oligomerizing at the caveolar neck. Upon mechanical stress, such as stretching, caveolae unfold to release additional surface and avoid damages to the cell **(2)**. Unfolding of caveolae results in a release of cavins in the cytoplasm and was shown to modulate the phosphorylation of caveolin-1. The fate of EHD2 is unknown. PM, plasma membrane.

Caveolae constitute important signaling platforms because they modulate the activity of several proteins such as the EGF receptor, the endothelial nitric oxide synthase (eNOS), Ras, or ion channels (Ariotti et al., 2014; Parton and del Pozo, 2013; Suzuki et al., 2013; Yamamoto et al., 2011; Zhang et al., 2007). The role of caveolae in endocytosis, more specifically in the transcytosis of albumin from the blood, is still under debate. Caveolin-1 can also be phosphorylated on Tyr14. Production of pY14-Cav-1 is linked to the mechanical state of the plasma membrane. While mechanical stress by strectching was shown induce phosphorylation of Cav1, thereby regulating focal adhesions and neogenesis of caveolae (Goetz et al., 2008; Joshi et al., 2012; Radel and Rizzo, 2005), it was also paradoxically shown that shear stress induces a dephosphorylation of caveolin-1 Tyr14 (Shin et al., 2006). Cavin-1 was also proposed to be released in the cytoplasm upon mechanical stress and to act as a transcription factor (Parton and del Pozo, 2013; Sinha et al., 2011).

The role of caveolae in intracellular signaling is exploited by several pathogens, including the fungus *Cryptococcus neoformans* and the bacterium *Chlamydia pneumoniae* (Hoffmann et al., 2010; Long et al., 2012; Mueller and Wolf, 2014). Interestingly, in epithelial cells, it was shown that caveolae sequentially inhibits and promotes the internalization of *N. gonorrhoeae*, depending on phase variation of the T4P (Boettcher et al., 2010; Faulstich et al., 2013).

Most importantly, the main function of caveolae is to act as plasma membrane reservoirs that protect the cell against mechanical stress (Cheng et al., 2015; Sinha et al., 2011). Upon stretching of endothelial cells for instance, caveolae invaginations unfold, thereby releasing an additional area of plasma membrane. Mobilization of caveolae upon mechanical stress is immediate and purely passive. It does not depend on actin polymerization or ATP (Fig. 18). On the contrary, reformation of caveolae at the plasma membrane after a mechanical challenge is active and depends on F-actin and energy (Sinha et al., 2011).

Since plasma membrane remodeling induced by *N. meningitidis* in endothelial cells is dependent on plasma membrane cholesterol but independent of actin polymerization and ATP, we hypothesized that caveolae could play a role in plasma membrane remodeling as initial plasma membrane reservoirs.

Results

We first reasoned that, if caveolae are unfolded upon T4P-mediated adhesion of meningococcus to endothelial cells, the components of caveolae should be diluted in the plasma membrane protrusions or completely absent. To test this hypothesis, we tested the recruitment of several caveolar components in endothelial cells underneath *N. meningitidis* microcolonies using different approaches (Fig. 19). Detection of endogenous caveolin-1 by immunofluorescence in HUVEC infected for 2h showed no recruitment of the protein within bacterial microcolonies as compared with the plasma membrane marker ezrin (Fig. 19A). Visualization of fluorescently tagged caveolin-1 and EHD2 in live cell imaging upon contact with pre-formed bacterial aggregates, as in (Soyer et al., 2014), consistently showed no recruitment of caveolin-1-mCherry but revealed an enrichment of EHD2-GFP (Fig. 19B). Finally, visualization of a fluorescently tagged cavin-1-mCherry in the same conditions but using oblique illumination showed no recruitment of cavin-1, while the plasma membrane maker PM-EGFP was recruited within the bacterial aggregate (Fig. 19C).

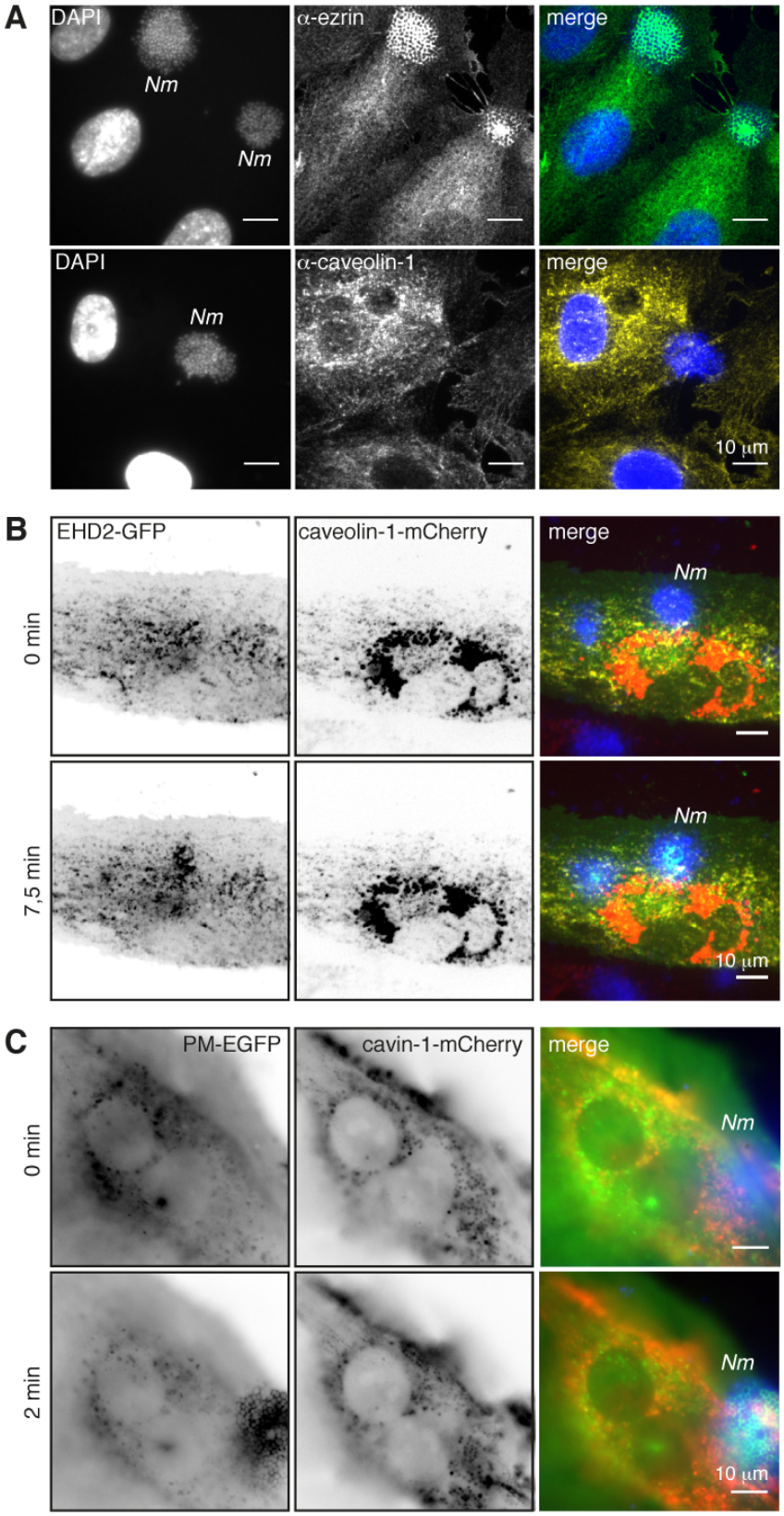

Figure 19 | Recruitment of caveolae components upon adhesion of meningococci to endothelial cells. (A) Immunodetection of endogenous ezrin or caveolin-1 in HUVEC after 2h infection by *N. meningitidis*. In both cases, the meningococcal strain used is the uncapsuated *siaD* mutant because the antibody against caveolin-1 reacted with the meningococcal capsule. n=1 experiment. **(B)** Fluorescence live cell spinning disc confocal imaging of the recruitment of EHD2-GFP and caveolin-1-mCherry. Shown are snapshots of the initial time of adhesion and of 7,5 min after adhesion. Representative of several events in one experiment. **(C)** Fluorescence live cell spinning disc confocal imaging, with oblique illumination, of the recruitment of cavin-1-mCherry and the plasma membrane marker PM-EGFP underneath preformed aggregates of WT *N. meningitidis*. Representative of several events in one experiment. *Nm*, *N. meningitidis* microcolonies or aggregates.

These data show that essential caveolae proteins are not recruited to sites of plasma membrane remodeling by meningococcus, and further suggests that caveolae could be disassembled by bacteria.

Since mechanical stress was shown to mediate phosphorylation or dephosphorylation of the Tyr14 residue of caveolin-1, we next tested whether caveolin-1 was phosphorylated or dephosphorylated in HUVEC in response to colonization by meningococcus (Fig. 20).

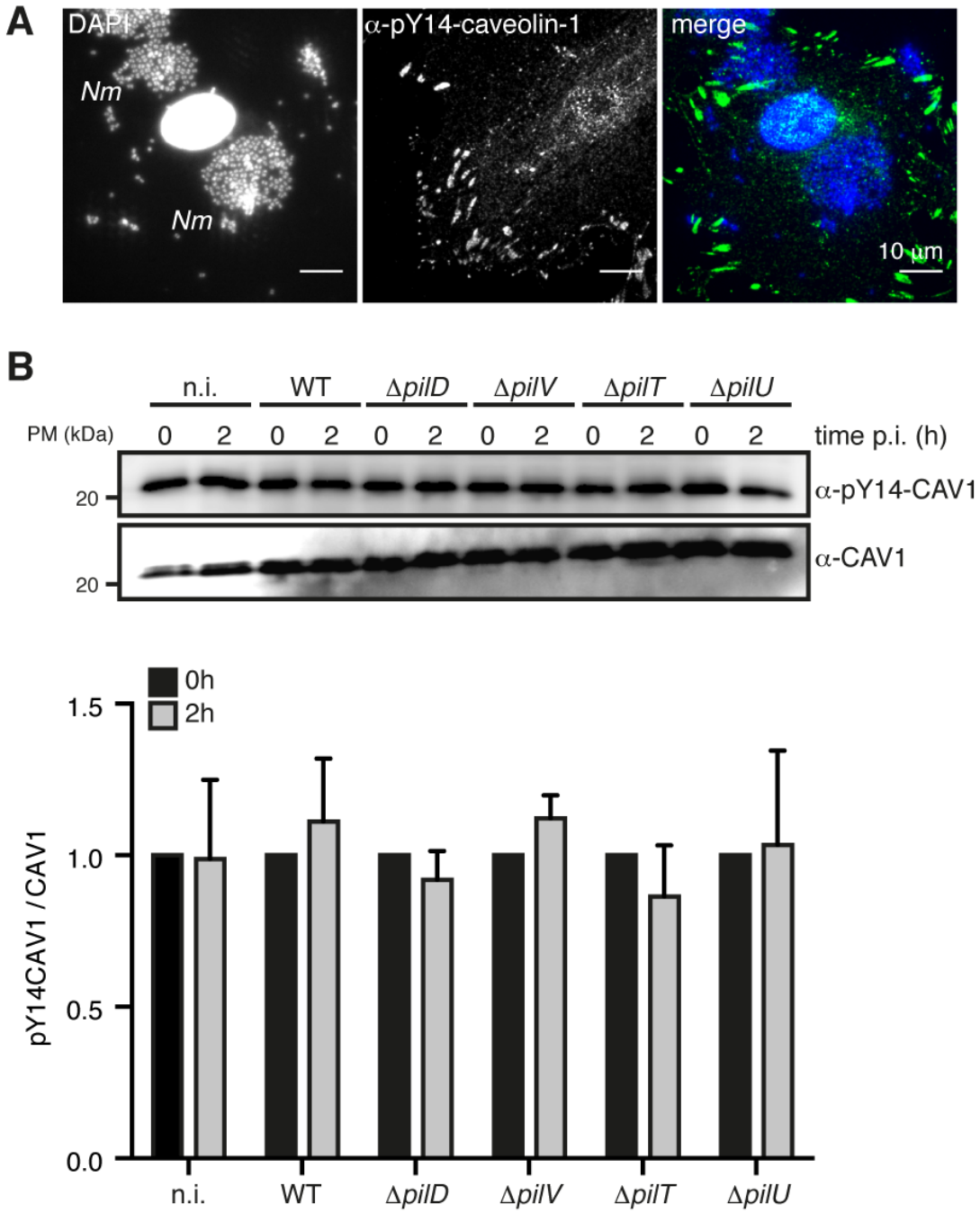

Figure 20 | Effect of the infection by *N. meningitidis* on the phosphorylation of caveolin-1. **(A)** Immunodetection of endogenous Tyr14-phosphorylated caveolin-1 in HUVEC (pY14-caveolin-1) after 2h infection by *N. meningitidis*. The meningococcal strain used is the uncapsuated *siaD* mutant. n=1 experiment. **(B)** Detection of endogenous levels of pY14-caveolin-1 and total caveolin-1 (CAV1) in HUVEC before and after 2h of infection with the indicated strains of *N. meningitidis* and in non-infected cells (n.i.). The ratio between pY14- and total CAV1 was measured in three independent experiments. Bars and error bars represent the mean ±SD. No statistical significance was observed between these different conditions. *Nm*, *N. meningitidis* microcolonies.

After 2h of infection, consistent with the absence of recruitment of caveolin-1 underneath bacterial microcolonies (Fig. 19A), we could not detect any recruitment of endogenous pY14-caveolin-1 by immunofluorescence at the site of bacterial adhesion (Fig. 20A). To detect a putative modification of the levels of phosphorylated caveolin-1 in the cytoplasm upon infection, we measured the amounts of phosphorylated and total caveolin-1 in HUVEC lysates by western blot before and after 2h of infection by meningococcus. No difference was observed between 0 and 2h and between non-infected and infected cells (Fig. 20B). No change in the phosphorylation of caveolin-1 was detected when cells were infected with non-piliated bacteria (Δ*pilD* mutant), bacteria deficient for host cell surface reorganization (Δ*pilV* mutant), bacteria defficient for pilus retraction and hyperpiliated (Δ*pilT* mutant) or bacteria known to induce a strong cell response (Δ*pilU* mutant) (Fig. 19B). These data show that, upon infection by meningococcus, no change in the phosphorylation state of caveolin-1 on the Tyr14 residue seems to occur.

Nevertheless, we finally tested whether caveolae were functionally involved in plasma membrane remodeling. To do so, we inhibited caveolae biogenesis by RNA interference against the main component of caveolae, caveolin-1. Upon silencing of caveolin-1 (Fig. 21A), cells were infected with *N. meningitidis* for 2h and host cell surface reorganization was assessed by immunofluorescence.

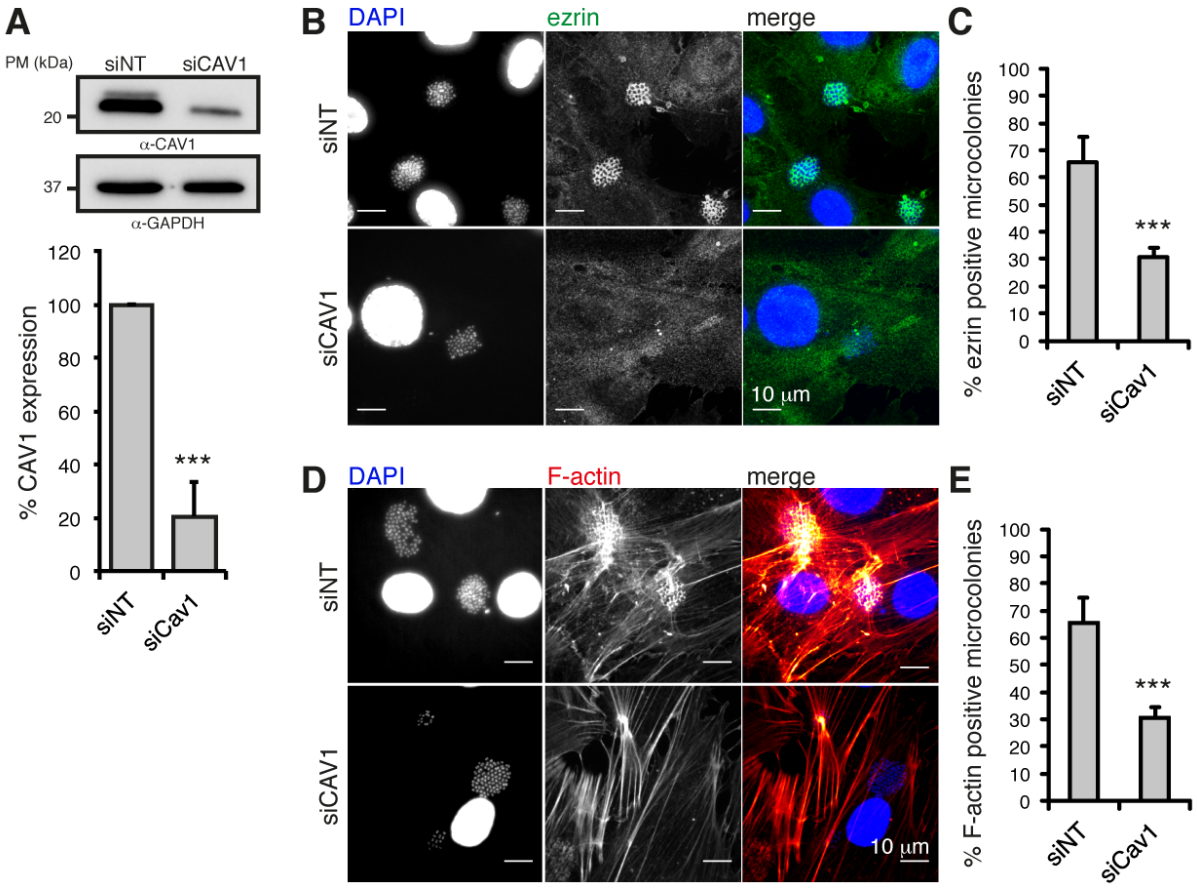

Figure 21 | Effect of the depletion of caveolin-1 on *N. meningitidis*-induced cell surface reorganization. **(A)** Detection of caveolin-1 and GAPDH by immunoblot in HUVEC treated with a siRNA against caveolin-1 (siCAV1) or a control siRNA (siNT) and quantification in 3 independent experiments. **(B)** Control and depleted cells were infected for 2h with *N. meningitidis* and endogenous ezrin was immunodetected and visualized by spinning disc confocal microscopy. **(C)** Microcolonies positive for ezrin in control and CAV1-depleted cells were counted in 3 independent experiments. **(D)** Same as in **(B)** except that F-actin was detected using fluorescently tagged phalloidin. **(E)** Quantification of F-actin positive microcolonies in control and CAV1-depleted cells in 3 independent experiments. Bars and error bars in bar plots represent the mean ±SD. ***, $p<0.005$ in a Student's *t*-test.

In cells treated with a non-targeting siRNA, after 2h of infection, 65% of meningococcal microcolonies had recruited the plasma membrane, as evidenced by immunostaining of ezrin (Fig. 20B and C), and 65% showed a rearrangement of F-actin (Fig. 21D and E). In contrast, when caveolin-1 expression was reduced by about 80%, approximately 30% of meningococcal microcolonies had recruited the plasma membrane and had induced a rearrangement of F-actin (Fig. 21 A-E).

Conclusion

These data suggest that caveolae are either excluded from or unfolded in *N. meningitidis*-induced plasma membrane protrusions. However, mechanical unfolding of the caveolae is not supported by the lack of modification of caveolin-1 phosphorylation upon infection. Nevertheless, caveolin-1 seems to plays a role in host cell surface reorganization by *N. meningitidis*, suggesting that caveolae could contribute to plasma membrane remodeling.

3.2. *N. meningitidis* recruits a specific plasma membrane compartment

Rationale

During the exploration of the different mechanisms that could be at play in *N. meningitidis*-induced plasma membrane remodeling, I had the opportunity to complete the description of the composition of the plasma membrane that is recruited by meningococcus. In particular, some host cell components that are not recruited can provide relevant information on *N. meningitidis* interaction with the endothelial cell. The summary of all the endothelial cell components whose recruitment was tested, by myself or by others, is reported in Table 1. It includes every component tested either at the level of the single bacterium, the pre-formed aggregate or the 2h microcolony.

Results

The host cell components that are recruited in the plasma membrane protrusions induced by meningococcus are lipids that are usually found in the plasma membrane, membrane receptors for T4P, proteins involved in meningococcus-induced signaling, cell-cell junction proteins, F-actin and regulators of actin polymerization. One can also find proteins that are known to be enriched at sites of negative membrane curvature such as I-BAR domains and I-BAR domain-containing proteins, ezrin and Exo70. The PtdIns(4,5)P_2 phosphatase oculocerebrorenal Lowe syndrome protein (OCRL) as well as the Rab35 GTPase that controls its activity can also be detected.

In contrast, no accumulation of the endosomal lipid PtdIns(3)*P* or of the vesicle-associated subunit of the exocyst complex, Exo84, is observed. Other non-recruited components include Sec61β, a protein from the endoplasmic reticulum, tubulin and the microtubules plus end binding protein EB1, the focal adhesion protein paxillin or the ESCRT-III complex subunit CHMP2A. Interestingly, proteins that are known to preferentially bind to positively curved membranes are not recruited by meningococcus either, such as clathrin, the transferrin receptor, cavin-1 and caveolin-1.

Conclusion

This summary suggests that the membrane pool recruited by meningococcus is the plasma membrane itself, and is not contributed by exocytosis of membranes from intracellular compartments, and shows that host cell proteins are differentially recruited upon T4P-mediated adhesion of meningococcus. Therefore, this list further suggests that the presence of a given cell component will be dictated by the curvature of the plasma membrane that is recruited by the bacterium.

Recruited components
Non-recruited components
Not clear

Molecule	Subcellular localization/Function	Detection method	Reference
Lipids			
Plasma membrane phospholipids (1)	Outer leaflet	Overexpressed GFP fused to a GPI (glycosylphosphatidylinositide) anchor	This work
Plasma membrane phospholipids (2)	Inner leaflet	Overexpressed EGFP-F or DsRed-Mono-F (farnesylated fluorescent proteins)	Soyer et al., 2014
Liquid-disordered phase phospholipids	-	Overexpressed EGFP-GG (polybasic contaning and geranylgernaylated EGFP)	This work
Liquid-ordered phase phospholipids	-	Overexpressed PM-EGFP (palmitoylated and myristoylated EGFP)	This work
Cholesterol	-	Endogenous (filipin III)	Mikaty et al., 2009
PtdIns(4,5)*P*2	Plasma membrane phosphatidylinositol phosphate	Overexpressed human GFP-PLCδ-PH	This work
PtdIns(3,4,5)*P*3	Plasma membrane phosphatidylinositol phosphate	Overexpressed GFP-Akt-PH and mouse PH-Gab2-GFP	Lambotin et al., 2005; this work
PtdIns(3)*P*	Endosomal phosphatidylinositol phosphate	Overexpressed human p40-PX-EGFP	This work
Endocytosis and exocytosis			
Clathrin light chain	Clathrin-coated pits/clathrin-coated vesicles	Overexpressed mouse CLC-GFP	This work
Transferrin receptor	Clathrin-coated pits/clathrin-coated vesicles	Overexpressed TfR-GFP	This work
Caveolin-1	Caveolae biogenesis and maintenance	Overexpressed dog CAV1-EGFP and dog CAV1-mCherry	This work
Phospho-caveolin-1	Caveolae biogenesis and maintenance	Endogenous	This work
Cavin-1 (PTRF)	Caveolae biogenesis and maintenance	Overexpressed mouse cavin1-mCherry	This work
EHD2	Caveolae biogenesis and maintenance/plasma membrane	Overexpressed human EHD2-mEGFP	This work
Exo70 (EXOC7)	Exocyst complex, plasma membrane associated subunit	Overexpressed human GFP-Exo70-HA	This work
Exo84 (EXOC8)	Exocyst complex, vesivle associated subunit	Overexpressed human mCherry-Exo84-HA	This work
Cytoskeleton and cytoskeleton regulators			
F-actin	Actin cytoskeleton	Overexpressed LifeAct-mCherry and endogenous (phalloidin)	Eugene et al., 2002; Soyer et al., 2014; this work
p16Arc (ARPC5)	Arp2/3 complex subunit/F-actin branching	Overexpressed p16-EGFP	This work
Cortactin	Actin binding/actin regulation	Overexpressed cortactin-GFP	Hoffmann et al., 2001
Rac1	F-actin regulation/small GTPase	Overexpressed GFP-Rac1	Lambotin et al., 2005

Table 1 | Differential recruitment of host cell components in human endothelial cells following adhesion of *N. meningitidis*. Host cell components are sorted according to their broad biological functions in the cell and then by alphabetical order, and the methods of detection are indicated. "This work" refers to cell components that were tested during the present PhD project.

Table 1 | *continued*

Ezrin	Linking of plasma membrane to cortical actin	Overexpressed EGFP-ezrin and endogenous	Eugene et al., 2002; Soyer et al., 2014; this work
Tubulin	Microtubules cytoskeleton	Endogenous	Unpublished lab data
EB1	Microtubules plus end binding protein	Overexpressed EB1-GFP	This work
Septins 6/8/10/11/14	Septin cytoskeleton	Endogenous (antibody against septin 11, recognizes the whole subfamily)	This work
Membrane remodeling proteins			
MIM (MTSS1)	I-BAR domain contaning protein	Overexpressed full length human MIM-GFP	This work
MIM-IMD (I-BAR domain)	I-BAR domain	Overexpressed human MIM-IMD-GFP (aa 1 254)	This work
IRSp53-IMD (I-BAR domain)	I-BAR domain	Overexpressed mouse IRSp53-IMD-GFP (aa 1-250)	This work
CHMP2A	ESCRTIII complex subunit	Overexpressed human CHMP2A-GFP	This work
Cell-cell junctions			
β-catenin	Adherens junctions	Endogenous	Coureuil et al., 2009
p120-catenin	Adherens junctions	Endogenous	Coureuil et al., 2009
VE-cadherin	Adherens junctions	Endogenous	Coureuil et al., 2009
Claudin-5	Tight junctions	Endogenous	Coureuil et al., 2009
ZO-1	Tight junctions	Endogenous	Coureuil et al., 2009
ZO-2	Tight junctions	Endogenous	Coureuil et al., 2009
Par3	Polarity complex	Overepressed Par3-myc	Coureuil et al., 2009
Par6	Polarity complex	Overexpressed Par6-YFP	Coureuil et al., 2009
Intracellular signaling			
β2-adrenergic receptor	GPCR	Overepressed β2AR-YFP	Coureuil et al., 2010
β-arrestin 2	GPCR to MAPK scaffold	Overepressed myc-βarr2 and endogenous	Coureuil et al., 2010
GRK2	GPCR phosphorylation to recruit β-arrestins	Overepressed GRK2-GFP	Coureuil et al., 2010
ErbB2	Receptor tyrosine kinase/EGFR family	Endogenous	Hoffmann et al., 2001
Src	Cortactin phosphorylation	Endogenous	Coureuil et al., 2010
Phospho-Src	Cortactin phosphorylation	Endogenous	Coureuil et al., 2010
Others			
α-actinin-4	Scaffolding protein	Endogenous	Maïssa et al., 2017
CD147	Pilus receptor	Endogenous	Bernard et al., 2014
CD44	Transmembrane protein/ERM-binding protein	Endogenous	Eugene et al., 2002
ICAM-1	Cell adhesion molecule	Endogenous	Eugene et al., 2002
OCRL1a	PtdIns(4,5)*P*2 PtdIns(3,4,5)P3 phosphatase at the plasma membrane and trans-Golgi network	Overexpressed OCRL1a-mCherry and human OCRL1a-GFP	This work
Paxillin	Focal adhesions	Endogenous	Eugene et al., 2002
Rab35	Endosomes recycling/actin dynamics/plasma membrane	Overexpressed human Rab35-GFP	This work
Cytoplasm	-	Overexpressed soluble GFP	Soyer et al., 2014
Sec61β	Endoplasmic reticulum	Overexpressed human mCherry-Sec61β	This work

DISCUSSION

1. On the mechanism of plasma membrane remodeling by *Neisseria meningitidis*

The first study that described endothelial cells surface reorganization by meningococcus had established that plasma membrane protrusions occur independently of actin cytoskeleton rearrangements (Eugene et al., 2002). Yet, paradoxically, subsequent studies have been based on the assumption that plasma membrane protrusions are driven by actin polymerization. As a result, not only plasma membrane reshaping per se has not been investigated, but also the very notion of it has not really existed in the field. Here, we sought to address the mechanisms of plasma membrane reshaping by *N. meningitidis*.

Dynamics of plasma membrane remodeling induced by pre-formed bacterial aggregates

The first important aspect of this work is the characterization of the dynamics of plasma membrane remodeling by meningococcus. At the beginning of the project, it was technically impossible to visualize plasma membrane remodeling at the level of the single bacterium by fluorescence microscopy. Therefore, we used pre-formed bacterial aggregates because they induce a macroscopically visible remodeling of the plasma membrane (Soyer et al., 2014). However, it can be argued that this is not relevant in terms of pathophysiology. Indeed, bacterial aggregates alone do not resist shear forces found in the bloodstream (Mikaty et al., 2009) and it was later found that bacteria initially bind to human blood vessels as individual cells (Melican et al., 2013). Yet, this configuration allowed us to robustly describe the early events of host cell surface reorganization by meningococcus for the first time. The first striking observation was that the accumulation of plasma membrane within the bacterial aggregate, which is usually observed after 2 h of infection, was actually completed within five minutes. Furthermore, it was initiated within seconds after adhesion of bacterial aggregates to the host cell surface. Most importantly, we confirmed that plasma membrane remodeling and actin polymerization at the site of bacterial adhesion are two separate steps, as inhibition of actin polymerization did not prevent accumulation of plasma membrane. Neither depletion of intracellular ATP or inhibition of β2-AR signaling blocked plasma membrane remodeling, further suggesting that plasma membrane remodeling by meningococcus is induced independently of any other events. In terms of timing, we found that plasma membrane reshaping occurs before accumulation of F-actin, which has two implications. First, it shows again that plasma membrane protrusions in this case are not pushed outward as a result of actin polymerization. Second, it suggests that actin polymerization occurs locally in response to plasma membrane negative curvature. In filopodia, proteins such as IRSp53 initiate negative curvature of the plasma membrane, which further promotes the clustering of IRSp53 by phase separation (Prevost et al., 2015). IRSp53 in turn recruits actin regulators such as the Vasodilator-stimulated phosphoprotein (VASP) (Disanza et al., 2013) and possibly generates clusters of PtdIns(4,5)P_2 that recruit Cdc42 (Zhao et al., 2013a), leading to actin polymerization and growth of the filopodium (Ahmed et al., 2010). Actin polymerization within the protrusions is likely promoted by plasma membrane reshaping, and perhaps similarly mediated by I-BAR domain-containing proteins that can be found in the protrusions (Table 1, Fig. 22 and Fig. 24). However, *N. meningitidis*-induced plasma membrane protrusions differ from filopodia because their growth does not depend on actin polymerization.

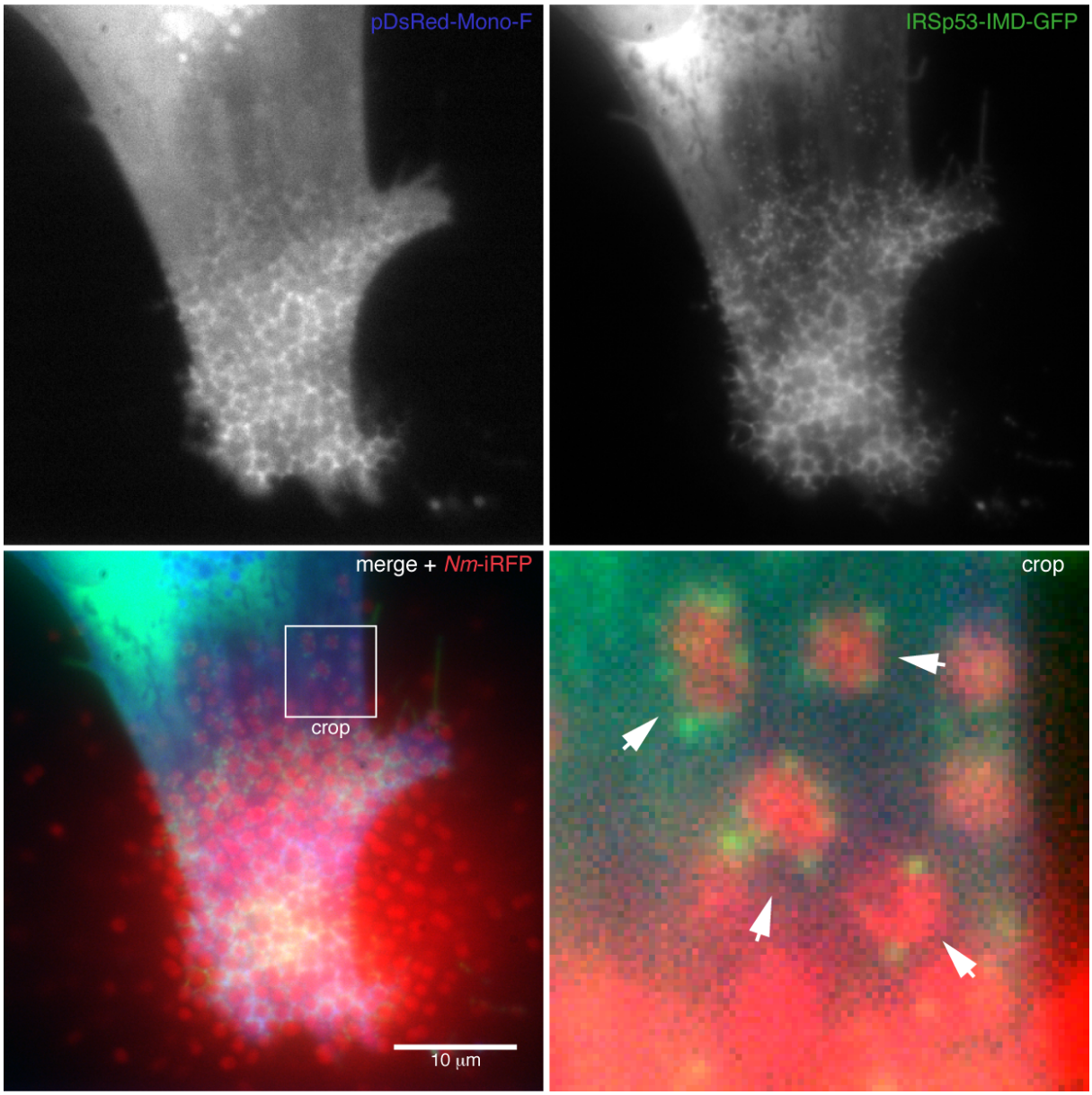

Figure 22 | Recruitment of the I-BAR domain of IRSp53 in *N. meningitidis*-induced plasma membrane protrusions. Endothelial cells overexpressing the I-BAR domain of IRSp53 fused to GFP and a farnesylated pDsRed (plasma membrane marker) were infected by pre-formed aggregates of iRFP-expressing *N. meningitidis* and observed with oblique illumination. Shown is one focal plane demonstrating the recruitment of the IMD-IRSp53-GFP construct in *Nm*-induced plasma membrane protrusions. The enlarged crop shows individual I-BAR domain-rich plasma membrane protrusions around bacteria (arrows) at the periphery of the aggregate.

On the path to identifying the mechanism of plasma membrane remodeling

As described earlier, there is a varied but limited number of mechanisms that are known to induce the bending of biological membranes in cells (see the section **5.1.** of the Introduction and Fig. 16). During my PhD project, we aimed at finding what factors promoted plasma membrane protrusions in the light of these mechanisms.

Modification of the shape of plasma membrane phospholipids by meningococcus

Several bacterial enzymes with a phospholipase activity are involved in pathogenic interactions with the host (Flores-Diaz et al., 2016; Istivan and Coloe, 2006). In our particular case, we hypothesized that a chemical modification of the host cell phospholipids by bacterial phospholipases could drive or contribute to plasma membrane reshaping (McMahon and Boucrot, 2015). Looking through the genome of our reference strain,

we found four genes possibly encoding for phospholipases: a phospholipase A1 (*pla1*, NMV_0510), a phospholipase D-like (*pld*, NMV_0954), a patatin-like (*plp*, NMV_2353) and GDSL motif-containing phospholipase (*gpl*, NMV_0698). The gene *pla1* was already shown to encode for a proper outer membrane phospholipase in *N. meningitidis* and *N. gonorrhoeae*. In meningococcus, it was proposed to contribute to bacterial autolysis. However, the role of Pla1 in virulence was not assessed (Bos et al., 2005; Senff et al., 1976). The three other genes were not described previously. Interestingly, *plp* and *gpl* are predicted to code for proteins that contain class II signal peptides and could therefore be expressed as periplasmic or outer membrane lipoproteins (Fig. 23). The product of the *pld* gene does not contain a lipoprotein signal peptide.

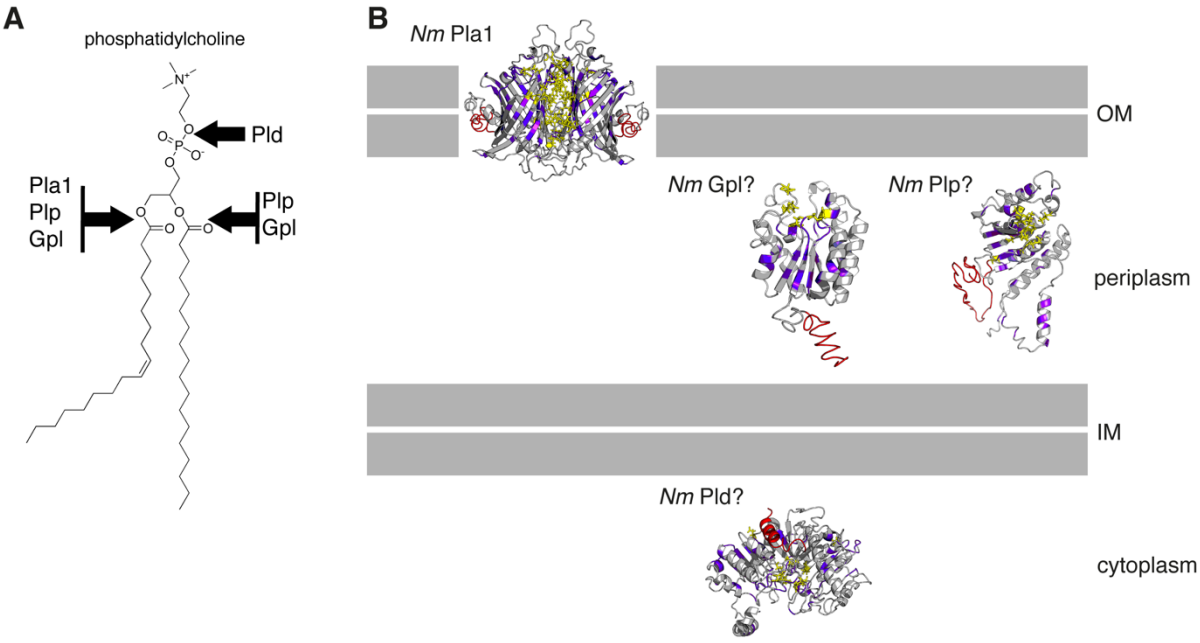

Figure 23 | Identification of putative phospholipases in *N. meningitidis*. (A) The phospholipase Pla1 and three putative phospholipases, Pld, Plp and Gpl, are encoded in the genome of *N. meningitidis*. They are predicted to be capable of cleaving phospholipids at different locations, as depicted on a phosphatidylcholine molecule. **(B)** The three-dimensional structure of each protein was predicted with the I-TASSER server (Roy et al., 2010; Yang et al., 2015; Zhang, 2008). Purple: conserved residues in homologous proteins of *N. gonorrhoeae*, *E. coli*, *K. pneumoniae*, *H. pylori*, *Y. pestis* and *V. parahaemolyticus*. Yellow: conserved catalytic residues. The possible subcellular localization of each protein is given according to the presence or absence of a lipoprotein signal peptide, as predicted by the LipoO 1.0 server (Juncker et al., 2003). Pla1, phospholipase A1; Pld, phospholipase D-like; Plp, patatin-like phospholipase; Gpl, GDSL motif-containing phospholipase; OM, outer membrane; IM, inner membrane; *Nm*, *N. meningitidis*.

Interestingly, meningococcal *pla1*, *pld*, *plp* and *gpl* genes are highly conserved between *N. meningitidis*, *N. gonorrhoeae* and commensal *Neisseria*, and homologs of each gene exist in other bacterial pathogens, such as *E. coli*, *K. pneumoniae*, *H. pylori*, *Y. pestis* and *V. parahaemolyticus*. In particular, the predicted catalytic domains of each protein are also highly conserved between meningococcus and these species (Fig. 23B).

To test the role of these proteins in the interaction of meningococcus with endothelial cells, we mutated all four of the putative phospholipase genes in order to test the ability of the mutant bacteria to remodel the host cell plasma membrane. Unfortunately, recombination events in *pilE* had occurred in all mutants, as determined by PCR, resulting in T4P that were distinct from the wildtype strain, as determined by mass spectrometry (data not shown). At the time of writing, we have not taken the characterization of these genes any further. Nevertheless, we cannot rule out a role of meningococcal phospholipases in plasma membrane remodeling or subsequent stabilization of plasma membrane curvature.

Utilization of caveolae as a reservoir of plasma membrane

Another hypothesis came from the paper by Sinha *et al.* demonstrating that caveolae flatten out to buffer mechanical stress at the plasma membrane in an ATP- and actin-independent fashion (Sinha et al., 2011). Since endothelial cells plasma membrane contains many caveolae, it was tempting to speculate that *N. meningitidis*-induced protrusions correspond to unfolded caveolar membrane. Alternatively, caveolae could facilitate plasma membrane remodeling by meningococcus by modulating plasma membrane tension. In the study by Sinha *et al.*, caveolae flattening is evidenced by a disappearance of caveolin-1-EGFP positive dots at the plasma membrane upon mechanical stress. Consistently, we found that caveolin-1 and cavin-1 were excluded from the plasma membrane protrusions induced by meningococcus. On the contrary, EHD2 was present, likely due to its affinity for negatively curved membranes. However, changes in the phosphorylation of caveolin-1, which are usually linked to caveolae disassembly (Joshi et al., 2012; Radel and Rizzo, 2005; Shin et al., 2006; Zhang et al., 2007), were not found in our infection experiments. This can mean i) that meningococcus does not induce a flattening of the caveolae or ii) that plasma membrane recruitment by meningococcus does not translate into a mechanical stress that is comparable to the stretching or osmotic stresses that are usually employed. Yet, upon caveolin-1 silencing in endothelial cells, we found that fewer bacterial microcolonies were capable of remodeling the host cell plasma membrane, consistent with a direct role of caveolae as plasma membrane reservoirs for meningococcus. However, caveolin-1 was shown to traffic from the Golgi to the plasma membrane along with cholesterol. Thus, silencing of caveolin-1 can impact cholesterol levels at the plasma membrane (Parat et al., 2002; Parton and del Pozo, 2013). Consequently, the negative effect of caveolin-1 knockdown in our experiments could be explained by a partial depletion of plasma membrane cholesterol, which is a potent way to inhibit plasma membrane reorganization by meningococcus (Mikaty et al., 2009). An obvious way to circumvent this problem would be to replenish plasma membrane cholesterol in caveolin-1 depleted cells prior to infection by meningococcus. Overall, it is still not clear from these experiments whether caveolae contribute to *N. meningitidis*-induced plasma protrusions.

Plasma membrane damage and the ESCRT-III complex

Physical damages to the plasma membrane can be fixed by the ESCRT-III complex (Jimenez et al., 2014) which incidentally induces the budding of the plasma membrane (Nabhan et al., 2012). Therefore, we tested whether T4P-mediated adhesion of meningococcus induces a damage to the plasma membrane, thereby recruiting the ESCRT-III complex. When infecting endothelial cells with pre-formed bacterial aggregates in the presence of the DNA marker and cell-impermeant propidium iodide, we did not detect any fluorescent signal in the cells nuclei (data not shown), suggesting that the plasma membrane remains intact upon meningococcal adhesion. In line with this, we could not detect any recruitment of a fluorescently tagged Chmp2A, a subunit of the ESCRT-III complex (Table 1). Therefore, we did not pursue this hypothesis any further.

Entry of water in the cell

We next wondered whether plasma membrane protrusions were induced by an influx of water, as demonstrated for aquaporin 9-driven membrane protrusions (Karlsson et al., 2013). To do so, we measured the fluorescence of a cell-permeable calcein probe, which is a hydrophobic molecule whose fluorescence self-quenches when concentrated. Upon dilution, the fluorescence dequenches and, thus, increases. However, we did not detect any increase in the cytoplasmic fluorescence of calcein upon plasma membrane remodeling, suggesting that there is no entry of water prior to, or along with, plasma membrane remodeling (data not shown).

T4P fibers as extracellular scaffolds driving plasma membrane remodeling

We finally focused our efforts on the role of T4P in the plasma membrane remodeling process. From a technical standpoint, this study was significantly aided by our original capability to visualize plasma membrane reshaping at the level of the single bacterium by live cell oblique imaging and to preserve T4P fibers in electron microscopy. What we found is that the endothelial cell plasma membrane is remodeled because it adheres along meningococcal T4P fibers, which act as an extracellular scaffold. Consequently, the geometry of plasma membrane protrusions is directly imposed by T4P fibers.

This mechanism fits well with the literature, with respect both to the bacterium and to the host cell. On the bacterial side, it is consistent with T4P being necessary to plasma membrane remodeling (Brissac et al., 2012; Mikaty et al., 2009), since they directly scaffold plasma membrane protrusions. It further suggests that plasma membrane remodeling and adhesion are two sides of a same coin, as plasma membrane remodeling relies on adhesion to T4P fibers. On the endothelial cell side, it is consistent with the need for plasma membrane cholesterol demonstrated in previous studies (Mikaty et al., 2009; Soyer et al., 2014), as cholesterol depletion alters the fluidity of the plasma membrane (Byfield et al., 2004; Sun et al., 2007; Wu et al., 2014) and since a stiff plasma membrane is unlikely to be permissive to such deformations. It also explains why plasma membrane remodeling is independent of actin polymerization and ATP, since the driving force for membrane protrusions does not originate from the host cell but from the bacterium.

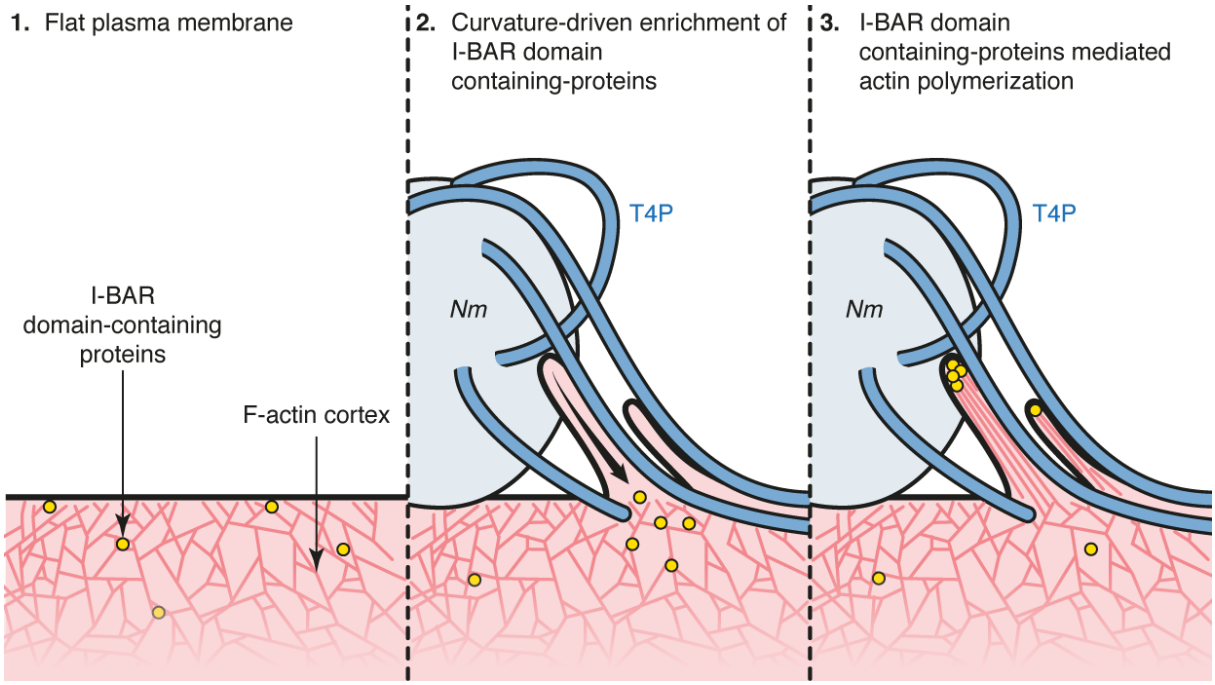

Figure 24 | Proposed mechanism for actin polymerization in T4P-driven plasma membrane protrusions. T4P fibers induce protrusions of the host cell plasma membrane in an actin-independent manner **(1 and 2)**. Recruitment of I-BAR domain-containing proteins such as IRSp53 could be promoted by the negative curvature of the F-actin-free plasma membrane protrusions **(2)**, leading to local actin polymerization, as observed *in vitro* and *in vivo*, from the cortical F-actin **(3)**.

Role of the actin cytoskeleton

In eukaryotic cells, there are other examples of plasma membrane remodeling processes that do not involve actin polymerization. On the one hand, unbending of the plasma membrane, like the rapid response of the plasma membrane to mechanical stress by the rapid disassembly of caveolae (Cheng et al., 2015; Sinha et al., 2011) or other membrane reservoirs (Kosmalska et al., 2015), occurs independently of actin polymerization or ATP. On the other hand, F-actin-independent plasma membrane bending can be driven

by the geometry of objects that bind to the plasma membrane. At small scales, BAR domain-containing proteins can impose their crescent shape to membranes, including the plasma membrane, leading to positive or negative curvature (also see (Simunovic et al., 2015) for a review). From the outside of the cell, plasma membrane invaginations can be induced by a similar nanoscaffolding effect, for example by the SV40 virus (Ewers et al., 2010) or by the protein galectin-3 alone (Lakshminarayan et al., 2014). At larger scales, it can be observed in the initial step of plasma membrane extension around a particle during phagocytosis (Lowry et al., 1998; Tollis et al., 2010), or in the internalization of the pathogen *Pseudomonas aeruginosa* that is triggered by direct adhesion to lipids in a zipper-like fashion (Tollis et al., 2010). In the particular case of *N. meningitidis*, the plasma membrane is remodeled towards the outside of the host cell, and remodeling is driven by the geometry of polymeric adhesive proteins assembled into fibers.

In both pre-formed bacterial aggregates and individual bacteria, we show however that inhibition of actin polymerization with cytochalasin D leads to a greater accumulation of plasma membrane by meningococcus. In the case of pre-formed aggregates, it is measured as a global increase of the macroscopic accumulation of the plasma membrane markers GFP-F and EGFP-ezrin underneath adherent bacteria (Soyer et al., 2014). In the case of single adhering bacteria, it consistently translates into an increased number of plasma membrane protrusions per bacterium. In this case, treatment with cytochalasin D also results in a decreased lifetime of the protrusions, suggesting that F-actin polymerizes inside plasma membrane protrusions and stabilizes them. This could possibly stem from an enhancement of T4P-host cell receptors interactions, as is the case for antigen-receptors interactions during phagocytosis (Andrews et al., 2008). As discussed before, it can be speculated that the negative curvature of the F-actin-free plasma membrane protrusions will recruit I-BAR domain-containing proteins, leading to local actin polymerization (Fig. 24). Yet, F-actin is hardly detectable in plasma membrane protrusions induced by individual bacteria. However, this could result from a detection threshold that is not reached at this scale, or from a specific F-actin architecture that is not detected by the LifeAct probe (Belin et al., 2014). Alternatively, cytochalasin D experiments suggest that the F-actin cortex could hinder plasma membrane remodeling. Indeed, plasma membrane protrusions are initially devoid of F-actin (Soyer et al., 2014), suggesting that the membrane locally detaches from the underlying cortex. Since low doses of cytochalasin D were shown to lower the density of the F-actin cortex and to alter its mechanics in cells (Kronlage et al., 2015; Wakatsuki et al., 2001), anchoring of the plasma membrane to cortical actin could mechanically counteract plasma membrane remodeling.

Role of T4P retraction

In this study, we addressed the hypothesis that pilus retraction powers plasma membrane remodeling in endothelial cells, which emerged from the study of the interaction of gonococcus with epithelial cells (Higashi et al., 2009; Lee et al., 2005). Our experiments show i) that T4P retraction is not necessary for plasma membrane reshaping and ii) that T4P retraction rather promotes the establishment of a close contact between meningococcus and the host cell surface, as previously demonstrated (Pujol et al., 1999).

However, our experiments also show that the dynamics of T4P fibers dictate the dynamics of the host cell plasma membrane protrusions. More specifically, we make a link between T4P retraction and the disappearance of the protrusions, meaning that plasma membrane and T4P dynamics mirror one another. Considering that typical T4P fibers measure between 5 and 20 μm and that they extend and retract at speeds in the order of 1 $\mu m.s^{-1}$ (Maier et al., 2002; Merz et al., 2000), we can predict that it would take a few tens of seconds for one fiber to completely extend and retract. This is in good accordance with the lifetime of the plasma protrusions that we estimated around 44 seconds. Consequently, the fact that plasma membrane protrusions appear very stable within a bacterial aggregate implies that T4P dynamics change as bacteria proliferate on top of the host cell. It can be imagined i) that T4P stop retracting within the microcolony or ii) that T4P accumulate in a way that every plasma membrane protrusion still interacts with at least one pilus

despite the retraction of other pili. Both hypotheses are consistent with the dense meshwork of T4P observed by electron microscopy within microcolonies.

Relevance to the pathophysiology of meningococcal disease

Finally, plasma membrane remodeling by adhesion along T4P fibers could conceivably occur *in vivo*. First, we show in this study that the plasma membrane of endothelial cells in human blood vessels is remodeled during vascular colonization. It is interesting to note that, in this case, plasma membrane reshaping occurs as actin-rich finger-like protrusions similar to what has been described *in vitro* and in 2D cell culture. Second, irreversible adhesion of bacteria in blood vessels occurs as individual cells and at very low shear stress, consistent with our experiments that are performed in the absence of flow. Therefore, adhesion of plasma membrane protrusions on T4P fibers could mediate initial irreversible adhesion of meningococcus along blood vessel walls *in vivo*. Furthermore, since no other modifications of the host cell surface occur upon T4P-mediated adhesion of individual bacteria, resistance to shear stress arguably stems from T4P-driven discrete plasma membrane protrusions.

2. On the wetting of the plasma membrane on nanoscale fibers

In our study on plasma membrane remodeling by single adhering bacteria, we show that the plasma membrane conforms to the shape of T4P fibers in a way that resembles the physical phenomenon of wetting, which raises several questions both on the biophysical properties of biological membranes and on the ability of cells to respond to nanotopographical cues from the environment, which are fundamental aspects of cell biology.

Wetting of a liquid on a flat surface

Wetting refers to the ability of a liquid to spread on a solid surface. It depends on a balance between the liquid/surface (adhesion) and the liquid/liquid interactions (cohesion). Ideally, when a reservoir of water (e.g. a droplet) is brought into contact with a perfectly flat surface, it spreads evenly and eventually forms a film at the interface between the air and that surface (Fig. 25). At the extreme opposite, on a surface that is perfectly not wettable, the droplet remains spherical and does not develop any contacts with the surface. Wetting of liquids on flat surfaces is often partial, and the degree of spreading of the droplet depends on its interactions with the solid, with which it forms a characteristic contact angle θ (Fig. 25A). $\theta = 0°$ corresponds to ideal wetting, while $\theta = 180°$ corresponds to perfect non-wetting.

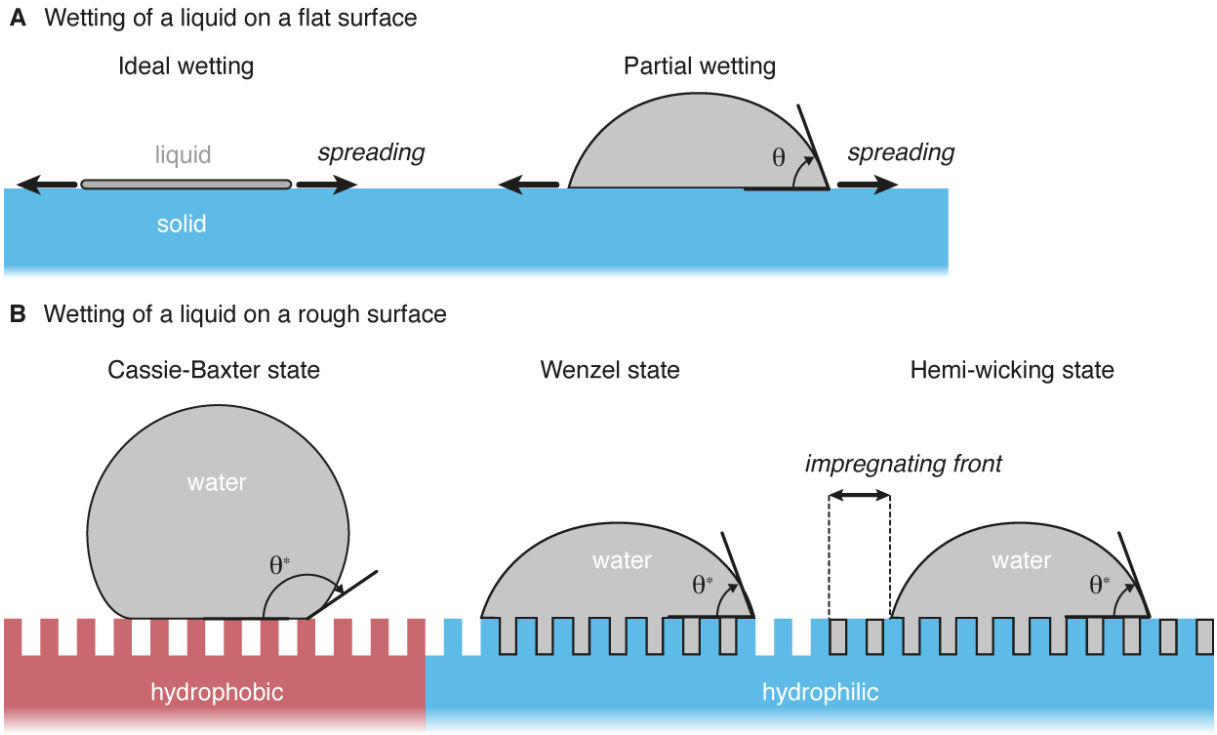

Figure 25 | Wetting of a water droplet on flat and rough surfaces in air. (A) Ideal wetting refers to the spreading of a liquid drop as a perfect film on a flat surface. However, wetting of a liquid is often partial. The liquid drop only partially spreads and forms a contact angle θ with the surface. **(B)** A liquid that partially wets on a rough surface has an apparent contact angle θ^*. It can be in a Cassie-Baxter state, a Wenzel state or a hemi-wicking state. In the latter case, the drop co-exists with a film of liquid that wicks within the surface texture.

Wetting of a liquid on a rough surface

In real life, these laws are challenged by the fact that very few solids are molecularly flat (Quere, 2008). A drop of liquid that spreads on a rough surface will successively interact with each defect of that surface with different contact angles. This contact angle hysteresis greatly varies with the surface roughness. The resulting

macroscopic contact angle between the droplet and the surface is then called the apparent contact angle θ* (Fig. 25B). Depending on the chemical interactions between the liquid and the solid surface, wetting on rough surfaces will fall into different regimes, or states. In the case of a very hydrophobic rough material, the liquid will not conform to the surface topography and air pockets will form in between the liquid droplet and the surface. This is called the Cassie-Baxter state (or the fakir state). The hydrophobicity of the material is enhanced by the surface roughness. Hydrophobic materials with very rough surfaces at the nanoscale are referred to as superhydrophobic. In the case of hydrophilic rough solids, the liquid will tend to interact with the surface defects and the droplet will spread by wetting the defects. This is the Wenzel state. Alternatively, the droplet will co-exist with a film of liquid that forms an impregnating front progressively wetting the surface defects by a process called hemi-wicking (wicking being the ability of a liquid to penetrate a tube or a slot). Hydrophilic materials with very rough surfaces will be more likely to be wetted via hemi-wicking. They are called hyperhydrophilic.

Wetting of the plasma membrane on T4P fibers

The case of plasma membrane wetting on T4P fibers implies that the interactions with T4P are strong enough so the energy cost for the membrane to wet on T4P is lower than not to wet. This is in good accordance with the adhesin function of T4P (i.e. proteins capable of interacting directly with components of the host cell surface) (Bernard et al., 2014; Lu et al., 2015; Maissa et al., 2017). It also implies that the surface tension of the plasma membrane is sufficiently low, consistent with the need for plasma membrane cholesterol in *N. meningitidis*-induced plasma membrane reshaping (Mikaty et al., 2009; Soyer et al., 2014). Indeed, cholesterol depletion stiffens the plasma membrane (Byfield et al., 2004; Sun et al., 2007; Wu et al., 2014) and wetting of liquids on surfaces depends on the liquid viscosity (Quere, 2008).

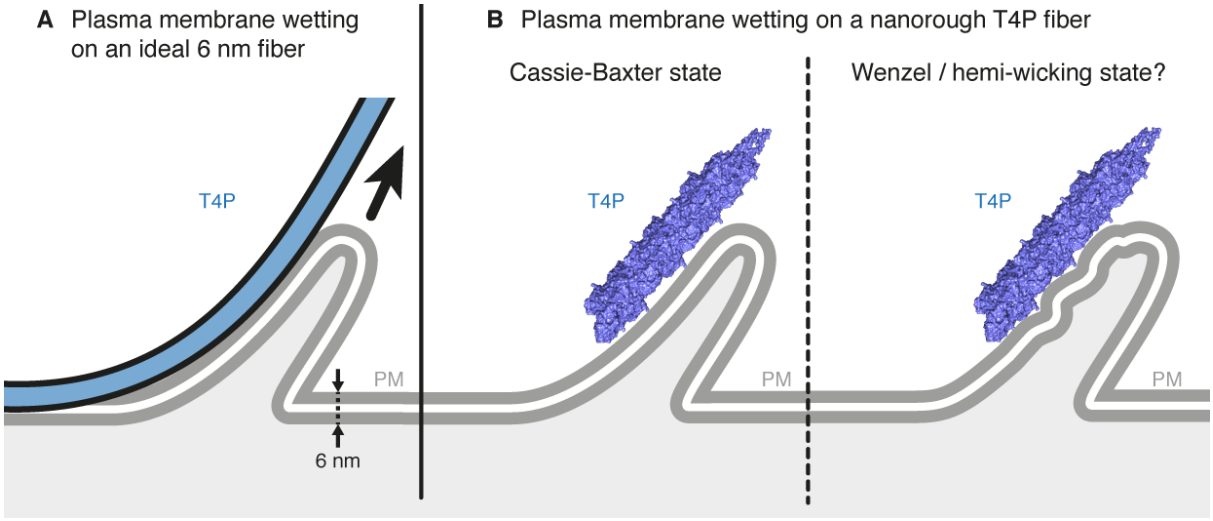

Figure 26 | Mechanisms of wetting applied to plasma membrane remodeling by T4P fibers. (A) Wetting of the plasma membrane on 6 nm fibers implies that the bilayer conforms to an object whose width is in the same order than the thickness of the lipid bilayer itself. **(B)** T4P fibers are not molecularly flat, which implies that wetting of the plasma membrane should follow a Cassie-Baxter state, a Wenzel state or a hemi-wicking state that occur during the wetting of liquids on rough surfaces. T4P, type IV pili; PM, plasma membrane.

However, T4P fibers are not two-dimensional plans but rather one-dimensional fibers with width in the order of the thickness of the plasma membrane itself (Fig. 26). Studies have shown that liposomes can wet onto adhesive fibers (Borghi et al., 2005) and that the wetting of supported lipid bilayers can be guided by the nanotopography of an adhesive substrate at the submicron scale (Bernard et al., 2000; Furukawa et al., 2007; Werner et al., 2009). Yet, to my knowledge, no study has addressed the physical possibility that a lipid

bilayer can wet on fibers in the order of a few nanometers. Therefore, plasma membrane remodeling by T4P fibers might be illustrative of a general biological process, since many biological macromolecules exist as fibers, in particular macromolecules that are found in the extracellular matrix.

Another aspect of T4P that might be of importance is that they are not molecularly flat. As described earlier for 2D plans, roughness can greatly influence the wetting of a liquid on a solid. In our particular case, one can wonder whether the roughness of a 1D fiber influences the wettability of that fiber. Another question is to know what regime would follow the wetting of a 6 nm-thick lipid bilayer on a rough 6 nm-wide fiber. The high adhesiveness of T4P towards the plasma membrane predicts that the plasma membrane should wet the defects of T4P fibers surface. However, the precise mechanism of adhesion of T4P to T4P receptors on the host cell surface is still elusive. For instance, adhesion could be mediated by specific amino acids that display periodic spacing along the T4P fiber, and wetting of the plasma membrane would then approach a Cassie-Baxter state (Fig. 26B). On the contrary, if adhesion occurs all along the T4P fibers surface, wetting of the plasma membrane should follow a Wenzel state or a hemi-wicking state. Yet, this would imply that the plasma membrane can accommodate deformations in the order of its own thickness, which can be predicted to be energetically unfavorable (Fig. 26B). Finally, roughness of T4P fibers is likely to be greatly modulated at the nanoscale by the ability of T4P to stretch and unwind under tension (Baker et al., 2013; Biais et al., 2010). Consequently, it can be imagined i) that T4P fibers roughness will vary in time and ii) that T4P fibers roughness will vary locally along the fiber length. Then, it can be speculated that wetting of the plasma membrane onto T4P fibers will follow different regimes according to the forces experienced by T4P fibers.

Implications for the interaction of cells with the extracellular matrix

It is well appreciated now that eukaryotic cells respond to biophysical parameters of the extracellular matrix (ECM) through the process of mechanosensing, where physical cues from the environment, such as rigidity or density, translate into intracellular signaling events. Mechanosensing can affect cell behavior transiently, as observed in directed cell migration, but can also have long-term effects on cell morphogenesis or cell differentiation via transcriptional regulation (see (Ruprecht et al., 2017) for a review). In particular, cells can sense submicron-scale defects in the topography of the substrate. For instance, filopodia allow the recognition of features of 35 to 75 nm high (Curtis and Wilkinson, 1999; Dalby et al., 2004; Dalby et al., 2002). Conversely, cells can sense nanoscale pores of the substrate (Bruggemann, 2013).

Numerous studies have demonstrated the effect of substrate nanoporosity on cells by performing cell culture on anodized aluminum oxide (AAO) membranes. Such materials feature a high density of nanopores whose diameter is highly controllable, from 20 to 300 nm. Different mammalian cell types, including neurons, fibroblasts, osteoblasts, muscle cells, epithelial and endothelial cells show optimal growth, differentiation or function on such nanoporous substrates (see (Bruggemann, 2013) for a review). Of note, nanoporous materials have become promising tools in regenerative medicine as cell culture substrates because of their beneficial effect on cell functions compared to flat surfaces. Interestingly, in hepatic cells and osteoblasts, filopodia were seen to protrude into pores as small as 100 nm (Hoess et al., 2012; Karlsson et al., 2003), in line with their role in nanotoporaphy sensing. However, in our hands, human endothelial cells were rarely seen to protrude into the 100 nm-pores of the RGD-coated AAO membranes. Instead, filopodia and plasma membrane on the cell contour tightly conformed to the topography of the pore walls, maybe reflecting cell type specificities. As a matter of fact, the reaction of the plasma membrane to nanoporosity is unknown in most cell types. A reason for that is the technical challenge of visualizing plasma membrane deformations in the order of a few tens of nanometers, even by high resolution scanning electron microscopy. Consequently, the vast majority of the studies on cells cultured on nanoporous substrates have been limited to biochemical assays, widefield fluorescence microscopy and, at best, macroscopic measurements of cell spreading by scanning electron microscopy.

More relevant to the architecture of the ECM, cells are known to react to the fibrous nature of the substrate. Fibroblasts in 3D collagen matrices or on synthetic nanofibers and neuron cultured in synthetic fibrous materials display long filopodia that entangle in the fibers or align to them (Albuschies and Vogel, 2013; Jiang and Grinnell, 2005; Sorkin et al., 2009). In line with this, our study shows that endothelial cells plasma membrane produces protrusions that conform to the morphology of T4P fibers. However, an important difference in our case is that plasma membrane protrusions are induced by extracellular fibers, as opposed to filopodia that interact with fibers once they are formed. More recently, Elkhatib *et al.* demonstrated that the plasma membrane of cells adjusts its shape to underlying collagen fibers in 3D matrices. Tubular clathrin lattices then assemble on the curved membrane and promote cell migration (Elkhatib et al., 2017). This finding is in good accordance with our study because the shape of the plasma membrane is imposed by collagen fibers. However, we show that plasma membrane deformation along adhesive fibers occurs at much smaller scales (collagen fibers in 3D gels matrices are about 100 nm thick, while T4P fibers are 6 nm wide). In addition, we show that plasma membrane reshaping at this scale does not depend on actin polymerization and resembles a wetting mechanism. Therefore, it would be of interest to see whether such wetting-like nanoscale deformations of the plasma membrane also exist at the cell-ECM interface, and whether cells use them as a means to detect the substrate topography. It can be speculated that strong adhesion of the plasma membrane to polymeric proteins in the ECM conceivably results in wetting. Furthermore, as for T4P, polymeric proteins are nanorough materials, which could enhance their wettability.

3. Three-dimensional pili meshworks: a common theme in prokaryotes?

A key aspect of this study is that we achieved the visualization, for the first time, of the 3D organization of T4P fibers on individual meningococci by electron microscopy. More specifically, we show that T4P organize a dense meshwork of fibers around bacterial bodies, in addition to producing long fibers that extend far away from the bacterium. This was surprising, as previous studies that used transmission or scanning electron microscopy showed only rare fibers emanating from meningococcal cells (Eugene et al., 2002; Mikaty et al., 2009; Pujol et al., 1997). Our finding is important because it allowed us to demonstrate that the endothelial host cell plasma membrane protrudes along T4P fibers at the level of the single bacterium. More generally, this is the first demonstration that the spatial organization of bacterial pili influence bacterial-host cell interactions.

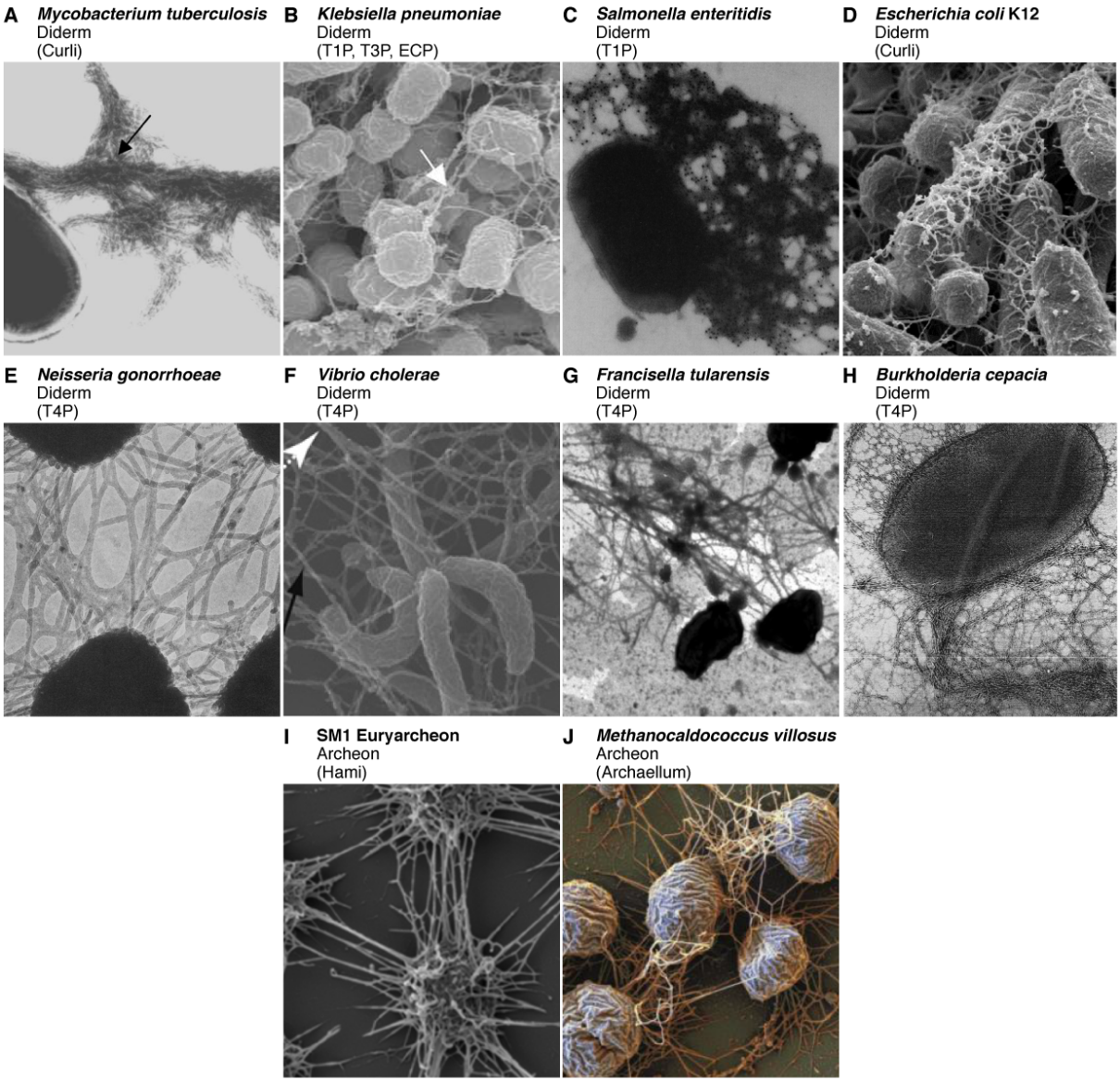

Figure 27 | Ultrastructure of filamentous organelles in other diderm bacteria and archaea. Transmission **(A, C, E, G, H)** and scanning **(B, D, F, I, J)** electron micrographs showing the ultrastructure of filamentous organelles in various prokaryotes. The type of organelle is indicated in brackets. **(A-D)** Non-T4P filamentous organelles in diderm bacteria. **(E-H)** T4P in other didern bacteria than *N. meningitidis*. **(I, J)** Filamentous organelles in archaea. Adapted from the following references (from **A** to **I**): (Alteri et al., 2007), (Alcantar-Curiel et al., 2013), (Collinson et al., 1991), (El Abed et al., 2012), (Todd et al., 1984), (Jude and Taylor, 2011), (Gil et al., 2004), (Sajjan et al., 1995), (Perras et al., 2014) and **J**: Prof. Gerhard Wanner. (Also see **Credits** section.)

Technically, it seems that meningococcal T4P do not withstand the dehydration steps involved in sample processing for electron microscopy, which required the optimization of more preservative techniques. For scanning electron microscopy, T4P were immunolabeled prior to processing, probably protecting the T4P meshwork from dehydration. In another study, authors had already noticed that incubation of bacteria with a serum directed against pili proteins allowed preservation of the pili structure in electron microscopy (Collinson et al., 1991). Alternatively, we used high pressure freezing and freeze substitution instead of conventional room temperature methods for transmission electron microscopy on bacterial microcolonies. This method allows a near-native preservation of biological samples because the cells are rapidly frozen without the formation of ice crystals and because dehydration is achieved at cryogenic temperatures (Hurbain and Sachse, 2011).

Here we show that *N. meningitidis* produces large amounts of T4P, from the single bacterium to the bacterial microcolony, which was not described before. However, the closely related species *Neisseria gonorrhoeae* is known to express large amounts of T4P that also organize in a meshwork-like fashion (Todd et al., 1984) (Fig. 27E). It is also the case in other human pathogens such as *Vibrio cholerae* (Jude and Taylor, 2011; Krebs and Taylor, 2011), *Francisella tularensis* (Gil et al., 2004) and *Burkholderia cepacia* (Sajjan et al., 1995) (Fig. 27F-H). Interestingly, the ability to form dense meshworks of fibers is not restricted to T4P as it seems to occur in other types of pili, like the curli pili of *Mycobacterium tuberculosis* (Alteri et al., 2007) and *Escherichia coli* (El Abed et al., 2012), the type I pili of *Salmonella enteritidis* (Collinson et al., 1991) and the mixed pili types of *Klebsiella pneumoniae* (Alcantar-Curiel et al., 2013) and *Enterococcus faecalis* (Kristich et al., 2008) (Fig. 27A-D). Even filamentous organelles produced by archaea (Jarrell et al., 2013), like the hami fibers in the SM1 Euryarcheon (Perras et al., 2014), display dense and complex architectures *in vitro* and in multispecies biofilms *in vivo* (Fig. 27I and J). To our knowledge however, the three-dimensional architecture of these different fibers at the single cell level has not been assessed. Therefore, it would be of great interest to see whether the 3D architecture of *N. meningitidis* T4P at the single bacterium level is shared by other prokaryotes, and whether this contributes to the interactions between microorganisms and their environment or host cells.

4. The extracellular lifestyle of meningococcus: a geometry problem?

Unlike other bacterial pathogens, *N. meningitidis* colonization of host cells does not lead to efficient internalization. Although meningococcus lacks bacterial factors used by other pathogens to invade host cells, such as secretion systems that deliver toxins into the host cell cytoplasm, it does trigger an important rearrangement of the plasma membrane and of the actin cytoskeleton, which could be expected to result in bacterial engulfment. Here, I propose that internalization of meningococci could presumably be hindered by i) the morphology of the bacterium and ii) the distinctive plasma membrane protrusions elicited by T4P fibers.

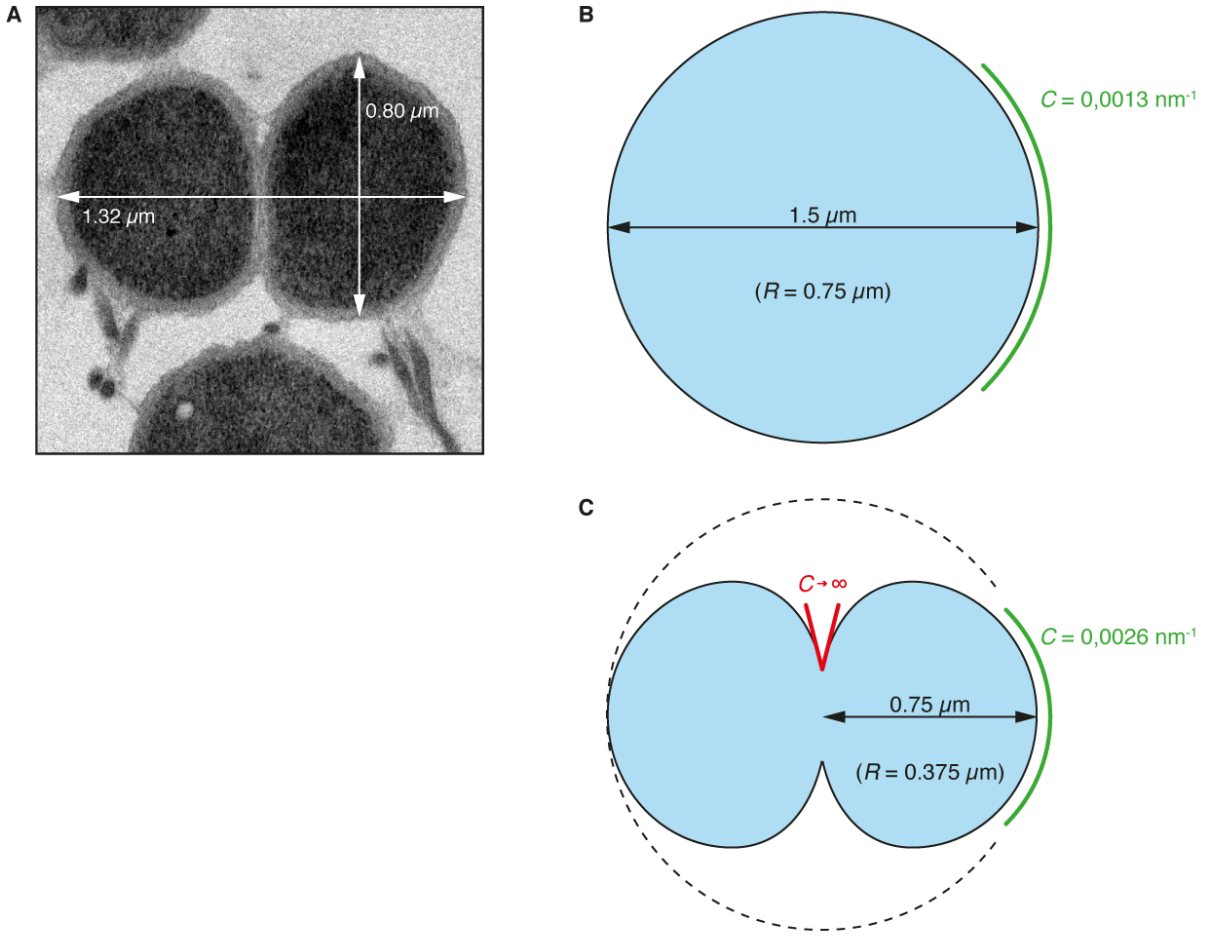

Figure 28 | Curvature in a diplococcus-shaped particle. **(A)** Transmission electron micrograph after high pressure freezing and freeze substitution of *N. meningitidis* on top of an endothelial cell, showing an individual diplococcus cell. The diplococcus can be compared as two joined partial spheres with a long axis of 1.32 μm and short axes of 0.8 μm. **(B)** A sphere of 1.5 μm diameter has a positive curvature *C* of 0.0013 nm^{-1} (*C* = 1/*R*, with *R* the radius of the sphere). **(C)** A theoretical diplococcus fitting a sphere of the same diameter displays two spherical ends with positive curvatures *C* of 0.0026 nm^{-1} (green), and two zones of negative curvature at the junction between the two spheres where *C* tends towards infinity (red).

Effect of the morphology of meningococcus

Uptake of particles by cells, for example by phagocytosis, shows a strong dependency on the shape of the particle. There is a higher energetic cost for the plasma membrane to adapt to highly curved surfaces. Thus, it is easier for a cell to engulf a spherical particle than a rod-shaped particle, unless it presents with its tip first as in *Mycobacteria* (Champion and Mitragotri, 2006; Champion and Mitragotri, 2009). After zippering of

the plasma membrane on the particle surface through receptors-ligands interactions, engulfment is further facilitated by actin polymerization, which stabilizes these interactions, independently of the particle size. Alternatively, it was shown that small spherical particles of radius 1.5 µm can be internalized by a passive zipper mechanism where no actin polymerization is required (Tollis et al., 2010). In that case, the particle radius R is 0.75 µm, giving a positive curvature $C = 1/R$ of 0.0013 nm^{-1} (Fig. 28B). A typical meningococcus cell (Fig. 28A) can be assimilated to two joined spheres with a long axis of around 1.5 µm and short axes of 0.75 µm (Fig. 28C). Therefore, meningococcus presents two spherical ends that are highly positively curved (C = 0.0026 nm^{-1}, Fig. 28C), and displays two zones of negative curvature at the junction between the two partial spheres where C tends towards infinity (red, Fig. 28C). Since *N. meningitidis* does not colonize its natural niche as an intracellular bacterium, it can be speculated that it has evolved a specific shape in relation to its interactions with host cells (i.e. epithelial cells in the nasopharynx). In the pathogens *Helicobacter pylori* and *Campylobacter jejuni*, the spiral shape of the bacteria was proposed to inhibit their phagocytosis by macrophages (Champion and Mitragotri, 2009). It is not easy to predict how the shape of meningococcus could influence its internalization, but it would be interesting to see how human cells engulf diplococcus-shaped particles.

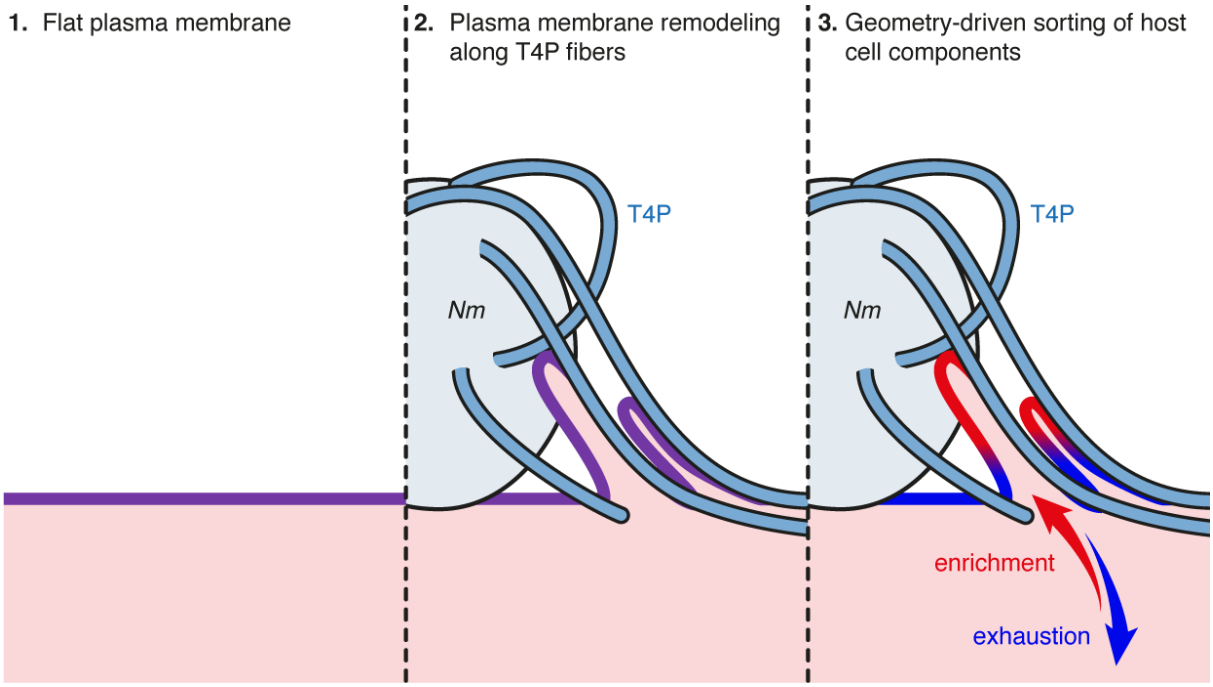

Figure 29 | Putative effect of the geometry of T4P-induced plasma membrane protrusions on the recruitment of host cell components. T4P fibers are able to induce protrusions of the host cell plasma membrane **(1 and 2)**. Negative curvature of the host cell plasma membrane could presumably lead to a local separation of host cell components, as observed *in vitro* **(3)**. T4P, type IV pili; *Nm*, *N. meningitidis*.

Effect of the geometry of plasma membrane protrusions

Another key parameter to particles internalization by eukaryotic cells is the supply of additional plasma membrane that supports the growth of the phagocytic cup. This can be achieved either by exocytosis of intracellular vesicles or by unfolding of plasma membrane wrinkles (Hallett and Dewitt, 2007; Levin et al., 2016). In the case of *N. meningitidis*, the plasma membrane that is in contact with the bacterium is not cup-shaped. Instead, we show that T4P fibers impose a finger-like geometry to the plasma membrane. Thus, meningococcus prevents continuous (or homogenous) adhesion of the plasma membrane, which is predicted to alter internalization dynamics (Tollis et al., 2010). Most importantly, the geometry of the protrusions induced by meningococcus could modulate the biological processes that take place at the plasma

membrane. First, membrane-associated biochemical reactions can be influenced by membrane shape and curvature. For example, the lipid phosphatase synaptojanin was shown to be only active on highly curved membranes (Chang-Ileto et al., 2011). Second, membrane curvature can drive the sorting of membrane proteins (Aimon et al., 2014). Experiments of nanotubes pulling from giant unilamellar vesicles (GUVs) also demonstrated that the diffusion of lipids and transmembrane proteins decreases with the tube diameter, and is significantly reduced for tubes diameters below 100 nm (Domanov et al., 2011; Quemeneur et al., 2014). In neurons, it was shown that the morphology of the neck of dendritic spines regulates the molecular composition of the spines by altering the diffusion of membrane proteins (Tonnesen et al., 2014). In our case, the host cell components recruited to *N. meningitidis*-induced plasma membrane protrusions (Table 1) show a differential recruitment of proteins that are naturally affine for negatively curved membranes. Oppositely, proteins that are usually found at sites of positive membrane curvature seem to be excluded from the protrusions. Thus, the local composition of the plasma membrane recruited by meningococcus differs from the surrounding plasma membrane, which could be due to the geometry of the plasma membrane protrusions (Fig. 29). In addition, this suggests that biochemical reactions could be locally modified by this geometrical effect. Proteins involved in endocytosis, such as clathrin, or in exocytosis of intracellular vesicles, such as Exo84, are excluded from *N. meningitidis*-induced protrusions, suggesting that the geometry of the plasma membrane protrusions triggered by T4P fibers could also locally impair intracellular trafficking. In line with this, only plasma membrane lipids are detected in plasma membrane protrusiosn, as compared to lipids from intracellular compartments. Paradoxically, delocalization of VE-cadherin at the site of bacterial adhesion depends on vesicular trafficking rather than lateral diffusion from the cell-cell junctions (Coureuil et al., 2009). However, the putative inhibitory effect of plasma membrane protrusions geometry on intracellular trafficking could act at very local scales. Overall, the distinctive remodeling of the host cell plasma membrane by meningococcus can be predicted to impact biological processes at the cell surface. Since meningococcus is an extracellular bacterium, it can be further speculated that this was also selected as a means to avoid internalization.

Together, both the distinctive morphology of *N. meningitidis* cells and the specific geometry of plasma membrane protrusions that it induces in host cells could conceivably influence the lifestyle of the bacterium. Yet, it can be argued that in piliated meningococci the effect of the morphology would be dominated by the action of T4P, which are the first structures in contact with the host cell surface and can sculpt the plasma membrane in the form of discrete protrusions. However, the diplococcus shape could provide non-piliated bacteria with a selective advantage over differently shaped microorganisms for proliferation in the nasopharynx.

GENERAL CONCLUSION & OUTLOOK

It has been well documented that upon T4P-mediated adhesion to human endothelial cells, *N. meningitidis* induces a reorganization of the cell surface, which includes a remodeling of the plasma membrane in the shape of fliopodia-like protrusions and a reorganization of the actin cytoskeleton. Remodeling of the host cell surface allows bacteria to resist shear forces present in the bloodstream. As such, it is believed to be essential to the pathophysiology of meningococcal disease, where vascular damage is induced by the colonization of blood vessels by the bacteria. Therefore, understanding how the bacterium achieves host cell surface reorganization has emerged as an important question.

Despite the widely-admitted idea that plasma membrane protrusions result from actin polymerization, convincing evidence had accumulated that *N. meningitidis*-induced plasma membrane remodeling is actin-independent. Yet, the underlying mechanisms were unknown. Therefore, here we investigated the mechanisms of plasma membrane remodeling by meningococcus, which was a new question in the field.

To address this question, we used different approaches of live cell imaging, super-resolution microscopy and high-resolution transmission and scanning electron microscopy. We found that the endothelial cell plasma membrane is remodeled by meningococcus because it spontaneously adheres to individual T4P fibers in a wetting-like manner, thereby protruding towards the bacterium. This novel mechanism has not been described in the study of bacterial virulence so far. The originality of this work is that we could assess the spatial organization of T4P fibers and visualize plasma membrane remodeling at the level of the single bacterium for the first time. Furthermore, this study demonstrates that the plasma membrane of human cells can spontaneously conform to the shape of nanoscale objects in an F-actin-independent, wetting-like fashion. Consequently, this work has potential implications for the fields of microbiology and cell biology. First, T4P are expressed by a wide number of bacterial pathogens. Therefore, the mechanism of plasma membrane remodeling along T4P fibers could be relevant to the interaction of other pathogens with their host cells. Second, this original mechanism could be added to the set of mechanisms of biological membranes deformation in cells. With respect to the emerging field of mechanobiology, it could also represent a new mechanism for the sensing of the environment nanotopography by cells.

Consistent with our *in vitro* experiments, we found that the plasma membrane of endothelial cells is reshaped within meningococcal microcolonies during vascular colonization of human blood vessels *in vivo*. Deformation of the plasma membrane by adhesion along T4P fibers is thus likely to occur during meningococcal disease in human, where it would convey bacterial resistance to blood flow-generated shear stress. Therefore, in this thesis, we describe a novel biophysical mechanism for plasma membrane remodeling in human cells that can impact our understanding of meningococcal disease progression.

EXPERIMENTAL PROCEDURES

Here are presented the experimental procedures that were used in the section **Results**, **3. Additional results**. *Procedures already described in the paper by Soyer et al. as well as in the manuscript in preparation are not described.*

Reactives

A mouse monoclonal antibody against human caveolin-1 (610058, BD Transduction Laboratories, BD Biosciences) was diluted 1:500 and 1:5,000 in immunofluorescence and western blot assays, respectively. Rabbit polyclonal antibodies against human phospho-caveolin-1 (phospho-Tyr14, 11090, Signalway Antibody) was diluted 1:200 and 1:1,000. For western blots, a mouse monoclonal antibody against human glyceraldehyde-3-phosphate dehydrogenase (GAPDH, MAB374, clone 6C5, Millipore) was used as a loading control and diluted 1:10,000. Goat secondary antibodies against mouse or rabbit IgG coupled to horseradish peroxidase (HRP, Invitrogen) were diluted 1:10,000.

For RNA interference experiments, we used a pool of four siRNAs targeting human caveolin-1 (siCAV1, ON-TARGETplus Human CAV1 (857) SMARTpool, Thermo Scientific) or a control siRNA (siNT, ON-TARGETplus non-targeting siRNA #1).

Complementary list of plasmids used in this study:

Plasmid name	Function/tagged gene	Species	Source	Reference
CAV1-mCherry	caveolae (caveolin-1)	*C. lupus*	C. Lamaze (origin A. Helenius)	(Hayer et al., 2010)
Cavin-1-mCherry	caveolae	*M. musculus*	C. Lamaze (origin R. Parton)	(Hill et al., 2008)
CHMP2A-GFP	ESCRTIII complex subunit	*H. sapiens*	Addgene 31805 (D. Gerlich)	(Guizetti et al., 2011)
CLC-GFP	clathrin light chain	*M. musculus*	C. Lamaze (origin J. Keen ?)	(Gaidarov et al., 1999)
EB1-GFP	microtubules plus end	-	G. Dumenil (origin ?)	-
EHD2-mEGFP	caveolae/PM	*H. sapiens*	C. Lamaze (origin A. Helenius)	(Stoeber et al., 2012)
GFP-Exo70-HA	exocyst complex subunit Exo70	*H. sapiens*	P. Chavrier	(Hertzog et al., 2012)
IRSp53-IMD-GFP	I-BAR domain from IRSp53 (aa 1-250)	*M. musculus*	P. Lappalainen	pPL485 - (Mattila et al., 2007)
MIM-GFP	full length MIM	*H. sapiens*	P. Lappalainen	pPL151 - (Mattila et al., 2007)
MIM-IMD-GFP	I-BAR domain from MIM (aa 1-254)	*H. sapiens*	P. Lappalainen	pPL271 - (Mattila et al., 2007)

OCRLa-mCherry	full length inositol 5-phosphatase OCRLa with N-terminal mCherry(mainly neuronal isoform)	*M. musculus*	D. Perrais (C. Merrifield, Addgene 27675)	(Taylor et al., 2011)
p16-GFP	Arp2/3 complex subunit	-	M. Piel (origin P. Chavrier)	-
p40-PX-EGFP	PI3P binding domain from p40phox	*H. sapiens*	Addgene 19010 (M Yaffe)	(Kanai et al., 2001)
GFP-PLC -PH	PIP2 binding domain from PLCd	*H. sapiens*	Addgene 21179 (T. Meyer)	(Stauffer et al., 1998)
PH-Gab2-GFP	PIP3 binding domain from Gab2 (x2)	*M. musculus*	Addgene 35147 (S. Grinstein)	(Gu et al., 2003)
GFP-GPI	GFP fused to the GPI (glycosylphosphatidylinositide) anchor of the folate receptor	-	C. Zurzolo (origin S. Lacey)	(Paladino et al., 2004)
GFP-Rab35	GFP fused to Rab35 GTPase	-	A. Echard	(Chesneau et al., 2012)
mCherry-Sec61β	endoplasmic reticulum (translocon)	*H. sapiens*	Addgene 49155 (G. Voeltz)	(Zurek et al., 2011)
TfR-GFP	transferrin receptor	-	A. Benmerah (origin?)	-

RNA interference

5.10^5 to 10^6 HUVEC cells were transfected with 200 nM siRNA on day 0, kept in culture and re-electroporated on day 2 with 200 nM siRNA prior to seeding in 6-well plates (for western blots) or 96-well plates (for imaging). Cells were used on day 3. When indicated, cells were also co- transfected with plasmid DNA on day 2.

Western blot

Cells were rinsed with ice-cold PBS 1X and lysed in homemade Laemmli 1X (2% SDS, 60mM Tris-HCl pH 6.8, 100mM dithiothreitol, 0.01% bromophenol blue, 20% glycerol). 100µL of Laemmli was used for each well (i.e. approximately 2.10^5 cells). Lysates were boiled at 95°C for 10 min. Samples were run on a 15% polyacrylamide gel. Proteins were blotted onto a PVDF membrane for 45 min at 15V through a semi dry transfer system (BioRad). Membranes were cut in two. Top part was incubated with anti-GAPDH, bottom part with anti-Cav1. Primary and secondary antibodies were diluted in PBST-5% milk and incubated for 1h at room temperature (Régilait). Cav1 was revealed with the Pierce ECL2 kit and GAPDH with the BioRad CLARITY kit. Chemiluminescence was detected and imaged with a LAS-4000 device (GE Healthcare). For the analysis of the phosphorylation of caveolin-1, Laemmli buffer contained 1 mM of the tyrosine phosphatase inhibitor Na_3VO_4. PBST was replaced with TBST in all subsequent steps.

REFERENCES

Ahmed, S., Goh, W. I. and Bu, W. (2010). I-BAR domains, IRSp53 and filopodium formation. *Semin Cell Dev Biol* **21**, 350-6.

Aho, E. L., Dempsey, J. A., Hobbs, M. M., Klapper, D. G. and Cannon, J. G. (1991). Characterization of the opa (class 5) gene family of Neisseria meningitidis. *Mol Microbiol* **5**, 1429-37.

Aimon, S., Callan-Jones, A., Berthaud, A., Pinot, M., Toombes, G. E. and Bassereau, P. (2014). Membrane shape modulates transmembrane protein distribution. *Dev Cell* **28**, 212-8.

Albers, S. V. and Jarrell, K. F. (2015). The archaellum: how Archaea swim. *Front Microbiol* **6**, 23.

Albuschies, J. and Vogel, V. (2013). The role of filopodia in the recognition of nanotopographies. *Sci Rep* **3**, 1658.

Alcantar-Curiel, M. D., Blackburn, D., Saldana, Z., Gayosso-Vazquez, C., Iovine, N. M., De la Cruz, M. A. and Giron, J. A. (2013). Multi-functional analysis of Klebsiella pneumoniae fimbrial types in adherence and biofilm formation. *Virulence* **4**, 129-38.

Allison, T. M., Conrad, S. and Castric, P. (2015). The group I pilin glycan affects type IVa pilus hydrophobicity and twitching motility in Pseudomonas aeruginosa 1244. *Microbiology* **161**, 1780-9.

Alm, R. A., Bodero, A. J., Free, P. D. and Mattick, J. S. (1996). Identification of a novel gene, pilZ, essential for type 4 fimbrial biogenesis in Pseudomonas aeruginosa. *J Bacteriol* **178**, 46-53.

Alrutz, M. A. and Isberg, R. R. (1998). Involvement of focal adhesion kinase in invasin-mediated uptake. *Proc Natl Acad Sci U S A* **95**, 13658-63.

Alteri, C. J., Xicohtencatl-Cortes, J., Hess, S., Caballero-Olin, G., Giron, J. A. and Friedman, R. L. (2007). Mycobacterium tuberculosis produces pili during human infection. *Proc Natl Acad Sci U S A* **104**, 5145-50.

Andrews, N. L., Lidke, K. A., Pfeiffer, J. R., Burns, A. R., Wilson, B. S., Oliver, J. M. and Lidke, D. S. (2008). Actin restricts FcepsilonRI diffusion and facilitates antigen-induced receptor immobilization. *Nat Cell Biol* **10**, 955-63.

Archibald, F. S. and DeVoe, I. W. (1978). Iron in Neisseria meningitidis: minimum requirements, effects of limitation, and characteristics of uptake. *J Bacteriol* **136**, 35-48.

Ariotti, N., Fernandez-Rojo, M. A., Zhou, Y., Hill, M. M., Rodkey, T. L., Inder, K. L., Tanner, L. B., Wenk, M. R., Hancock, J. F. and Parton, R. G. (2014). Caveolae regulate the nanoscale organization of the plasma membrane to remotely control Ras signaling. *J Cell Biol* **204**, 777-92.

Asmat, T. M., Tenenbaum, T., Jonsson, A. B., Schwerk, C. and Schroten, H. (2014). Impact of calcium signaling during infection of Neisseria meningitidis to human brain microvascular endothelial cells. *PLoS One* **9**, e114474.

Assalkhou, R., Balasingham, S., Collins, R. F., Frye, S. A., Davidsen, T., Benam, A. V., Bjoras, M., Derrick, J. P. and Tonjum, T. (2007). The outer membrane secretin PilQ from Neisseria meningitidis binds DNA. *Microbiology* **153**, 1593-603.

Baker, J. L., Biais, N. and Tama, F. (2013). Steered molecular dynamics simulations of a type IV pilus probe initial stages of a force-induced conformational transition. *PLoS Comput Biol* **9**, e1003032.

Balaban, M., Battig, P., Muschiol, S., Tirier, S. M., Wartha, F., Normark, S. and Henriques-Normark, B. (2014). Secretion of a pneumococcal type II secretion system pilus correlates with DNA uptake during transformation. *Proc Natl Acad Sci U S A* **111**, E758-65.

Balasingham, S. V., Collins, R. F., Assalkhou, R., Homberset, H., Frye, S. A., Derrick, J. P. and Tonjum, T. (2007). Interactions between the lipoprotein PilP and the secretin PilQ in Neisseria meningitidis. *J Bacteriol* **189**, 5716-27.

Banks, W. A. (2016). From blood-brain barrier to blood-brain interface: new opportunities for CNS drug delivery. *Nat Rev Drug Discov* **15**, 275-92.

Basquin, C., Trichet, M., Vihinen, H., Malarde, V., Lagache, T., Ripoll, L., Jokitalo, E., Olivo-Marin, J. C., Gautreau, A. and Sauvonnet, N. (2015). Membrane protrusion powers clathrin-independent endocytosis of interleukin-2 receptor. *Embo J* **34**, 2147-61.

Belin, B. J., Goins, L. M. and Mullins, R. D. (2014). Comparative analysis of tools for live cell imaging of actin network architecture. *Bioarchitecture* **4**, 189-202.

Berger, C. N., Billker, O., Meyer, T. F., Servin, A. L. and Kansau, I. (2004). Differential recognition of members of the carcinoembryonic antigen family by Afa/Dr adhesins of diffusely adhering Escherichia coli (Afa/Dr DAEC). *Mol Microbiol* **52**, 963-83.

Bernard, A. L., Guedeau-Boudeville, M. A., Sandre, O., Palacin, S., di Meglio, J. M. and Jullien, L. (2000). Permeation through lipid bilayers by adhesion of giant vesicles on decorated surfaces. *Langmuir* **16**, 6801-6808.

Bernard, S. C., Simpson, N., Join-Lambert, O., Federici, C., Laran-Chich, M. P., Maissa, N., Bouzinba-Segard, H., Morand, P. C., Chretien, F., Taouji, S. et al. (2014). Pathogenic Neisseria meningitidis utilizes CD147 for vascular colonization. *Nat Med* **20**, 725-31.

Berry, J. L. and Pelicic, V. (2015). Exceptionally widespread nanomachines composed of type IV pilins: the prokaryotic Swiss Army knives. *FEMS Microbiol Rev* **39**, 134-54.

Berry, J. L., Phelan, M. M., Collins, R. F., Adomavicius, T., Tonjum, T., Frye, S. A., Bird, L., Owens, R., Ford, R. C., Lian, L. Y. et al. (2012). Structure and assembly of a trans-periplasmic channel for type IV pili in Neisseria meningitidis. *PLoS Pathog* **8**, e1002923.

Biais, N., Higashi, D. L., Brujic, J., So, M. and Sheetz, M. P. (2010). Force-dependent polymorphism in type IV pili reveals hidden epitopes. *Proc Natl Acad Sci U S A* **107**, 11358-63.

Biais, N., Ladoux, B., Higashi, D., So, M. and Sheetz, M. (2008). Cooperative retraction of bundled type IV pili enables nanonewton force generation. *PLoS Biol* **6**, e87.

Bille, E., Meyer, J., Jamet, A., Euphrasie, D., Barnier, J. P., Brissac, T., Larsen, A., Pelissier, P. and Nassif, X. (2017). A virulence-associated filamentous bacteriophage of Neisseria meningitidis increases host-cell colonisation. *PLoS Pathog* **13**, e1006495.

Bille, E., Ure, R., Gray, S. J., Kaczmarski, E. B., McCarthy, N. D., Nassif, X., Maiden, M. C. and Tinsley, C. R. (2008). Association of a bacteriophage with meningococcal disease in young adults. *PLoS One* **3**, e3885.

Bille, E., Zahar, J. R., Perrin, A., Morelle, S., Kriz, P., Jolley, K. A., Maiden, M. C., Dervin, C., Nassif, X. and Tinsley, C. R. (2005). A chromosomally integrated bacteriophage in invasive meningococci. *J Exp Med* **201**, 1905-13.

Biswas, G. D., Sox, T., Blackman, E. and Sparling, P. F. (1977). Factors affecting genetic transformation of Neisseria gonorrhoeae. *J Bacteriol* **129**, 983-92.

Blackwell, C. C., Weir, D. M., James, V. S., Todd, W. T., Banatvala, N., Chaudhuri, A. K., Gray, H. G., Thomson, E. J. and Fallon, R. J. (1990). Secretor status, smoking and carriage of Neisseria meningitidis. *Epidemiol Infect* **104**, 203-9.

Blattner, F. R., Plunkett, G., 3rd, Bloch, C. A., Perna, N. T., Burland, V., Riley, M., Collado-Vides, J., Glasner, J. D., Rode, C. K., Mayhew, G. F. et al. (1997). The complete genome sequence of Escherichia coli K-12. *Science* **277**, 1453-62.

Boesen, T. and Nielsen, L. P. (2013). Molecular dissection of bacterial nanowires. *MBio* **4**, e00270-13.

Boettcher, J. P., Kirchner, M., Churin, Y., Kaushansky, A., Pompaiah, M., Thorn, H., Brinkmann, V., Macbeath, G. and Meyer, T. F. (2010). Tyrosine-phosphorylated caveolin-1 blocks bacterial uptake by inducing Vav2-RhoA-mediated cytoskeletal rearrangements. *PLoS Biol* **8**.

Boisier, P., Nicolas, P., Djibo, S., Taha, M. K., Jeanne, I., Mainassara, H. B., Tenebray, B., Kairo, K. K., Giorgini, D. and Chanteau, S. (2007). Meningococcal meningitis: unprecedented incidence of serogroup X-related cases in 2006 in Niger. *Clin Infect Dis* **44**, 657-63.

Borghi, N., Alias, K., de Gennes, P. G. and Brochard-Wyart, F. (2005). Wetting fibers with liposomes. *Journal of Colloid and Interface Science* **285**, 61-66.

Borst, P. (1991). Molecular genetics of antigenic variation. *Immunol Today* **12**, A29-33.

Bos, M. P., Tefsen, B., Voet, P., Weynants, V., van Putten, J. P. and Tommassen, J. (2005). Function of neisserial outer membrane phospholipase a in autolysis and assessment of its vaccine potential. *Infect Immun* **73**, 2222-31.

Boucrot, E., Ferreira, A. P., Almeida-Souza, L., Debard, S., Vallis, Y., Howard, G., Bertot, L., Sauvonnet, N. and McMahon, H. T. (2015). Endophilin marks and controls a clathrin-independent endocytic pathway. *Nature* **517**, 460-5.

Bougneres, L., Girardin, S. E., Weed, S. A., Karginov, A. V., Olivo-Marin, J. C., Parsons, J. T., Sansonetti, P. J. and Van Nhieu, G. T. (2004). Cortactin and Crk cooperate to trigger actin polymerization during Shigella invasion of epithelial cells. *J Cell Biol* **166**, 225-35.

Bourdet-Sicard, R., Rudiger, M., Jockusch, B. M., Gounon, P., Sansonetti, P. J. and Nhieu, G. T. (1999). Binding of the Shigella protein IpaA to vinculin induces F-actin depolymerization. *Embo J* **18**, 5853-62.

Bradley, D. E. (1972). Shortening of Pseudomonas aeruginosa pili after RNA-phage adsorption. *J Gen Microbiol* **72**, 303-19.

Brandtzaeg, P., Kierulf, P., Gaustad, P., Skulberg, A., Bruun, J. N., Halvorsen, S. and Sorensen, E. (1989a). Plasma endotoxin as a predictor of multiple organ failure and death in systemic meningococcal disease. *J Infect Dis* **159**, 195-204.

Brandtzaeg, P., Mollnes, T. E. and Kierulf, P. (1989b). Complement activation and endotoxin levels in systemic meningococcal disease. *J Infect Dis* **160**, 58-65.

Brandtzaeg, P. and van Deuren, M. (2012). Classification and pathogenesis of meningococcal infections. *Methods Mol Biol* **799**, 21-35.

Brissac, T., Mikaty, G., Dumenil, G., Coureuil, M. and Nassif, X. (2012). The meningococcal minor pilin PilX is responsible for type IV pilus conformational changes associated with signaling to endothelial cells. *Infect Immun* **80**, 3297-306.

Broome, C. V. (1986). The carrier state: Neisseria meningitidis. *J Antimicrob Chemother* **18 Suppl A**, 25-34.

Brown, D. R., Helaine, S., Carbonnelle, E. and Pelicic, V. (2010). Systematic functional analysis reveals that a set of seven genes is involved in fine-tuning of the multiple functions mediated by type IV pili in Neisseria meningitidis. *Infect Immun* **78**, 3053-63.

Bruce-Staskal, P. J., Weidow, C. L., Gibson, J. J. and Bouton, A. H. (2002). Cas, Fak and Pyk2 function in diverse signaling cascades to promote Yersinia uptake. *J Cell Sci* **115**, 2689-700.

Bruggemann, D. (2013). Nanoporous Aluminium Oxide Membranes as Cell Interfaces. *Journal of Nanomaterials*.

Burton, E. A., Plattner, R. and Pendergast, A. M. (2003). Abl tyrosine kinases are required for infection by Shigella flexneri. *Embo J* **22**, 5471-9.

Byfield, F. J., Aranda-Espinoza, H., Romanenko, V. G., Rothblat, G. H. and Levitan, I. (2004). Cholesterol depletion increases membrane stiffness of aortic endothelial cells. *Biophys J* **87**, 3336-43.

Caltagarone, J., Ma, S. and Sorkin, A. (2015). Dopamine transporter is enriched in filopodia and induces filopodia formation. *Mol Cell Neurosci* **68**, 120-30.

Campellone, K. G. and Leong, J. M. (2005). Nck-independent actin assembly is mediated by two phosphorylated tyrosines within enteropathogenic Escherichia coli Tir. *Mol Microbiol* **56**, 416-32.

Campellone, K. G., Robbins, D. and Leong, J. M. (2004). EspFU is a translocated EHEC effector that interacts with Tir and N-WASP and promotes Nck-independent actin assembly. *Dev Cell* **7**, 217-28.

Capecchi, B., Adu-Bobie, J., Di Marcello, F., Ciucchi, L., Masignani, V., Taddei, A., Rappuoli, R., Pizza, M. and Arico, B. (2005). Neisseria meningitidis NadA is a new invasin which promotes bacterial adhesion to and penetration into human epithelial cells. *Mol Microbiol* **55**, 687-98.

Carbonnelle, E., Helaine, S., Nassif, X. and Pelicic, V. (2006). A systematic genetic analysis in Neisseria meningitidis defines the Pil proteins required for assembly, functionality, stabilization and export of type IV pili. *Mol Microbiol* **61**, 1510-22.

Carbonnelle, E., Helaine, S., Prouvensier, L., Nassif, X. and Pelicic, V. (2005). Type IV pilus biogenesis in Neisseria meningitidis: PilW is involved in a step occurring after pilus assembly, essential for fibre stability and function. *Mol Microbiol* **55**, 54-64.

Caugant, D. A. (2008). Genetics and evolution of Neisseria meningitidis: importance for the epidemiology of meningococcal disease. *Infect Genet Evol* **8**, 558-65.

Caugant, D. A., Hoiby, E. A., Magnus, P., Scheel, O., Hoel, T., Bjune, G., Wedege, E., Eng, J. and Froholm, L. O. (1994). Asymptomatic carriage of Neisseria meningitidis in a randomly sampled population. *J Clin Microbiol* **32**, 323-30.

Caugant, D. A., Hoiby, E. A., Rosenqvist, E., Froholm, L. O. and Selander, R. K. (1992). Transmission of Neisseria meningitidis among asymptomatic military recruits and antibody analysis. *Epidemiol Infect* **109**, 241-53.

Caugant, D. A. and Maiden, M. C. (2009). Meningococcal carriage and disease--population biology and evolution. *Vaccine* **27 Suppl 2**, B64-70.

Caugant, D. A., Tzanakaki, G. and Kriz, P. (2007). Lessons from meningococcal carriage studies. *FEMS Microbiol Rev* **31**, 52-63.

Cehovin, A., Simpson, P. J., McDowell, M. A., Brown, D. R., Noschese, R., Pallett, M., Brady, J., Baldwin, G. S., Lea, S. M., Matthews, S. J. et al. (2013). Specific DNA recognition mediated by a type IV pilin. *Proc Natl Acad Sci U S A* **110**, 3065-70.

Chaban, B., Voisin, S., Kelly, J., Logan, S. M. and Jarrell, K. F. (2006). Identification of genes involved in the biosynthesis and attachment of Methanococcus voltae N-linked glycans: insight into N-linked glycosylation pathways in Archaea. *Mol Microbiol* **61**, 259-68.

Chamot-Rooke, J., Mikaty, G., Malosse, C., Soyer, M., Dumont, A., Gault, J., Imhaus, A. F., Martin, P., Trellet, M., Clary, G. et al. (2011). Posttranslational modification of pili upon cell contact triggers N. meningitidis dissemination. *Science* **331**, 778-82.

Champion, J. A. and Mitragotri, S. (2006). Role of target geometry in phagocytosis. *Proc Natl Acad Sci U S A* **103**, 4930-4.

Champion, J. A. and Mitragotri, S. (2009). Shape induced inhibition of phagocytosis of polymer particles. *Pharm Res* **26**, 244-9.

Chang, Y. W., Kjaer, A., Ortega, D. R., Kovacikova, G., Sutherland, J. A., Rettberg, L. A., Taylor, R. K. and Jensen, G. J. (2017). Architecture of the Vibrio cholerae toxin-coregulated pilus machine revealed by electron cryotomography. *Nat Microbiol* **2**, 16269.

Chang, Y. W., Rettberg, L. A., Treuner-Lange, A., Iwasa, J., Sogaard-Andersen, L. and Jensen, G. J. (2016). Architecture of the type IVa pilus machine. *Science* **351**, aad2001.

Chang-Ileto, B., Frere, S. G., Chan, R. B., Voronov, S. V., Roux, A. and Di Paolo, G. (2011). Synaptojanin 1-mediated PI(4,5)P2 hydrolysis is modulated by membrane curvature and facilitates membrane fission. *Dev Cell* **20**, 206-18.

Chappie, J. S., Mears, J. A., Fang, S., Leonard, M., Schmid, S. L., Milligan, R. A., Hinshaw, J. E. and Dyda, F. (2011). A pseudoatomic model of the dynamin polymer identifies a hydrolysis-dependent powerstroke. *Cell* **147**, 209-22.

Charles-Orszag, A., Lemichez, E., Tran Van Nhieu, G. and Dumenil, G. (2016). Microbial pathogenesis meets biomechanics. *Curr Opin Cell Biol* **38**, 31-7.

Chen, I. and Dubnau, D. (2004). DNA uptake during bacterial transformation. *Nat Rev Microbiol* **2**, 241-9.

Chen, I., Provvedi, R. and Dubnau, D. (2006). A macromolecular complex formed by a pilin-like protein in competent Bacillus subtilis. *J Biol Chem* **281**, 21720-7.

Cheng, J. P., Mendoza-Topaz, C., Howard, G., Chadwick, J., Shvets, E., Cowburn, A. S., Dunmore, B. J., Crosby, A., Morrell, N. W. and Nichols, B. J. (2015). Caveolae protect endothelial cells from membrane rupture during increased cardiac output. *J Cell Biol* **211**, 53-61.

Chesneau, L., Dambournet, D., Machicoane, M., Kouranti, I., Fukuda, M., Goud, B. and Echard, A. (2012). An ARF6/Rab35 GTPase cascade for endocytic recycling and successful cytokinesis. *Curr Biol* **22**, 147-53.

Chimileski, S., Franklin, M. J. and Papke, R. T. (2014). Biofilms formed by the archaeon Haloferax volcanii exhibit cellular differentiation and social motility, and facilitate horizontal gene transfer. *BMC Biol* **12**, 65.

Cisneros, D. A., Bond, P. J., Pugsley, A. P., Campos, M. and Francetic, O. (2012). Minor pseudopilin self-assembly primes type II secretion pseudopilus elongation. *Embo J* **31**, 1041-53.

Claus, H., Maiden, M. C., Wilson, D. J., McCarthy, N. D., Jolley, K. A., Urwin, R., Hessler, F., Frosch, M. and Vogel, U. (2005). Genetic analysis of meningococci carried by children and young adults. *J Infect Dis* **191**, 1263-71.

Collins, A., Warrington, A., Taylor, K. A. and Svitkina, T. (2011). Structural organization of the actin cytoskeleton at sites of clathrin-mediated endocytosis. *Curr Biol* **21**, 1167-75.

Collins, R. F., Davidsen, L., Derrick, J. P., Ford, R. C. and Tonjum, T. (2001). Analysis of the PilQ secretin from Neisseria meningitidis by transmission electron microscopy reveals a dodecameric quaternary structure. *J Bacteriol* **183**, 3825-32.

Collins, R. F., Frye, S. A., Kitmitto, A., Ford, R. C., Tonjum, T. and Derrick, J. P. (2004). Structure of the Neisseria meningitidis outer membrane PilQ secretin complex at 12 A resolution. *J Biol Chem* **279**, 39750-6.

Collinson, S. K., Emody, L., Muller, K. H., Trust, T. J. and Kay, W. W. (1991). Purification and characterization of thin, aggregative fimbriae from Salmonella enteritidis. *J Bacteriol* **173**, 4773-81.

Comanducci, M., Bambini, S., Caugant, D. A., Mora, M., Brunelli, B., Capecchi, B., Ciucchi, L., Rappuoli, R. and Pizza, M. (2004). NadA diversity and carriage in Neisseria meningitidis. *Infect Immun* **72**, 4217-23.

Cooke, I. R. and Deserno, M. (2006). Coupling between lipid shape and membrane curvature. *Biophys J* **91**, 487-95.

Coureuil, M., Lecuyer, H., Bourdoulous, S. and Nassif, X. (2017). A journey into the brain: insight into how bacterial pathogens cross blood-brain barriers. *Nat Rev Microbiol* **15**, 149-159.

Coureuil, M., Lecuyer, H., Scott, M. G., Boularan, C., Enslen, H., Soyer, M., Mikaty, G., Bourdoulous, S., Nassif, X. and Marullo, S. (2010). Meningococcus Hijacks a beta2-adrenoceptor/beta-Arrestin pathway to cross brain microvasculature endothelium. *Cell* **143**, 1149-60.

Coureuil, M., Mikaty, G., Miller, F., Lecuyer, H., Bernard, C., Bourdoulous, S., Dumenil, G., Mege, R. M., Weksler, B. B., Romero, I. A. et al. (2009). Meningococcal type IV pili recruit the polarity complex to cross the brain endothelium. *Science* **325**, 83-7.

Craig, L., Pique, M. E. and Tainer, J. A. (2004). Type IV pilus structure and bacterial pathogenicity. *Nat Rev Microbiol* **2**, 363-78.

Curtis, A. and Wilkinson, C. (1999). New depths in cell behaviour: reactions of cells to nanotopography. *Biochem Soc Symp* **65**, 15-26.

Dalby, M. J., Gadegaard, N., Riehle, M. O., Wilkinson, C. D. and Curtis, A. S. (2004). Investigating filopodia sensing using arrays of defined nano-pits down to 35 nm diameter in size. *Int J Biochem Cell Biol* **36**, 2005-15.

Dalby, M. J., Riehle, M. O., Johnstone, H., Affrossman, S. and Curtis, A. S. (2002). In vitro reaction of endothelial cells to polymer demixed nanotopography. *Biomaterials* **23**, 2945-54.

Davidsen, T. and Tonjum, T. (2006). Meningococcal genome dynamics. *Nat Rev Microbiol* **4**, 11-22.

de Greeff, S. C., de Melker, H. E., Schouls, L. M., Spanjaard, L. and van Deuren, M. (2008). Pre-admission clinical course of meningococcal disease and opportunities for the earlier start of appropriate intervention: a prospective epidemiological study on 752 patients in the Netherlands, 2003-2005. *Eur J Clin Microbiol Infect Dis* **27**, 985-92.

de Jonge, M. I., Hamstra, H. J., van Alphen, L., Dankert, J. and van der Ley, P. (2003). Mapping the binding domains on meningococcal Opa proteins for CEACAM1 and CEA receptors. *Mol Microbiol* **50**, 1005-15.

de Vries, F. P., Cole, R., Dankert, J., Frosch, M. and van Putten, J. P. (1998). Neisseria meningitidis producing the Opc adhesin binds epithelial cell proteoglycan receptors. *Mol Microbiol* **27**, 1203-12.

de Vries, F. P., van Der Ende, A., van Putten, J. P. and Dankert, J. (1996). Invasion of primary nasopharyngeal epithelial cells by Neisseria meningitidis is controlled by phase variation of multiple surface antigens. *Infect Immun* **64**, 2998-3006.

Deghmane, A. E., Giorgini, D., Larribe, M., Alonso, J. M. and Taha, M. K. (2002). Down-regulation of pili and capsule of Neisseria meningitidis upon contact with epithelial cells is mediated by CrgA regulatory protein. *Mol Microbiol* **43**, 1555-64.

Dehio, C., Meyer, M., Berger, J., Schwarz, H. and Lanz, C. (1997). Interaction of Bartonella henselae with endothelial cells results in bacterial aggregation on the cell surface and the subsequent engulfment and internalisation of the bacterial aggregate by a unique structure, the invasome. *J Cell Sci* **110 (Pt 18)**, 2141-54.

Deitsch, K. W., Lukehart, S. A. and Stringer, J. R. (2009). Common strategies for antigenic variation by bacterial, fungal and protozoan pathogens. *Nat Rev Microbiol* **7**, 493-503.

DeVoe, I. W. and Gilchrist, J. E. (1975). Pili on meningococci from primary cultures of nasopharyngeal carriers and cerebrospinal fluid of patients with acute disease. *J Exp Med* **141**, 297-305.

Disanza, A., Bisi, S., Winterhoff, M., Milanesi, F., Ushakov, D. S., Kast, D., Marighetti, P., Romet-Lemonne, G., Muller, H. M., Nickel, W. et al. (2013). CDC42 switches IRSp53 from inhibition of actin growth to elongation by clustering of VASP. *Embo J* **32**, 2735-50.

Doherty, G. J. and McMahon, H. T. (2009). Mechanisms of endocytosis. *Annu Rev Biochem* **78**, 857-902.

Dolan-Livengood, J. M., Miller, Y. K., Martin, L. E., Urwin, R. and Stephens, D. S. (2003). Genetic basis for nongroupable Neisseria meningitidis. *J Infect Dis* **187**, 1616-28.

Domanov, Y. A., Aimon, S., Toombes, G. E., Renner, M., Quemeneur, F., Triller, A., Turner, M. S. and Bassereau, P. (2011). Mobility in geometrically confined membranes. *Proc Natl Acad Sci U S A* **108**, 12605-10.

Drogari-Apiranthitou, M., Kuijper, E. J., Dekker, N. and Dankert, J. (2002). Complement activation and formation of the membrane attack complex on serogroup B Neisseria meningitidis in the presence or absence of serum bactericidal activity. *Infect Immun* **70**, 3752-8.

Dumenil, G. (2011). Revisiting the extracellular lifestyle. *Cell Microbiol* **13**, 1114-21.

Dunger, G., Guzzo, C. R., Andrade, M. O., Jones, J. B. and Farah, C. S. (2014). Xanthomonas citri subsp. citri type IV Pilus is required for twitching motility, biofilm development, and adherence. *Mol Plant Microbe Interact* **27**, 1132-47.

Dupin, N., Lecuyer, H., Carlotti, A., Poyart, C., Coureuil, M., Chanal, J., Schmitt, A., Vacher-Lavenu, M. C., Taha, M. K., Nassif, X. et al. (2012). Chronic meningococcemia cutaneous lesions involve meningococcal perivascular invasion through the remodeling of endothelial barriers. *Clin Infect Dis* **54**, 1162-5.

Echenique-Rivera, H., Muzzi, A., Del Tordello, E., Seib, K. L., Francois, P., Rappuoli, R., Pizza, M. and Serruto, D. (2011). Transcriptome analysis of Neisseria meningitidis in human whole blood and mutagenesis studies identify virulence factors involved in blood survival. *PLoS Pathog* **7**, e1002027.

Eicher, S. C. and Dehio, C. (2012). Bartonella entry mechanisms into mammalian host cells. *Cell Microbiol* **14**, 1166-73.

El Abed, S., Ibnsouda, S. K., Latrache, H., Meftah, H., Tahri, N. J. and Hamadi, F. (2012). Environmental Scanning Electron Microscopy characterization of the adhesion of conidia from Penicillium expansum to cedar wood substrata at different pH values. *World Journal of Microbiology & Biotechnology* **28**, 1707-1713.

Elkhatib, N., Bresteau, E., Baschieri, F., Rioja, A. L., van Niel, G., Vassilopoulos, S. and Montagnac, G. (2017). Tubular clathrin/AP-2 lattices pinch collagen fibers to support 3D cell migration. *Science* **356**.

Elkins, C., Thomas, C. E., Seifert, H. S. and Sparling, P. F. (1991). Species-specific uptake of DNA by gonococci is mediated by a 10-base-pair sequence. *J Bacteriol* **173**, 3911-3.

Eugene, E., Hoffmann, I., Pujol, C., Couraud, P. O., Bourdoulous, S. and Nassif, X. (2002). Microvilli-like structures are associated with the internalization of virulent capsulated Neisseria meningitidis into vascular endothelial cells. *J Cell Sci* **115**, 1231-41.

Evans, R. W., Crawley, J. B., Joannou, C. L. and Sharma, N. D. (1999). Iron proteins. In *Iron and infection: molecular, physiological, and clinical aspects*, vol. 1 (ed. J. J. B. a. E. Griffiths), pp. 27-86: John Wiley & Sons, Ltd., West Sussex, United Kingdom.

Ewers, H., Romer, W., Smith, A. E., Bacia, K., Dmitrieff, S., Chai, W., Mancini, R., Kartenbeck, J., Chambon, V., Berland, L. et al. (2010). GM1 structure determines SV40-induced membrane invagination and infection. *Nat Cell Biol* **12**, 11-8; sup pp 1-12.

Fackler, O. T. and Grosse, R. (2008). Cell motility through plasma membrane blebbing. *J Cell Biol* **181**, 879-84.

Faulstich, M., Bottcher, J. P., Meyer, T. F., Fraunholz, M. and Rudel, T. (2013). Pilus phase variation switches gonococcal adherence to invasion by caveolin-1-dependent host cell signaling. *PLoS Pathog* **9**, e1003373.

Figueroa, J., Andreoni, J. and Densen, P. (1993). Complement deficiency states and meningococcal disease. *Immunol Res* **12**, 295-311.

Figueroa, J. E. and Densen, P. (1991). Infectious diseases associated with complement deficiencies. *Clin Microbiol Rev* **4**, 359-95.

Findlow, H., Vogel, U., Mueller, J. E., Curry, A., Njanpop-Lafourcade, B. M., Claus, H., Gray, S. J., Yaro, S., Traore, Y., Sangare, L. et al. (2007). Three cases of invasive meningococcal disease caused by a capsule null locus strain circulating among healthy carriers in Burkina Faso. *J Infect Dis* **195**, 1071-7.

Finne, J., Bitter-Suermann, D., Goridis, C. and Finne, U. (1987). An IgG monoclonal antibody to group B meningococci cross-reacts with developmentally regulated polysialic acid units of glycoproteins in neural and extraneural tissues. *J Immunol* **138**, 4402-7.

Flores-Diaz, M., Monturiol-Gross, L., Naylor, C., Alape-Giron, A. and Flieger, A. (2016). Bacterial Sphingomyelinases and Phospholipases as Virulence Factors. *Microbiol Mol Biol Rev* **80**, 597-628.

Ford, M. G., Mills, I. G., Peter, B. J., Vallis, Y., Praefcke, G. J., Evans, P. R. and McMahon, H. T. (2002). Curvature of clathrin-coated pits driven by epsin. *Nature* **419**, 361-6.

Forest, K. T., Dunham, S. A., Koomey, M. and Tainer, J. A. (1999). Crystallographic structure reveals phosphorylated pilin from Neisseria: phosphoserine sites modify type IV pilus surface chemistry and fibre morphology. *Mol Microbiol* **31**, 743-52.

Fransen, F., Heckenberg, S. G., Hamstra, H. J., Feller, M., Boog, C. J., van Putten, J. P., van de Beek, D., van der Ende, A. and van der Ley, P. (2009). Naturally occurring lipid A mutants in neisseria meningitidis from patients with invasive meningococcal disease are associated with reduced coagulopathy. *PLoS Pathog* **5**, e1000396.

Fribourg, P. F., Chami, M., Sorzano, C. O., Gubellini, F., Marabini, R., Marco, S., Jault, J. M. and Levy, D. (2014). 3D cryo-electron reconstruction of BmrA, a bacterial multidrug ABC transporter in an inward-facing conformation and in a lipidic environment. *J Mol Biol* **426**, 2059-69.

Fu, Y. and Galan, J. E. (1999). A salmonella protein antagonizes Rac-1 and Cdc42 to mediate host-cell recovery after bacterial invasion. *Nature* **401**, 293-7.

Furukawa, K., Sumitomo, K., Nakashima, H., Kashimura, Y. and Torimitsu, K. (2007). Supported lipid bilayer self-spreading on a nanostructured silicon surface. *Langmuir* **23**, 367-371.

Gaidarov, I., Santini, F., Warren, R. A. and Keen, J. H. (1999). Spatial control of coated-pit dynamics in living cells. *Nat Cell Biol* **1**, 1-7.

Ganesh, K., Allam, M., Wolter, N., Bratcher, H. B., Harrison, O. B., Lucidarme, J., Borrow, R., de Gouveia, L., Meiring, S., Birkhead, M. et al. (2017). Molecular characterization of invasive capsule null Neisseria meningitidis in South Africa. *BMC Microbiol* **17**, 40.

Garcia, E., Jones, G. E., Machesky, L. M. and Anton, I. M. (2012). WIP: WASP-interacting proteins at invadopodia and podosomes. *Eur J Cell Biol* **91**, 869-77.

Garmendia, J., Phillips, A. D., Carlier, M. F., Chong, Y., Schuller, S., Marches, O., Dahan, S., Oswald, E., Shaw, R. K., Knutton, S. et al. (2004). TccP is an enterohaemorrhagic Escherichia coli O157:H7 type III effector protein that couples Tir to the actin-cytoskeleton. *Cell Microbiol* **6**, 1167-83.

Gault, J., Ferber, M., Machata, S., Imhaus, A. F., Malosse, C., Charles-Orszag, A., Millien, C., Bouvier, G., Bardiaux, B., Pehau-Arnaudet, G. et al. (2015). Neisseria meningitidis Type IV Pili Composed of Sequence Invariable Pilins Are Masked by Multisite Glycosylation. *PLoS Pathog* **11**, e1005162.

Gault, J., Malosse, C., Dumenil, G. and Chamot-Rooke, J. (2013). A combined mass spectrometry strategy for complete posttranslational modification mapping of Neisseria meningitidis major pilin. *J Mass Spectrom* **48**, 1199-206.

Gedde-Dahl, T. W., Hoiby, E. A., Schillinger, A., Lystad, A. and Bovre, K. (1983). An epidemiological, clinical and microbiological follow-up study of incident meningococcal disease cases in Norway, winter 1981-1982. Material and epidemiology in the MenOPP project. *NIPH Ann* **6**, 155-68.

Georgiadou, M., Castagnini, M., Karimova, G., Ladant, D. and Pelicic, V. (2012). Large-scale study of the interactions between proteins involved in type IV pilus biology in Neisseria meningitidis: characterization of a subcomplex involved in pilus assembly. *Mol Microbiol* **84**, 857-73.

Gil, H., Benach, J. L. and Thanassi, D. G. (2004). Presence of pili on the surface of Francisella tularensis. *Infect Immun* **72**, 3042-7.

Giltner, C. L., Nguyen, Y. and Burrows, L. L. (2012). Type IV pilin proteins: versatile molecular modules. *Microbiol Mol Biol Rev* **76**, 740-72.

Giron, J. A., Gomez-Duarte, O. G., Jarvis, K. G. and Kaper, J. B. (1997). Longus pilus of enterotoxigenic Escherichia coli and its relatedness to other type-4 pili--a minireview. *Gene* **192**, 39-43.

Goetz, J. G., Joshi, B., Lajoie, P., Strugnell, S. S., Scudamore, T., Kojic, L. D. and Nabi, I. R. (2008). Concerted regulation of focal adhesion dynamics by galectin-3 and tyrosine-phosphorylated caveolin-1. *J Cell Biol* **180**, 1261-75.

Goldschneider, I., Gotschlich, E. C. and Artenstein, M. S. (1969a). Human immunity to the meningococcus. I. The role of humoral antibodies. *J Exp Med* **129**, 1307-26.

Goldschneider, I., Gotschlich, E. C. and Artenstein, M. S. (1969b). Human immunity to the meningococcus. II. Development of natural immunity. *J Exp Med* **129**, 1327-48.

Goosens, V. J., Busch, A., Georgiadou, M., Castagnini, M., Forest, K. T., Waksman, G. and Pelicic, V. (2017). Reconstitution of a minimal machinery capable of assembling periplasmic type IV pili. *Proc Natl Acad Sci U S A* **114**, E4978-E4986.

Graves, J. F., Biswas, G. D. and Sparling, P. F. (1982). Sequence-specific DNA uptake in transformation of Neisseria gonorrhoeae. *J Bacteriol* **152**, 1071-7.

Griffiths, E. (1999). Iron in biological systems. In *Iron and infection: molecular, physiological and clinical aspects, 2nd ed.*, vol. 1 (ed. J. J. B. a. E. Griffiths), pp. 1-26: John Wiley & Sons, Ltd., West Sussex, United Kingdom.

Griffiths, E. and Williams, P. (1999). The iron-uptake systems of pathogenic bacteria, fungi and protozoa. In *Iron and infection: molecular, physiological and clinical aspects*, vol. 1 (ed. J. J. B. a. E. Griffiths), pp. 87-212: John Wiley & Sons, Ltd., West Sussex, United Kingdom.

Griffiths, N. J., Bradley, C. J., Heyderman, R. S. and Virji, M. (2007). IFN-gamma amplifies NFkappaB-dependent Neisseria meningitidis invasion of epithelial cells via specific upregulation of CEA-related cell adhesion molecule 1. *Cell Microbiol* **9**, 2968-83.

Griffiths, N. J., Hill, D. J., Borodina, E., Sessions, R. B., Devos, N. I., Feron, C. M., Poolman, J. T. and Virji, M. (2011). Meningococcal surface fibril (Msf) binds to activated vitronectin and inhibits the terminal complement pathway to increase serum resistance. *Mol Microbiol* **82**, 1129-49.

Groffen, A. J., Martens, S., Diez Arazola, R., Cornelisse, L. N., Lozovaya, N., de Jong, A. P., Goriounova, N. A., Habets, R. L., Takai, Y., Borst, J. G. et al. (2010). Doc2b is a high-affinity Ca2+ sensor for spontaneous neurotransmitter release. *Science* **327**, 1614-8.

Gu, H., Botelho, R. J., Yu, M., Grinstein, S. and Neel, B. G. (2003). Critical role for scaffolding adapter Gab2 in Fc gamma R-mediated phagocytosis. *J Cell Biol* **161**, 1151-61.

Guarner, J., Greer, P. W., Whitney, A., Shieh, W. J., Fischer, M., White, E. H., Carlone, G. M., Stephens, D. S., Popovic, T. and Zaki, S. R. (2004). Pathogenesis and diagnosis of human meningococcal disease using immunohistochemical and PCR assays. *Am J Clin Pathol* **122**, 754-64.

Guizetti, J., Schermelleh, L., Mantler, J., Maar, S., Poser, I., Leonhardt, H., Muller-Reichert, T. and Gerlich, D. W. (2011). Cortical constriction during abscission involves helices of ESCRT-III-dependent filaments. *Science* **331**, 1616-20.

Hacker, J. and Kaper, J. B. (2000). Pathogenicity islands and the evolution of microbes. *Annu Rev Microbiol* **54**, 641-79.

Hadi, H. A., Wooldridge, K. G., Robinson, K. and Ala'Aldeen, D. A. (2001). Identification and characterization of App: an immunogenic autotransporter protein of Neisseria meningitidis. *Mol Microbiol* **41**, 611-23.

Hallett, M. B. and Dewitt, S. (2007). Ironing out the wrinkles of neutrophil phagocytosis. *Trends Cell Biol* **17**, 209-14.

Halstensen, A., Pedersen, S. H., Haneberg, B., Bjorvatn, B. and Solberg, C. O. (1987). Case fatality of meningococcal disease in western Norway. *Scand J Infect Dis* **19**, 35-42.

Hammarstrom, S. (1999). The carcinoembryonic antigen (CEA) family: structures, suggested functions and expression in normal and malignant tissues. *Semin Cancer Biol* **9**, 67-81.

Hammerschmidt, S., Muller, A., Sillmann, H., Muhlenhoff, M., Borrow, R., Fox, A., van Putten, J., Zollinger, W. D., Gerardy-Schahn, R. and Frosch, M. (1996). Capsule phase variation in Neisseria meningitidis serogroup B by slipped-strand mispairing in the polysialyltransferase gene (siaD): correlation with bacterial invasion and the outbreak of meningococcal disease. *Mol Microbiol* **20**, 1211-20.

Hansen, C. G., Bright, N. A., Howard, G. and Nichols, B. J. (2009). SDPR induces membrane curvature and functions in the formation of caveolae. *Nat Cell Biol* **11**, 807-14.

Hansen, C. G., Howard, G. and Nichols, B. J. (2011). Pacsin 2 is recruited to caveolae and functions in caveolar biogenesis. *J Cell Sci* **124**, 2777-85.

Hansen, C. G., Shvets, E., Howard, G., Riento, K. and Nichols, B. J. (2013). Deletion of cavin genes reveals tissue-specific mechanisms for morphogenesis of endothelial caveolae. *Nat Commun* **4**, 1831.

Hansen, S. D. and Mullins, R. D. (2015). Lamellipodin promotes actin assembly by clustering Ena/VASP proteins and tethering them to actin filaments. *Elife* **4**.

Hardt, W. D., Chen, L. M., Schuebel, K. E., Bustelo, X. R. and Galan, J. E. (1998). S. typhimurium encodes an activator of Rho GTPases that induces membrane ruffling and nuclear responses in host cells. *Cell* **93**, 815-26.

Harrison, O. B., Claus, H., Jiang, Y., Bennett, J. S., Bratcher, H. B., Jolley, K. A., Corton, C., Care, R., Poolman, J. T., Zollinger, W. D. et al. (2013). Description and nomenclature of Neisseria meningitidis capsule locus. *Emerg Infect Dis* **19**, 566-73.

Harrison, O. B., Schoen, C., Retchless, A. C., Wang, X., Jolley, K. A., Bray, J. E. and Maiden, M. C. J. (2017). Neisseria genomics: current status and future perspectives. *Pathog Dis*.

Hartsock, A. and Nelson, W. J. (2008). Adherens and tight junctions: structure, function and connections to the actin cytoskeleton. *Biochim Biophys Acta* **1778**, 660-9.

Hartung, S., Arvai, A. S., Wood, T., Kolappan, S., Shin, D. S., Craig, L. and Tainer, J. A. (2011). Ultrahigh resolution and full-length pilin structures with insights for filament assembly, pathogenic functions, and vaccine potential. *J Biol Chem* **286**, 44254-65.

Havarstein, L. S., Coomaraswamy, G. and Morrison, D. A. (1995). An unmodified heptadecapeptide pheromone induces competence for genetic transformation in Streptococcus pneumoniae. *Proc Natl Acad Sci U S A* **92**, 11140-4.

Hayer, A., Stoeber, M., Bissig, C. and Helenius, A. (2010). Biogenesis of caveolae: stepwise assembly of large caveolin and cavin complexes. *Traffic* **11**, 361-82.

Hayward, R. D. and Koronakis, V. (1999). Direct nucleation and bundling of actin by the SipC protein of invasive Salmonella. *Embo J* **18**, 4926-34.

Hegge, F. T., Hitchen, P. G., Aas, F. E., Kristiansen, H., Lovold, C., Egge-Jacobsen, W., Panico, M., Leong, W. Y., Bull, V., Virji, M. et al. (2004). Unique modifications with phosphocholine and phosphoethanolamine define alternate antigenic forms of Neisseria gonorrhoeae type IV pili. *Proc Natl Acad Sci U S A* **101**, 10798-803.

Heiniger, R. W., Winther-Larsen, H. C., Pickles, R. J., Koomey, M. and Wolfgang, M. C. (2010). Infection of human mucosal tissue by Pseudomonas aeruginosa requires sequential and mutually dependent virulence factors and a novel pilus-associated adhesin. *Cell Microbiol* **12**, 1158-73.

Helaine, S., Carbonnelle, E., Prouvensier, L., Beretti, J. L., Nassif, X. and Pelicic, V. (2005). PilX, a pilus-associated protein essential for bacterial aggregation, is a key to pilus-facilitated attachment of Neisseria meningitidis to human cells. *Mol Microbiol* **55**, 65-77.

Helaine, S., Dyer, D. H., Nassif, X., Pelicic, V. and Forest, K. T. (2007). 3D structure/function analysis of PilX reveals how minor pilins can modulate the virulence properties of type IV pili. *Proc Natl Acad Sci U S A* **104**, 15888-93.

Helfrich, P. and Jakobsson, E. (1990). Calculation of deformation energies and conformations in lipid membranes containing gramicidin channels. *Biophys J* **57**, 1075-84.

Helfrich, W. (1973). Elastic properties of lipid bilayers: theory and possible experiments. *Z Naturforsch C* **28**, 693-703.

Hellerud, B. C., Stenvik, J., Espevik, T., Lambris, J. D., Mollnes, T. E. and Brandtzaeg, P. (2008). Stages of meningococcal sepsis simulated in vitro, with emphasis on complement and Toll-like receptor activation. *Infect Immun* **76**, 4183-9.

Helm, R. A. and Seifert, H. S. (2010). Frequency and rate of pilin antigenic variation of Neisseria meningitidis. *J Bacteriol* **192**, 3822-3.

Henne, W. M., Boucrot, E., Meinecke, M., Evergren, E., Vallis, Y., Mittal, R. and McMahon, H. T. (2010). FCHo proteins are nucleators of clathrin-mediated endocytosis. *Science* **328**, 1281-4.

Henne, W. M., Kent, H. M., Ford, M. G., Hegde, B. G., Daumke, O., Butler, P. J., Mittal, R., Langen, R., Evans, P. R. and McMahon, H. T. (2007). Structure and analysis of FCHo2 F-BAR domain: a dimerizing and membrane recruitment module that effects membrane curvature. *Structure* **15**, 839-52.

Henrichsen, J., Froholm, L. O. and Bovre, K. (1972). Studies on bacterial surface translocation. 2. Correlation of twitching motility and fimbriation in colony variants of Moraxella nonliquefaciens, M. bovis, and M. kingii. *Acta Pathol Microbiol Scand B Microbiol Immunol* **80**, 445-52.

Hertzog, M., Monteiro, P., Le Dez, G. and Chavrier, P. (2012). Exo70 subunit of the exocyst complex is involved in adhesion-dependent trafficking of caveolin-1. *PLoS One* **7**, e52627.

Higashi, D. L., Biais, N., Weyand, N. J., Agellon, A., Sisko, J. L., Brown, L. M. and So, M. (2011). N. elongata produces type IV pili that mediate interspecies gene transfer with N. gonorrhoeae. *PLoS One* **6**, e21373.

Higashi, D. L., Zhang, G. H., Biais, N., Myers, L. R., Weyand, N. J., Elliott, D. A. and So, M. (2009). Influence of type IV pilus retraction on the architecture of the Neisseria gonorrhoeae-infected cell cortex. *Microbiology* **155**, 4084-92.

Hill, M. M., Bastiani, M., Luetterforst, R., Kirkham, M., Kirkham, A., Nixon, S. J., Walser, P., Abankwa, D., Oorschot, V. M., Martin, S. et al. (2008). PTRF-Cavin, a conserved cytoplasmic protein required for caveola formation and function. *Cell* **132**, 113-24.

Hill, W. R. and Kinney, T. D. (1947). The cutaneous lesions in acute meningococcemia; a clinical and pathologic study. *J Am Med Assoc* **134**, 513-8.

Hoang, L. M., Thomas, E., Tyler, S., Pollard, A. J., Stephens, G., Gustafson, L., McNabb, A., Pocock, I., Tsang, R. and Tan, R. (2005). Rapid and fatal meningococcal disease due to a strain of Neisseria meningitidis containing the capsule null locus. *Clin Infect Dis* **40**, e38-42.

Hobbs, M. M., Malorny, B., Prasad, P., Morelli, G., Kusecek, B., Heckels, J. E., Cannon, J. G. and Achtman, M. (1998). Recombinational reassortment among opa genes from ET-37 complex Neisseria meningitidis isolates of diverse geographical origins. *Microbiology* **144 (Pt 1)**, 157-66.

Hoess, A., Thormann, A., Friedmann, A. and Heilmann, A. (2012). Self-supporting nanoporous alumina membranes as substrates for hepatic cell cultures. *Journal of Biomedical Materials Research Part A* **100**, 2230-8.

Hoffmann, C., Berking, A., Agerer, F., Buntru, A., Neske, F., Chhatwal, G. S., Ohlsen, K. and Hauck, C. R. (2010). Caveolin limits membrane microdomain mobility and integrin-mediated uptake of fibronectin-binding pathogens. *J Cell Sci* **123**, 4280-91.

Hoffmann, I., Eugene, E., Nassif, X., Couraud, P. O. and Bourdoulous, S. (2001). Activation of ErbB2 receptor tyrosine kinase supports invasion of endothelial cells by Neisseria meningitidis. *J Cell Biol* **155**, 133-43.

Howie, H. L., Glogauer, M. and So, M. (2005). The N. gonorrhoeae type IV pilus stimulates mechanosensitive pathways and cytoprotection through a pilT-dependent mechanism. *PLoS Biol* **3**, e100.

Hubert, K., Pawlik, M. C., Claus, H., Jarva, H., Meri, S. and Vogel, U. (2012). Opc expression, LPS immunotype switch and pilin conversion contribute to serum resistance of unencapsulated meningococci. *PLoS One* **7**, e45132.

Hui, E., Johnson, C. P., Yao, J., Dunning, F. M. and Chapman, E. R. (2009). Synaptotagmin-mediated bending of the target membrane is a critical step in Ca(2+)-regulated fusion. *Cell* **138**, 709-21.

Hurbain, I. and Sachse, M. (2011). The future is cold: cryo-preparation methods for transmission electron microscopy of cells. *Biol Cell* **103**, 405-20.

Hyland, R. M., Sun, J., Griener, T. P., Mulvey, G. L., Klassen, J. S., Donnenberg, M. S. and Armstrong, G. D. (2008). The bundlin pilin protein of enteropathogenic Escherichia coli is an N-acetyllactosamine-specific lectin. *Cell Microbiol* **10**, 177-87.

Imhaus, A. F. and Dumenil, G. (2014). The number of Neisseria meningitidis type IV pili determines host cell interaction. *Embo J*.

Insall, R. H. and Machesky, L. M. (2009). Actin dynamics at the leading edge: from simple machinery to complex networks. *Dev Cell* **17**, 310-22.

Isas, J. M., Ambroso, M. R., Hegde, P. B., Langen, J. and Langen, R. (2015). Tubulation by amphiphysin requires concentration-dependent switching from wedging to scaffolding. *Structure* **23**, 873-81.

Isberg, R. R. and Leong, J. M. (1990). Multiple beta 1 chain integrins are receptors for invasin, a protein that promotes bacterial penetration into mammalian cells. *Cell* **60**, 861-71.

Isberg, R. R., Voorhis, D. L. and Falkow, S. (1987). Identification of invasin: a protein that allows enteric bacteria to penetrate cultured mammalian cells. *Cell* **50**, 769-78.

Istivan, T. S. and Coloe, P. J. (2006). Phospholipase A in Gram-negative bacteria and its role in pathogenesis. *Microbiology* **152**, 1263-74.

Jacobs, J. H., Viboud, C., Tchetgen, E. T., Schwartz, J., Steiner, C., Simonsen, L. and Lipsitch, M. (2014). The association of meningococcal disease with influenza in the United States, 1989-2009. *PLoS One* **9**, e107486.

Jacquemet, G., Hamidi, H. and Ivaska, J. (2015). Filopodia in cell adhesion, 3D migration and cancer cell invasion. *Curr Opin Cell Biol* **36**, 23-31.

Jafri, R. Z., Ali, A., Messonnier, N. E., Tevi-Benissan, C., Durrheim, D., Eskola, J., Fermon, F., Klugman, K. P., Ramsay, M., Sow, S. et al. (2013). Global epidemiology of invasive meningococcal disease. *Popul Health Metr* **11**, 17.

Jain, S., Moscicka, K. B., Bos, M. P., Pachulec, E., Stuart, M. C., Keegstra, W., Boekema, E. J. and van der Does, C. (2011). Structural characterization of outer membrane components of the type IV pili system in pathogenic Neisseria. *PLoS One* **6**, e16624.

Janeway, C. A., Jr. and Medzhitov, R. (2002). Innate immune recognition. *Annu Rev Immunol* **20**, 197-216.

Jarrell, K. F., Ding, Y., Nair, D. B. and Siu, S. (2013). Surface appendages of archaea: structure, function, genetics and assembly. *Life (Basel)* **3**, 86-117.

Jarsch, I. K., Daste, F. and Gallop, J. L. (2016). Membrane curvature in cell biology: An integration of molecular mechanisms. *J Cell Biol* **214**, 375-87.

Jarva, H., Ram, S., Vogel, U., Blom, A. M. and Meri, S. (2005). Binding of the complement inhibitor C4bp to serogroup B Neisseria meningitidis. *J Immunol* **174**, 6299-307.

Jennings, M. P., Srikhanta, Y. N., Moxon, E. R., Kramer, M., Poolman, J. T., Kuipers, B. and van der Ley, P. (1999). The genetic basis of the phase variation repertoire of lipopolysaccharide immunotypes in Neisseria meningitidis. *Microbiology* **145 (Pt 11)**, 3013-21.

Jennissen, H. P. (2012). Hyperhydrophilic rough surfaces and imaginary contact angles. *Materialwissenschaft Und Werkstofftechnik* **43**, 743-750.

Jiang, H. and Grinnell, F. (2005). Cell-matrix entanglement and mechanical anchorage of fibroblasts in three-dimensional collagen matrices. *Mol Biol Cell* **16**, 5070-6.

Jimenez, A. J., Maiuri, P., Lafaurie-Janvore, J., Divoux, S., Piel, M. and Perez, F. (2014). ESCRT machinery is required for plasma membrane repair. *Science* **343**, 1247136.

Joberty, G., Petersen, C., Gao, L. and Macara, I. G. (2000). The cell-polarity protein Par6 links Par3 and atypical protein kinase C to Cdc42. *Nat Cell Biol* **2**, 531-9.

Johansson, L., Rytkonen, A., Bergman, P., Albiger, B., Kallstrom, H., Hokfelt, T., Agerberth, B., Cattaneo, R. and Jonsson, A. B. (2003). CD46 in meningococcal disease. *Science* **301**, 373-5.

Johnson, M. D., Garrett, C. K., Bond, J. E., Coggan, K. A., Wolfgang, M. C. and Redinbo, M. R. (2011). Pseudomonas aeruginosa PilY1 binds integrin in an RGD- and calcium-dependent manner. *PLoS One* **6**, e29629.

Join-Lambert, O., Lecuyer, H., Miller, F., Lelievre, L., Jamet, A., Furio, L., Schmitt, A., Pelissier, P., Fraitag, S., Coureuil, M. et al. (2013). Meningococcal interaction to microvasculature triggers the tissular lesions of purpura fulminans. *J Infect Dis* **208**, 1590-7.

Jones, D. M., Borrow, R., Fox, A. J., Gray, S., Cartwright, K. A. and Poolman, J. T. (1992). The lipooligosaccharide immunotype as a virulence determinant in Neisseria meningitidis. *Microb Pathog* **13**, 219-24.

Jonsson, A. B., Nyberg, G. and Normark, S. (1991). Phase variation of gonococcal pili by frameshift mutation in pilC, a novel gene for pilus assembly. *Embo J* **10**, 477-88.

Joshi, B., Bastiani, M., Strugnell, S. S., Boscher, C., Parton, R. G. and Nabi, I. R. (2012). Phosphocaveolin-1 is a mechanotransducer that induces caveola biogenesis via Egr1 transcriptional regulation. *J Cell Biol* **199**, 425-35.

Jude, B. A. and Taylor, R. K. (2011). The physical basis of type 4 pilus-mediated microcolony formation by Vibrio cholerae O1. *J Struct Biol* **175**, 1-9.

Juncker, A. S., Willenbrock, H., Von Heijne, G., Brunak, S., Nielsen, H. and Krogh, A. (2003). Prediction of lipoprotein signal peptides in Gram-negative bacteria. *Protein Sci* **12**, 1652-62.

Jyssum, K. and Lie, S. (1965). Genetic Factors Determining Competence in Transformation of Neisseria Meningitidis. 1. A Permanent Loss of Competence. *Acta Pathol Microbiol Scand* **63**, 306-16.

Kallstrom, H., Liszewski, M. K., Atkinson, J. P. and Jonsson, A. B. (1997). Membrane cofactor protein (MCP or CD46) is a cellular pilus receptor for pathogenic Neisseria. *Mol Microbiol* **25**, 639-47.

Kanai, F., Liu, H., Field, S. J., Akbary, H., Matsuo, T., Brown, G. E., Cantley, L. C. and Yaffe, M. B. (2001). The PX domains of p47phox and p40phox bind to lipid products of PI(3)K. *Nat Cell Biol* **3**, 675-8.

Karlsson, M., Palsgard, E., Wilshaw, P. R. and Di Silvio, L. (2003). Initial in vitro interaction of osteoblasts with nano-porous alumina. *Biomaterials* **24**, 3039-46.

Karlsson, T., Bolshakova, A., Magalhaes, M. A., Loitto, V. M. and Magnusson, K. E. (2013). Fluxes of water through aquaporin 9 weaken membrane-cytoskeleton anchorage and promote formation of membrane protrusions. *PLoS One* **8**, e59901.

Kenny, B., DeVinney, R., Stein, M., Reinscheid, D. J., Frey, E. A. and Finlay, B. B. (1997). Enteropathogenic E. coli (EPEC) transfers its receptor for intimate adherence into mammalian cells. *Cell* **91**, 511-20.

Kenny, B., Ellis, S., Leard, A. D., Warawa, J., Mellor, H. and Jepson, M. A. (2002). Co-ordinate regulation of distinct host cell signalling pathways by multifunctional enteropathogenic Escherichia coli effector molecules. *Mol Microbiol* **44**, 1095-1107.

Kirchhausen, T. (2012). Bending membranes. *Nat Cell Biol* **14**, 906-8.

Kirchner, M., Heuer, D. and Meyer, T. F. (2005). CD46-independent binding of neisserial type IV pili and the major pilus adhesin, PilC, to human epithelial cells. *Infect Immun* **73**, 3072-82.

Kirn, T. J., Lafferty, M. J., Sandoe, C. M. and Taylor, R. K. (2000). Delineation of pilin domains required for bacterial association into microcolonies and intestinal colonization by Vibrio cholerae. *Mol Microbiol* **35**, 896-910.

Knutton, S., Rosenshine, I., Pallen, M. J., Nisan, I., Neves, B. C., Bain, C., Wolff, C., Dougan, G. and Frankel, G. (1998). A novel EspA-associated surface organelle of enteropathogenic Escherichia coli involved in protein translocation into epithelial cells. *Embo J* **17**, 2166-76.

Koh, W., Mahan, R. D. and Davis, G. E. (2008). Cdc42- and Rac1-mediated endothelial lumen formation requires Pak2, Pak4 and Par3, and PKC-dependent signaling. *J Cell Sci* **121**, 989-1001.

Kohler, R., Schafer, K., Muller, S., Vignon, G., Diederichs, K., Philippsen, A., Ringler, P., Pugsley, A. P., Engel, A. and Welte, W. (2004). Structure and assembly of the pseudopilin PulG. *Mol Microbiol* **54**, 647-64.

Kolappan, S., Coureuil, M., Yu, X., Nassif, X., Egelman, E. H. and Craig, L. (2016). Structure of the Neisseria meningitidis Type IV pilus. *Nat Commun* **7**, 13015.

Koomey, J. M. and Falkow, S. (1987). Cloning of the recA gene of Neisseria gonorrhoeae and construction of gonococcal recA mutants. *J Bacteriol* **169**, 790-5.

Kosmalska, A. J., Casares, L., Elosegui-Artola, A., Thottacherry, J. J., Moreno-Vicente, R., Gonzalez-Tarrago, V., del Pozo, M. A., Mayor, S., Arroyo, M., Navajas, D. et al. (2015). Physical principles of membrane remodelling during cell mechanoadaptation. *Nat Commun* **6**, 7292.

Kovtun, O., Tillu, V. A., Jung, W., Leneva, N., Ariotti, N., Chaudhary, N., Mandyam, R. A., Ferguson, C., Morgan, G. P., Johnston, W. A. et al. (2014). Structural insights into the organization of the cavin membrane coat complex. *Dev Cell* **31**, 405-19.

Krebs, S. J. and Taylor, R. K. (2011). Protection and attachment of Vibrio cholerae mediated by the toxin-coregulated pilus in the infant mouse model. *J Bacteriol* **193**, 5260-70.

Kristich, C. J., Nguyen, V. T., Le, T., Barnes, A. M., Grindle, S. and Dunny, G. M. (2008). Development and use of an efficient system for random mariner transposon mutagenesis to identify novel genetic determinants of biofilm formation in the core Enterococcus faecalis genome. *Appl Environ Microbiol* **74**, 3377-86.

Kroll, J. S., Wilks, K. E., Farrant, J. L. and Langford, P. R. (1998). Natural genetic exchange between Haemophilus and Neisseria: intergeneric transfer of chromosomal genes between major human pathogens. *Proc Natl Acad Sci U S A* **95**, 12381-5.

Kronlage, C., Schafer-Herte, M., Boning, D., Oberleithner, H. and Fels, J. (2015). Feeling for Filaments: Quantification of the Cortical Actin Web in Live Vascular Endothelium. *Biophys J* **109**, 687-98.

Kueltzo, L. A., Osiecki, J., Barker, J., Picking, W. L., Ersoy, B., Picking, W. D. and Middaugh, C. R. (2003). Structure-function analysis of invasion plasmid antigen C (IpaC) from Shigella flexneri. *J Biol Chem* **278**, 2792-8.

Kuhn, S., Erdmann, C., Kage, F., Block, J., Schwenkmezger, L., Steffen, A., Rottner, K. and Geyer, M. (2015). The structure of FMNL2-Cdc42 yields insights into the mechanism of lamellipodia and filopodia formation. *Nat Commun* **6**, 7088.

Kurre, R., Hone, A., Clausen, M., Meel, C. and Maier, B. (2012). PilT2 enhances the speed of gonococcal type IV pilus retraction and of twitching motility. *Mol Microbiol*.

Kuzemenska, P., Burian, V. and Hausenblasova, M. (1978). Circulation of N. meningitidis in a child community. *J Hyg Epidemiol Microbiol Immunol* **22**, 90-107.

Lakshminarayan, R., Wunder, C., Becken, U., Howes, M. T., Benzing, C., Arumugam, S., Sales, S., Ariotti, N., Chambon, V., Lamaze, C. et al. (2014). Galectin-3 drives glycosphingolipid-dependent biogenesis of clathrin-independent carriers. *Nat Cell Biol* **16**, 595-606.

Lam, T. T., Claus, H., Frosch, M. and Vogel, U. (2011). Sequence analysis of serotype-specific synthesis regions II of Haemophilus influenzae serotypes c and d: evidence for common ancestry of capsule synthesis in Pasteurellaceae and Neisseria meningitidis. *Res Microbiol* **162**, 483-7.

Lambotin, M., Hoffmann, I., Laran-Chich, M. P., Nassif, X., Couraud, P. O. and Bourdoulous, S. (2005). Invasion of endothelial cells by Neisseria meningitidis requires cortactin recruitment by a phosphoinositide-3-kinase/Rac1 signalling pathway triggered by the lipo-oligosaccharide. *J Cell Sci* **118**, 3805-16.

Laurenceau, R., Pehau-Arnaudet, G., Baconnais, S., Gault, J., Malosse, C., Dujeancourt, A., Campo, N., Chamot-Rooke, J., Le Cam, E., Claverys, J. P. et al. (2013). A type IV pilus mediates DNA binding during natural transformation in Streptococcus pneumoniae. *PLoS Pathog* **9**, e1003473.

Lecuit, M., Dramsi, S., Gottardi, C., Fedor-Chaiken, M., Gumbiner, B. and Cossart, P. (1999). A single amino acid in E-cadherin responsible for host specificity towards the human pathogen Listeria monocytogenes. *Embo J* **18**, 3956-63.

Lecuit, M., Hurme, R., Pizarro-Cerda, J., Ohayon, H., Geiger, B. and Cossart, P. (2000). A role for alpha-and beta-catenins in bacterial uptake. *Proc Natl Acad Sci U S A* **97**, 10008-13.

Lecuit, M., Nelson, D. M., Smith, S. D., Khun, H., Huerre, M., Vacher-Lavenu, M. C., Gordon, J. I. and Cossart, P. (2004). Targeting and crossing of the human maternofetal barrier by Listeria monocytogenes: role of internalin interaction with trophoblast E-cadherin. *Proc Natl Acad Sci U S A* **101**, 6152-7.

Lecuit, M., Vandormael-Pournin, S., Lefort, J., Huerre, M., Gounon, P., Dupuy, C., Babinet, C. and Cossart, P. (2001). A transgenic model for listeriosis: role of internalin in crossing the intestinal barrier. *Science* **292**, 1722-5.

Lecuyer, H., Nassif, X. and Coureuil, M. (2012). Two strikingly different signaling pathways are induced by meningococcal type IV pili on endothelial and epithelial cells. *Infect Immun* **80**, 175-86.

Lee, S. W., Higashi, D. L., Snyder, A., Merz, A. J., Potter, L. and So, M. (2005). PilT is required for PI(3,4,5)P3-mediated crosstalk between Neisseria gonorrhoeae and epithelial cells. *Cell Microbiol* **7**, 1271-84.

Levin, R., Grinstein, S. and Canton, J. (2016). The life cycle of phagosomes: formation, maturation, and resolution. *Immunol Rev* **273**, 156-79.

Lewis, L. A. and Dyer, D. W. (1995). Identification of an iron-regulated outer membrane protein of Neisseria meningitidis involved in the utilization of hemoglobin complexed to haptoglobin. *J Bacteriol* **177**, 1299-306.

Lewis, L. A., Gipson, M., Hartman, K., Ownbey, T., Vaughn, J. and Dyer, D. W. (1999). Phase variation of HpuAB and HmbR, two distinct haemoglobin receptors of Neisseria meningitidis DNM2. *Mol Microbiol* **32**, 977-89.

Lewis, L. A., Ngampasutadol, J., Wallace, R., Reid, J. E., Vogel, U. and Ram, S. (2010). The meningococcal vaccine candidate neisserial surface protein A (NspA) binds to factor H and enhances meningococcal resistance to complement. *PLoS Pathog* **6**, e1001027.

Lewis, L. A. and Ram, S. (2014). Meningococcal disease and the complement system. *Virulence* **5**, 98-126.

Lewis, L. A., Vu, D. M., Vasudhev, S., Shaughnessy, J., Granoff, D. M. and Ram, S. (2013). Factor H-dependent alternative pathway inhibition mediated by porin B contributes to virulence of Neisseria meningitidis. *MBio* **4**, e00339-13.

Li, H. and Walker, D. H. (1998). rOmpA is a critical protein for the adhesion of Rickettsia rickettsii to host cells. *Microb Pathog* **24**, 289-98.

Li, J., Egelman, E. H. and Craig, L. (2012). Structure of the Vibrio cholerae Type IVb Pilus and stability comparison with the Neisseria gonorrhoeae type IVa pilus. *J Mol Biol* **418**, 47-64.

Li, N., Xiang, G. S., Dokainish, H., Ireton, K. and Elferink, L. A. (2005). The Listeria protein internalin B mimics hepatocyte growth factor-induced receptor trafficking. *Traffic* **6**, 459-73.

Lieberman, J. A., Petro, C. D., Thomas, S., Yang, A. and Donnenberg, M. S. (2015). Type IV pilus secretins have extracellular C termini. *MBio* **6**.

Liu, G. Y., Tang, C. M. and Exley, R. M. (2015). Non-pathogenic Neisseria: members of an abundant, multi-habitat, diverse genus. *Microbiology-Sgm* **161**, 1297-1312.

Loh, E., Kugelberg, E., Tracy, A., Zhang, Q., Gollan, B., Ewles, H., Chalmers, R., Pelicic, V. and Tang, C. M. (2013). Temperature triggers immune evasion by Neisseria meningitidis. *Nature* **502**, 237-40.

Long, M., Huang, S. H., Wu, C. H., Shackleford, G. M. and Jong, A. (2012). Lipid raft/caveolae signaling is required for Cryptococcus neoformans invasion into human brain microvascular endothelial cells. *J Biomed Sci* **19**, 19.

Loscalzo, J. and Schafer, A. (2002). Thrombosis and Hemorrhage: Lippincott Williams and Wilkins, Philadelphia.

Lowry, M. B., Duchemin, A. M., Robinson, J. M. and Anderson, C. L. (1998). Functional separation of pseudopod extension and particle internalization during Fc gamma receptor-mediated phagocytosis. *J Exp Med* **187**, 161-76.

Lu, S., Giuliani, M., Harvey, H., Burrows, L. L., Wickham, R. A. and Dutcher, J. R. (2015). Nanoscale Pulling of Type IV Pili Reveals Their Flexibility and Adhesion to Surfaces over Extended Lengths of the Pili. *Biophys J* **108**, 2865-75.

Lundmark, R., Doherty, G. J., Howes, M. T., Cortese, K., Vallis, Y., Parton, R. G. and McMahon, H. T. (2008). The GTPase-activating protein GRAF1 regulates the CLIC/GEEC endocytic pathway. *Curr Biol* **18**, 1802-8.

MacFadyen, L. P., Chen, D., Vo, H. C., Liao, D., Sinotte, R. and Redfield, R. J. (2001). Competence development by Haemophilus influenzae is regulated by the availability of nucleic acid precursors. *Mol Microbiol* **40**, 700-7.

Machesky, L., Jurdic, P. and Hinz, B. (2008). Grab, stick, pull and digest: the functional diversity of actin-associated matrix-adhesion structures. Workshop on Invadopodia, Podosomes and Focal Adhesions in Tissue Invasion. *EMBO Rep* **9**, 139-43.

Mackinnon, F. G., Borrow, R., Gorringe, A. R., Fox, A. J., Jones, D. M. and Robinson, A. (1993). Demonstration of lipooligosaccharide immunotype and capsule as virulence factors for Neisseria meningitidis using an infant mouse intranasal infection model. *Microb Pathog* **15**, 359-66.

Madico, G., Welsch, J. A., Lewis, L. A., McNaughton, A., Perlman, D. H., Costello, C. E., Ngampasutadol, J., Vogel, U., Granoff, D. M. and Ram, S. (2006). The meningococcal vaccine candidate GNA1870 binds the complement regulatory protein factor H and enhances serum resistance. *J Immunol* **177**, 501-10.

Maiden, M. C., Bygraves, J. A., Feil, E., Morelli, G., Russell, J. E., Urwin, R., Zhang, Q., Zhou, J., Zurth, K., Caugant, D. A. et al. (1998). Multilocus sequence typing: a portable approach to the identification of clones within populations of pathogenic microorganisms. *Proc Natl Acad Sci U S A* **95**, 3140-5.

Maier, B., Potter, L., So, M., Long, C. D., Seifert, H. S. and Sheetz, M. P. (2002). Single pilus motor forces exceed 100 pN. *Proc Natl Acad Sci U S A* **99**, 16012-7.

Mairey, E., Genovesio, A., Donnadieu, E., Bernard, C., Jaubert, F., Pinard, E., Seylaz, J., Olivo-Marin, J. C., Nassif, X. and Dumenil, G. (2006). Cerebral microcirculation shear stress levels determine Neisseria meningitidis attachment sites along the blood-brain barrier. *J Exp Med* **203**, 1939-50.

Maissa, N., Covarelli, V., Janel, S., Durel, B., Simpson, N., Bernard, S. C., Pardo-Lopez, L., Bouzinba-Segard, H., Faure, C., Scott, M. G. H. et al. (2017). Strength of Neisseria meningitidis binding to endothelial cells requires highly-ordered CD147/beta2-adrenoceptor clusters assembled by alpha-actinin-4. *Nat Commun* **8**, 15764.

Marathe, R., Meel, C., Schmidt, N. C., Dewenter, L., Kurre, R., Greune, L., Schmidt, M. A., Muller, M. J., Lipowsky, R., Maier, B. et al. (2014). Bacterial twitching motility is coordinated by a two-dimensional tug-of-war with directional memory. *Nat Commun* **5**, 3759.

Martin, D., Cadieux, N., Hamel, J. and Brodeur, B. R. (1997). Highly conserved Neisseria meningitidis surface protein confers protection against experimental infection. *J Exp Med* **185**, 1173-83.

Martin, P., van de Ven, T., Mouchel, N., Jeffries, A. C., Hood, D. W. and Moxon, E. R. (2003). Experimentally revised repertoire of putative contingency loci in Neisseria meningitidis strain MC58: evidence for a novel mechanism of phase variation. *Mol Microbiol* **50**, 245-57.

Martinez, J. J. and Cossart, P. (2004). Early signaling events involved in the entry of Rickettsia conorii into mammalian cells. *J Cell Sci* **117**, 5097-106.

Martinez, J. J., Seveau, S., Veiga, E., Matsuyama, S. and Cossart, P. (2005). Ku70, a component of DNA-dependent protein kinase, is a mammalian receptor for Rickettsia conorii. *Cell* **123**, 1013-23.

Matthey, N. and Blokesch, M. (2016). The DNA-Uptake Process of Naturally Competent Vibrio cholerae. *Trends Microbiol* **24**, 98-110.

Mattila, P. K. and Lappalainen, P. (2008). Filopodia: molecular architecture and cellular functions. *Nat Rev Mol Cell Biol* **9**, 446-54.

Mattila, P. K., Pykalainen, A., Saarikangas, J., Paavilainen, V. O., Vihinen, H., Jokitalo, E. and Lappalainen, P. (2007). Missing-in-metastasis and IRSp53 deform PI(4,5)P2-rich membranes by an inverse BAR domain-like mechanism. *J Cell Biol* **176**, 953-64.

McCallum, M., Tammam, S., Khan, A., Burrows, L. L. and Howell, P. L. (2017). The molecular mechanism of the type IVa pilus motors. *Nat Commun* **8**, 15091.

McGhie, E. J., Hayward, R. D. and Koronakis, V. (2004). Control of actin turnover by a salmonella invasion protein. *Mol Cell* **13**, 497-510.

McMahon, H. T. and Boucrot, E. (2011). Molecular mechanism and physiological functions of clathrin-mediated endocytosis. *Nat Rev Mol Cell Biol* **12**, 517-33.

McMahon, H. T. and Boucrot, E. (2015). Membrane curvature at a glance. *J Cell Sci* **128**, 1065-70.

McNeil, L. K., Zagursky, R. J., Lin, S. L., Murphy, E., Zlotnick, G. W., Hoiseth, S. K., Jansen, K. U. and Anderson, A. S. (2013). Role of factor H binding protein in Neisseria meningitidis virulence and its potential as a vaccine candidate to broadly protect against meningococcal disease. *Microbiol Mol Biol Rev* **77**, 234-52.

Melican, K., Michea Veloso, P., Martin, T., Bruneval, P. and Dumenil, G. (2013). Adhesion of Neisseria meningitidis to dermal vessels leads to local vascular damage and purpura in a humanized mouse model. *PLoS Pathog* **9**, e1003139.

Merz, A. J., Enns, C. A. and So, M. (1999). Type IV pili of pathogenic Neisseriae elicit cortical plaque formation in epithelial cells. *Mol Microbiol* **32**, 1316-32.

Merz, A. J. and So, M. (1997). Attachment of piliated, Opa- and Opc- gonococci and meningococci to epithelial cells elicits cortical actin rearrangements and clustering of tyrosine-phosphorylated proteins. *Infect Immun* **65**, 4341-9.

Merz, A. J., So, M. and Sheetz, M. P. (2000). Pilus retraction powers bacterial twitching motility. *Nature* **407**, 98-102.

Meyer, J., Brissac, T., Frapy, E., Omer, H., Euphrasie, D., Bonavita, A., Nassif, X. and Bille, E. (2016). Characterization of MDAPhi, a temperate filamentous bacteriophage of Neisseria meningitidis. *Microbiology* **162**, 268-82.

Mickelsen, P. A., Blackman, E. and Sparling, P. F. (1982). Ability of Neisseria gonorrhoeae, Neisseria meningitidis, and commensal Neisseria species to obtain iron from lactoferrin. *Infect Immun* **35**, 915-20.

Mickelsen, P. A. and Sparling, P. F. (1981). Ability of Neisseria gonorrhoeae, Neisseria meningitidis, and commensal Neisseria species to obtain iron from transferrin and iron compounds. *Infect Immun* **33**, 555-64.

Mikaty, G., Soyer, M., Mairey, E., Henry, N., Dyer, D., Forest, K. T., Morand, P., Guadagnini, S., Prevost, M. C., Nassif, X. et al. (2009). Extracellular bacterial pathogen induces host cell surface reorganization to resist shear stress. *PLoS Pathog* **5**, e1000314.

Miller, F., Phan, G., Brissac, T., Bouchiat, C., Lioux, G., Nassif, X. and Coureuil, M. (2014). The hypervariable region of meningococcal major pilin PilE controls the host cell response via antigenic variation. *MBio* **5**, e01024-13.

Mim, C. and Unger, V. M. (2012). Membrane curvature and its generation by BAR proteins. *Trends Biochem Sci* **37**, 526-33.

Moore, J., Bailey, S. E., Benmechernene, Z., Tzitzilonis, C., Griffiths, N. J., Virji, M. and Derrick, J. P. (2005). Recognition of saccharides by the OpcA, OpaD, and OpaB outer membrane proteins from Neisseria meningitidis. *J Biol Chem* **280**, 31489-97.

Morand, P. C., Bille, E., Morelle, S., Eugene, E., Beretti, J. L., Wolfgang, M., Meyer, T. F., Koomey, M. and Nassif, X. (2004). Type IV pilus retraction in pathogenic Neisseria is regulated by the PilC proteins. *Embo J* **23**, 2009-17.

Morand, P. C., Tattevin, P., Eugene, E., Beretti, J. L. and Nassif, X. (2001). The adhesive property of the type IV pilus-associated component PilC1 of pathogenic Neisseria is supported by the conformational structure of the N-terminal part of the molecule. *Mol Microbiol* **40**, 846-56.

Moren, B., Shah, C., Howes, M. T., Schieber, N. L., McMahon, H. T., Parton, R. G., Daumke, O. and Lundmark, R. (2012). EHD2 regulates caveolar dynamics via ATP-driven targeting and oligomerization. *Mol Biol Cell* **23**, 1316-29.

Morlot, S., Galli, V., Klein, M., Chiaruttini, N., Manzi, J., Humbert, F., Dinis, L., Lenz, M., Cappello, G. and Roux, A. (2012). Membrane shape at the edge of the dynamin helix sets location and duration of the fission reaction. *Cell* **151**, 619-29.

Morrow, I. C. and Parton, R. G. (2005). Flotillins and the PHB domain protein family: rafts, worms and anaesthetics. *Traffic* **6**, 725-40.

Moxon, E. R., Rainey, P. B., Nowak, M. A. and Lenski, R. E. (1994). Adaptive evolution of highly mutable loci in pathogenic bacteria. *Curr Biol* **4**, 24-33.

Mueller, K. E. and Wolf, K. (2014). C. pneumoniae disrupts eNOS trafficking and impairs NO production in human aortic endothelial cells. *Cell Microbiol*.

Muenzner, P., Dehio, C., Fujiwara, T., Achtman, M., Meyer, T. F. and Gray-Owen, S. D. (2000). Carcinoembryonic antigen family receptor specificity of Neisseria meningitidis Opa variants influences adherence to and invasion of proinflammatory cytokine-activated endothelial cells. *Infect Immun* **68**, 3601-7.

Nabhan, J. F., Hu, R., Oh, R. S., Cohen, S. N. and Lu, Q. (2012). Formation and release of arrestin domain-containing protein 1-mediated microvesicles (ARMMs) at plasma membrane by recruitment of TSG101 protein. *Proc Natl Acad Sci U S A* **109**, 4146-51.

Nakane, D. and Nishizaka, T. (2017). Asymmetric distribution of type IV pili triggered by directional light in unicellular cyanobacteria. *Proc Natl Acad Sci U S A* **114**, 6593-6598.

Namork, E. and Brandtzaeg, P. (2002). Fatal meningococcal septicaemia with "blebbing" meningococcus. *Lancet* **360**, 1741.

Nassif, X., Beretti, J. L., Lowy, J., Stenberg, P., O'Gaora, P., Pfeifer, J., Normark, S. and So, M. (1994). Roles of pilin and PilC in adhesion of Neisseria meningitidis to human epithelial and endothelial cells. *Proc Natl Acad Sci U S A* **91**, 3769-73.

Nassif, X., Lowy, J., Stenberg, P., O'Gaora, P., Ganji, A. and So, M. (1993). Antigenic variation of pilin regulates adhesion of Neisseria meningitidis to human epithelial cells. *Mol Microbiol* **8**, 719-25.

Neisser, A. (1879). Ueber eine der Gonorrhoe eigentümliche Micrococcusform. In *Centralbatt für die medicinischen Wissenschaften*, vol. No. 28 (eds J. Rosenthal and H. Senator).

Nguyen, Y., Sugiman-Marangos, S., Harvey, H., Bell, S. D., Charlton, C. L., Junop, M. S. and Burrows, L. L. (2015). Pseudomonas aeruginosa minor pilins prime type IVa pilus assembly and promote surface display of the PilY1 adhesin. *J Biol Chem* **290**, 601-11.

Niebuhr, K., Giuriato, S., Pedron, T., Philpott, D. J., Gaits, F., Sable, J., Sheetz, M. P., Parsot, C., Sansonetti, P. J. and Payrastre, B. (2002). Conversion of PtdIns(4,5)P(2) into PtdIns(5)P by the S.flexneri effector IpgD reorganizes host cell morphology. *Embo J* **21**, 5069-78.

Nivaskumar, M., Bouvier, G., Campos, M., Nadeau, N., Yu, X., Egelman, E. H., Nilges, M. and Francetic, O. (2014). Distinct docking and stabilization steps of the Pseudopilus conformational transition path suggest rotational assembly of type IV pilus-like fibers. *Structure* **22**, 685-96.

Nivaskumar, M. and Francetic, O. (2014). Type II secretion system: a magic beanstalk or a protein escalator. *Biochim Biophys Acta* **1843**, 1568-77.

Obergfell, K. P. and Seifert, H. S. (2016). The Pilin N-terminal Domain Maintains Neisseria gonorrhoeae Transformation Competence during Pilus Phase Variation. *PLoS Genet* **12**, e1006069.

Olcen, P., Kjellander, J., Danielsson, D. and Lindquist, B. L. (1981). Epidemiology of Neisseria meningitidis; prevalence and symptoms from the upper respiratory tract in family members to patients with meningococcal disease. *Scand J Infect Dis* **13**, 105-9.

Opitz, D. and Maier, B. (2011). Rapid cytoskeletal response of epithelial cells to force generation by type IV pili. *PLoS One* **6**, e17088.

Ottow, J. C. (1975). Ecology, physiology, and genetics of fimbriae and pili. *Annu Rev Microbiol* **29**, 79-108.

Ovstebo, R., Brandtzaeg, P., Brusletto, B., Haug, K. B., Lande, K., Hoiby, E. A. and Kierulf, P. (2004). Use of robotized DNA isolation and real-time PCR to quantify and identify close correlation between levels of Neisseria meningitidis DNA and lipopolysaccharides in plasma and cerebrospinal fluid from patients with systemic meningococcal disease. *J Clin Microbiol* **42**, 2980-7.

Ozdemir, H., Kendirli, T., Ciftci, E. and Ince, E. (2012). Purpura fulminans in a child due to Neisseria meningitidis. *Infection* **40**, 717-8.

Paget, M. S. (2015). Bacterial Sigma Factors and Anti-Sigma Factors: Structure, Function and Distribution. *Biomolecules* **5**, 1245-65.

Paladino, S., Sarnataro, D., Pillich, R., Tivodar, S., Nitsch, L. and Zurzolo, C. (2004). Protein oligomerization modulates raft partitioning and apical sorting of GPI-anchored proteins. *J Cell Biol* **167**, 699-709.

Palander, O., El-Zeiry, M. and Trimble, W. S. (2017). Uncovering the Roles of Septins in Cilia. *Front Cell Dev Biol* **5**, 36.

Parat, M. O., Stachowicz, R. Z. and Fox, P. L. (2002). Oxidative stress inhibits caveolin-1 palmitoylation and trafficking in endothelial cells. *Biochem J* **361**, 681-8.

Parida, S. K., Domann, E., Rohde, M., Muller, S., Darji, A., Hain, T., Wehland, J. and Chakraborty, T. (1998). Internalin B is essential for adhesion and mediates the invasion of Listeria monocytogenes into human endothelial cells. *Mol Microbiol* **28**, 81-93.

Parkhill, J., Achtman, M., James, K. D., Bentley, S. D., Churcher, C., Klee, S. R., Morelli, G., Basham, D., Brown, D., Chillingworth, T. et al. (2000). Complete DNA sequence of a serogroup A strain of Neisseria meningitidis Z2491. *Nature* **404**, 502-6.

Parton, R. G. and del Pozo, M. A. (2013). Caveolae as plasma membrane sensors, protectors and organizers. *Nat Rev Mol Cell Biol* **14**, 98-112.

Parton, R. G., Hanzal-Bayer, M. and Hancock, J. F. (2006). Biogenesis of caveolae: a structural model for caveolin-induced domain formation. *J Cell Sci* **119**, 787-96.

Peak, I. R., Srikhanta, Y., Dieckelmann, M., Moxon, E. R. and Jennings, M. P. (2000). Identification and characterisation of a novel conserved outer membrane protein from Neisseria meningitidis. *FEMS Immunol Med Microbiol* **28**, 329-34.

Perras, A. K., Wanner, G., Klingl, A., Mora, M., Auerbach, A. K., Heinz, V., Probst, A. J., Huber, H., Rachel, R., Meck, S. et al. (2014). Grappling archaea: ultrastructural analyses of an uncultivated, cold-loving archaeon, and its biofilm. *Front Microbiol* **5**, 397.

Peter, B. J., Kent, H. M., Mills, I. G., Vallis, Y., Butler, P. J., Evans, P. R. and McMahon, H. T. (2004). BAR domains as sensors of membrane curvature: the amphiphysin BAR structure. *Science* **303**, 495-9.

Phillips, N., Hayward, R. D. and Koronakis, V. (2004). Phosphorylation of the enteropathogenic E. coli receptor by the Src-family kinase c-Fyn triggers actin pedestal formation. *Nat Cell Biol* **6**, 618-25.

Pizarro-Cerda, J. and Cossart, P. (2006). Bacterial adhesion and entry into host cells. *Cell* **124**, 715-27.

Pizza, M., Scarlato, V., Masignani, V., Giuliani, M. M., Arico, B., Comanducci, M., Jennings, G. T., Baldi, L., Bartolini, E., Capecchi, B. et al. (2000). Identification of vaccine candidates against serogroup B meningococcus by whole-genome sequencing. *Science* **287**, 1816-20.

Plancon, L., Du Merle, L., Le Friec, S., Gounon, P., Jouve, M., Guignot, J., Servin, A. and Le Bouguenec, C. (2003). Recognition of the cellular beta1-chain integrin by the bacterial AfaD invasin is implicated in the internalization of afa-expressing pathogenic Escherichia coli strains. *Cell Microbiol* **5**, 681-93.

Platonov, A. E., Vershinina, I. V., Kuijper, E. J., Borrow, R. and Kayhty, H. (2003). Long term effects of vaccination of patients deficient in a late complement component with a tetravalent meningococcal polysaccharide vaccine. *Vaccine* **21**, 4437-47.

Pohlschroder, M. and Esquivel, R. N. (2015). Archaeal type IV pili and their involvement in biofilm formation. *Front Microbiol* **6**, 190.

Poolman, J. T., Hopman, C. T. and Zanen, H. C. (1983). Immunogenicity of meningococcal antigens as detected in patient sera. *Infect Immun* **40**, 398-406.

Postle, K. and Kadner, R. J. (2003). Touch and go: tying TonB to transport. *Mol Microbiol* **49**, 869-82.

Poweleit, N., Ge, P., Nguyen, H. H., Loo, R. R., Gunsalus, R. P. and Zhou, Z. H. (2016). CryoEM structure of the Methanospirillum hungatei archaellum reveals structural features distinct from the bacterial flagellum and type IV pili. *Nat Microbiol* **2**, 16222.

Prevost, C., Zhao, H., Manzi, J., Lemichez, E., Lappalainen, P., Callan-Jones, A. and Bassereau, P. (2015). IRSp53 senses negative membrane curvature and phase separates along membrane tubules. *Nat Commun* **6**, 8529.

Pries, A. R., Secomb, T. W., Gessner, T., Sperandio, M. B., Gross, J. F. and Gaehtgens, P. (1994). Resistance to blood flow in microvessels in vivo. *Circ Res* **75**, 904-15.

Prince, S. M., Achtman, M. and Derrick, J. P. (2002). Crystal structure of the OpcA integral membrane adhesin from Neisseria meningitidis. *Proc Natl Acad Sci U S A* **99**, 3417-21.

Pujol, C., Eugene, E., de Saint Martin, L. and Nassif, X. (1997). Interaction of Neisseria meningitidis with a polarized monolayer of epithelial cells. *Infect Immun* **65**, 4836-42.

Pujol, C., Eugene, E., Marceau, M. and Nassif, X. (1999). The meningococcal PilT protein is required for induction of intimate attachment to epithelial cells following pilus-mediated adhesion. *Proc Natl Acad Sci U S A* **96**, 4017-22.

Putonti, C., Nowicki, B., Shaffer, M., Fofanov, Y. and Nowicki, S. (2013). Where does Neisseria acquire foreign DNA from: an examination of the source of genomic and pathogenic islands and the evolution of the Neisseria genus. *BMC Evol Biol* **13**, 184.

Quemeneur, F., Sigurdsson, J. K., Renner, M., Atzberger, P. J., Bassereau, P. and Lacoste, D. (2014). Shape matters in protein mobility within membranes. *Proc Natl Acad Sci U S A* **111**, 5083-7.

Quere, D. (2008). Wetting and roughness. *Annual Review of Materials Research* **38**, 71-99.

Radel, C. and Rizzo, V. (2005). Integrin mechanotransduction stimulates caveolin-1 phosphorylation and recruitment of Csk to mediate actin reorganization. *Am J Physiol Heart Circ Physiol* **288**, H936-45.

Rao, Y. and Haucke, V. (2011). Membrane shaping by the Bin/amphiphysin/Rvs (BAR) domain protein superfamily. *Cell Mol Life Sci* **68**, 3983-93.

Reardon, P. N. and Mueller, K. T. (2013). Structure of the type IVa major pilin from the electrically conductive bacterial nanowires of Geobacter sulfurreducens. *J Biol Chem* **288**, 29260-6.

Rhomberg, T. A., Truttmann, M. C., Guye, P., Ellner, Y. and Dehio, C. (2009). A translocated protein of Bartonella henselae interferes with endocytic uptake of individual bacteria and triggers uptake of large bacterial aggregates via the invasome. *Cell Microbiol* **11**, 927-45.

Ridley, A. J. (2006). Rho GTPases and actin dynamics in membrane protrusions and vesicle trafficking. *Trends Cell Biol* **16**, 522-9.

Ridley, A. J. (2011). Life at the leading edge. *Cell* **145**, 1012-22.

Romer, W., Berland, L., Chambon, V., Gaus, K., Windschiegl, B., Tenza, D., Aly, M. R., Fraisier, V., Florent, J. C., Perrais, D. et al. (2007). Shiga toxin induces tubular membrane invaginations for its uptake into cells. *Nature* **450**, 670-5.

Roy, A., Kucukural, A. and Zhang, Y. (2010). I-TASSER: a unified platform for automated protein structure and function prediction. *Nat Protoc* **5**, 725-38.

Rudel, T., Scheurerpflug, I. and Meyer, T. F. (1995). Neisseria PilC protein identified as type-4 pilus tip-located adhesin. *Nature* **373**, 357-9.

Ruprecht, V., Monzo, P., Ravasio, A., Yue, Z., Makhija, E., Strale, P. O., Gauthier, N., Shivashankar, G. V., Studer, V., Albiges-Rizo, C. et al. (2017). How cells respond to environmental cues - insights from bio-functionalized substrates. *Journal of Cell Science* **130**, 51-61.

Sajjan, U. S., Sun, L., Goldstein, R. and Forstner, J. F. (1995). Cable (cbl) type II pili of cystic fibrosis-associated Burkholderia (Pseudomonas) cepacia: nucleotide sequence of the cblA major subunit pilin gene and novel morphology of the assembled appendage fibers. *J Bacteriol* **177**, 1030-8.

Sarkari, J., Pandit, N., Moxon, E. R. and Achtman, M. (1994). Variable expression of the Opc outer membrane protein in Neisseria meningitidis is caused by size variation of a promoter containing poly-cytidine. *Mol Microbiol* **13**, 207-17.

Sauvonnet, N., Vignon, G., Pugsley, A. P. and Gounon, P. (2000). Pilus formation and protein secretion by the same machinery in Escherichia coli. *Embo J* **19**, 2221-8.

Scarselli, M., Serruto, D., Montanari, P., Capecchi, B., Adu-Bobie, J., Veggi, D., Rappuoli, R., Pizza, M. and Arico, B. (2006). Neisseria meningitidis NhhA is a multifunctional trimeric autotransporter adhesin. *Mol Microbiol* **61**, 631-44.

Schlegel, A. and Lisanti, M. P. (2000). A molecular dissection of caveolin-1 membrane attachment and oligomerization. Two separate regions of the caveolin-1 C-terminal domain mediate membrane binding and oligomer/oligomer interactions in vivo. *J Biol Chem* **275**, 21605-17.

Schmitt, C., Turner, D., Boesl, M., Abele, M., Frosch, M. and Kurzai, O. (2007). A functional two-partner secretion system contributes to adhesion of Neisseria meningitidis to epithelial cells. *J Bacteriol* **189**, 7968-76.

Schoen, C., Blom, J., Claus, H., Schramm-Gluck, A., Brandt, P., Muller, T., Goesmann, A., Joseph, B., Konietzny, S., Kurzai, O. et al. (2008). Whole-genome comparison of disease and carriage strains provides insights into virulence evolution in Neisseria meningitidis. *Proc Natl Acad Sci U S A* **105**, 3473-8.

Scholten, R. J., Kuipers, B., Valkenburg, H. A., Dankert, J., Zollinger, W. D. and Poolman, J. T. (1994). Lipo-oligosaccharide immunotyping of Neisseria meningitidis by a whole-cell ELISA with monoclonal antibodies. *J Med Microbiol* **41**, 236-43.

Schryvers, A. B. and Gonzalez, G. C. (1990). Receptors for transferrin in pathogenic bacteria are specific for the host's protein. *Can J Microbiol* **36**, 145-7.

Schryvers, A. B. and Lee, B. C. (1989). Comparative analysis of the transferrin and lactoferrin binding proteins in the family Neisseriaceae. *Can J Microbiol* **35**, 409-15.

Schryvers, A. B. and Morris, L. J. (1988a). Identification and characterization of the human lactoferrin-binding protein from Neisseria meningitidis. *Infect Immun* **56**, 1144-9.

Schryvers, A. B. and Morris, L. J. (1988b). Identification and characterization of the transferrin receptor from Neisseria meningitidis. *Mol Microbiol* **2**, 281-8.

Schryvers, A. B. and Stojiljkovic, I. (1999). Iron acquisition systems in the pathogenic Neisseria. *Mol Microbiol* **32**, 1117-23.

Schubert-Unkmeir, A., Konrad, C., Slanina, H., Czapek, F., Hebling, S. and Frosch, M. (2010). Neisseria meningitidis induces brain microvascular endothelial cell detachment from the matrix and cleavage of occludin: a role for MMP-8. *PLoS Pathog* **6**, e1000874.

Segal, E., Hagblom, P., Seifert, H. S. and So, M. (1986). Antigenic variation of gonococcal pilus involves assembly of separated silent gene segments. *Proc Natl Acad Sci U S A* **83**, 2177-81.

Senff, L. M., Wegener, W. S., Brooks, G. F., Finnerty, W. R. and Makula, R. A. (1976). Phospholipid composition and phospholipase A activity of Neisseria gonorrhoeae. *J Bacteriol* **127**, 874-80.

Senju, Y., Itoh, Y., Takano, K., Hamada, S. and Suetsugu, S. (2011). Essential role of PACSIN2/syndapin-II in caveolae membrane sculpting. *J Cell Sci* **124**, 2032-40.

Serruto, D., Adu-Bobie, J., Scarselli, M., Veggi, D., Pizza, M., Rappuoli, R. and Arico, B. (2003). Neisseria meningitidis App, a new adhesin with autocatalytic serine protease activity. *Mol Microbiol* **48**, 323-34.

Serruto, D., Bottomley, M. J., Ram, S., Giuliani, M. M. and Rappuoli, R. (2012). The new multicomponent vaccine against meningococcal serogroup B, 4CMenB: immunological, functional and structural characterization of the antigens. *Vaccine* **30 Suppl 2**, B87-97.

Seveau, S., Bierne, H., Giroux, S., Prevost, M. C. and Cossart, P. (2004). Role of lipid rafts in E-cadherin- - and HGF-R/Met--mediated entry of Listeria monocytogenes into host cells. *J Cell Biol* **166**, 743-53.

Shahapure, R., Driessen, R. P., Haurat, M. F., Albers, S. V. and Dame, R. T. (2014). The archaellum: a rotating type IV pilus. *Mol Microbiol* **91**, 716-23.

Shen, Y., Naujokas, M., Park, M. and Ireton, K. (2000). InlB-dependent internalization of Listeria is mediated by the Met receptor tyrosine kinase. *Cell* **103**, 501-10.

Shin, J., Jo, H. and Park, H. (2006). Caveolin-1 is transiently dephosphorylated by shear stress-activated protein tyrosine phosphatase mu. *Biochem Biophys Res Commun* **339**, 737-41.

Sidikou, F., Zaneidou, M., Alkassoum, I., Schwartz, S., Issaka, B., Obama, R., Lingani, C., Tate, A., Ake, F., Sakande, S. et al. (2016). Emergence of epidemic Neisseria meningitidis serogroup C in Niger, 2015: an analysis of national surveillance data. *Lancet Infect Dis* **16**, 1288-1294.

Simunovic, M., Voth, G. A., Callan-Jones, A. and Bassereau, P. (2015). When Physics Takes Over: BAR Proteins and Membrane Curvature. *Trends Cell Biol* **25**, 780-92.

Singh, R. N. and Pitale, M. P. (1968). Competence and deoxyribonucleic acid uptake in Bacillus subtilis. *J Bacteriol* **95**, 864-6.

Sinha, B., Koster, D., Ruez, R., Gonnord, P., Bastiani, M., Abankwa, D., Stan, R. V., Butler-Browne, G., Vedie, B., Johannes, L. et al. (2011). Cells respond to mechanical stress by rapid disassembly of caveolae. *Cell* **144**, 402-13.

Siryaporn, A., Kuchma, S. L., O'Toole, G. A. and Gitai, Z. (2014). Surface attachment induces Pseudomonas aeruginosa virulence. *Proc Natl Acad Sci U S A* **111**, 16860-5.

Sit, S. T. and Manser, E. (2011). Rho GTPases and their role in organizing the actin cytoskeleton. *J Cell Sci* **124**, 679-83.

Skerker, J. M. and Shapiro, L. (2000). Identification and cell cycle control of a novel pilus system in Caulobacter crescentus. *Embo J* **19**, 3223-34.

Sorkin, R., Greenbaum, A., David-Pur, M., Anava, S., Ayali, A., Ben-Jacob, E. and Hanein, Y. (2009). Process entanglement as a neuronal anchorage mechanism to rough surfaces. *Nanotechnology* **20**, 015101.

Soyer, M., Charles-Orszag, A., Lagache, T., Machata, S., Imhaus, A. F., Dumont, A., Millien, C., Olivo-Marin, J. C. and Dumenil, G. (2014). Early sequence of events triggered by the interaction of Neisseria meningitidis with endothelial cells. *Cell Microbiol* **16**, 878-95.

Sparling, P. F. (1966). Genetic transformation of Neisseria gonorrhoeae to streptomycin resistance. *J Bacteriol* **92**, 1364-71.

Spratt, B. G., Bowler, L. D., Zhang, Q. Y., Zhou, J. and Smith, J. M. (1992). Role of interspecies transfer of chromosomal genes in the evolution of penicillin resistance in pathogenic and commensal Neisseria species. *J Mol Evol* **34**, 115-25.

Sprong, T., Moller, A. S., Bjerre, A., Wedege, E., Kierulf, P., van der Meer, J. W., Brandtzaeg, P., van Deuren, M. and Mollnes, T. E. (2004). Complement activation and complement-dependent inflammation by Neisseria meningitidis are independent of lipopolysaccharide. *Infect Immun* **72**, 3344-9.

Stachowiak, J. C., Hayden, C. C. and Sasaki, D. Y. (2010). Steric confinement of proteins on lipid membranes can drive curvature and tubulation. *Proc Natl Acad Sci U S A* **107**, 7781-6.

Stachowiak, J. C., Schmid, E. M., Ryan, C. J., Ann, H. S., Sasaki, D. Y., Sherman, M. B., Geissler, P. L., Fletcher, D. A. and Hayden, C. C. (2012). Membrane bending by protein-protein crowding. *Nat Cell Biol* **14**, 944-9.

Stauffer, T. P., Ahn, S. and Meyer, T. (1998). Receptor-induced transient reduction in plasma membrane PtdIns(4,5)P2 concentration monitored in living cells. *Curr Biol* **8**, 343-6.

Steeg, P. S., Camphausen, K. A. and Smith, Q. R. (2011). Brain metastases as preventive and therapeutic targets. *Nat Rev Cancer* **11**, 352-63.

Steeghs, L., den Hartog, R., den Boer, A., Zomer, B., Roholl, P. and van der Ley, P. (1998). Meningitis bacterium is viable without endotoxin. *Nature* **392**, 449-50.

Stephens, D. S., Greenwood, B. and Brandtzaeg, P. (2007). Epidemic meningitis, meningococcaemia, and Neisseria meningitidis. *Lancet* **369**, 2196-2210.

Stephens, D. S., Hoffman, L. H. and McGee, Z. A. (1983). Interaction of Neisseria meningitidis with human nasopharyngeal mucosa: attachment and entry into columnar epithelial cells. *J Infect Dis* **148**, 369-76.

Stephens, D. S. and McGee, Z. A. (1981). Attachment of Neisseria meningitidis to human mucosal surfaces: influence of pili and type of receptor cell. *J Infect Dis* **143**, 525-32.

Stern, A. and Meyer, T. F. (1987). Common mechanism controlling phase and antigenic variation in pathogenic neisseriae. *Mol Microbiol* **1**, 5-12.

Stoeber, M., Stoeck, I. K., Hanni, C., Bleck, C. K., Balistreri, G. and Helenius, A. (2012). Oligomers of the ATPase EHD2 confine caveolae to the plasma membrane through association with actin. *Embo J* **31**, 2350-64.

Stojiljkovic, I., Hwa, V., de Saint Martin, L., O'Gaora, P., Nassif, X., Heffron, F. and So, M. (1995). The Neisseria meningitidis haemoglobin receptor: its role in iron utilization and virulence. *Mol Microbiol* **15**, 531-41.

Stojiljkovic, I., Larson, J., Hwa, V., Anic, S. and So, M. (1996). HmbR outer membrane receptors of pathogenic Neisseria spp.: iron-regulated, hemoglobin-binding proteins with a high level of primary structure conservation. *J Bacteriol* **178**, 4670-8.

Stojiljkovic, I. and Srinivasan, N. (1997). Neisseria meningitidis tonB, exbB, and exbD genes: Ton-dependent utilization of protein-bound iron in Neisseriae. *J Bacteriol* **179**, 805-12.

Suetsugu, S. and Gautreau, A. (2012). Synergistic BAR-NPF interactions in actin-driven membrane remodeling. *Trends Cell Biol* **22**, 141-50.

Sun, M., Northup, N., Marga, F., Huber, T., Byfield, F. J., Levitan, I. and Forgacs, G. (2007). The effect of cellular cholesterol on membrane-cytoskeleton adhesion. *J Cell Sci* **120**, 2223-31.

Suzuki, Y., Yamamura, H., Ohya, S. and Imaizumi, Y. (2013). Caveolin-1 facilitates the direct coupling between large conductance Ca2+-activated K+ (BKCa) and Cav1.2 Ca2+ channels and their clustering to regulate membrane excitability in vascular myocytes. *J Biol Chem* **288**, 36750-61.

Svitkina, T. M., Bulanova, E. A., Chaga, O. Y., Vignjevic, D. M., Kojima, S., Vasiliev, J. M. and Borisy, G. G. (2003). Mechanism of filopodia initiation by reorganization of a dendritic network. *J Cell Biol* **160**, 409-21.

Swanson, J. (1978). Studies on gonococcus infection. XIV. Cell wall protein differences among color/opacity colony variants of Neisseria gonorrhoeae. *Infect Immun* **21**, 292-302.

Swimm, A., Bommarius, B., Li, Y., Cheng, D., Reeves, P., Sherman, M., Veach, D., Bornmann, W. and Kalman, D. (2004). Enteropathogenic Escherichia coli use redundant tyrosine kinases to form actin pedestals. *Mol Biol Cell* **15**, 3520-9.

Szabo, Z., Stahl, A. O., Albers, S. V., Kissinger, J. C., Driessen, A. J. and Pohlschroder, M. (2007). Identification of diverse archaeal proteins with class III signal peptides cleaved by distinct archaeal prepilin peptidases. *J Bacteriol* **189**, 772-8.

Tala, A., Progida, C., De Stefano, M., Cogli, L., Spinosa, M. R., Bucci, C. and Alifano, P. (2008). The HrpB-HrpA two-partner secretion system is essential for intracellular survival of Neisseria meningitidis. *Cell Microbiol* **10**, 2461-82.

Tan, Y., Adhikari, R. Y., Malvankar, N. S., Ward, J. E., Woodard, T. L., Nevin, K. P. and Lovley, D. R. (2017). Expressing the Geobacter metallireducens PilA in Geobacter sulfurreducens Yields Pili with Exceptional Conductivity. *MBio* **8**.

Taylor, M. J., Perrais, D. and Merrifield, C. J. (2011). A high precision survey of the molecular dynamics of mammalian clathrin-mediated endocytosis. *PLoS Biol* **9**, e1000604.

Tettelin, H., Saunders, N. J., Heidelberg, J., Jeffries, A. C., Nelson, K. E., Eisen, J. A., Ketchum, K. A., Hood, D. W., Peden, J. F., Dodson, R. J. et al. (2000). Complete genome sequence of Neisseria meningitidis serogroup B strain MC58. *Science* **287**, 1809-15.

Todd, W. J., Wray, G. P. and Hitchcock, P. J. (1984). Arrangement of pili in colonies of Neisseria gonorrhoeae. *J Bacteriol* **159**, 312-20.

Tollis, S., Dart, A. E., Tzircotis, G. and Endres, R. G. (2010). The zipper mechanism in phagocytosis: energetic requirements and variability in phagocytic cup shape. *BMC Syst Biol* **4**, 149.

Tonnesen, J., Katona, G., Rozsa, B. and Nagerl, U. V. (2014). Spine neck plasticity regulates compartmentalization of synapses. *Nat Neurosci* **17**, 678-85.

Tosi, T., Estrozi, L. F., Job, V., Guilvout, I., Pugsley, A. P., Schoehn, G. and Dessen, A. (2014). Structural Similarity of Secretins from Type II and Type III Secretion Systems. *Structure* **22**, 1348-55.

Trotter, C. L. and Greenwood, B. M. (2007). Meningococcal carriage in the African meningitis belt. *Lancet Infect Dis* **7**, 797-803.

Truttmann, M. C., Rhomberg, T. A. and Dehio, C. (2011). Combined action of the type IV secretion effector proteins BepC and BepF promotes invasome formation of Bartonella henselae on endothelial and epithelial cells. *Cell Microbiol* **13**, 284-99.

Turner, D. P., Marietou, A. G., Johnston, L., Ho, K. K., Rogers, A. J., Wooldridge, K. G. and Ala'Aldeen, D. A. (2006). Characterization of MspA, an immunogenic autotransporter protein that mediates adhesion to epithelial and endothelial cells in Neisseria meningitidis. *Infect Immun* **74**, 2957-64.

Tzeng, Y. L., Bazan, J. A., Turner, A. N., Wang, X., Retchless, A. C., Read, T. D., Toh, E., Nelson, D. E., Del Rio, C. and Stephens, D. S. (2017). Emergence of a new Neisseria meningitidis clonal complex 11 lineage 11.2 clade as an effective urogenital pathogen. *Proc Natl Acad Sci U S A*.

Tzeng, Y. L., Martin, L. E. and Stephens, D. S. (2014). Environmental survival of Neisseria meningitidis. *Epidemiol Infect* **142**, 187-90.

Uchiyama, T. (2003). Adherence to and invasion of Vero cells by recombinant Escherichia coli expressing the outer membrane protein rOmpB of Rickettsia japonica. *Ann N Y Acad Sci* **990**, 585-90.

Unkmeir, A., Latsch, K., Dietrich, G., Wintermeyer, E., Schinke, B., Schwender, S., Kim, K. S., Eigenthaler, M. and Frosch, M. (2002). Fibronectin mediates Opc-dependent internalization of Neisseria meningitidis in human brain microvascular endothelial cells. *Mol Microbiol* **46**, 933-46.

Unwin, N. (2005). Refined structure of the nicotinic acetylcholine receptor at 4A resolution. *J Mol Biol* **346**, 967-89.

Uria, M. J., Zhang, Q., Li, Y., Chan, A., Exley, R. M., Gollan, B., Chan, H., Feavers, I., Yarwood, A., Abad, R. et al. (2008). A generic mechanism in Neisseria meningitidis for enhanced resistance against bactericidal antibodies. *J Exp Med* **205**, 1423-34.

Uruno, T., Liu, J., Zhang, P., Fan, Y., Egile, C., Li, R., Mueller, S. C. and Zhan, X. (2001). Activation of Arp2/3 complex-mediated actin polymerization by cortactin. *Nat Cell Biol* **3**, 259-66.

van der Ende, A., Hopman, C. T., Zaat, S., Essink, B. B., Berkhout, B. and Dankert, J. (1995). Variable expression of class 1 outer membrane protein in Neisseria meningitidis is caused by variation in the spacing between the -10 and -35 regions of the promoter. *J Bacteriol* **177**, 2475-80.

van Deuren, M., Brandtzaeg, P. and van der Meer, J. W. (2000). Update on meningococcal disease with emphasis on pathogenesis and clinical management. *Clin Microbiol Rev* **13**, 144-66, table of contents.

van Schaik, E. J., Giltner, C. L., Audette, G. F., Keizer, D. W., Bautista, D. L., Slupsky, C. M., Sykes, B. D. and Irvin, R. T. (2005). DNA binding: a novel function of Pseudomonas aeruginosa type IV pili. *J Bacteriol* **187**, 1455-64.

van Ulsen, P., Rutten, L., Feller, M., Tommassen, J. and van der Ende, A. (2008). Two-partner secretion systems of Neisseria meningitidis associated with invasive clonal complexes. *Infect Immun* **76**, 4649-58.

Vandeputte-Rutten, L., Bos, M. P., Tommassen, J. and Gros, P. (2003). Crystal structure of Neisserial surface protein A (NspA), a conserved outer membrane protein with vaccine potential. *J Biol Chem* **278**, 24825-30.

VanDyke, D. J., Wu, J., Ng, S. Y., Kanbe, M., Chaban, B., Aizawa, S. and Jarrell, K. F. (2008). Identification of a putative acetyltransferase gene, MMP0350, which affects proper assembly of both flagella and pili in the archaeon Methanococcus maripaludis. *J Bacteriol* **190**, 5300-7.

Vargas, M., Malvankar, N. S., Tremblay, P. L., Leang, C., Smith, J. A., Patel, P., Snoeyenbos-West, O., Nevin, K. P. and Lovley, D. R. (2013). Aromatic amino acids required for pili conductivity and long-range extracellular electron transport in Geobacter sulfurreducens. *MBio* **4**, e00105-13.

Vasioukhin, V., Bauer, C., Yin, M. and Fuchs, E. (2000). Directed actin polymerization is the driving force for epithelial cell-cell adhesion. *Cell* **100**, 209-19.

Veiga, E. and Cossart, P. (2005). Listeria hijacks the clathrin-dependent endocytic machinery to invade mammalian cells. *Nat Cell Biol* **7**, 894-900.

Vidarsson, G., Overbeeke, N., Stemerding, A. M., van den Dobbelsteen, G., van Ulsen, P., van der Ley, P., Kilian, M. and van de Winkel, J. G. (2005). Working mechanism of immunoglobulin A1 (IgA1) protease: cleavage of IgA1 antibody to Neisseria meningitidis PorA requires de novo synthesis of IgA1 Protease. *Infect Immun* **73**, 6721-6.

Vignon, G., Kohler, R., Larquet, E., Giroux, S., Prevost, M. C., Roux, P. and Pugsley, A. P. (2003). Type IV-like pili formed by the type II secreton: specificity, composition, bundling, polar localization, and surface presentation of peptides. *J Bacteriol* **185**, 3416-28.

Virji, M., Evans, D., Hadfield, A., Grunert, F., Teixeira, A. M. and Watt, S. M. (1999). Critical determinants of host receptor targeting by Neisseria meningitidis and Neisseria gonorrhoeae: identification of Opa adhesiotopes on the N-domain of CD66 molecules. *Mol Microbiol* **34**, 538-51.

Virji, M., Makepeace, K., Ferguson, D. J., Achtman, M., Sarkari, J. and Moxon, E. R. (1992). Expression of the Opc protein correlates with invasion of epithelial and endothelial cells by Neisseria meningitidis. *Mol Microbiol* **6**, 2785-95.

Virji, M., Makepeace, K. and Moxon, E. R. (1994). Distinct mechanisms of interactions of Opc-expressing meningococci at apical and basolateral surfaces of human endothelial cells; the role of integrins in apical interactions. *Mol Microbiol* **14**, 173-84.

Virji, M., Makepeace, K., Peak, I. R., Ferguson, D. J., Jennings, M. P. and Moxon, E. R. (1995). Opc- and pilus-dependent interactions of meningococci with human endothelial cells: molecular mechanisms and modulation by surface polysaccharides. *Mol Microbiol* **18**, 741-54.

Vogel, U., Claus, H., von Muller, L., Bunjes, D., Elias, J. and Frosch, M. (2004). Bacteremia in an immunocompromised patient caused by a commensal Neisseria meningitidis strain harboring the capsule null locus (cnl). *J Clin Microbiol* **42**, 2898-901.

Wakatsuki, T., Schwab, B., Thompson, N. C. and Elson, E. L. (2001). Effects of cytochalasin D and latrunculin B on mechanical properties of cells. *J Cell Sci* **114**, 1025-36.

Wang, S., Parsek, M. R., Wozniak, D. J. and Ma, L. Z. (2013). A spider web strategy of type IV pili-mediated migration to build a fibre-like Psl polysaccharide matrix in Pseudomonas aeruginosa biofilms. *Environ Microbiol* **15**, 2238-53.

Watanabe, S. and Boucrot, E. (2017). Fast and ultrafast endocytosis. *Curr Opin Cell Biol* **47**, 64-71.

Weaver, A. M., Heuser, J. E., Karginov, A. V., Lee, W. L., Parsons, J. T. and Cooper, J. A. (2002). Interaction of cortactin and N-WASp with Arp2/3 complex. *Curr Biol* **12**, 1270-8.

Weaver, A. M., Karginov, A. V., Kinley, A. W., Weed, S. A., Li, Y., Parsons, J. T. and Cooper, J. A. (2001). Cortactin promotes and stabilizes Arp2/3-induced actin filament network formation. *Curr Biol* **11**, 370-4.

Werner, J. H., Montano, G. A., Garcia, A. L., Zurek, N. A., Akhadov, E. A., Lopez, G. P. and Shreve, A. P. (2009). Formation and Dynamics of Supported Phospholipid Membranes on a Periodic Nanotextured Substrate. *Langmuir* **25**, 2986-2993.

Wolfgang, M., Lauer, P., Park, H. S., Brossay, L., Hebert, J. and Koomey, M. (1998). PilT mutations lead to simultaneous defects in competence for natural transformation and twitching motility in piliated Neisseria gonorrhoeae. *Mol Microbiol* **29**, 321-30.

Wolfgang, M., van Putten, J. P., Hayes, S. F. and Koomey, M. (1999). The comP locus of Neisseria gonorrhoeae encodes a type IV prepilin that is dispensable for pilus biogenesis but essential for natural transformation. *Mol Microbiol* **31**, 1345-57.

Wong, K. W. and Isberg, R. R. (2003). Arf6 and phosphoinositol-4-phosphate-5-kinase activities permit bypass of the Rac1 requirement for beta1 integrin-mediated bacterial uptake. *J Exp Med* **198**, 603-14.

Wormann, M. E., Horien, C. L., Bennett, J. S., Jolley, K. A., Maiden, M. C., Tang, C. M., Aho, E. L. and Exley, R. M. (2014). Sequence, distribution and chromosomal context of class I and class II pilin genes of Neisseria meningitidis identified in whole genome sequences. *BMC Genomics* **15**, 253.

Wu, L., Huang, J., Yu, X., Zhou, X., Gan, C., Li, M. and Chen, Y. (2014). AFM of the ultrastructural and mechanical properties of lipid-raft-disrupted and/or cold-treated endothelial cells. *J Membr Biol* **247**, 189-200.

Yamamoto, K., Furuya, K., Nakamura, M., Kobatake, E., Sokabe, M. and Ando, J. (2011). Visualization of flow-induced ATP release and triggering of Ca2+ waves at caveolae in vascular endothelial cells. *J Cell Sci* **124**, 3477-83.

Yamanaka, T., Horikoshi, Y., Suzuki, A., Sugiyama, Y., Kitamura, K., Maniwa, R., Nagai, Y., Yamashita, A., Hirose, T., Ishikawa, H. et al. (2001). PAR-6 regulates aPKC activity in a novel way and mediates cell-cell contact-induced formation of the epithelial junctional complex. *Genes Cells* **6**, 721-31.

Yang, J., Yan, R., Roy, A., Xu, D., Poisson, J. and Zhang, Y. (2015). The I-TASSER Suite: protein structure and function prediction. *Nat Methods* **12**, 7-8.

Yonemura, S., Tsukita, S. and Tsukita, S. (1999). Direct involvement of ezrin/radixin/moesin (ERM)-binding membrane proteins in the organization of microvilli in collaboration with activated ERM proteins. *J Cell Biol* **145**, 1497-509.

Yoshida, S., Katayama, E., Kuwae, A., Mimuro, H., Suzuki, T. and Sasakawa, C. (2002). Shigella deliver an effector protein to trigger host microtubule destabilization, which promotes Rac1 activity and efficient bacterial internalization. *Embo J* **21**, 2923-35.

Yoshida, T., Kim, S. R. and Komano, T. (1999). Twelve pil genes are required for biogenesis of the R64 thin pilus. *J Bacteriol* **181**, 2038-43.

Yurist-Doutsch, S., Chaban, B., VanDyke, D. J., Jarrell, K. F. and Eichler, J. (2008). Sweet to the extreme: protein glycosylation in Archaea. *Mol Microbiol* **68**, 1079-84.

Zarantonelli, M. L., Szatanik, M., Giorgini, D., Hong, E., Huerre, M., Guillou, F., Alonso, J. M. and Taha, M. K. (2007). Transgenic mice expressing human transferrin as a model for meningococcal infection. *Infect Immun* **75**, 5609-14.

Zhang, B., Peng, F., Wu, D., Ingram, A. J., Gao, B. and Krepinsky, J. C. (2007). Caveolin-1 phosphorylation is required for stretch-induced EGFR and Akt activation in mesangial cells. *Cell Signal* **19**, 1690-700.

Zhang, Y. (2008). I-TASSER server for protein 3D structure prediction. *BMC Bioinformatics* **9**, 40.

Zhao, H., Michelot, A., Koskela, E. V., Tkach, V., Stamou, D., Drubin, D. G. and Lappalainen, P. (2013a). Membrane-sculpting BAR domains generate stable lipid microdomains. *Cell Rep* **4**, 1213-23.

Zhao, Y., Liu, J., Yang, C., Capraro, B. R., Baumgart, T., Bradley, R. P., Ramakrishnan, N., Xu, X., Radhakrishnan, R., Svitkina, T. et al. (2013b). Exo70 generates membrane curvature for morphogenesis and cell migration. *Dev Cell* **26**, 266-78.

Zschiedrich, C. P., Keidel, V. and Szurmant, H. (2016). Molecular Mechanisms of Two-Component Signal Transduction. *J Mol Biol* **428**, 3752-75.

Zurek, N., Sparks, L. and Voeltz, G. (2011). Reticulon short hairpin transmembrane domains are used to shape ER tubules. *Traffic* **12**, 28-41.

APPENDIX

1. *Neisseria meningitidis* type IV pili composed of sequence invariable pilins are masked by multisite glycosylation

As described in the Introduction, meningococcal type IV pilin are subject to phase and antigenic variation, and the major pilin PilE can be post-translationally modified, generating a large repertoire of T4P variants among a given strain which is believed to help escape the immune system.

While this is true for class I type IV pilins, class II pilins do not show antigenic variation. However, a number of disease-associated strains happen to possess class II pilins. Therefore, Gault et al. wondered how meningococcal T4P with sequence invariable pilins could contribute to immune evasion during meningococcal disease.

It was found that, unlike class I pilins that possess only one glycosylation site, class II pilins possess up to five of them. This results in an enhanced coverage of the pilus fibers with glycans. Eventually, phase variation of the *pgl* genes responsible for pilin glycosylation generates strain-specific glycosylation patterns that modulate pilus coverage and could be of importance in the avoidance of recognition by antibodies during infection (Gault et al., 2015).

My contribution to this paper, in addition to help with the writing of the manuscript, was to demonstrate that the glycosylation of class II pilins in several clinical isolates has no impact on the ability of these bacteria to adhere to human epithelial cells.

PLOS | PATHOGENS

RESEARCH ARTICLE

Neisseria meningitidis Type IV Pili Composed of Sequence Invariable Pilins Are Masked by Multisite Glycosylation

Joseph Gault[1¤], Mathias Ferber[2], Silke Machata[3,4], Anne-Flore Imhaus[3,4], Christian Malosse[1], Arthur Charles-Orszag[3,4], Corinne Millien[3,4], Guillaume Bouvier[2], Benjamin Bardiaux[2], Gérard Péhau-Arnaudet[5], Kelly Klinge[6], Isabelle Podglajen[7], Marie Cécile Ploy[8], H. Steven Seifert[6], Michael Nilges[2], Julia Chamot-Rooke[1], Guillaume Dumenil[3,4]*

1 Structural Mass Spectrometry and Proteomics Unit, Institut Pasteur, CNRS UMR 3528, Paris, France, **2** Institut Pasteur, Unité de Bioinformatique Structurale, CNRS UMR 3528, Département de Biologie Structurale et Chimie, Paris, France, **3** INSERM, U970, Paris Cardiovascular Research Center, Paris, France, **4** Université Paris Descartes, Faculté de Médecine Paris Descartes, Paris, France, **5** CNRS, UMR3528, Paris, France, **6** Department of Microbiology-Immunology, Northwestern University Feinberg School of Medicine, Chicago, Illinois, United States of America, **7** Service de Microbiologie, Assistance Publique-Hôpitaux de Paris, Hôpital Européen Georges-Pompidou, Paris, France, **8** INSERM UMR1092, Faculté de Médecine, Université de Limoges, Limoges, France

¤ Current address: Department of Chemistry, Physical and Theoretical Chemistry Laboratory, University of Oxford, Oxford OX1 3QZ, UK
* guillaume.dumenil@inserm.fr

OPEN ACCESS

Citation: Gault J, Ferber M, Machata S, Imhaus A-F, Malosse C, Charles-Orszag A, et al. (2015) *Neisseria meningitidis* Type IV Pili Composed of Sequence Invariable Pilins Are Masked by Multisite Glycosylation. PLoS Pathog 11(9): e1005162. doi:10.1371/journal.ppat.1005162

Editor: Tomoko Kubori, Osaka University, JAPAN

Received: May 15, 2015

Accepted: August 20, 2015

Published: September 14, 2015

Data Availability Statement: The genomic sequences of two strains described in the study are available at BIGSdb (http://pubmlst.org/software/database/bigsdb/): Id 31214 for strain LIM707 and Id 31215 for strain LIM534.

Funding: This work was supported by: the Avenir INSERM Starting Grant (GD); a CODDIM equipment grant (Région Ile de France, GD); the Integrative Biology of Emerging Infectious Diseases (IBEID) laboratory of excellence (GD), the VIP European Research Council (ERC) starting grant (GD); the Wellcome Trust grant WT093470AIA and NIH grant R37 AI033493 (HSS); a Monge PhD scholarship at

Abstract

The ability of pathogens to cause disease depends on their aptitude to escape the immune system. Type IV pili are extracellular filamentous virulence factors composed of pilin monomers and frequently expressed by bacterial pathogens. As such they are major targets for the host immune system. In the human pathogen *Neisseria meningitidis*, strains expressing class I pilins contain a genetic recombination system that promotes variation of the pilin sequence and is thought to aid immune escape. However, numerous hypervirulent clinical isolates express class II pilins that lack this property. This raises the question of how they evade immunity targeting type IV pili. As glycosylation is a possible source of antigenic variation it was investigated using top-down mass spectrometry to provide the highest molecular precision on the modified proteins. Unlike class I pilins that carry a single glycan, we found that class II pilins display up to 5 glycosylation sites per monomer on the pilus surface. Swapping of pilin class and genetic background shows that the pilin primary structure determines multisite glycosylation while the genetic background determines the nature of the glycans. Absence of glycosylation in class II pilins affects pilus biogenesis or enhances pilus-dependent aggregation in a strain specific fashion highlighting the extensive functional impact of multisite glycosylation. Finally, molecular modeling shows that glycans cover the surface of class II pilins and strongly decrease antibody access to the polypeptide chain. This strongly supports a model where strains expressing class II pilins evade the immune system by changing their sugar structure rather than pilin primary structure. Overall these

Ecole Polytechnique (JG); and the European Union (FP7-IDEAS- ERC 294809) (MN). The funders had no role in study design, data collection and analysis, decision to publish, or preparation of the manuscript.

Competing Interests: The authors have declared that no competing interests exist.

results show that sequence invariable class II pilins are cloaked in glycans with extensive functional and immunological consequences.

Author Summary

During infection pathogens and their host engage in a series of measures and counter-measures to promote their own survival: pathogens express virulence factors, the immune system targets these surface structures and pathogens modify them to evade detection. Like numerous bacterial pathogens, *Neisseria meningitidis* express type IV pili, long filamentous adhesive structures composed of pilins. Intriguingly the amino acid sequences of pilins from most hypervirulent strains do not vary, raising the question of how they evade the immune system. This study shows that the pilus structure is completely coated with sugars thus limiting access of antibodies to the pilin polypeptide chain. We propose that multisite glycosylation and thus variation in the type of sugar mediates immune evasion in these strains.

Introduction

Members of the *Neisseria* genus are Gram-negative proteobacteria that include several commensals such as *N. sicca*, *N. lactamica* or *N. elongata* and two human pathogens, *N. gonorrheae* and *N. meningitidis*. Both of these are highly adapted for interaction with humans, their unique host. *N. gonorrheae* colonizes the human urogenital tract and is responsible for a sexually transmitted infection characterized by a massive inflammatory response and purulent discharge. *Neisseria meningitis* is responsible for devastating sepsis and meningitis [1]. *N. meningitidis* proliferates on the surface of epithelial cells lining the nasopharynx in approximately 5 to 30% of the total human population. Pathogenesis is initiated when bacteria access the bloodstream from the throat, survive and multiply in the blood. Systemic infection and perturbation of vascular function lead to sepsis, the most severe form of the disease associated with organ dysfunction, limb necrosis and death in certain cases. *N. meningitidis* can also cross the blood-brain barrier and access the cerebrospinal fluid, leading to meningitis.

Type IV pili (Tfp) are extracellular filamentous organelles that can be found on a large number of bacterial species [2]. In the case of *Neisseria spp*. they are key virulence factors. These abundant structures are 6–8 nm wide, can measure several microns in length and are expressed by all pathogenic *Neisseria spp*. strains. Type IV pili are primarily composed of a single protein or major pilin, called PilE in *Neisseria spp*., which is assembled in a polymeric helical fiber. *Neisseria* type IV pilins have been grouped in two classes (class I and class II) based on the recognition of the SM1 antibody. This antibody reacts with the linear epitope $E^{49}YYLN^{53}$, which is specific to class I pilins [3]. It was later recognized that the genomic location of the class I and II pilin genes are also different [4, 5]. Type IV pili provide several properties to the bacteria: autoaggregation, adhesion to host cells, intracellular signaling, competence and a form of motility called twitching motility [6]. The importance of this structure during *N. gonorrheae* infection has been demonstrated in human volunteers [7]. Male volunteers inoculated with a type IV pili deficient strain only developed a watery urethral discharge or none at all. More recently, using mice grafted with human skin, Melican *et al.* showed that type IV pili mediated adhesion of *N. meningitidis* is a determining factor in vascular damage observed during *purpura fulminans* [8].

As a countermeasure against this virulence factor the immune system produces antibodies against type IV pili [9]. The efficacy of *N. meningitidis* to proliferate in the throat and in blood

during productive infection thus depends on its ability to evade type IV pili specific antibodies. The amino acid sequence of class I pilins can vary by a process called antigenic variation [10]. Beside the expression locus of the major pilins a variable number of non-expressed (silent) *pilS* loci with different but homologous sequences are present in *Neisseria spp*. genomes. Pilin antigenic variation results from a gene conversion, which transfers DNA from the silent cassettes to the expression locus. Thus, the pilin sequence can change generating multiple different antigens. Surprisingly, it was recently recognized that pilins belonging to class II lack this antigenic variation in *Neisseria meningitidis* [11, 12]. Strains with sequence invariable *pilE* genes are frequently isolated worldwide independently of serogroup, year or country of isolation [5]. Interestingly class II pilin genes are restricted to certain clonal complexes, and all pilin genes from clonal complexes cc1, cc5, cc8, cc11 and cc174 are class II. Importantly, these clonal complexes display among the highest disease to carriage ratio, in other words they are hypervirulent [13]. Another interesting feature of these clonal complexes is the association with epidemic meningococcal disease (cc1, cc5 and cc11). Countries in the "meningitis belt" in sub-Saharan Africa have the highest burden of meningococcal disease with both large seasonal epidemics, and much higher incidence rates compared to other areas of the world where outbreaks are small and sporadic. These studies therefore raise the question of how, in absence of primary structure variation, do class II expressing strains evade immunity targeted against type IV pili?

Another potential source of surface variation is post translational modification and in particular glycosylation. Pilin glycosylation has been identified in strains expressing class I pilins that display a single glycosylation site on Ser^{63} [14–17] but has never been studied in class II pilin expressing strains. Importantly, genes involved in the glycosylation of surface structures (*pgl* genes) are submitted to phase variation. As a consequence, oligosaccharides present on the bacterial surface vary between strains and change for one strain during the course of nasopharynx colonization and infection. The *Neisseria spp*. glycosylation pathway starts with the synthesis of an undecaprenyl diphosphate (Undpp) monosaccharide in the cytoplasm. Three enzymes are involved in this step, PglB, C and D. In strains expressing the *pglB1* allele these enzymes synthesize an undecaprenyl-DATDH (diacetamido trideoxyhexose) and in strains expressing the *pglB2* allele a GATDH (glyceramido trideoxyhexose) core [18]. The Unpp-monosaccharide can then be modified with additional sugars by three glycosyltransferases *pglH*, *pglA and pglE*, the latter two being submitted to phase variation. When in the ON-phase, *pglA* leads to the addition of a galactosyl residue on GATDH or DATDH [19]. PglH adds a glycosyl residue on the same site [20]. Recently a *pglH2* allele was described whose product adds an N-acetyl glucosamine residue on the first sugar [21]. When a disaccharide is formed a third sugar can be added by the PglE transferase. PglF is then responsible for the translocation of this structure to the periplasmic side of the inner membrane [22]. Finally, the PglO/L oligosaccharide transferase adds the sugar chain onto the pilin [23, 24].

Given the clinical importance of strains expressing class II pilins and the invariable nature of their sequences, we decided to explore how such strains could evade immunity directed against type IV pili. Since pilin glycosylation is a potential source of surface structure variation we determined the nature of class II pilin glycosylation and show that this could provide immune escape in the absence of primary structure variation.

Results

The class II pilin from the FAM20 strain displays multiple glycosylation sites

The prototypical strain expressing a class II pilin is the FAM18 strain that was isolated from the cerebrospinal fluid of a patient in North Carolina USA in the 1980s. Its genome has been

sequenced and is publicly available [25]. We used a Nalidixic acid resistant variant of this strain called FAM20 to characterize the posttranslational modifications of this representative class II pilin [26]. Type IV pili were purified and characterized using a combination of high-resolution mass profiling and top-down mass spectrometry [27].

Mass profiling of the FAM20 strain produced an exceptionally complex spectrum with over 20 different proteoforms [28] clearly distinguishable (Fig 1A, FAM20). Pilin masses ranged from 15967 Da to over 16850 Da while the molecular mass predicted from the genome is only 14524 Da strongly indicating that numerous post translational modifications (PTMs) were present. Pilin sequences from individual clones were identical indicating that differences in mass were not due to recombination at the pilin locus as expected from previous studies [12]. In order to identify the different PTMs on this pilin we proceeded to simplify the spectral pattern using specific mutants deficient for genes involved in PTMs. Certain proteoforms of the FAM20 major pilin were separated by 124 Da suggesting that phosphoethanolamine (PE) was present. As *pptA* is responsible for PE modification a *pptA* deletion mutant was generated (Fig 1A, *pptA*) and type IV pili were purified from this strain [29, 30]. The overall pattern of pilin purified from the FAM20*pptA* strain was shifted towards lower masses and the number of major proteoforms was reduced to about 12. Peaks with differences of mass corresponding to one hexose were also frequently observed in the spectra (162 Da). Since FAM18 PglH was found to add a glucose residue onto DATDH (glycosyl transferase) we generated and tested a *pglH* mutant [20]. The complexity of the spectrum obtained with the *pglH* strain was also greatly reduced confirming the activity of this enzyme (Fig 1A, *pglH*). To combine the effects of each mutation a double mutant was made. The *pglHpptA* double mutant generated pili with only 3 major proteoforms (15693, 15967 and 16241 Da). Strikingly, the mass difference between the 3 peaks corresponded to one GATDH moiety (274 Da, Fig 1, *pglHpptA*). This result is a strong indication that the FAM20 pilin is glycosylated at least at 3 sites in contrast with previously analyzed strains that showed only one glycosylation site [18, 23].

The reduced complexity of the *pptApglH* double mutant allowed us to identify the PTMs found on the 3 proteoforms using top-down mass spectrometry (Fig 1B, S1 Fig and S1 Table). Different charge states corresponding to each proteoform were submitted to Electron Transfer Dissociation (ETD) fragmentation. As expected, the 3 proteoforms were found to be modified with the usual pilin modifications: N-terminal methylation, disulfide bond between the two cysteine residues and two phosphoglycerol moieties on Ser^{69} and Ser^{97} (Table 1). Proteoform 1 displayed two glycosylation sites with GATDH at Ser^{63} and Ser^{90}. Proteoform 2 harbored three glycosylation sites at Ser^{63}, Ser^{87} and Ser^{98}. Proteoform 3 harbored a fourth glycosylation site at Ser^{90} in addition to those found on proteoform 2. The FAM20 strain can therefore harbor up to 4 different glycans on the same pilin monomer. This detailed top-down analysis of the mutant strain allowed us to precisely assign specific PTMs to the 23 different proteoforms found in the wild type FAM20 highlighting the tremendous diversity of structures found on the pilin of this strain (Fig 2).

The presence of multiple glycosylation sites is a common feature of strains expressing class II pilins

The presence of a strikingly high number of pilin glycosylation sites in FAM20 raised the question of whether this is a particularity of FAM20 or a common feature of strains expressing class II pilins. We therefore collected several class II pilin expressing strains, isolated during a 2003–2006 period from patients suffering from sepsis and meningitis at the Limoges university hospital in France and analyzed their PTM (Table 2). Strains were selected to be part of different serogroups and sequence types to represent a diverse panel with the common feature of

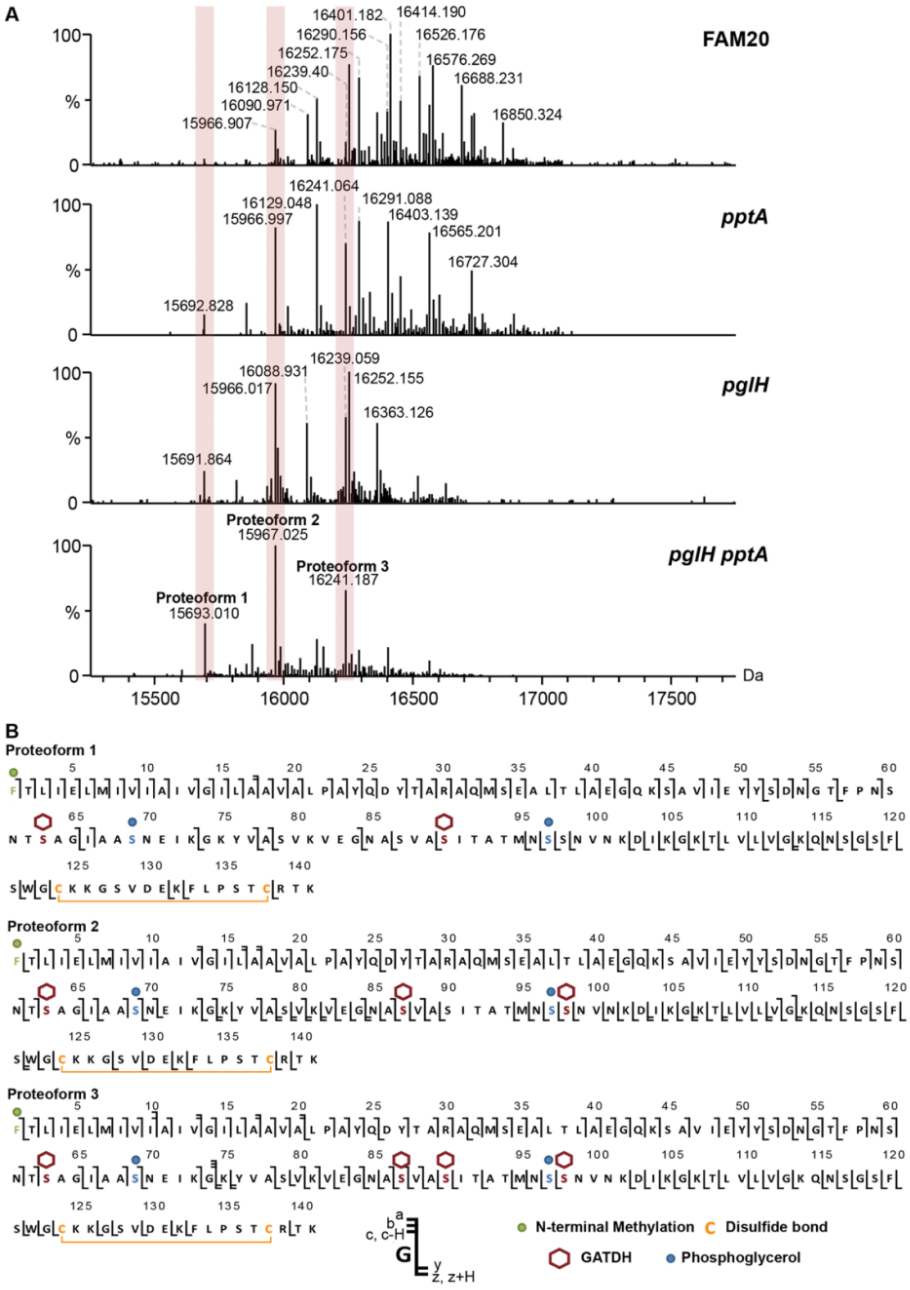

Fig 1. Analysis of the posttranslational modifications of the class II pilin expressing strain FAM20. (A) Whole protein analysis of type IV pili prepared from the FAM20 strain and mutants of the same strain *pptA*, *pglH* and the double mutant *pglHpptA*. (B) Top-down fragmentation maps of the three main proteoforms found in the FAM20*pglHpptA* strain showing identified PTMs localized to sites on the PilE primary structure.

doi:10.1371/journal.ppat.1005162.g001

Table 1. Measured neutral monoisotopic masses of PilE proteoforms from the FAM20*pglHpptA* double mutant and comparison with theoretical masses calculated from the FAM20 sequence plus indicated PTMs.

FAM20 *pglHpptA* proteoform	Measured monoisotopic neutral Mass (Da)	Theoretical mass (Da)	Error (ppm)	PTM present*
1	15693.0104	15692.8603	9.6	Methylated N-ter, C-C, 2 PG, 2 GATDH
2	15967.0251	15966.9768	3.0	Methylated N-ter, C-C, 2 PG, 3 GATDH
3	16241.1870	16241.0933	5.8	Methylated N-ter, C-C, 2 PG, 4 GATDH

* C-C, disulfide bond; PG, phosphoglycerol; GATDH, glyceramido trideoxyhexose

doi:10.1371/journal.ppat.1005162.t001

expressing class II pilins. To allow detailed genetic analysis the entire genomic sequence of two of these clinical strains was established and genes involved in pilin production and its glycosylation characterized (Fig 3A and 3B, LIM534 and LIM707). In both cases sequences of the major pilin are closely related to the FAM20 type II sequence (S2 Fig) and the pilin gene is also located between the *katA* and *prlC* genes as expected for class II expressing strains (Fig 3A). Type IV pili were purified from these strains and submitted to high resolution intact mass profiling. Overall, spectra were less complex than the FAM20 strain with 3–6 major proteoforms (Fig 3C). Nevertheless pilin purified from LIM534, LIM712, LIM675 and LIM707, consistently displayed evidence of multiple glycosylation sites (Fig 3C). The difference in mass between major proteoforms could be explained by the sequential addition of several DATDH/GATDH or DATDH-Hex/GATDH-Hex glycans depending on the strain. Top-down MS analysis of

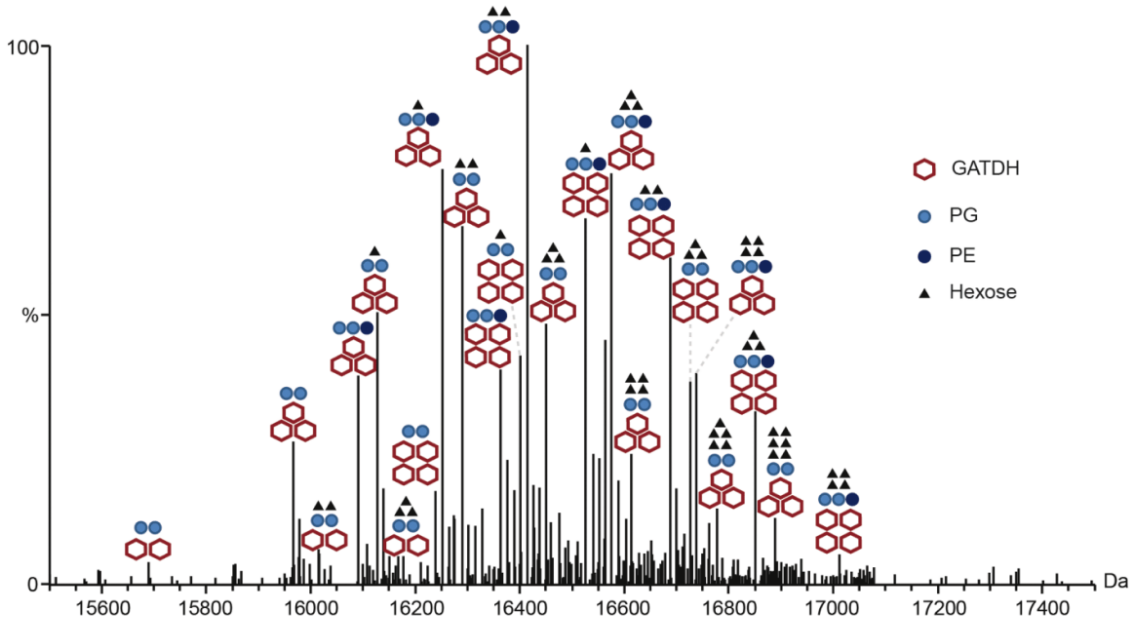

Fig 2. Complete description of the 23 proteoforms expressed by the FAM20 strain.

doi:10.1371/journal.ppat.1005162.g002

Table 2. Clinical isolates used in this study.

Strain	Isolation	Date	Pilin Class	CC*	Serogroup	Reference
8013	Blood	1989	I	ST-18	C	[58]
FAM20	CSF	1980s	II	ST-11	C	[26]
LIM534	Throat	2006	II	ST-5	A	[27]
LIM712	Blood	2005	II	ST- 11	C	This study
LIM675	Blood	2003	II	ST-11	C	This study
LIM707	CSF	2003	II	ST-11	C	This study

*CC, clonal complex

doi:10.1371/journal.ppat.1005162.t002

these different proteoforms demonstrated that proteoforms contained 2–5 glycosylation sites (Fig 3D). These results show that strains expressing class II pilins from different clonal complexes isolated from different continents and in different time periods share the common feature of carrying multiple glycosylation sites. This strongly suggests that such multisite pilin glycosylation is a general feature of class II expressing strains.

The number of glycosylation sites is determined by the pilin primary structure

The observation that class II pilin-carrying strains bear multiple glycosylation sites as opposed to class I strains that carry only one, could be explained by two non-exclusive hypotheses. First, the particular primary structure of class II pilins may itself be more favorable to glycosylation due to a larger number of accessible serine residues. Second, this difference is due to the genetic background and in particular to the *pgl* genes expressed by these strains.

As a first attempt to address this question the genomic regions carrying the *pgl* genes were analyzed in two of the isolated class II pilin expressing strains, LIM534 and LIM707 but this did not reveal any obvious explanation for the number of glycosylation sites. For instance, the PglO/L oligosaccharide transferase was highly conserved between the class I (8013) and class II (FAM18, LIM534 and LIM707) pilin-expressing strains with identity scores between 98 and 100%. As in the class I pilin-expressing strains the *pglBCDFH* genes are localized between the *ribD* and *avtA* genes apart from the *pglA* and *pglE* genes which are located on a separate region (Fig 3B). The LIM707 strain carries a split *pglB2* gene (GATDH) previously found to maintain functionality and an insertion containing *orf2* and *pglH* between the *pglF* and *pglB* genes [20, 31]. The LIM534 strain expresses a *pglB1* (DATDH) gene and displays an insertion containing the *orf2* and *pglH* genes but, interestingly, the *pglH* gene is interrupted by a transposase explaining why only a monosaccharide is found on the pilin.

To address the potential role of the pilin sequence in determining the number of glycosylation sites we generated two "class swap" mutant strains, the first with a class II pilin in a class I pilin-expressing genetic background and the reciprocal strain with a class I pilin in a class II background. In the first case, a class II LIM707 pilin was expressed in the context of the 8013 background (8013*pilE*LIM707, Fig 4A). Pilin from the 8013 strain normally harbors GATDH at a single glycosylation site [18]. Expression of the class II LIM707 pilin in the 8013 background strain led to a pilin modified with up to 3 GATDH moieties (Fig 4B and 4C). The glycosylation sites were the same as in the original LIM707 strain. This result indicates that the *pgl* genes from the 8013 strain are capable of modifying the pilin at multiple sites and that the number of glycosylation sites is determined by the pilin sequence itself rather than the *pgl* genes. To confirm this result the reverse situation was generated and the 8013 pilin (class I)

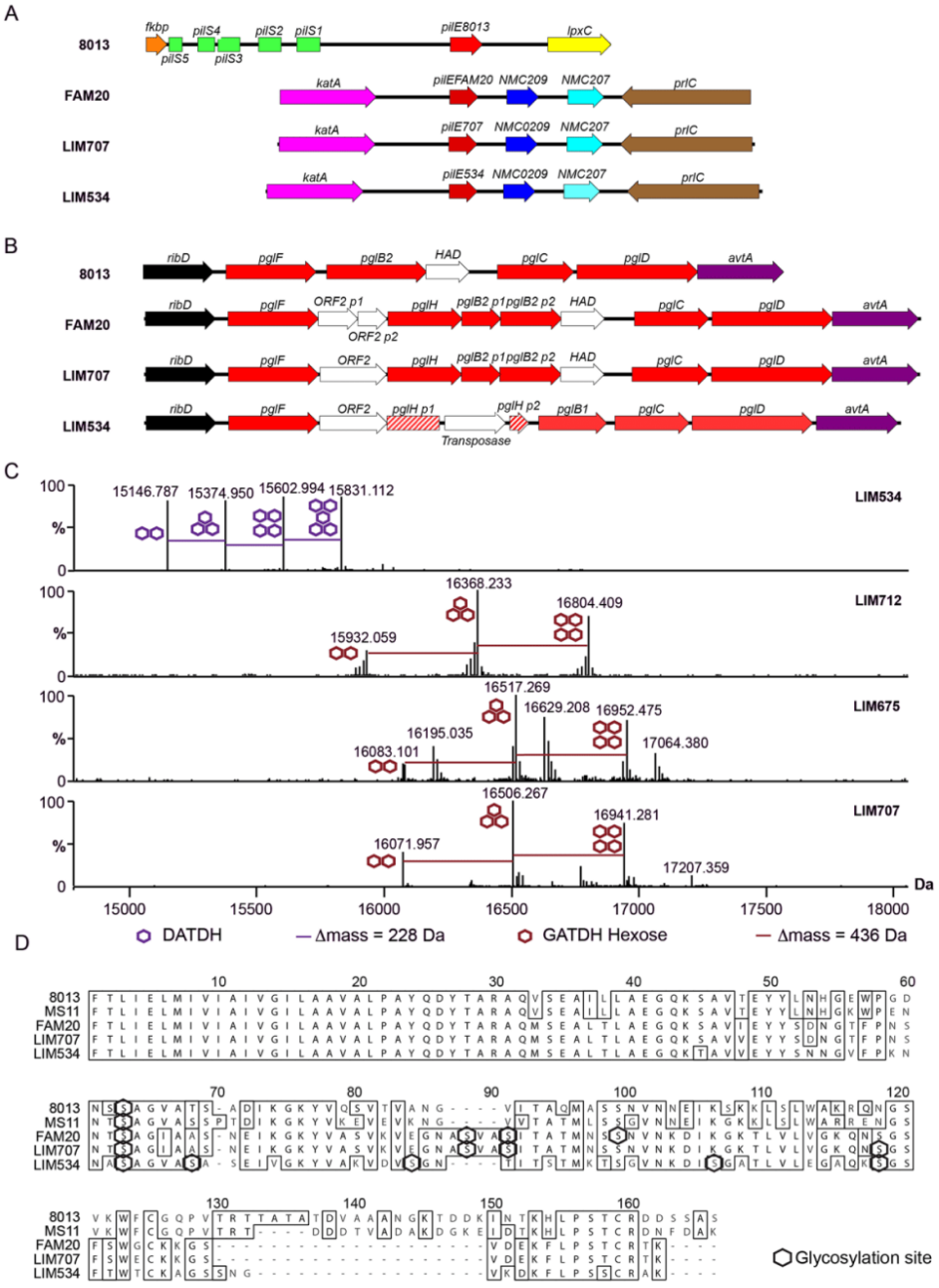

Fig 3. Genomic and biochemical description of class II pilin expressing strains isolated at different sites and at different times. (A) Genetic organization of the pilin locus in the 8013, FAM20, LIM707, and LIM534 strains. (B) Genetic organization of the core *pgl* locus in the same strains. (C) High resolution intact protein mass profiling of 4 class II pilin expressing strains demonstrating multisite glycosylation. (D) Alignment of the pilin sequences from collected class II pilin expressing clinical strains. Sequences of the *N. meningitidis* 8013 and FAM20 strains and the *N. gonorrhoeae* MS11 strain [35] are included for reference. Glycosylation sites irrespective of their nature appear as black hexagons.

doi:10.1371/journal.ppat.1005162.g003

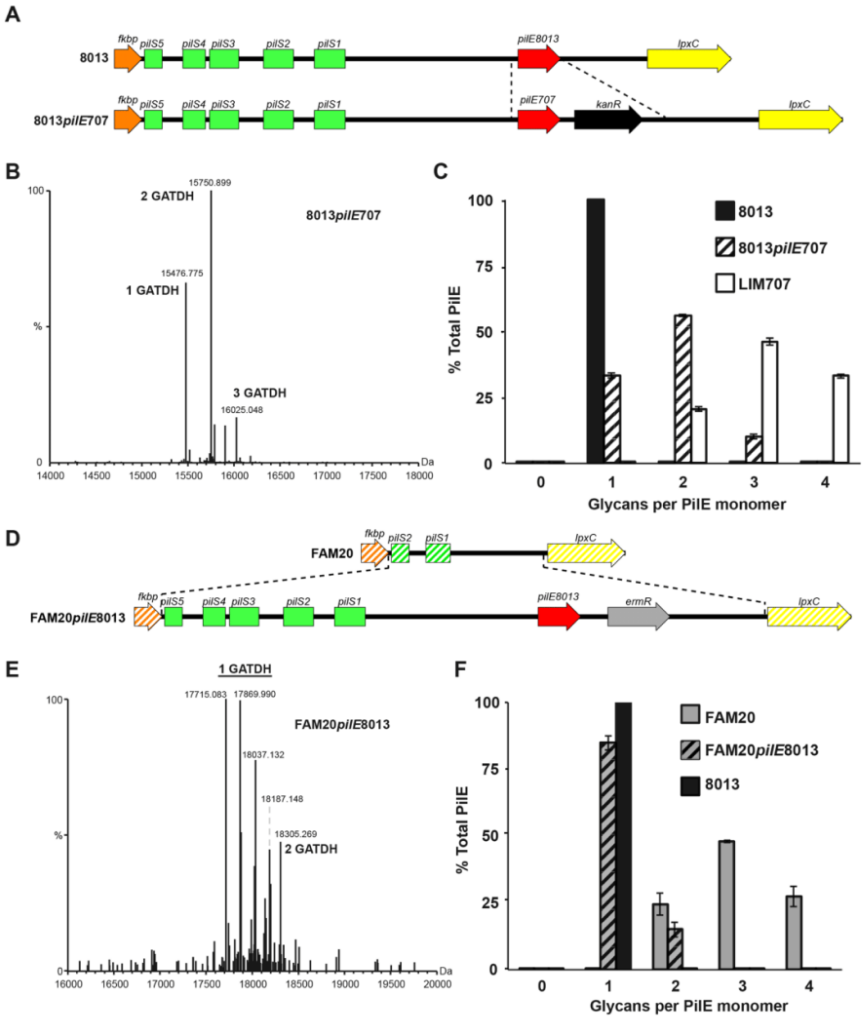

Fig 4. Roles of pilin amino-acid sequence and genetic environment in determining the number of glycosylation sites. (A) Schematic representation of the genetic modification introduced in the 8013 strain to express the class II pilin from the LIM707 strain (8013*pilE*707). (B) Whole protein mass spectrometry analysis of the 8013*pilE*707 strain. (C) Distribution of the number of glycans per monomer in the 8013, 8013*pilE*707 and LIM707 strains. (D) Schematic representation of the insertion introduced in the FAM20 strain to express the class I pilin from the 8013 strain (FAM20*pilE*8013). (E) Whole protein mass spectrometry analysis of the FAM20*pilE*8013 strain. In this case there are multiple proteoforms harboring one glycosylation site. This is due to different phosphoform content and the presence of either di or monosaccharide on Ser^{63}. (F) Distribution of the number of glycans per monomer in the FAM20, FAM20*pilE*8013 and 8013 strains. For panels D and F, average and standard deviations are indicated from 3 independent pili preparations.

doi:10.1371/journal.ppat.1005162.g004

was expressed in the FAM20 background (FAM20*pilE*8013, Fig 4D). High resolution MS analysis showed that pilins purified from this strain comprised of a more complex array of proteoforms due to modification with PE, PC, di and trisaccharides but the vast majority contained a single glycosylation site at Ser^{63} (Fig 4E and 4F). Interestingly, in this case about 10% of the pilin also contained a second glycosylation. Taken together these results show that the genetic environment of the strain determines the type of sugar added, DATDH or GATDH, mono, di

or trisaccharide but the presence of multiple glycosylation sites in class II pilins is largely determined by the primary structure of this class of pilins.

Multiple glycosylation sites on class II pilins affect type IV function in a strain-specific fashion

Neisseria meningitidis class I pilin glycosylation has been shown to contribute to adhesion by interacting with the platelet activating factor (PAF) receptor on the surface of human airway cells [32]. In contrast, in *Neisseria gonorrhoeae* strains deficient for pilin glycosylation exhibited an early hyper-adhesive phenotype but were attenuated in their ability to invade primary cervical epithelial cells [33]. The multiple glycosylation sites found on the class II pilins raised the question of their function more acutely. To explore the function of glycosylation FAM20, LIM707, LIM534 and 8013 strains deleted for the *pglC* and *pglD* genes were generated. Surprisingly, however, despite repeated attempts we were unable to purify pili from the FAM20*pglC* and FAM20*pglD* strains. Electron microscopy observation showed that these two strains do not display any type IV pili on their surface (S2 Fig). Complementation of mutant strains with the corresponding genes restored piliation. In the case of the FAM20 strain, glycosylation appears to be necessary for efficient pilus assembly. This result was unique to the FAM20 strain as the other two class II pilin expressing strains showed normal piliation in absence of glycosylation.

The impact of the loss of glycosylation on the typical pilus properties of adhesion to endothelial cells and auto-aggregation was then determined (Fig 5A–5D). As expected from the absence of pili, the FAM20*pglD* strain showed very low adhesive capacity indistinguishable from the non-piliated mutant (Fig 5A). In contrast, adhesion by the LIM707, LIM534 and 8013 strains were unaffected by the absence of pilin glycosylation. Similar results were found on pulmonary epithelial cells (S3 Fig). Bacterial aggregation was evaluated as a second type IV pilus-dependent property (Fig 5B–5D). As expected, the FAM20*pglC* and *pglD* mutants did not show any aggregation. Bacterial aggregation of LIM534 and LIM707 was higher in the absence of glycosylation. Interestingly, instead of being spherical, bacterial aggregates formed by the unglycosylated LIM707 and LIM534 strains displayed unusual heterogeneous shapes. Such an aggregation phenotype characterized by more aggregation and polymorphous aggregates is reminiscent of strains deficient for the PilT retraction ATPase [34]. To evaluate whether the absence of glycosylation was altering pilus retraction the motility of these strains was evaluated (S4 Fig). Twitching motility depends on cycles of pilus extension and retraction that drag the bacteria on a surface. The glycosylation mutants of the LIM534 and LIM707 strains did not show any defect in motility indicating normal retraction on individual bacteria (S4 Fig). This suggests that class II pilin glycosylation destabilizes pilus-pilus contacts allowing for dynamic interactions between pili in the context of aggregates.

Taken together these results show that the absence of glycosylation on class II pilins leads to strong functional changes, and such changes vary depending on the strain. In the most dramatic situation pili were not expressed on the surface. In other cases, pilus-pilus interactions were stabilized leading to enhanced aggregation.

Modeling pili structures with multiple glycosylations reveals extensive pilus surface coverage

The important functional impact of the multisite glycosylation displayed by class II pilins described above suggests that sugars occupy a large percentage of the pilus surface. To explore this hypothesis the structures of pilin fibers were modeled using the *N. gonorrhoeae* MS11 pilin as a template [35] and taking into account glycan PTM. Three glycans per monomer were

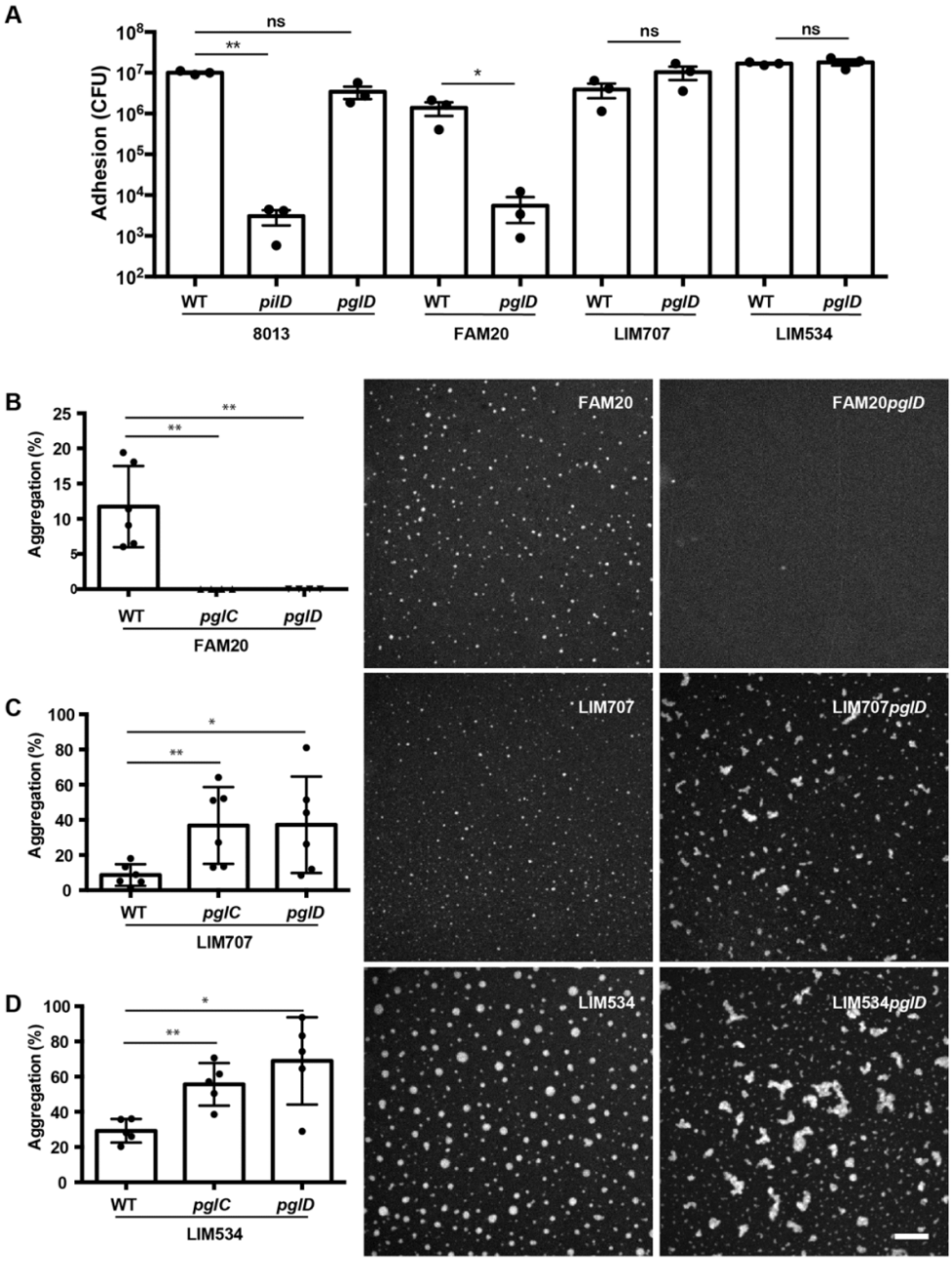

Fig 5. Functional consequences of absence of glycosylation in class II strains. (A) Impact of class II pilin glycosylation on adhesion to endothelial cells. Strains 8013, LIM707, LIM534, FAM20 and their corresponding *pglD* mutants were allowed to adhere to endothelial cells for 4 hours and the number of adherent bacteria analyzed. A non-piliated *pilD* mutant of the 8013 strain was used as a negative control. (B-D) Quantitative and qualitative impact of pilin glycosylation on bacterial aggregation in three class II pilin-harboring strains: (B) FAM20, (C) LIM707 and (D) LIM534. Bacteria were allowed to aggregate in suspension and the size and number of aggregates determined using fluorescence microscopy following DAPI staining. The scale bar indicates 200 μm.

Mean ± standard deviation was determined and indicated on the figures. Statistical analysis was done by paired two-tailed t-test; * indicates $P \leq 0.05$; ** indicates $P \leq 0.01$.

doi:10.1371/journal.ppat.1005162.g005

included in the model as it represents the dominant and average proteoform. Pilus assembly was performed as previously described [36] and corresponding sugars were built by energy minimization and added onto the pilus fiber. Organization of the whole structure was then refined first *in vacuo* and then in water. Glycosylated pilus structures formed of class II pilins consistently show global coverage of the fibers by sugars (Fig 6A). Higher magnification of the FAM20 pilus glycosylated on 3 sites per monomer, the most abundant proteoform, shows extensive coverage of the pilus surface (Fig 6B). Glycosylation therefore strongly changes the structure of the pilus fiber.

These results also suggest that glycosylation will perturb antibody recognition of the pilus fibers. In particular, antibodies directed against the pilus structures would have limited direct access to the protein backbone. As this could compensate for the absence of sequence variation in the class II pilins we decided to investigate this point further. All atoms of the pilus in cylindric coordinates were projected on a plane according to their height and angular coordinate, in order to obtain a flat representation of the pilus surface on a 2D grid (Fig 6C). The surface at the tip of antibodies, typically involved in antigen binding, is roughly circular in shape with a diameter in the order of 5 nm. Since interaction with the antigen does not require the whole surface we approximated the antibody-antigen binding site by using a 2 nm diameter disc [37]. The disc was tested against each position along a grid covering the pilus surface and for each position the presence of sugar was evaluated. The percentage of positions where antibody binding was not affected by sugars was then determined (Fig 6D). For the 8013 class I expressing strain that displays a single glycosylation site the presence of sugars decreased antibody accessibility to 65% of the surface. In the case of the class II pilins that carry multiple glycosylation sites, antibody accessibility was reduced to 15%, 11% and 9% of the surface in the FAM20, LIM534 and LIM707 strains respectively. These results show that the surface-accessible amino-acid residues of class II pilins are largely masked by glycosylation sites.

Discussion

Our results show that, unlike in class I pilins, a large portion of the pilus surface is coated with sugars in class II pilins. Over the years pilin glycosylation of class I pilins has been studied from 3 different *Neisseria meningitidis* strains demonstrating a single conserved glycosylation site at Ser^{63} (Table 3). Strain C311#3 displays a Gal(β1–4)Gal(α1–3)2,4-DATDH [16], strain 8013 one GATDH residue [14] and NIID280 a DATDH residue [17]. In addition, *N. gonorrhoeae* strain N400 presents a hexose residue linked to a DATDH on its class I pilin also at Ser^{63} [15]. In this single study using top-down mass spectrometry, we describe for the first time the glycosylation pattern of 5 different strains expressing class II pilins including the FAM18 reference strain. Pilins from all of these 5 strains display 3 to 5 glycosylation sites (Table 3). Independently of the serogroup, clonal complex, geographic site or temporal period of isolation of the strains (Table 2), class I pilins show a single site of glycosylation while class II pilins have multiple sites of glycosylation.

Molecular modeling reveals that multisite glycosylation of the pilin monomer leads to the coverage of the pilus surface. This could have important consequences in terms of adaptation of the bacteria to the host immune response. More specifically, this could explain why amino-acid sequence variation is not required in class II strains because the polypeptide chain is not exposed to the extracellular milieu and thus not submitted to pressure by the immune system. That is not to say that antibodies cannot recognize glycosylated class II pilins: indeed

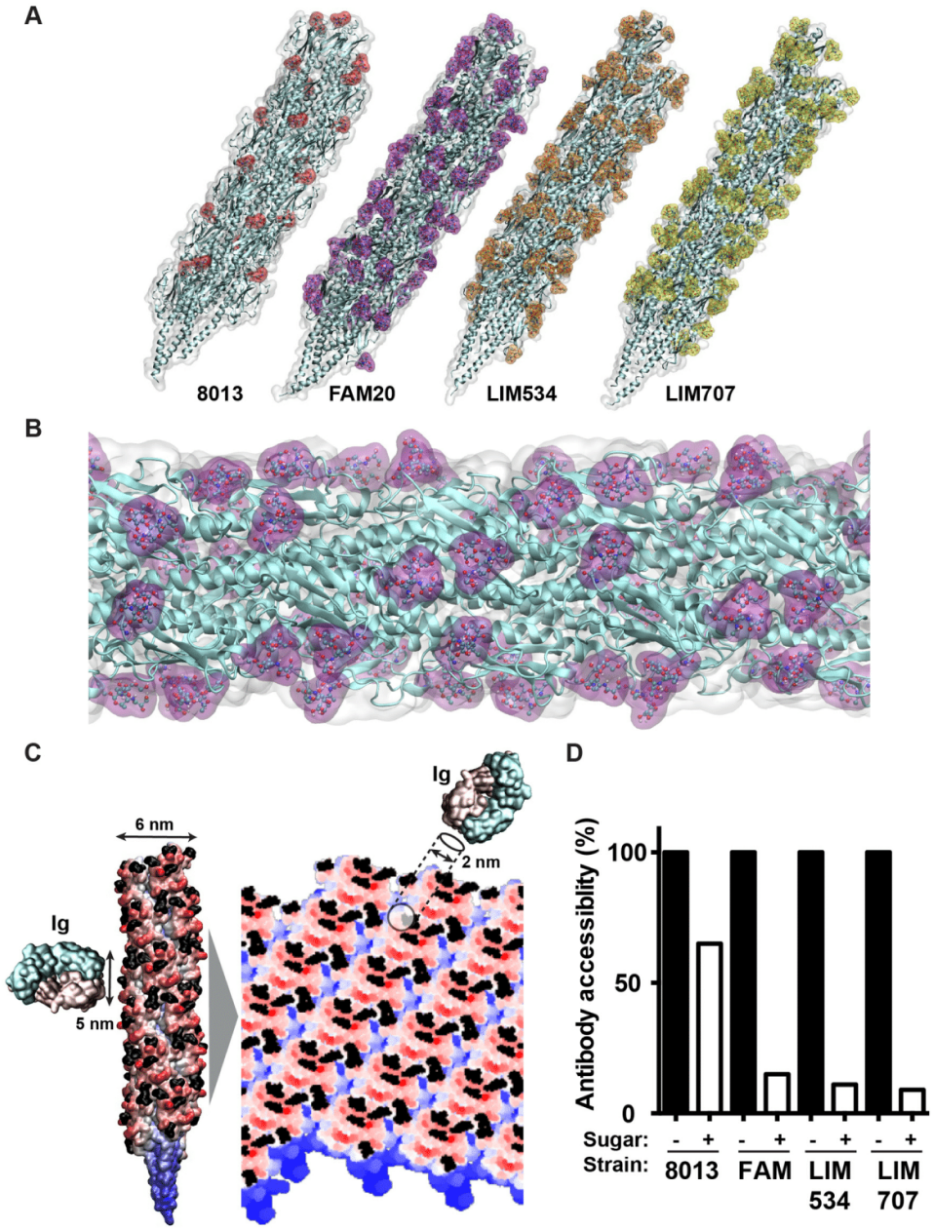

Fig 6. Molecular modeling of antibody accessibility to the primary structure of class II pilins. (A) Overall aspect of the glycosylated pilus fibers from the 8013, FAM20, LIM534 and LIM707 strains. The polypeptide structure appears in cyan and the surface representation of the sugars appears in color. (B) Detailed view of the FAM20 fiber formed with the proteoform with three glycosylation sites. Sugars appear in purple. (C) Projection of the pilus surface on a 2D grid. The antigen-binding tip of an antibody is represented at the same scale. Sugar moieties appear in black. (D) Antibody accessibility to the polypeptide chain in the presence or absence of sugar modifications. Results are presented as the percentage of positions along the grid that allow a 2 nm disc to be placed on the pilus surface without touching sugar moieties relative to all positions on the grid.

doi:10.1371/journal.ppat.1005162.g006

Table 3. Summary of the number of glycosylation sites found in the different *Neisseria meningitidis* strains.

Strain	Pilin class	Number of sites	Reference
C311	I	1	[16]
8013	I	1	[14]
NIID280	I	1	[17]
N400	I	1	[15]
FAM20	II	4	This study
LIM534	II	5	This study
LIM712	II	4	This study
LIM675	II	4	This study
LIM707	II	4	This study

doi:10.1371/journal.ppat.1005162.t003

glycopeptides from type IV pili are immunogenic [38, 39]. Rather, these results suggest that the immune escape scenario would then be different between class I and II pilins. In the case of class I pilins, after throat colonization by a given strain the IgAs specific for the pilin primary sequence will be produced and lead to killing of the initial strain, but variants arising from recombination at the pilin genetic locus will survive until a second adaptation of the immune system. This cycle can potentially repeat itself numerous times. In the case of class II strains the primary structure is cloaked in oligosaccharides, and only antibodies targeted to epitopes that include sugar moieties will efficiently lead to bacterial killing. In this case variants in the sugar structure will survive. Type IV pili have been considered as potential vaccine antigens against *Neisseria gonorrhoeae* infections but sequence variation in class I pilins has hampered these attempts [40, 41]. In the absence of sequence variation in class II pilins it could be tempting to use such proteins as vaccine antigens but our results show that glycosylation would complicate this approach.

A number of arguments support the idea that sugar structure does change during infection of individuals and during epidemics. It has been shown that sera from infected patients during acute and convalescent stage meningococcal disease recognize the major pilin [9] and thus establishes that type IV pili are indeed a target of the immune system and its pressure. It is also well documented that certain *pgl* genes such as *pglA* and *pglE* are submitted to phase variation [42]. This implies that the functionality of these genes and thus the nature of pilin glycosylation can vary at rates between 10^{-2} to 10^{-6} per cell per generation giving the bacteria the opportunity to evade antibody response against type IV pili [43, 44]. Beyond phase variation, *pgl* genes appear to be the site of rapid changes including at the epidemic scale. Lamelas *et al.* performed a longitudinal study in Northern Ghana between 2001 and 2009 [45] where they collected and sequenced the genomes of 100 strains in order to identify evolutionary changes during these epidemic waves. This revealed that the *pgl* genes were the site of no less than 5 successive recombination events during this period. Importantly, all of the strains in this study display class II pilins (Gerd Pluschke, personal communication). Our work also provides evidence of changes in pilin glycosylation. In the case of the LIM534 strain the *pglH* gene is interrupted by an insertion sequence. This insertion event is a molecular signature of changes in the nature of the sugars coating a class II pilin. Taken together these studies underline the high level of variation undergone by class II pilin glycosylation likely to evade the immune response directed against pili.

Our results also provide an explanation for the molecular mechanism that leads to multisite glycosylation in class II pilins. We showed that expression of a class II pilin in a strain normally expressing a class I pilin leads to glycosylation on multiple sites on the pilin backbone. This

result shows that the pilin amino-acid sequence is a determining factor for multisite glycosylation. Alignment of the pilin sequences from class I and II strains suggests two scenarios. Certain glycosylated serines present on class II pilins are simply absent in class I pilins (e.g. serines at alignment positions 88, 91 or 118 in class II are absent in class I). Alternatively the serine is present on class I pilins but the local sequence is different (e.g. serines at alignment position 68 and 99) and this would likely affect glycosyltransferase recognition. Predominance of pilin sequence in the determination of glycosylation sites is confirmed by the reciprocal situation. When a class I sequence is expressed in the class II expressing background, the vast majority of the pilin contains only one sugar. It is noteworthy however that the genetic background, and most probably the *pgl* genes, also plays a partial role in determining the number of glycosylation sites. Indeed, when the class II pilin is expressed in its normal background the main proteoform contains 3 glycans per monomer whereas when it is expressed in the class I expressing background the main proteoform contains only 2. Furthermore, when the class I sequence is expressed in the class II expressing background the main proteoform contains one sugar but 10% of pilins also contain 2 sugars. It is therefore likely that pilins of different classes have co-evolved with their respective *pgl* systems and the glycosylation systems in class II pilin expressing strains are more efficient.

Independently of the number of glycosylation sites, the nature of the sugars on the pilin is determined by the *pgl* genes. The FAM20 strain expresses a *pglB2* allele, *pglA* and *pglE* genes are in the OFF phase and the insertion with the ORF2 and *pglH* genes is present. Accordingly, pilins from this strain are modified with a GATDH core, determined by the *pglB2* allele, and between 1 and 2 hexose residues likely being a glucose transferred by PglH. Interestingly, the PglH transferase expressed by this strain is partially functional in the sense that certain sites display a GATDH-hexose while others a GATDH monosaccharide. This specificity of the *pglH* allele contributes to the complexity of the pattern found on pilins expressed by the FAM20 strain. The LIM707 strain contains the same expression pattern of *pgl* genes as the FAM20 (*pglB2* allele, $pglA_{OFF}$, $pglE_{OFF}$, *pglH* present) leading to the production of a GATDH-Hexose type of sugar. In contrast to the FAM20 strain, all sugars on the LIM707 pilin are disaccharides. For the LIM534 strain, we observe the *pglB1* allele, *pglA* and *pglE* alleles are in the OFF phase and the *pglH* gene is present but interrupted by an insertion sequence. In this case, only DATDH is present as predicted by the genomic data. When pilin sequences are introduced into a different genetic background the nature of sugar changes with the genetic background of the strain. When the pilin gene from the LIM707 strain is introduced in the 8013 background, the pilin becomes modified with a GATDH residue as found in the 8013 strain rather than with a GATDH-Hexose disaccharide. Similarly, introduction of the 8013 pilin gene into the FAM20 strain leads to the expression of pilin modified with GATDH-hexose. Overall these results show that the pilin sequence determines the *number* of glycosylation sites and the *pgl* gene pattern the *nature* of the sugar.

An intriguing result of this study is the difference in functional consequence of the lack of glycosylation in the different class II pilin expressing strains. The most striking phenotype is in the FAM20 strain where type IV pili are simply not expressed on the surface of the bacteria in absence of glycosylation. This phenotype is specific to the FAM20 strain as the LIM707 or LIM534 strains still adhere to host cells via their type IV pili despite inactivation of the *pgl* genes. Another specificity of the FAM20 strain is the high number of proteoforms expressed. In addition to the 2–4 glycosylation sites displayed by this strain, phosphoglycerol (2) phosphoethanolamine (1–3) and phosphocholine (2) modifications are also present. It is possible that in absence of sugar these numerous modifications generate a specific structural environment that is incompatible with pilus expression. It is also possible that the piliation machinery has co-evolved with the glycosylation of this strain and that specific interactions with the

machinery such as with the PilQ secretin require glycosylation. Further work is required to elucidate at which step glycosylation is necessary for piliation in the FAM20 strain. For instance, identification of the point at which pilus biogenesis is blocked in the FAM20*pglC/D* strains will yield useful information to understand the mechanisms of pilus biogenesis. A role for glycosylation in the assembly and function of pili in other organisms has been described. In *Neisseria gonorrhoeae*, pilin (class I) glycosylation has subtle effects on pilus dynamics [46]. Perhaps a similar but more prevalent mechanism is at play in the FAM20 strain. Glycosylation of the *Pseudomonas aeruginosa* major pilin is also necessary for efficient piliation [47]. In Archea, the archaellum, a swimming organelle closely related to type IV pili bears glycosylation sites that are required for assembly [48]

Surprisingly, in strains LIM707 and LIM534 absence of glycosylation of their class II pilins did not affect adhesion to either endothelial or epithelial cells. This is in contrast with previous studies on strains expressing class I pillins that reported a decrease of adhesion in strains lacking pilin glycosylation due to direct interactions of the sugars with cellular receptors [33]. Recently, the recombinant non-glycosylated class I pilin from the 8013 strain was shown to interact with the surface protein CD147 [49]. In principle class II pilins could mediate interactions with cellular receptors through the polypeptidic chain but modeling shows that its accessibility is limited by the numerous surface exposed glycans. Intriguingly, our results thus make a direct interaction between the major pilin and a cellular receptor difficult to imagine at the structural level. Further structural work is required to clarify this point. In contrast, the absence of glycosylation of the pilins expressed by LIM707 and LIM534 led to enhanced aggregation and to an unusual aggregation behavior likely due to stabilized pilus-pilus interactions. These results are consistent with the idea that multisite class II pilin glycosylation leads to changes in surface properties of type IV pili. These results also point out that the functional consequences of pilin glycosylation could be different in class I and class II pilins.

Overall, our work revises the current view of pilin glycosylation. Starting from a single modification per pilin in class I strains we now realize that a large proportion of *N. meningitidis* strains express class II pilins and carry multiple glycosylation sites. Our study first reveals the profound implications in terms of pilus biogenesis, structure and function. The results presented here also have important implications in terms of immunity against type IV pili, vaccine design and how *N. meningitidis* manages to escape the immune system. In particular the presence of multiple glycosylation sites provides a simple explanation for the absence of pilin sequence variation in class II pilins and suggests that variations in sugar structure are the main motor for immune evasion in these strains. The worldwide distribution, hypervirulence and association with epidemic forms of the disease of strains carrying class II pilins underscore the importance of these results to understand *Neisseria meningitidis* infections. In the more global context of infectious diseases our study highlights the wealth of strategies exploited by pathogens to escape the immune system and the key role played by glycosylation.

Materials and Methods

Bacterial strains and growth conditions

N. meningitidis strains were grown on GC agar base plates (Conda Laboratorios, Spain) containing Kellogg's supplements [7] and, when required, 5 μg/ml chloramphenicol at 37°C in moist atmosphere containing 5% CO_2. *Escherichia coli* transformants were grown in liquid or solid Luria-Bertani medium (Difco) containing 100 μg/ml ampicillin. *Neisseria meningitidis* strains used in this study are described in Table 4.

Table 4. Genetically modified strains used in this study.

Strain	Genotype	Reference
8013*pglC*	8013Δ*pglC*::*mariner*	[59]
8013*pglD*	8013Δ*pglD*::*mariner*	[59]
FAM20*pglH*	FAM20Δ*pglH*::*alphA-3*	This study
FAM20*pptA*	FAM20Δ*pptA*::*mariner*	This study
FAM20*pglHpptA*	FAM20Δ*pglH*::*cat* Δ*pptA*::*mariner*	This study
FAM20*pglC*	FAM20Δ*pglC*::*mariner*	This study
FAM20*pglD*	FAM20Δ*pglD*::*mariner*	This study
LIM707*pglC*	LIM707Δ*pglC*::*mariner*	This study
LIM707*pglD*	LIM707Δ*pglD*::*mariner*	This study
LIM534*pglC*	LIM534Δ*pglC*::*mariner*	This study
LIM534*pglD*	LIM534Δ*pglD*::*mariner*	This study
FAM20*pilE*8013	FAM20 Δ*pilE*::*pilE8013*	This study
8013*pilE*707	8013 Δ*pilE*::*pilE707*	This study

doi:10.1371/journal.ppat.1005162.t004

Molecular biology techniques

Genomic sequencing of clinical strains. Genomic sequencing of the LIM534 and LIM707 strains was performed with an Illumina sequencer with 2x74 paired-end sequences. Sequencing was performed at the sequencing platform IMAGIF (Centre de Recherche de Gif– www.imagif.CNRS.fr). Sequences were then assembled with the CLC Genomics Workbench 7 software using the assembly tool and submitted to the BIGSdb (http://pubmlst.org/software/database/bigsdb/).

Gene inactivation. Mutations in the *pptB*, *pptA* and *pglD* genes were described elsewhere [36]. To delete the *pglH* gene, an upstream region amplified with PglH-NF and PglH-NR primers (Table 5) and a downstream region amplified with PglH-CF and PglH-CR primers were restricted by the corresponding enzymes and ligated in the pBluescript plasmid restricted with SalI and SacI (Stratagene), then the kanamycin resistance cassette was cloned in the BamHI site.

Allelic exchange. The megaprimer strategy [50] was used to substitute the type II pilin sequence from the LIM707 strain into the 8013 strain normally expressing a class I pilin (8013*pilE*707). The first amplification was done using E707-F and E707-R primers using genomic DNA from the LIM707 strain as a template. The amplicon was used as a megaprimer to amplify the TopoPCR2.1 vector containing the 8013 pilin sequence followed by a kanamicyn resistance cassette [51]. Amplification products were treated with DpnI and transformed into *E. coli*. Plasmids from resulting clones were sequenced to identify those carrying the LIM707 pilin sequence. A positive plasmid was selected for transformation into the 8013 strain.

To introduce the 8013 *pilE* and *pilS* loci into FAM20, first the *lxpC* to *pilE* fragment was amplified from 8013 chromosomal DNA using the primers 8013-lpxC-pilE_FWD and 8013-lpxC-pilE_REV. and cloned into the plasmid pBlunt (Life Technologies). The *ermC* resistance gene was cloned downstream of *pilE* into the PmeI site. This construct was transformed into 8013 selecting for ErmR and the adjacent DNA sequenced. Chromosomal DNA from the ErmR 8013 was used to transform FAM20 selecting for ErmR, and transformants were screened by PCR using primers McPilRBS and3-end-ErmR_FWD to identify transformants that had recombined the *pilE* gene along with *ermC*. These transformants were further analyzed using primers Mid_pilEandS1FWD, Late_pilEandS1FWD, 3'end_pilS1 FWD, 5'end_fkbP REV, 3'end_pilS5 REV, 3end8013REVpilS1, 3end8013FORpilS1,

Table 5. Oligonucleotides used in this study.

Primer	Sequence*	Enz.
***pglH*NF2**	**GTCGAC**GGAATTTCATTTCCGGAAAAC	*SalI*
***pglH*NR**	**GGATCC**AGCAATAAGGGGCGACGATG	*BamHI*
***pglH*CF**	**GGATCC**AAGTTGCCGAAGTCCTTAC	*BamHI*
***pglH*CR**	**GAGCTC**ACCGCCAGATTGAAAATGC	*SacI*
E707F	GAGGCATTTCCTTTCCAATTAGGAGTAATTTTATGAAAGCAATCCAAAAAGGTTTC	
E707R	CCATTTATTATTTCCTTCCTCTTTTCTGATCCTTACTTATTTGGTGCGGCAGGTAGA	
8013-lpxC-pilE_FWD	GCCGTCTGAAGCGTCGGGCAAATCATCGC	
8013-lpxC-pilE_REV	GATTGTGATTGCCATCGTCG	
FAM20-pilE_FWD	gccgtctgaaATTTGGTGCGGCAGGTAG	
FAM20-pilE_REV	AGGTTTCACCCTGATCGAG	
McPilRBS	gcatttcctttccaattaggag	
3-end-ErmR_FWD	cgttatgaaatgggttaaca	
Mid_pilEandS1FWD	GTCAGCAGTGCCGAAAATTGTCAG	
Late_pilEandS1FWD	CCTCGTCGGTGCAGAAACTTA	
3'end_pilS1 FWD	ctcggtgacggctgatttttgac	
5'END_FKBP REV	gctgaaagtgtacgaataaAGC	
3'END_PILS5 REV	CTGACATAAtggcttcaag	
3END8013REVPILS1	CATCCTTTTGGTCgaaggtc	
3END8013FORPILS1	gaccttcGACCAAAAGGATG	
3END8013REVPILS2	GACGAAGCTATCCTTttggccg	
428BP_PRE-PILS1 FOR	CATCGGTACGGAAACTTATCG	
FAM18-PILE_FWD	gccgtctgaaATTTGGTGCGGCAGGTAG	
FAM18-PILE_REV	AGGTTTCACCCTGATCGAG	

* Restriction sites in bold

doi:10.1371/journal.ppat.1005162.t005

3end8013REVpilS2, and 428bp_pre-pilS1 and long PCR conditions (LongAmp Taq, NEB) to identify transformants carrying the entire *pilS* locus from 8013. DNA sequence analysis of PCR products was performed to confirm the presence of all 8013 sequences between *lpxC* and *fkbP* in FAM20.

The FAM20 native, class II *pilE locus* was cloned by amplifying the FAM20 *pilE* using primers FAM20-pilE_FWD and FAM18-pilE_REV and cloning into pSMART HC Amp (Lucigen). After confirmation by sequence analysis, plasmid DNA was treated with EZ-Tn5<KAN-2> (Epicenter) and the mini-transposon insertion site identified by PCR as 95 bp downstream of the translation start site. This construct was then transformed in the FAM20 strain to interrupt the endogenous *pilE* gene and to generate the FAM20*pilE*8013 strain.

Mass spectrometry techniques

PilE preparation. Pili were prepared as described previously [36]. Briefly, bacteria from 10–12 Petri dishes were harvested in 5 mL of 150 mM ethanolamine at pH 10.5. Pili were sheared by vortexing for 1 min. Bacteria were centrifuged at 4,000xg for 30 min at 4°C and the resulting supernatant further centrifuged at 15,000 x g, 30 min, ambient temperature. The supernatant was removed, pili precipitated from the suspension by the addition of 10% (vol/vol) ammonium sulfate saturated in 150 mM ethanolamine pH 10.5 and allowed to stand for 1 h. The precipitate was pelleted by centrifugation at 4,000xg for 1 h at 20°C. Pellets were washed twice with PBS and suspended in 100 μL distilled water.

High resolution mass profiling. Protein samples were desalted by C_4 ZipTip (Millipore) and eluted directly into a 10 μL spray solution of methanol:water:formic acid (75:25:3). A small amount, 2–6 μL, was introduced into either an Orbitrap Velos mass spectrometer, equipped with ETD module (Thermo Fisher Scientific, Bremen, Germany) or Orbitrap Fusion mass spectrometer (Thermo Scientific, San Jose CA) using a TriVersa NanoMate (Advion Biosciences, Ithaca, NY, USA) in positive ion mode. The spray voltage was set to 1.2–1.6 kV and back-pressure to 0.3–0.4 psi. A full set of automated positive ion calibrations was performed immediately prior to mass measurement.

For Orbitrap Velos MS the transfer capillary temperature was lowered to 100°C, sheath and auxiliary gasses switched off and source transfer parameters optimised using the auto tune feature. Helium was used as the collision gas in the linear ion trap. The FT automatic gain control (AGC) was set at $1x10^6$ for MS experiments. Spectra were acquired in the FTMS in full profile mode with between 1 and 20 microscans over several minutes, with averaging on and set to the maximum value, and a resolution of 60,000 at *m/z* 400. The final few spectra were then averaged using Qualbrowser in Thermo Xcalibur 2.1 and deconvoluted using Xtract to produce zero charge mass spectra.

For Orbitrap Fusion MS transfer capillary temperature was lowered to 100°C, sheath and auxiliary gasses switched off and protein mode switched on. The pressure in the ion routing multiple was lowered to 4 mTorr and ions detected directly in the Orbitrap. Spectra were acquired at resolutions of 120,000 at *m/z* 200 with between 1 and 20 microscans over several minutes with averaging. Processing was performed as for spectra acquired with the Orbitrap Velos.

Top-down mass spectrometry & data analysis. For top-down MS/MS experiments performed on the Orbitrap Velos the FT automatic gain control (AGC) was set at $2x10^5$. Ions corresponding to the isotopic distribution of a single charge state were selected with the largest possible window to avoid overlap with neighbouring species but minimize signal loss. ETD was performed using fluoranthene as the reagent gas. Interaction times were varied to maximise sequence coverage but were kept below 20 ms. Supplemental activation was used as noted. Spectra were acquired in the FTMS in full profile mode at a resolution of 60,000 at m/z 400, with between 10 and 50 microscans and with averaging on and set to the maximum value. The final few spectra were then averaged using Qualbrowser in Thermo Xcalibur 2.1 and deconvoluted using Xtract to produce singly charged MS/MS spectra.

Top-down experiments on the Orbitrap Fusion were done in a similar way with ion selection performed in the quadrupole, ETD performed in the linear ion trap at interaction times of 3–10 ms and fragment ions detected in the Orbitrap at high resolution.

Peak list data resulting from the deconvolution of several spectra (often different charge states of the same species or ETD experiments performed on the same charge state but with different interaction times) were combined and imported into a home built package for ion assignment and automated fragmentation map creation. Low mass, low charge ions that are often clearly present in the spectra but missed by the Xtract algorithm were added manually to the list and PTM assignment was performed with this software tool.

Functional assays

Bacterial aggregation assay. Bacteria grown on GCB agar plates were adjusted to OD_{600} of 0.05 and incubated for 2 hours at 37°C in RPMI containing 10% FBS. The bacterial suspension was concentrated to OD_{600} of 0.3 by centrifugation at 15000 x g for 1 min followed by resuspension in medium containing DAPI (4', 6- diamidino-2-phenylindol; 0.1 μg/ml). Bacterial suspensions were briefly vortexed and transferred in a glass-bottom 96-well plate (Ibidi

GmbH, München, Germany). After a 30 min incubation step, aggregates were observed microscopically with a 4x lens and size and numbers of bacteria involved in aggregates relative to the total amount of bacteria were determined with the ImageJ software, as previously described [36].

Bacterial adhesion assay. Adhesion of meningococci to human umbilical vein endothelial cells (HUVECs) was done as described previously [52]. Cells were grown at 37°C in a humidified incubator under 5% CO2. HUVECs (Promo- Cell, Heidelberg, Germany) were used between passages 1 and 8 and grown in Endo-SFM (Gibco) supplemented with 10% heat-inactivated fetal bovine serum (FBS, PAA Laboratories GmbH, Pasching, Austria) and endothelial cell growth supplement (Harbor Bioproducts, Norwood, USA). Monolayers of 10^5 cells in 24-well plates were infected with 10^7 bacteria (MOI of 100). The inoculum was characterized by CFU counts. After 30 min, unbound bacteria were removed by three washes and the infection was continued for 4h. Finally, after 3 washes adherent bacteria were recovered by scraping the wells and counted by plating appropriate dilutions on GCB agar plates.

Adhesion of meningococci to the human epithelial cell line A549 was performed as described for HUVECs except that a MOI of 500 was used instead of 100. A459 cells were a gift from Prof. Claire Poyart (Institut Cochin, Paris), cultured in DMEM high glucose, GlutaMAX, pyruvate (Life-Technologies) supplemented with 10% heat-inactivated FBS and maintained at 37°C and 5%CO2 in a humidified incubator.

Twitching motility assay. Twitching motility assays of *N.meningitidis* were performed inside a flow chamber (Ibidi GmbH, München, Germany). Bacteria ($2.5x10^7$) were introduced into the flow chamber and incubated for 30 min at 37°C. Unbound bacteria were removed by 3 washes. Bacterial motility was monitored by video microscopy over a 2-minute period with the acquisition of 2 frames per second. Cell tracking was then analyzed with the ImageJ software using the spot tracking plug-in (http://icy.bioimageanalysis.org). Velocities of single bacterial tracks were calculated in time intervals of 2 s.

Molecular modeling

Homology modeling. Target sequences were aligned to the MS11 *N. gonorrhoeae* pilin sequence, which shares high sequence identity with our strains: 77%, 56%, 59% and 59% for 8013, LIM534, LIM707 and FAM20, respectively. Individual pilin were modeled with Modeller 9v8 [53], using unmodified amino-acids sequences. The *N. gonorrhoeae* pilin structure (PDB code 2HIL) was used as template. 500 homology models were built with the standard procedure, clustered with the MMTSB Tool Set (www.mmtsb.org), and the best structure was selected according to the Dope assessment score [54], in the most populated cluster.

Pilus modeling. The approach for building the pilus was adapted from the multi-stage procedure described by Chamot-Rooke *et al.* [36]. We used CNS [55] with a modified version of the CHARMM19 force field, which included hand-made topology and parameters for the glycosylated sites (DATDH, GATDH, GATDH-Hex). The helical properties of the pili were taken from the *N. Gonorrhoeae* structure (rise 10.5 Å, angle 105.5°) and enforced throughout the modeling using the NCS STRICT command in CNS. In this way, only one unit is explicitly modeled with 20 virtual neighbors. First, we built the structures of the glycosylated sites by quick minimization with a simplified non-bonded interaction (repulsive Van der Waals only). The rest of the pilin was kept rigid during this stage. The second stage was a refinement *in vacuo* of the whole pilin, using adapted non-bonded parameters [36]. The third stage was a refinement in water, similar to the one used in NMR structure determination [56]. During the second and the third stage, the initial structures were maintained in a flexible and adaptive way using log-harmonic distance restraints and automated weighting [57].

Supporting Information

S1 Fig. Top-down analysis of the glycosylation sites present on the three main proteoforms of the FAM20*pglHpptA* strain. For each proteoform 3 panels describe: (A) A representative top-down ETD MS/MS Orbitrap spectrum that has been performed on a single charge state of PilE; (B) shows the full fragmentation maps resulting from PTM assignment for individual experiments perform on single charge states of each proteoform and (C) The combined full fragmentation map from all experiments in panel B. Details of the assigned ions can be found in S1 Table.
(TIF)

S2 Fig. Transmission electron microscopy of negatively stained bacteria as previously described [36]. (A) LIM707; (B) LIM707*pglD*; (C) LIM354; (D) LIM534*pglD*; (E) FAM20; and (F) FAM20*pglD*.
(TIF)

S3 Fig. Impact of pilin glycosylation on adhesion to human epithelial cells. Strains 8013, LIM707, LIM 534 and their corresponding *pglD* mutants were allowed to adhere to A549 human epithelial cells for 4 hours and the number of adherent bacteria analyzed. A non-piliated *pilD* mutant of the 8013 strain was used as a negative control. Average and standard deviations are indicated from three independent experiments.
(TIF)

S4 Fig. Twitching motility in absence of glycosylation in the class II pilin expressing strains.
(TIF)

S1 Table. c/z fragment ions of the three proteoforms found in the FAM20*pglHpptA* strain.
(XLSX)

Acknowledgments

Authors wish to thank Dr. Mark Anderson (Northwestern University) for technical assistance and Ana-maria Lennon-Dumenil for critical reading of the manuscript. This work has benefited from the facilities and expertise of the high-throughput sequencing platform IMAGIF (Centre de Recherche de Gif– www.imagif.CNRS.fr).

Author Contributions

Conceived and designed the experiments: JG MF SM AFI CMa ACO GB BB IP HSS MN JCR GD. Performed the experiments: JG MF SM AFI CMa CMi GPA KK HSS ACO. Analyzed the data: JG MF SM AFI GB ACO BB CMa IP MCP MN JCR GD. Contributed reagents/materials/analysis tools: MCP HSS. Wrote the paper: JG MF ACO SM AFI JCR GD.

References

1. Brandtzaeg P, van Deuren M. Classification and pathogenesis of meningococcal infections. Methods in molecular biology. 2012; 799:21–35. doi: 10.1007/978-1-61779-346-2_2 PMID: 21993637.
2. Pelicic V. Type IV pili: e pluribus unum? Mol Microbiol. 2008; 68(4):827–37. PMID: 18399938. doi: 10.1111/j.1365-2958.2008.06197.x
3. Virji M, Heckels JE, Potts WJ, Hart CA, Saunders JR. Identification of epitopes recognized by monoclonal antibodies SM1 and SM2 which react with all pili of Neisseria gonorrhoeae but which differentiate between two structural classes of pili expressed by Neisseria meningitidis and the distribution of their encoding sequences in the genomes of Neisseria spp. Journal of general microbiology. 1989; 135 (12):3239–51. PMID: 2483993.

4. Cehovin A, Winterbotham M, Lucidarme J, Borrow R, Tang CM, Exley RM, et al. Sequence conservation of pilus subunits in Neisseria meningitidis. Vaccine. 2010; 28(30):4817–26.: doi: 10.1016/j.vaccine.2010.04.065 PMID: 20457291.

5. Wormann ME, Horien CL, Bennett JS, Jolley KA, Maiden MC, Tang CM, et al. Sequence, distribution and chromosomal context of class I and class II pilin genes of Neisseria meningitidis identified in whole genome sequences. BMC genomics. 2014; 15:253. doi: 10.1186/1471-2164-15-253 PMID: 24690385; PubMed Central PMCID: PMC4023411.

6. Giltner CL, Nguyen Y, Burrows LL. Type IV pilin proteins: versatile molecular modules. Microbiology and molecular biology reviews: MMBR. 2012; 76(4):740–72. doi: 10.1128/MMBR.00035-12 PMID: 23204365; PubMed Central PMCID: PMC3510520.

7. Kellogg DS Jr., Cohen IR, Norins LC, Schroeter AL, Reising G. Neisseria gonorrhoeae. II. Colonial variation and pathogenicity during 35 months in vitro. J Bacteriol. 1968; 96(3):596–605. PMID: 4979098; PubMed Central PMCID: PMC252347.

8. Melican K, Michea Veloso P, Martin T, Bruneval P, Dumenil G. Adhesion of Neisseria meningitidis to dermal vessels leads to local vascular damage and purpura in a humanized mouse model. PLoS Pathog. 2013; 9(1):e1003139. doi: 10.1371/journal.ppat.1003139 PMID: 23359320; PubMed Central PMCID: PMC3554624.

9. Poolman JT, Hopman CT, Zanen HC. Immunogenicity of meningococcal antigens as detected in patient sera. Infect Immun. 1983; 40(1):398–406. PMID: 6131872; PubMed Central PMCID: PMC264860.

10. Rotman E, Seifert HS. The Genetics of Neisseria Species. Annual review of genetics. 2014. doi: 10.1146/annurev-genet-120213-092007 PMID: 25251852.

11. Davies JK, Harrison PF, Lin YH, Bartley S, Khoo CA, Seemann T, et al. The use of high-throughput DNA sequencing in the investigation of antigenic variation: application to Neisseria species. PloS one. 2014; 9(1):e86704. doi: 10.1371/journal.pone.0086704 PMID: 24466206; PubMed Central PMCID: PMC3899283.

12. Helm RA, Seifert HS. Frequency and rate of pilin antigenic variation of Neisseria meningitidis. J Bacteriol. 2010; 192(14):3822–3. doi: 10.1128/JB.00280-10 PMID: 20472803; PubMed Central PMCID: PMC2897326.

13. Caugant DA, Maiden MC. Meningococcal carriage and disease—population biology and evolution. Vaccine. 2009; 27 Suppl 2:B64–70. doi: 10.1016/j.vaccine.2009.04.061 PMID: 19464092; PubMed Central PMCID: PMC2719693.

14. Gault J, Malosse C, Dumenil G, Chamot-Rooke J. A combined mass spectrometry strategy for complete posttranslational modification mapping of Neisseria meningitidis major pilin. Journal of mass spectrometry: JMS. 2013; 48(11):1199–206. doi: 10.1002/jms.3262 PMID: 24259208.

15. Hegge FT, Hitchen PG, Aas FE, Kristiansen H, Lovold C, Egge-Jacobsen W, et al. Unique modifications with phosphocholine and phosphoethanolamine define alternate antigenic forms of Neisseria gonorrhoeae type IV pili. Proc Natl Acad Sci U S A. 2004; 101(29):10798–803. PMID: 15249686.

16. Stimson E, Virji M, Makepeace K, Dell A, Morris HR, Payne G, et al. Meningococcal pilin: a glycoprotein substituted with digalactosyl 2,4-diacetamido-2,4,6-trideoxyhexose. Mol Microbiol. 1995; 17(6):1201–14. PMID: 8594338.

17. Takahashi H, Yanagisawa T, Kim KS, Yokoyama S, Ohnishi M. Meningococcal PilV potentiates Neisseria meningitidis type IV pilus-mediated internalization into human endothelial and epithelial cells. Infect Immun. 2012; 80(12):4154–66. doi: 10.1128/IAI.00423-12 PMID: 22988016; PubMed Central PMCID: PMC3497409.

18. Chamot-Rooke J, Rousseau B, Lanternier F, Mikaty G, Mairey E, Malosse C, et al. Alternative Neisseria spp. type IV pilin glycosylation with a glyceramido acetamido trideoxyhexose residue. Proc Natl Acad Sci U S A. 2007; 104(37):14783–8. PMID: 17804791.

19. Jennings MP, Virji M, Evans D, Foster V, Srikhanta YN, Steeghs L, et al. Identification of a novel gene involved in pilin glycosylation in Neisseria meningitidis. Mol Microbiol. 1998; 29(4):975–84. PMID: 9767566.

20. Borud B, Viburiene R, Hartley MD, Paulsen BS, Egge-Jacobsen W, Imperiali B, et al. Genetic and molecular analyses reveal an evolutionary trajectory for glycan synthesis in a bacterial protein glycosylation system. Proc Natl Acad Sci U S A. 2011; 108(23):9643–8. doi: 10.1073/pnas.1103321108 PMID: 21606362; PubMed Central PMCID: PMC3111294.

21. Borud B, Anonsen JH, Viburiene R, Cohen EH, Samuelsen AB, Koomey M. Extended glycan diversity in a bacterial protein glycosylation system linked to allelic polymorphisms and minimal genetic alterations in a glycosyltransferase gene. Mol Microbiol. 2014. doi: 10.1111/mmi.12789 PMID: 25213144.

22. Kahler CM, Martin LE, Tzeng YL, Miller YK, Sharkey K, Stephens DS, et al. Polymorphisms in pilin glycosylation Locus of Neisseria meningitidis expressing class II pili. Infect Immun. 2001; 69(6):3597–604. PMID: 11349019.

23. Aas FE, Vik A, Vedde J, Koomey M, Egge-Jacobsen W. Neisseria gonorrhoeae O-linked pilin glycosylation: functional analyses define both the biosynthetic pathway and glycan structure. Mol Microbiol. 2007; 65(3):607–24. doi: 10.1111/j.1365-2958.2007.05806.x PMID: 17608667; PubMed Central PMCID: PMC1976384.

24. Power PM, Seib KL, Jennings MP. Pilin glycosylation in Neisseria meningitidis occurs by a similar pathway to wzy-dependent O-antigen biosynthesis in Escherichia coli. Biochem Biophys Res Commun. 2006; 347(4):904–8. PMID: 16870136.

25. Bentley SD, Vernikos GS, Snyder LA, Churcher C, Arrowsmith C, Chillingworth T, et al. Meningococcal genetic variation mechanisms viewed through comparative analysis of serogroup C strain FAM18. PLoS genetics. 2007; 3(2):e23. doi: 10.1371/journal.pgen.0030023 PMID: 17305430; PubMed Central PMCID: PMC1797815.

26. Dyer DW, McKenna W, Woods JP, Sparling PF. Isolation by streptonigrin enrichment and characterization of a transferrin-specific iron uptake mutant of Neisseria meningitidis. Microbial pathogenesis. 1987; 3(5):351–63. PMID: 3143887.

27. Gault J, Malosse C, Machata S, Millien C, Podglajen I, Ploy MC, et al. Complete posttranslational modification mapping of pathogenic Neisseria meningitidis pilins requires top-down mass spectrometry. Proteomics. 2014; 14(10):1141–51. doi: 10.1002/pmic.201300394 PMID: 24459079; PubMed Central PMCID: PMC4201860.

28. Smith LM, Kelleher NL, Consortium for Top Down P. Proteoform: a single term describing protein complexity. Nat Methods. 2013; 10(3):186–7. doi: 10.1038/nmeth.2369 PMID: 23443629; PubMed Central PMCID: PMC4114032.

29. Naessan CL, Egge-Jacobsen W, Heiniger RW, Wolfgang MC, Aas FE, Rohr A, et al. Genetic and functional analyses of PptA, a phospho-form transferase targeting type IV pili in Neisseria gonorrhoeae. J Bacteriol. 2008; 190(1):387–400. PMID: 17951381.

30. Warren MJ, Jennings MP. Identification and characterization of pptA: a gene involved in the phase-variable expression of phosphorylcholine on pili of Neisseria meningitidis. Infect Immun. 2003; 71 (12):6892–8. PMID: 14638777.

31. Viburiene R, Vik A, Koomey M, Borud B. Allelic variation in a simple sequence repeat element of neisserial pglB2 and its consequences for protein expression and protein glycosylation. J Bacteriol. 2013; 195(15):3476–85. doi: 10.1128/JB.00276-13 PMID: 23729645; PubMed Central PMCID: PMC3719539.

32. Jen FE, Warren MJ, Schulz BL, Power PM, Swords WE, Weiser JN, et al. Dual pili post-translational modifications synergize to mediate meningococcal adherence to platelet activating factor receptor on human airway cells. PLoS Pathog. 2013; 9(5):e1003377. doi: 10.1371/journal.ppat.1003377 PMID: 23696740; PubMed Central PMCID: PMC3656113.

33. Jennings MP, Jen FE, Roddam LF, Apicella MA, Edwards JL. Neisseria gonorrhoeae pilin glycan contributes to CR3 activation during challenge of primary cervical epithelial cells. Cell Microbiol. 2011; 13 (6):885–96. doi: 10.1111/j.1462-5822.2011.01586.x PMID: 21371235; PubMed Central PMCID: PMC3889163.

34. Merz AJ, So M, Sheetz MP. Pilus retraction powers bacterial twitching motility. Nature. 2000; 407 (6800):98–102. doi: 10.1038/35024105 PMID: 10993081.

35. Parge HE, Forest KT, Hickey MJ, Christensen DA, Getzoff ED, Tainer JA. Structure of the fibre-forming protein pilin at 2.6 A resolution. Nature. 1995; 378(6552):32–8. PMID: 7477282.

36. Chamot-Rooke J, Mikaty G, Malosse C, Soyer M, Dumont A, Gault J, et al. Posttranslational modification of pili upon cell contact triggers N. meningitidis dissemination. Science. 2011; 331(6018):778–82. doi: 10.1126/science.1200729 PMID: 21311024.

37. Mortezaei N, Singh B, Bullitt E, Uhlin BE, Andersson M. P-fimbriae in the presence of anti-PapA antibodies: new insight of antibodies action against pathogens. Scientific reports. 2013; 3:3393. doi: 10.1038/srep03393 PMID: 24292100; PubMed Central PMCID: PMC3848023.

38. Borud B, Aas FE, Vik A, Winther-Larsen HC, Egge-Jacobsen W, Koomey M. Genetic, structural, and antigenic analyses of glycan diversity in the O-linked protein glycosylation systems of human Neisseria species. J Bacteriol. 2010; 192(11):2816–29. doi: 10.1128/JB.00101-10 PMID: 20363948; PubMed Central PMCID: PMC2876500.

39. Shewell LK, Ku SC, Schulz BL, Jen FE, Mubaiwa TD, Ketterer MR, et al. Recombinant truncated AniA of pathogenic Neisseria elicits a non-native immune response and functional blocking antibodies. Biochem Biophys Res Commun. 2013; 431(2):215–20. doi: 10.1016/j.bbrc.2012.12.132 PMID: 23313483; PubMed Central PMCID: PMC4326246.

40. Boslego JW, Tramont EC, Chung RC, McChesney DG, Ciak J, Sadoff JC, et al. Efficacy trial of a parenteral gonococcal pilus vaccine in men. Vaccine. 1991; 9(3):154–62. PMID: 1675029.

41. Tramont EC, Sadoff JC, Boslego JW, Ciak J, McChesney D, Brinton CC, et al. Gonococcal pilus vaccine. Studies of antigenicity and inhibition of attachment. The Journal of clinical investigation. 1981; 68 (4):881–8. PMID: 6116723; PubMed Central PMCID: PMC370875.

42. Power PM, Roddam LF, Rutter K, Fitzpatrick SZ, Srikhanta YN, Jennings MP. Genetic characterization of pilin glycosylation and phase variation in Neisseria meningitidis. Mol Microbiol. 2003; 49(3):833–47. PMID: 12864863.

43. Mayer LW. Rates in vitro changes of gonococcal colony opacity phenotypes. Infect Immun. 1982; 37 (2):481–5. PMID: 6126433; PubMed Central PMCID: PMC347559.

44. Richardson AR, Stojiljkovic I. Mismatch repair and the regulation of phase variation in Neisseria meningitidis. Mol Microbiol. 2001; 40(3):645–55. PMID: 11359570.

45. Lamelas A, Harris SR, Roltgen K, Dangy JP, Hauser J, Kingsley RA, et al. Emergence of a New Epidemic Neisseria meningitidis Serogroup A Clone in the African Meningitis Belt: High-Resolution Picture of Genomic Changes That Mediate Immune Evasion. mBio. 2014; 5(5). doi: 10.1128/mBio.01974-14 PMID: 25336458.

46. Vik A, Aspholm M, Anonsen JH, Borud B, Roos N, Koomey M. Insights into type IV pilus biogenesis and dynamics from genetic analysis of a C-terminally tagged pilin: a role for O-linked glycosylation. Mol Microbiol. 2012; 85(6):1166–78. doi: 10.1111/j.1365-2958.2012.08166.x PMID: 22882659.

47. Harvey H, Kus JV, Tessier L, Kelly J, Burrows LL. Pseudomonas aeruginosa D-arabinofuranose biosynthetic pathway and its role in type IV pilus assembly. J Biol Chem. 2011; 286(32):28128–37. doi: 10.1074/jbc.M111.255794 PMID: 21676874; PubMed Central PMCID: PMC3151058.

48. VanDyke DJ, Wu J, Logan SM, Kelly JF, Mizuno S, Aizawa S, et al. Identification of genes involved in the assembly and attachment of a novel flagellin N-linked tetrasaccharide important for motility in the archaeon Methanococcus maripaludis. Mol Microbiol. 2009; 72(3):633–44. doi: 10.1111/j.1365-2958.2009.06671.x PMID: 19400781.

49. Bernard SC, Simpson N, Join-Lambert O, Federici C, Laran-Chich MP, Maissa N, et al. Pathogenic Neisseria meningitidis utilizes CD147 for vascular colonization. Nature medicine. 2014; 20(7):725–31. doi: 10.1038/nm.3563 PMID: 24880614.

50. Ke SH, Madison EL. Rapid and efficient site-directed mutagenesis by single-tube 'megaprimer' PCR method. Nucleic Acids Res. 1997; 25(16):3371–2. PMID: 9241254; PubMed Central PMCID: PMC146891.

51. Marceau M, Beretti JL, Nassif X. High adhesiveness of encapsulated Neisseria meningitidis to epithelial cells is associated with the formation of bundles of pili. Mol Microbiol. 1995; 17(5):855–63. PMID: 8596435.

52. Eugene E, Hoffmann I, Pujol C, Couraud PO, Bourdoulous S, Nassif X. Microvilli-like structures are associated with the internalization of virulent capsulated Neisseria meningitidis into vascular endothelial cells. J Cell Sci. 2002; 115(Pt 6):1231–41. PMID: 11884522.

53. Sali A, Blundell TL. Comparative protein modelling by satisfaction of spatial restraints. Journal of Molecular Biology. 1993; 234(3):779–815. doi: 10.1006/jmbi.1993.1626 PMID: 8254673.

54. Shen M-Y, Sali A. Statistical potential for assessment and prediction of protein structures. Protein science: a publication of the Protein Society. 2006; 15(11):2507–24. doi: 10.1110/ps.062416606 PMID: 17075131; PubMed Central PMCID: PMCPMC2242414.

55. Brünger AT, Adams PD, Clore GM, DeLano WL, Gros P, Grosse-Kunstleve RW, et al. Crystallography & NMR system: A new software suite for macromolecular structure determination. Acta crystallographica Section D, Biological crystallography. 1998; 54(Pt 5):905–21. PMID: 9757107.

56. Linge JP, Williams MA, Spronk CA, Bonvin AM, Nilges M. Refinement of protein structures in explicit solvent. Proteins. 2003; 50(3):496–506. PMID: 12557191.

57. Nilges M, Bernard A, Bardiaux B, Malliavin T, Habeck M, Rieping W. Accurate NMR structures through minimization of an extended hybrid energy. Structure. 2008; 16(9):1305–12. PMID: 18786394. doi: 10.1016/j.str.2008.07.008

58. Nassif X, Lowy J, Stenberg P, O'Gaora P, Ganji A, So M. Antigenic variation of pilin regulates adhesion of Neisseria meningitidis to human epithelial cells. Mol Microbiol. 1993; 8(4):719–25. PMID: 8332064.

59. Geoffroy MC, Floquet S, Metais A, Nassif X, Pelicic V. Large-scale analysis of the meningococcus genome by gene disruption: resistance to complement-mediated lysis. Genome Res. 2003; 13(3):391–8. PMID: 12618369.

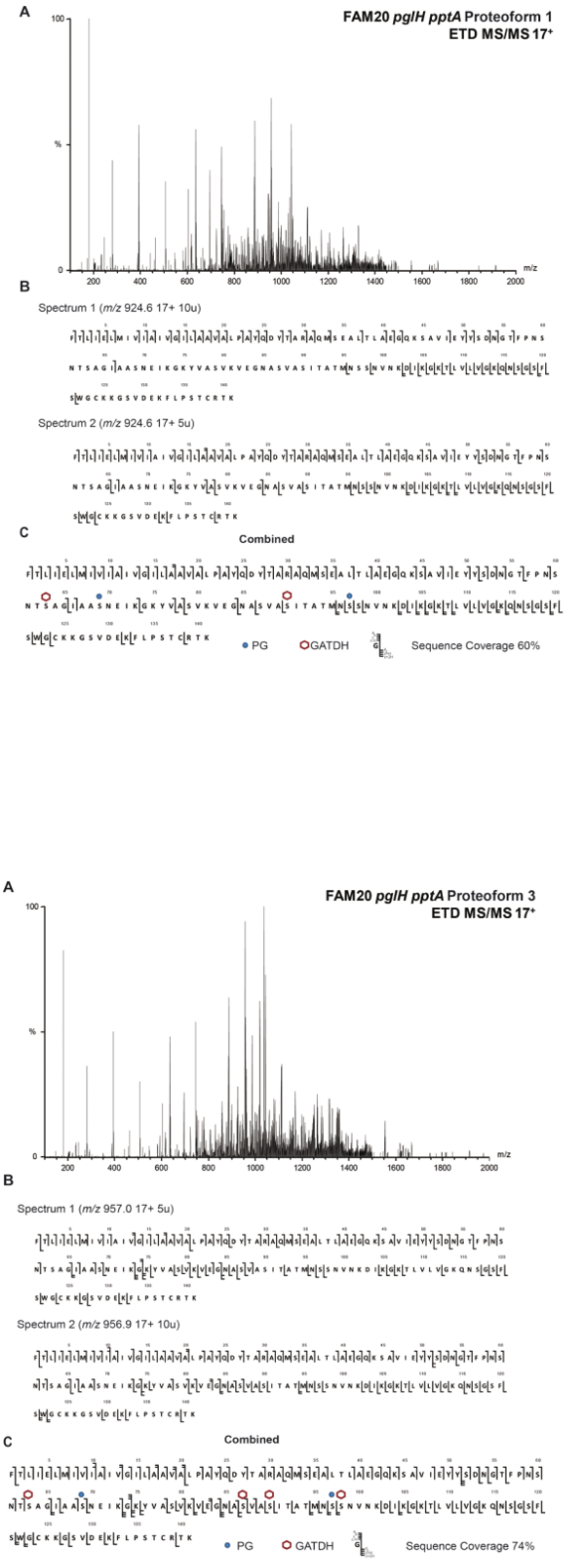
A
FAM20 pglH pptA Proteoform 1
ETD MS/MS 17+
B
Spectrum 1 (m/z 924.6 17+ 10u)
Spectrum 2 (m/z 924.6 17+ 5u)
C
Combined
PG
GATDH
Sequence Coverage 60%

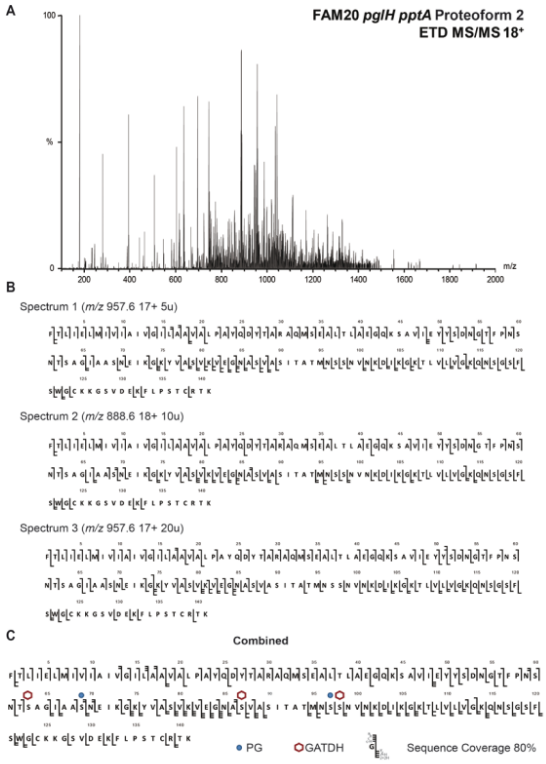
A
FAM20 pglH pptA Proteoform 2
ETD MS/MS 18+
B
Spectrum 1 (m/z 957.6 17+ 5u)
Spectrum 2 (m/z 888.6 18+ 10u)
Spectrum 3 (m/z 957.6 17+ 20u)
C
Combined
PG
GATDH
Sequence Coverage 80%

A
FAM20 pglH pptA Proteoform 3
ETD MS/MS 17+
B
Spectrum 1 (m/z 957.0 17+ 5u)
Spectrum 2 (m/z 956.9 17+ 10u)
C
Combined
PG
GATDH
Sequence Coverage 74%

Fig. S1

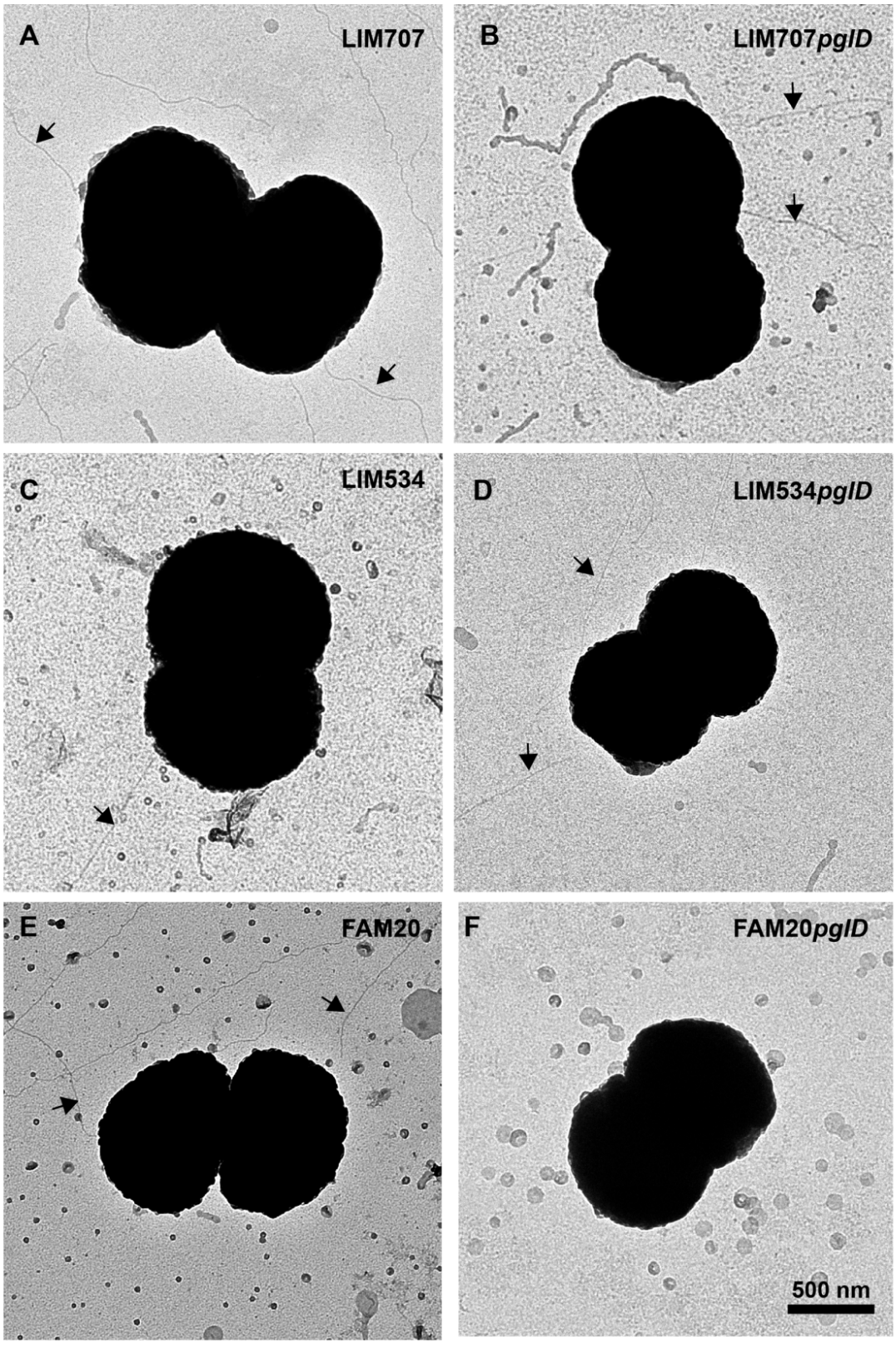
A
LIM707
B
LIM707pglD
C
LIM534
D
LIM534pglD
E
FAM20
F
FAM20pglD
500 nm

Fig. S2

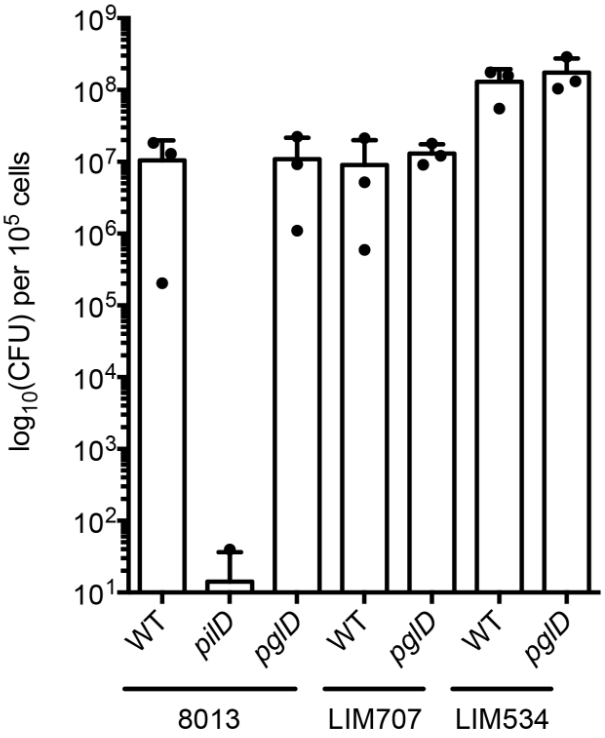
log10(CFU) per 10^5 cells
10^9
10^8
10^7
10^6
10^5
10^4
10^3
10^2
10^1
WT
pilD
pglD
WT
pglD
WT
pglD
8013
LIM707
LIM534

Fig. S3

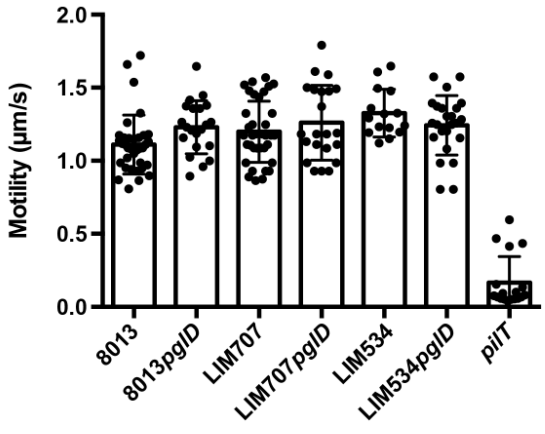
Motility (µm/s)
2.0
1.5
1.0
0.5
0.0
8013
8013pglD
LIM707
LIM707pglD
LIM534
LIM534pglD
pilT

Fig. S4

2. Microbial pathogenesis meets biomechanics

During this PhD, I also had the opportunity to co-author a review article in a special issue of Current Opinion in Cell Biology on cell architecture.

In this review, we describe three examples where the study of physical forces has been crucial to the understanding of the interactions between bacterial pathogens, or toxins, and their target cells. We stress that inputs from the different fields of physics will likely shine light on many biological questions in the future.

Available online at www.sciencedirect.com

ScienceDirect

Current Opinion in Cell Biology

Microbial pathogenesis meets biomechanics

Arthur Charles-Orszag[1], Emmanuel Lemichez[2], Guy Tran Van Nhieu[3,4,5,6] and Guillaume Duménil[1]

Introducing concepts from soft matter physics and mechanics has largely contributed to our understanding of a variety of biological processes. In this review, we argue that this holds true for bacterial pathogenesis. We base this argument on three examples of bacterial pathogens and their interaction with host cells during infection: (i) *Shigella flexneri* exploits actin-dependent forces to come into close contact with epithelial cells prior to invasion of the epithelium; (ii) *Neisseria meningitidis* manipulates endothelial cells to resist shear stress during vascular colonization; (iii) bacterial toxins take advantage of the biophysical properties of the host cell plasma membrane to generate transcellular macroapertures in the vascular wall. Together, these examples show that a multidisciplinary approach integrating physics and biology is more necessary than ever to understand complex infectious phenomena. Moreover, this avenue of research will allow the exploration of general processes in cell biology, highlighted by pathogens, in the context of other non-communicable human diseases.

Addresses
[1] Pathogenesis of vascular infections unit, INSERM, Institut Pasteur, 75015 Paris, France
[2] INSERM, U1065, Microbial Toxins in Host–Pathogen Interactions, Centre Méditerranéen De Médecine Moléculaire, C3M, 151 Route St Antoine de Ginestière, 06204 Nice, France
[3] Equipe Communication Intercellulaire et Infections Microbiennes, Centre de Recherche Interdisciplinaire en Biologie (CIRB), Collège de France, Paris, France
[4] Institut National de la Santé et de la Recherche Médicale U1050, Paris, France
[5] Centre National de la Recherche Scientifique UMR 7241, Paris, France
[6] MEMOLIFE Laboratory of Excellence and Paris Science Lettre, Paris, France

Corresponding author: Duménil, Guillaume (guillaume.dumenil@inserm.fr)

Current Opinion in Cell Biology 2016, **38**:31–37

This review comes from a themed issue on **Cell architecture**

Edited by **Margaret L Gardel** and **Matthieu Piel**

http://dx.doi.org/10.1016/j.ceb.2016.01.005

Introduction

The study of bacterial pathogenesis has revealed a wealth of interactions between bacteria and their host. This is crucial for a successful colonization and invasion of host tissues by pathogenic bacteria. Depending on the site of entry and bacterial niches during infection, different cell types are encountered. Epithelial cells are particularly exposed during initial infection stages, but pathogens also interact with immune and endothelial cells during invasive diseases. Pathogens use elaborate molecular machineries to manipulate host cells. Dedicated secretion systems act as nano-syringes to translocate effector proteins that modulate cellular functions across the plasma membrane. Bacterial filamentous structures, such as pili, sometimes reaching several times the length of the bacterium itself, provide the means to adhere to the cellular surface. Bacteria can also act on cells at a distance, by secreting toxins that affect the plasma membrane integrity and/or perturb various host cell processes upon internalization.

When 'cellular microbiology' was still an emerging field, Stanley Falkow and Brett Finlay wrote a seminal review entitled 'Common themes in microbial pathogenicity' mostly focusing on the molecular mechanisms involved [1]. We would like to argue that coping with and exploiting mechanical forces is an emerging common theme in bacterial pathogenesis. This is well illustrated in pioneering works on the *Escherichia coli* type 1 fimbriae, depicting the 'catch-bond' mechanism through elastic adhesin tethers that enables bacterial optimal adhesion under the shear stress conditions encountered in the urinary tract [2••]. In general, infections take place in the context of the mechanical forces generated within host tissues, related for instance to blood flow, muscular contraction or cytoskeletal contractility at the level of individual cells. Furthermore, it has become apparent that host membranes can be described as a composite material endowed with specific biomechanical properties, and that it can be reshaped by pathogenic bacteria [3]. Objects as small as cells, for which inertial forces are not dominant, is best described by principles borrowed from the soft inert matter field [4,5]. A recent review has described the impact of mechanical forces in the context of microbial ecology [6•]. The present review focuses on bacterial pathogenesis. We discuss three examples where the impact of forces during the interaction of bacteria and their toxins with host cells has been explored. These examples highlight the importance of mechanical forces at prototypical stages of infection and at the scale of molecules, cells and tissues.

Pulling its way through the epithelium

Upon ingestion of contaminated foodstuff, *Shigella* reaches the colonic mucosa and invades it, leading to

an intense inflammatory reaction responsible for tissue destruction and bloody diarrhea. *Shigella* expresses a so-called type III secretion system (T3SS), which is responsible for the injection of bacterial effectors upon cell contact [7], triggering the formation of membrane ruffles and bacterial invasion (Figure 1a).

Initial studies focused on the global bacterial population suggested that contrary to other invasive bacteria, *Shigella* does not display constitutive adhesion to the host cell surface. Real-time microscopy and single bacterium analysis then revealed that only a minority of bacteria adheres to filopodia tips, often transiently (Figure 1a,b). Upon contact, filopodia retract bringing bound bacteria in close contact with the cell body, where membrane ruffles are induced and bacterial internalization occurs. *Shigella* capture by filopodial extensions consistently precedes bacterial invasion and appears to act as a bottleneck sorting out proficient interactions with bacteria, thus providing a mechanism for invasion without constitutive adhesion. This process implies that mechanical forces are exerted on bacteria bound to the filopodia tips, and that the strength of the interaction at this tip determines retraction towards the cell body, hence invasion.

At the molecular level, filopodia interaction occurs through a specific set of proteins located at the tip of the T3SS, explaining their interaction with the bacterial pole where active secretion predominantly occurs [8,9]. The receptors involved in *Shigella* capture by filopodia have not been identified yet, but appear to be sensitive to the depletion of extracellular Ca^{2+}, consistent with cadherins or integrins [10]. Only a limited number of bacteria and filopodia, however, are involved in capture, suggesting heterogeneity among bacteria as well as filopodia [9]. While not fully elucidated, key insights into the mechanism of bacteria-induced filopodial retraction have been provided through force measurements. Using optical tweezers, it was found that beads coated with bacterial membranes containing the *Shigella* T3SS are pulled by single filopodia with a maximal force of 15 pN. This force equals or even exceeds that of beads coated with the *Yersinia* Invasin, a beta 1 integrin ligand, at a density allowing the interaction of thousands of molecules with the filopodial tip. Since only a discrete number (<10) of *Shigella* T3SSs are expected to interact with a filopodial tip, the T3SS tip complex appears to optimally promote filopodial retraction [10]. As opposed to what is described for viruses targeting filopodia, filopodial retraction following *Shigella* contact occurs in the presence of myosin II inhibitors but is impaired in the presence of actin polymerization inhibitors [9]. Consistently, it was found that the F-actin retrograde flow linked to actin treadmilling at the cell cortex is the major driving force pulling filopodial actin filaments inwards [11••]. Because actin polymerization in the cell cortex generates forces in the hundreds of

Figure 1

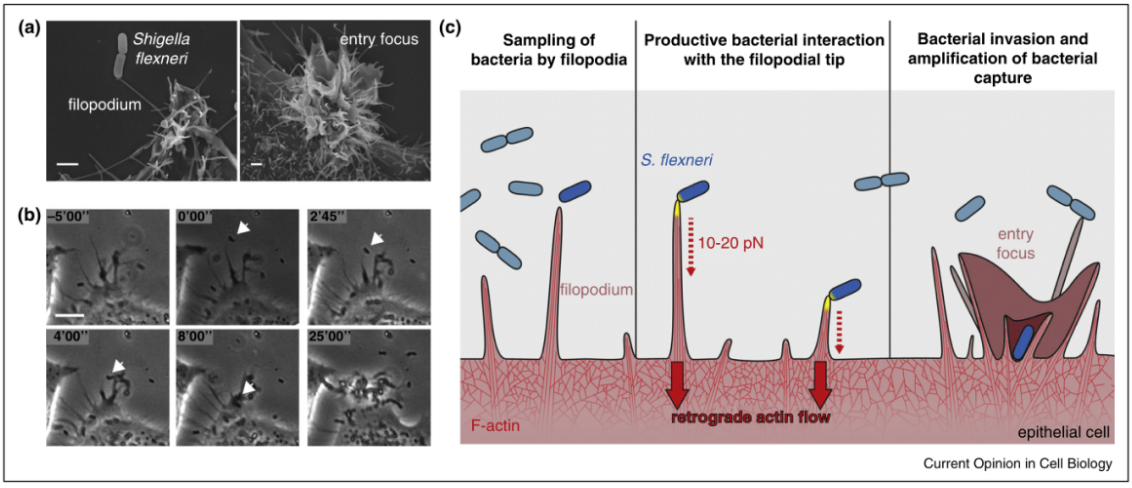

Filopodial retraction forces exploited by *S. flexneri* for invasion. **(a)** Scanning electron micrograph showing *S. flexneri* interacting with a filopodium emanating from an epithelial cell (left) prior to engulfment of the bacterium at the entry focus characterized by localized membrane ruffling (right). Scale bars = 1 μm. **(b)** Snapshots from a live cell imaging experiment showing the dynamics of one bacterium (white arrow) being sampled and captured by a filopodium. Scale bar = 5 μm. **(c)** Proposed model for filopodial retraction following bacterial capture. Epithelial cells sample invasion-proficient *S. flexneri* through filopodial extensions (left panel). Productive interaction between one bacterial pole and the filopodial tip triggers filopodial retraction that exerts forces in the 10–20 pN range powered by the actin retrograde flow (middle panel). Reorganization of the cell surface upon contact of *S. flexneri* with the cell body leads to bacterial internalization at the entry focus and subsequent amplification of the bacterial capture.

nanoN range, it cannot represent a limiting factor to the force exerted by retracting filopodia. Rather, the link between receptors and actin filaments at the filopodial tip likely limits the retraction force.

These findings have important implications and are supportive of the model depicted in Figure 1c: filopodia sample bacteria that are proficient for invasion; receptor clustering by the *Shigella* T3SS tip complex components leads to the recruitment of a cytoskeletal linker physically bridging bacteria to filopodial actin filaments; inhibition of actin polymerization at the tip of filopodia, possibly mediated by the cytoskeletal linker, results in filopodial retraction powered by the retrograde flow. Bacterial sampling by filopodia is consistent with the sensor function of these organelles and supports the notion of a discrete mode of invasion limiting bacterial exposure associated with constitutive cell adhesion [12]. Filopodia sampling of bacteria may also allow the targeting of specific sites within the intestinal epithelium [13]. Deciphering the mechanics of bacterial invasion emerges as an exciting challenge, key to an in-depth understanding of bacterial pathogenesis.

Coping with blood flow-generated shear stress while adhering to the endothelium

Infections caused by *Neisseria meningitidis* fall into the group of severe infections that occur when the pathogen makes its way to the bloodstream leading to sepsis and meningitis. Sepsis is arguably the most severe form of such infections. *N. meningitidis* adheres along the microvessels in multiple organs and proliferates in the form of aggregates eventually filling the vessel lumen [14•]. This complex process termed *vascular colonization* [15] is of key importance as it determines the vascular damage observed during the infection [16].

An important, and generally overlooked, implication of the circulation as an infection site is the presence of blood flow and the mechanical forces generated by it. Blood flow generates drag forces parallel to the vascular wall on objects depending on their geometry, on the blood viscosity and its velocity, and on the vessel diameter and geometry. These forces are often expressed as a function of wall shear stress, the force per area expressed in dynes/cm^2. Interestingly, shear stress levels in the vasculature vary greatly along the vascular tree. In particular, arteries have the highest shear stress levels, veins present lower levels and capillaries show the highest heterogeneity over time [17]. In capillaries, shear stress can be as high as 80 dynes/cm^2 and suddenly decrease to values close to zero during a few seconds to a few minutes. Contrary to other bacteria such as uropathogenic *E. coli* [18], *N. meningitidis* adhesion only occurs at low levels of shear stress [14•]. As a result the initial adhesion occurs only when the shear stress level is sufficiently low, that is, in capillaries (Figure 2a). This is supported experimentally by adhesion assays in flow chambers as well as by *post-mortem* analysis of human cases where the bacterium is found only in the microcirculation. In this case, the mechanical properties of the blood flow determine where the bacterium will eventually bind. Interestingly, similar processes occur in cancer where metastatic seeding is proposed to occur at sites of optimal flow patterns [19].

After initial adhesion bacteria proliferate on the endothelial surface. *N. meningitidis* also has the ability to autoaggregate and proliferation leads to the formation of compact groups of bacteria tightly bound to the endothelial cell surface (Figure 2b). Since the lumen size of the capillaries is only in the order of 10 μm and one bacterium is about 1 μm in diameter, a few cycles of division are sufficient for bacteria to fill the vessel lumen. Progressive occlusion of the microcirculation is likely to play an important role in the vascular damage and the organ failures observed during infection. The presence of bacterial aggregates inside the vessel lumen implies strong mechanical cohesion. Surprisingly, bacterial aggregates in suspension are disrupted by the kind of forces found in the circulation, indicating that interaction with endothelial cells modifies the mechanical properties of the aggregates [20••]. Close observation of *N. meningitidis* proliferating on the endothelial surface shows that an intense cross talk is taking place [21]. Multiple filopodia-like structures extend from the plasma membrane and invade the bacterial microcolony, generating a compact structure that allows the aggregate to resist the highest shear stress levels (Figure 1b). Beyond a clear role of type IV pili, how this bacterium triggers the formation of these membrane structures is not yet fully understood [20••,22–24].

Overall, in the case of *N. meningitidis* infections, the biophysical properties of the blood circulation have a strong impact on the infection process: first, by determining the site of infection; second, by imposing a complex cross talk between endothelial cells and bacteria, enabling them to resist blood flow-generated shear stress.

Opening secret passages through the endothelium

Intoxication of endothelial cells by a group of potent toxins secreted by bacteria causes vascular leakages, gelatinous edema and contributes to the dissemination of bacteria via the hematogenous route [25–27]. These tunnel-forming toxins (TFTx) are endowed with the capacity to open giant transcellular holes across the endothelium called trans-endothelial macroapertures (TEMs) that can reach up to 20 μm in width, by a phenomenon analogous to the dewetting of liquid films (Figure 3a,b) [25]. Opposite to spreading, dewetting refers to the spontaneous withdrawal of a liquid film from a non-wettable surface by nucleation and growth of dry regions (Figure 3c) [28]. TFTx have in common the

Figure 2

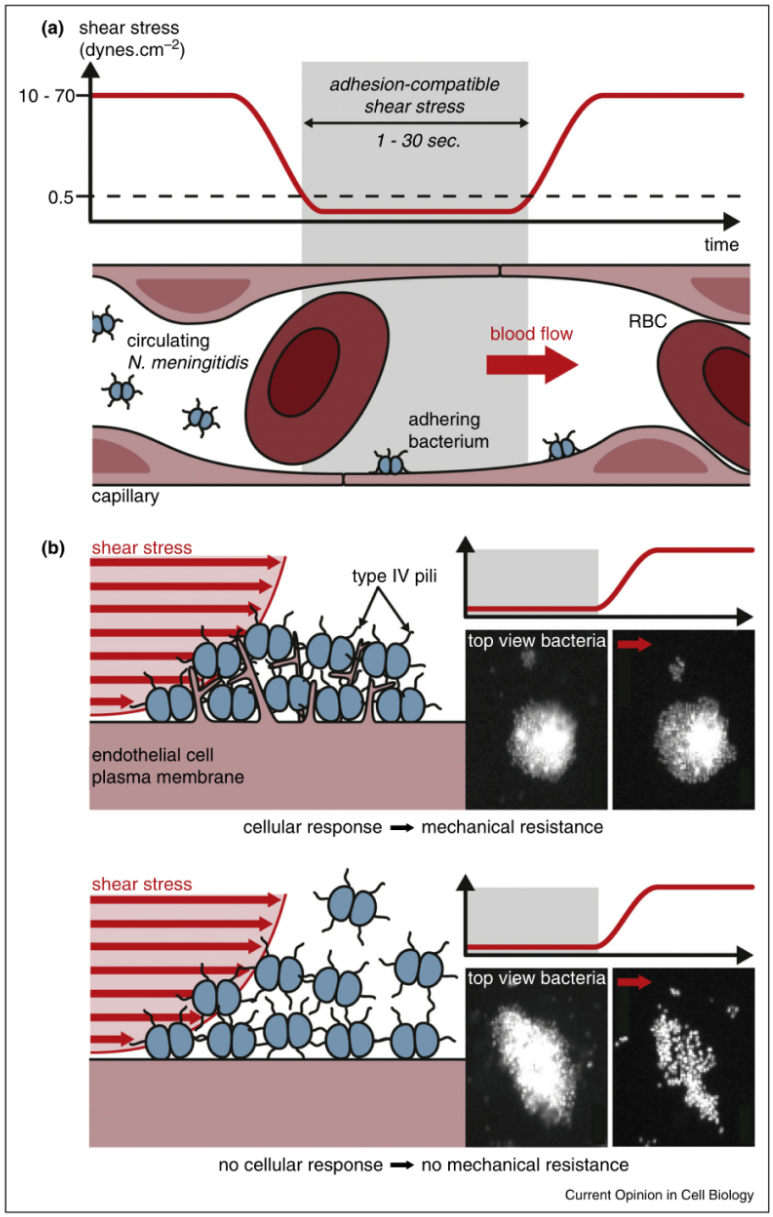

Impacts of blood shear stress on *N. meningitidis* physiopathology. **(a)** *N. meningitidis* that has entered the human circulation cannot bind vessels walls until the blood flow-generated shear stress levels reach values compatibles with bacterial adhesion. Irreversible adhesion of meningococcus to the endothelial cells through type IV pili allows bacterial proliferation and subsequent damage to the vessels. **(b)** Reshaping of the endothelial cell plasma membrane by adherent meningococci provides bacterial microcolonies mechanical resistance to high shear stress levels (top panel). Mutants that are unable to trigger this cellular response lack mechanical resistance and remain sensitive to shear stress (bottom panel). For each case, snapshots from live cell imaging experiments show bacterial microcolonies adhering to human endothelial cells before (left) and after (right) the addition of flow.

Figure 3

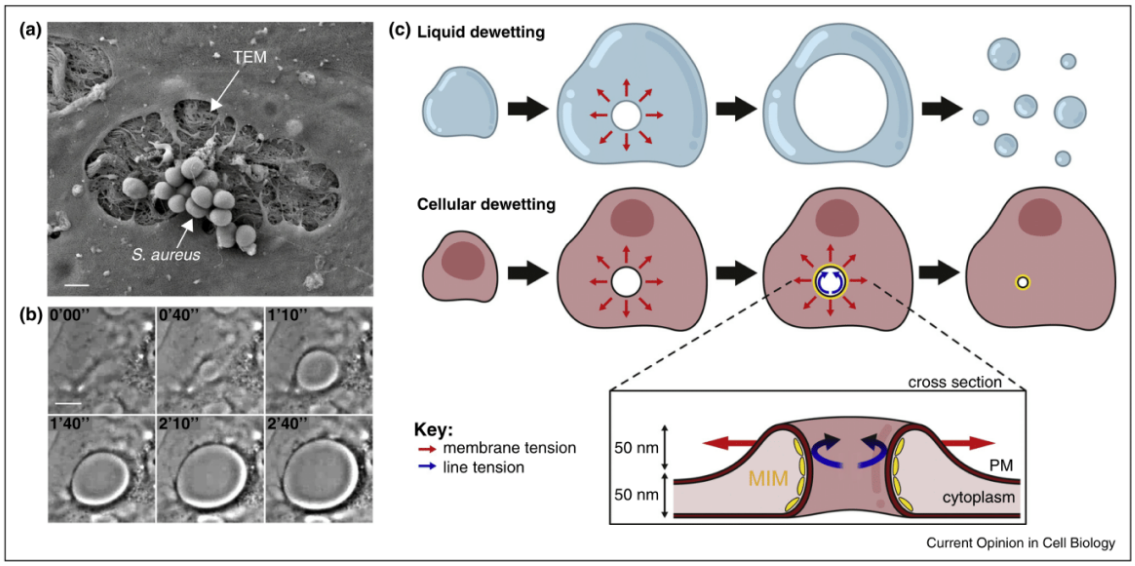

Physical principles in cellular dewetting induced by bacterial toxins. **(a)** Scanning electron micrograph showing transendothelial cell macroaperture (TEM) tunnels induced by EDIN-expressing *S. aureus* on the surface of artery-lining endothelial cells. This unmasks the matrix fibers, which serve as substrate for bacterial adhesion. Scale bar = 1 μm. **(b)** Snapshots from a live cell imaging experiment showing the formation and enlargement of TEMs in an endothelial cell intoxicated with EDIN. Scale bar = 5 μm. **(c)** Liquid dewetting classically describes the rupture of a thin liquid film on a non-wettable surface and the formation of droplets (top panel). In the cellular mode of dewetting, cells limit TEM enlargement to a diameter of about ten microns. Holes widen as a function of the tension of the membrane that originates from cell spreading, exerting a tensile force on the tunnel (red arrows). Membrane tension itself depends on the radius of the tunnel and decreases as the tunnel size increases. In addition, enlargement of the holes is resisted by the induction of a line tension along TEM edges (blue arrows) partially supported by the activity of the I-BAR domain containing protein missing-in-metastasis (MIM). PM: plasma membrane.

property of triggering actomyosin relaxation, thereby causing endothelial cell spreading [29]. This is caused by: (i) the direct inhibition of the small GTPase RhoA by EDIN-like factor virulence attributes from *S. aureus* [30] or (ii) the action of adenylate-cyclases from *Bacillus anthracis* or *Bordetella pertussis*, which exacerbate the flux of cyclic adenosine monophosphate (cAMP) broad signaling molecule and the downstream EPAC/Rap and protein kinase A (PKA) signaling pathways [26••]. Endothelial cell spreading induced by toxins likely involves a disruption of the cytoskeletal mechanical network which, in non-pathological cells, balances membrane tension and controls cell shape [31]. As discussed in recent reviews, the deformation, contractility and compliance properties of biological tissues make them akin to soft inert matter, such as viscoelastic liquids [32••,33]. Physical principles of soft matter have been instrumental in characterizing the dynamics of TEMs [25,32••]. Indeed, exploiting these phenomenological similarities, Gonzalez-Rodriguez and collaborators have modeled cellular dewetting leading to several deductions on the dynamics of TEM opening [32••] (Figure 3c). In good agreement with the experimental data, the driving force to form and enlarge a hole is given by the increase of membrane tension of spread cells. Membrane tension is then locally relaxed by opening the TEM until an equilibrium size is attained, where membrane tension and line tension balance out [25,32••] (Figure 3c). Analogous to liquid dewetting, the cellular material removed from the hole is collected in a ridge that forms at the edge of TEMs. This ridge has been evidenced by video microscopy coupled to atomic force microscopy [26••].

Comparison of both forms of dewetting has also highlighted a major behavior difference between inert and active matter. While liquids undergo complete dewetting up to the formation of droplets, cellular dewetting progresses only up to a maximum TEM size. This difference is due to two specific features of cellular dewetting: relaxation of membrane tension with hole size and building up of line tension along the TEM's edge in order to resist to the enlargement (Figure 3c). These studies have opened the search for cellular factors controlling line tension, taking into account that dewetting generates curved membrane at the edge of TEMs (Figure 3c). In this context, one good candidate would be a curvature-sensitive protein such as Bin-Amphiphysin-Rvs (BAR)-domain containing proteins that form homodimers of crescent shape

endowed with the capacity to sense and/or deform membranes depending on protein concentration [34]. Interestingly, the subfamily of inverse-BAR (I-BAR) proteins possesses a unique convex membrane-binding interface offering a good fit with membrane curvature at the edge of TEMs [35•]. The I-BAR protein missing-in-metastasis (MIM) starts to accumulate at the edge of TEMs a few hundred milliseconds after their opening, offering *in vivo* evidence of its capacity to sense a curved membrane [26••]. MIM depletion leads to opening of TEMs of a larger size, pointing to its contributing role to line tension together with other uncharacterized factors [32••]. MIM is a bifunctional protein that sets the recruitment of the ARP2/3-dependent actin polymerization machinery along the edge of TEMs thereby promoting the formation of protruding membrane waves [35•]. This activity of MIM is essential for promoting the closure of TEMs, making such structures transitional passages. Study of TEM dewetting offers a good cell biology model and theoretical frame to determine how cells control the strength and compliance of the plasma membrane.

Conclusions and perspectives

The three examples described above only represent selected facets and we anticipate that biophysical considerations are unavoidable to understand mechanisms relevant for virtually all bacterial infection models. For instance, in addition to blood flow, shear stress is also generated by various mucosal fluids including urine or mucus at the epithelial surfaces. Such shear stress will not only affect the adhesive or invasive properties of pathogens, but also their interaction with immune cells [36]. Beyond mechanical forces, electric and magnetic fields are also likely to influence microbial pathogenesis as they do for other cellular processes such as migration and polarity [37]. Soft matter physics of bacterial aggregation in particular in the context of biofilm formation is another rapidly moving field relevant for pathogenesis [38]. It should be emphasized that the emergence of these different research directions is currently made possible by the availability of novel techniques derived from the physical field that are now being adapted to biological systems. A non-exhaustive list would include microfluidics, micropipette aspiration, surface micropatterns, artificial lipid membranes and optical tweezers. Another key element of success for this type of studies is a close collaboration between biologists and physicists. Work at the interface with physics will undoubtedly allow us to make a quantum leap in our understanding of microbial pathogenesis.

Acknowledgments

Authors would like to thank Daria Bonazzi for discussions and critical reading of the manuscript. This work was supported by the French ministry for research and higher education (ACO); the Avenir INSERM Starting Grant (GD); the Integrative Biology of Emerging Infectious Diseases (IBEID) laboratory of excellence (GD); a European Research Council starting grant (GD); the BUGS-IN-FLOW ANR (agence nationale pour la recherche) grant; the investments for the future LABEX SIGNALIFE program reference ANR-11-LABX-0028-01 (EL); the ANR *TransEndotheliaTunnel* grant (EL); the Memolife LABEX (GTVN) and the IDEX Paris Science et Lettres, inter-institutions structuring program (GTVN).

References and recommended reading

Papers of particular interest, published within the period of review, have been highlighted as:

- • of special interest
- •• of outstanding interest

1. Finlay BB, Falkow S: **Common themes in microbial pathogenicity revisited**. *Microbiol Mol Biol Rev* 1997, **61**: 136-169.

2. •• Sokurenko EV, Vogel V, Thomas WE: **Catch-bond mechanism of force-enhanced adhesion: counterintuitive, elusive, but … widespread?** *Cell Host Microbe* 2008, **4**:314-323.
This review presents the latest views on how, through catch-bond interactions mediated by the type I fimbriae adhesion FimH, uropathogenic *E. coli* adapts its adhesion as a function of shear stress.

3. Salbreux G, Charras G, Paluch E: **Actin cortex mechanics and cellular morphogenesis**. *Trends Cell Biol* 2012, **22**:536-545.

4. de Gennes PG: **Soft matter**. *Science* 1992, **256**:495-497.

5. Gonzalez-Rodriguez D, Guevorkian K, Douezan S, Brochard-Wyart F: **Soft matter models of developing tissues and tumors**. *Science* 2012, **338**:910-917.

6. • Persat A, Nadell CD, Kim MK, Ingremeau F, Siryaporn A, Drescher K, Wingreen NS, Bassler BL, Gitai Z, Stone HA: **The mechanical world of bacteria**. *Cell* 2015, **161**:988-997.
An insightful and thorough review of the impact of mechanics in bacterial ecology.

7. Cossart P, Sansonetti PJ: **Bacterial invasion: the paradigms of enteroinvasive pathogens**. *Science* 2004, **304**:242-248.

8. Jaumouille V, Francetic O, Sansonetti PJ, Tran Van Nhieu G: **Cytoplasmic targeting of IpaC to the bacterial pole directs polar type III secretion in *Shigella***. *EMBO J* 2008, **27**:447-457.

9. Romero S, Grompone G, Carayol N, Mounier J, Guadagnini S, Prevost MC, Sansonetti PJ, Van Nhieu GT: **ATP-mediated Erk1/2 activation stimulates bacterial capture by filopodia, which precedes *Shigella* invasion of epithelial cells**. *Cell Host Microbe* 2011, **9**:508-519.

10. Romero S, Quatela A, Bornschlog T, Guadagnini S, Bassereau P, Tran Van Nhieu G: **Filopodium retraction is controlled by adhesion to its tip**. *J Cell Sci* 2012, **125**:4999-5004.

11. •• Bornschlogl T, Romero S, Vestergaard CL, Joanny JF, Van Nhieu GT, Bassereau P: **Filopodial retraction force is generated by cortical actin dynamics and controlled by reversible tethering at the tip**. *Proc Natl Acad Sci U S A* 2013, **110**: 18928-18933.
Using force measurements, this article shows that filopodial retraction is powered by actin treadmilling at the cell cortex and membrane tension, a process relevant for invasion by enteroinvasive *Shigella*.

12. Heckman CA, Plummer HK 3rd: **Filopodia as sensors**. *Cell Signal* 2013, **25**:2298-2311.

13. Carayol N, Tran Van Nhieu G: **Tips and tricks about *Shigella* invasion of epithelial cells**. *Curr Opin Microbiol* 2013, **16**:32-37.

14. • Mairey E, Genovesio A, Donnadieu E, Bernard C, Jaubert F, Pinard E, Seylaz J, Olivo-Marin JC, Nassif X, Dumenil G: **Cerebral microcirculation shear stress levels determine *Neisseria meningitidis* attachment sites along the blood–brain barrier**. *J Exp Med* 2006, **203**:1939-1950.
The first demonstration of the importance of shear stress in the determination of the adhesion site of *Neisseria meningitidis* along the cerebral microcirculation.

15. Melican K, Dumenil G: **Vascular colonization by *Neisseria meningitidis***. *Curr Opin Microbiol* 2012, **15**:50-56.

16. Melican K, Michea Veloso P, Martin T, Bruneval P, Dumenil G: **Adhesion of *Neisseria meningitidis* to dermal vessels leads to**

local vascular damage and purpura in a humanized mouse model. *PLoS Pathog* 2013, **9**:e1003139.

17. Pries AR, Secomb TW, Gessner T, Sperandio MB, Gross JF, Gaehtgens P: **Resistance to blood flow in microvessels in vivo**. *Circ Res* 1994, **75**:904-915.

18. Thomas WE, Trintchina E, Forero M, Vogel V, Sokurenko EV: **Bacterial adhesion to target cells enhanced by shear force**. *Cell* 2002, **109**:913-923.

19. Azevedo AS, Follain G, Patthabhiraman S, Harlepp S, Goetz JG: **Metastasis of circulating tumor cells: Favorable soil or suitable biomechanics, or both?** *Cell Adh Migr* 2015, **9**: 345-356.

20. •• Mikaty G, Soyer M, Mairey E, Henry N, Dyer D, Forest KT, Morand P, Guadagnini S, Prevost MC, Nassif X: **Extracellular bacterial pathogen induces host cell surface reorganization to resist shear stress**. *PLoS Pathog* 2009, **5**:e1000314.
This article shows how the crosstalk between *Neisseria meningitidis* and endothelial cells enhances the mechanical cohesion of adhering micro-colonies in the face of blood flow.

21. Eugene E, Hoffmann I, Pujol C, Couraud PO, Bourdoulous S, Nassif X: **Microvilli-like structures are associated with the internalization of virulent capsulated *Neisseria meningitidis* into vascular endothelial cells**. *J Cell Sci* 2002, **115**:1231-1241.

22. Coureuil M, Lecuyer H, Scott MG, Boularan C, Enslen H, Soyer M, Mikaty G, Bourdoulous S, Nassif X, Marullo S: **Meningococcus Hijacks a beta2-adrenoceptor/beta-Arrestin pathway to cross brain microvasculature endothelium**. *Cell* 2010, **143**:1149-1160.

23. Merz AJ, Enns CA, So M: **Type IV pili of pathogenic Neisseriae elicit cortical plaque formation in epithelial cells**. *Mol Microbiol* 1999, **32**:1316-1332.

24. Soyer M, Charles-Orszag A, Lagache T, Machata S, Imhaus AF, Dumont A, Millien C, Olivo-Marin JC, Dumenil G: **Early sequence of events triggered by the interaction of *Neisseria meningitidis* with endothelial cells**. *Cell Microbiol* 2014, **16**:878-895.

25. Lemichez E, Gonzalez-Rodriguez D, Bassereau P, Brochard-Wyart F: **Transcellular tunnel dynamics: control of cellular dewetting by actomyosin contractility and I-BAR proteins**. *Biol Cell* 2013, **105**:109-117.

26. •• Maddugoda MP, Stefani C, Gonzalez-Rodriguez D, Saarikangas J, Torrino S, Janel S, Munro P, Doye A, Prodon F, Aurrand-Lions M *et al.*: **cAMP signaling by anthrax edema toxin induces transendothelial cell tunnels, which are resealed by MIM via Arp2/3-driven actin polymerization**. *Cell Host Microbe* 2011, **10**:464-474.
This article reports that the flux of cyclic-AMP broad signaling molecule stimulated by bacterial toxins or pharmacological compounds sensitized the endothelial cells to transcellular tunnel opening. This work also allowed to visualize the accumulation of MIM I-BAR domain at the membrane-curvature driven by TEMs a few hundreds milliseconds after the opening.

27. Munro P, Benchetrit M, Nahori MA, Stefani C, Clement R, Michiels JF, Landraud L, Dussurget O, Lemichez E: **The *Staphylococcus aureus* epidermal cell differentiation inhibitor toxin promotes formation of infection foci in a mouse model of bacteremia**. *Infect Immun* 2010, **78**:3404-3411.

28. de Gennes P-G, Brochard-Wyart F, Quere D: *Capillarity and Wetting Phenomena*. Springer Media, Inc.; 2004.

29. Lemichez E, Aktories K: **Hijacking of Rho GTPases during bacterial infection**. *Exp Cell Res* 2013, **319**:2329-2336.

30. Boyer L, Doye A, Rolando M, Flatau G, Munro P, Gounon P, Clement R, Pulcini C, Popoff MR, Mettouchi A *et al.*: **Induction of transient macroapertures in endothelial cells through RhoA inhibition by *Staphylococcus aureus* factors**. *J Cell Biol* 2006, **173**:809-819.

31. Cai Y, Rossier O, Gauthier NC, Biais N, Fardin MA, Zhang X, Miller LW, Ladoux B, Cornish VW, Sheetz MP: **Cytoskeletal coherence requires myosin-IIA contractility**. *J Cell Sci* 2010, **123**:413-423.

32. •• Gonzalez-Rodriguez D, Maddugoda MP, Stefani C, Janel S, Lafont F, Cuvelier D, Lemichez E, Brochard-Wyart F: **Cellular dewetting: opening of macroapertures in endothelial cells**. *Phys Rev Lett* 2012, **108**:218105.
Modelisation of the cellular form of dewetting

33. Paluch EK, Nelson CM, Biais N, Fabry B, Moeller J, Pruitt BL, Wollnik C, Kudryasheva G, Rehfeldt F, Federle W: **Mechanotransduction: use the force(s)**. *BMC Biol* 2015, **13**:47.

34. Frost A, Unger VM, De Camilli P: **The BAR domain superfamily: membrane-molding macromolecules**. *Cell* 2009, **137**:191-196.

35. • Saarikangas J, Zhao H, Pykalainen A, Laurinmaki P, Mattila PK, Kinnunen PK, Butcher SJ, Lappalainen P: **Molecular mechanisms of membrane deformation by I-BAR domain proteins**. *Curr Biol* 2009, **19**:95-107.
Functional and biochemical characterization of the family of proteins with the properties of deforming artificial cell membranes outwardly of the cell in opposite direction to deformation induced by BAR proteins.

36. Moller J, Luhmann T, Chabria M, Hall H, Vogel V: **Macrophages lift off surface-bound bacteria using a filopodium-lamellipodium hook-and-shovel mechanism**. *Sci Rep* 2013, **3**:2884.

37. Chang F, Minc N: **Electrochemical control of cell and tissue polarity**. *Annu Rev Cell Dev Biol* 2014, **30**:317-336.

38. Galy O, Latour-Lambert P, Zrelli K, Ghigo JM, Beloin C, Henry N: **Mapping of bacterial biofilm local mechanics by magnetic microparticle actuation**. *Biophys J* 2012, **103**:1400-1408.

CREDITS

FIGURES

Figure 3.	Adapted from (Ozdemir et al., 2012), © 2012, with permission of Springer.
Figure 4. A	Adapted from (Mairey et al., 2006), licensed under a Creative Commons License.
Figure 4. B	Adapted from (Melican et al., 2013), licensed under a Creative Commons License.
Figure 6. A	Reproduced from (Deitsch et al., 2009) by permission from Macmillan Publishers Ltd.: Nature Reviews Microbiology, © 2009.
Figure 6. B	Reproduced from (Davidsen and Tonjum, 2006) by permission from Macmillan Publishers Ltd.: Nature Reviews Microbiology, © 2006.
Figure 7. A	Adapted from (Berry and Pelicic, 2015), licensed under a Creative Commons License.
Figure 7. B	Adapted from (Poweleit et al., 2016) by permission from Macmillan Publishers Ltd.: Nature Microbiology, © 2016.
Figure 8. A	Reproduced from (Berry and Pelicic, 2015), licensed under a Creative Commons License.
Figure 8. B	Adapted from (Kolappan et al., 2016), licensed under a Creative Commons License.
Figure 9. A	Adapted from (Chang et al., 2016) with permission from AAAS.
Figure 10. B	Adapted from (Higashi et al., 2011), licensed under a Creative Commons License.
Figure 11.	Reproduced from (Wormann et al., 2014), licensed under a Creative Commons License.
Figure 14. A	Reproduced from (Coureuil et al., 2017) by permission from Macmillan Publishers Ltd.: Nature Reviews Microbiology, © 2017.
Figure 14. B	Reproduced from (Steeg et al., 2011) by permission from Macmillan Publishers Ltd.: Nature Reviews Cancer, © 2011.
Figure 15.	Reproduced from (Charles-Orszag et al., 2016), © 2016, with permission from Elsevier.
Figure 17.	Adapted from (Parida et al., 1998) and (Knutton et al., 1998), © 1998, with permission from John Wiley & Sons, and from (Charles-Orszag et al., 2016), © 2016, with permission from Elsevier.
Figure 27. A	Reproduced from (Alteri et al., 2007) © 2007 National Academy of Sciences, U.S.A..
Figure 27. B	Reproduced from (Alcantar-Curiel et al., 2013), courtesy of Taylor & Francis.
Figure 27. C	Reproduced from (Collinson et al., 1991), courtesy of the American Society for Microbiology.
Figure 27. D	Reproduced from (El Abed et al., 2012), licensed under a Creative Commons License.
Figure 27. E	Reproduced from (Todd et al., 1984), courtesy of the American Society for Microbiology.
Figure 27. F	Reproduced from (Jude and Taylor, 2011), © 2011, with permission from Elsevier.
Figure 27. G	Reproduced from (Gil et al., 2004), courtesy of the American Society for Microbiology.
Figure 27. H	Reproduced from (Sajjan et al., 1995), courtesy of the American Society for Microbiology.
Figure 27. I	Reproduced from (Perras et al., 2014), licensed under a Creative Commons License.
Figure 27. J	Courtesy of Professor Gerhard Wanner, University of Münich.

FULL ARTICLES

Soyer *et al*., Cell. Microbiol. 2014, © 2014, reproduced with permission from John Wiley & Sons.
Gault *et al*., PLOS Pathog. 2015, licensed under a Creative Commons License.
Charles-Orszag *et al*., Curr. Opin. Cell. Biol. 2016, © 2016, reproduced with permission from Elsevier.

Cellular and molecular mechanisms of human endothelial cell plasma membrane remodeling by *Neisseria meningitidis*

Doctoral Thesis in Cell Biology by **Arthur Charles-Orszag**

Abstract

Neisseria meningitidis is a diderm bacterium that is naturally found in the human nasopharynx as a commensal. Occasionally, it can cross the mucosa and reach the underlying blood vessels where it enters the circulation. Once in the bloodstream, it can cause severe septic shock and/or meningitis.

The ability of *N. meningitidis* to cause disease is tightly linked to its ability to interact with human endothelial cells. In particular, upon bacterial adhesion via filamentous organelles called type IV pili, bacteria remodel the host cell plasma membrane in the form of actin-rich, filopodia-like protrusions. These protrusions allow bacteria to resist blood flow-generated shear stress and proliferate on top of the host cells. Unlike many other bacterial pathogens, plasma membrane remodeling induced by *N. meningitidis* does not require actin polymerization. Yet, the cellular and molecular mechanisms of this process are unknown.

Here, we show that upon adhesion of individual bacteria, the host cell plasma membrane deforms by adhering along type IV pili fibers in a wetting-like fashion. Therefore, type IV pili act as an extracellular scaffold that guide plasma membrane protrusions in an F-actin-independent manner.

We further show that the ability of the plasma membrane to deform along nanoscale adhesive structures is an intrinsic property of endothelial cells.

Therefore, this study uncovers the mechanism of a key step of *N. meningitidis* pathophysiology and reveals novel properties of human cell plasma membrane that could be at play in other fundamental cellular processes.

Résumé

Neisseria meningitidis est une bactérie diderme qui colonise le nasopharynx humain de façon commensale. Occasionnellement, elle franchit la barrière nasopharyngée et accède à la circulation sanguine où elle peut provoquer un choc septique et/ou une méningite

Le pouvoir pathogène de *N. meningitidis* est lié à sa capacité à interagir avec les cellules endothéliales humaines. Après avoir adhéré aux cellules grâce à des organelles filamenteux, les pili de type IV, les bactéries induisent une déformation de la membrane plasmique de la cellule hôte sous la forme de protrusions riches en actine ressemblant à des filopodes. Ces protrusions permettent aux bactéries de résister aux forces de cisaillements générées par le flux sanguin et de proliférer à la surface des cellules. Contrairement à de nombreuses autres bactéries pathogènes, cette déformation de la membrane plasmique ne nécessite pas de polymérisation d'actine. Cependant, les mécanismes cellulaires et moléculaires de cette déformation sont inconnus.

Dans cette étude, nous montrons que lorsque des bactéries individuelles adhèrent à la cellule hôte, la membrane plasmique se déforme en adhérant le long des fibres de pili de type IV de façon similaire au mouillage d'un liquide sur un solide. Les pili de type IV agissent donc comme un échafaudage extracellulaire qui guide les protrusions de membrane plasmique indépendamment du cytosquelette d'actine.

Nous montrons également que la capacité de la membrane plasmique à se déformer le long de structures adhésives nanométriques est une propriété intrinsèque des cellules endothéliales.

Ces travaux décrivent le mécanisme d'une étape importante de la pathophysiologie de *N. meningitidis* et mettent en évidence des propriétés nouvelles de la membrane plasmique des cellules humaines qui pourraient être impliquées dans d'autres processus fondamentaux de biologie cellulaire.